COMPUTER-AIDED MODELING AND ANALYSIS OF PASSIVE MICROWAVE AND MILLIMETER-WAVE HIGH-TEMPERATURE SUPERCONDUCTOR CIRCUITS AND COMPONENTS

Thesis by
Dimitrios Antsos

In Partial Fulfillment of the Requirements
for the Degree of
Doctor of Philosophy

California Institute of Technology
Pasadena, California

1994
(Defended November 5, 1993)

ACKNOWLEDGMENTS

Early in the morning of June 15,1993, my thesis advisor Professor Edward C. Posner of Caltech was killed in a traffic accident, while riding his bicycle to work. Part of me died with him that day and things are never going to be quite the same again. As I write this emotional eulogy and acknowledgment, which admittedly has no place in any thesis, I cannot but think how really essential it is to this one. Without Ed (I have only posthumously and lovingly started to call him Ed; when he was living the aura of wisdom, love and respect his person projected "forced" me to use the more formal Dr. Posner), or another person of his caliber, it simply wouldn't have been possible. Unfortunately - and this is my own opinion - persons of Ed's caliber represent a species that is virtually extinct in today's society. Hence the huge vacuum that he left behind him will not be easy to fill. This thesis is *In Memoriam* of a worthy person with a great mind and heart.

With similar gratitude, I would like to thank and acknowledge Robert C. Clauss (Bob), former manager of the TDA Systems Development Program at JPL and current JPL Member of Technical Staff, without whose help and support (moral, judicial and mechanical amongst others) I might not have even had a BS. today (he doesn't either; yet his thoughts and suggestions induce academic nightmares to many "educated" Ph.D.'s- myself not excluded).

From Caltech: I wish to thank professor R. J. McEliece who, after Dr. Posner's death, became my advisor and helped me along in the critical final months of my graduate studies. Additionally, I would like to acknowledge professors Vaidyanathan and Rutledge of the Electrical Engineering department and professor Brattkus and Sebius Doedler of the Applied Mathematics department for the time that they devoted to me, selflessly and willingly, for discussions at various times during the development of my thesis.

From JPL: I would like to thank my boss Dan Rascoe, Supervisor of group 3363 (who probably lost quite a few tenths of a degree of his eyesight trying to untangle my Gordian knot of syntax and spelling) for helpful suggestions and discussions and for taking the considerable time entailed in being part of my thesis committee. Also Wilbert Chew provided valuable suggestions and references. Gratitude is also due to all my colleagues, the group who tolerated me for 2.5 years, sharing their facilities and taking up office space, with minimal productivity in return. Many thanks are due Section 336 in general and its Manager, Tom Komarek, for the nurturing nest they provided me in these research years.

Gratitude is due Marc Matzner who volunteered his professional proof-reading and editing services. Without his comments, suggestions and edits, implemented in their entirety in this thesis, the latter would have been considerably harder to read.

Support for the computing research presented in chapter 8 was provided by the JPL Supercomputing Project on the CRAY computers at the Jet Propulsion Laboratory and at Goddard Space Flight Center. The JPL Supercomputing Project is sponsored by the Jet Propulsion Laboratory and the NASA Office of Space Science and Applications. Finally, I have been asked to mention Brian Hunt and his group at JPL who fabricated the HTS circuits used for the experimental verifications in chapters 5, 6 and 7.

Conductus Inc., provided me with a "student-priced" HTS YBCO resonator, which is used for the experimental verification in chapter 4, for which I am grateful.

Last and foremost I would like to thank and acknowledge my fiancee, Judith Din, who, with her love and patience, provided the haven of peace and concentration necessary for the successful completion of my work.

ABSTRACT

As their critical temperatures continue to rise, high-temperature superconductors (HTS) promise applications in microwave, and to some extent in millimeter-wave circuits, because they should exhibit lower loss, in these frequencies, than their normal metal counterparts. However, in the case of passive circuits, fundamental performance limits (finite insertion loss) still exist and apply, as explored in this thesis.

Commercial computer-aided design (CAD) and analysis software tools exist, that permit design and analysis of normal metal microwave and millimeter-wave circuits. These tools minimize design and manufacturing errors and the need for costly re-work and design iterations. In the case of HTS circuits these tools are insufficient because of three effects present in HTS circuits that do not exist in normal metal circuits. First, because of manufacturing practices, the HTS layers on substrates are usually very thin; of the order of the magnetic field penetration depth. Second, there is an additional internal inductance, the kinetic inductance, which is due to the inertia of the superelectrons. Third, high input power induces high magnetic fields and current densities which drive the superconductor into its normal state, in which it is an insulator.

This thesis is a study of these phenomena and their effects on quasi-TEM transmission line circuit performance. Methods for accounting for these effects and introducing them into currently available CAD tools are presented. These methods are applied to three example circuits for which modeled and measured performance is compared.

The viability and advantages of HTS waveguides are also studied and analyzed. A finite difference analysis program is presented.

CONTENTS

LIST OF FIGURES

LIST OF TABLES

CHAPTER 1

INTRODUCTION

1.1 The Current State of Development of CAD Tools

This thesis is devoted to Computer Aided Design (CAD) and Modeling of High-Temperature Superconductor (HTS) Microwave Circuits.

Microwave circuits, which are important and widely used in communications, are, unlike their lower frequency counterparts, difficult to model by equations that involve simple circuit parameters like voltage and current. Much research, during the latter half of this century, has been devoted to understanding these circuits and overcoming this difficulty. Today, with the advent of digital computers, CAD and modeling of "conventional" microwave circuits is a very developed science. Kirchhoff's voltage and current laws together with Ohm's law go a long way in modeling low frequency circuits, circuits for which the wavelength of the electric and magnetic fields is large compared to the linear dimensions of the elements of the circuit.

Conversely, in microwave circuits the wavelength of the excitation is comparable to one or more of the linear dimensions of the elements of the circuit. If additional linear dimensions of the circuit are comparable to the wavelength, it becomes harder to model the circuit because of the greater number of field-modes that have to be considered. Thus, a microstrip patch antenna ,which has its width *and* length comparable to a wavelength, is harder to model than a microstrip transmission line, which has only its length comparable to a wavelength.

Modeling is important in the design and fabrication of microwave circuits because it helps avoid expensive rework and manufacturing iterations. Yet today, microwave engineering is still considered, by many within the engineering community, "black magic," as it remains one of the fields of engineering in which there is no substitute for intuition and experience.

The advent of powerful computers has had an impact here in recent years. Hewlett Packard (HP) has, in the last three years, released a CAD software package, the High Frequency Structure Simulator (HFSS), which analyzes the steady-state response of circuits of arbitrary shape (of which all dimensions may be comparable to a wavelength) to electromagnetic sinusoidal excitation. It performs a finite difference solution of Maxwell's equations in arbitrary volumes by sub-sectioning these volumes into elementary sub-volumes (bounded by tetrahedra) in which the fields are assumed constant.

Nonetheless, while most modern microwave CAD programs are successful in predicting the direction of change of the response of circuits with respect to their design variables, I have yet to see one that accurately predicts the response of the circuit given the design parameters. Although the partial derivative of the response parameters with respect to the design variables can, usually, be predicted fairly accurately, the absolute values of the response parameters are more elusive. This is because, among other reasons, material uniformity over small spatial dimensions (that are comparable to the short wavelength of high frequencies) is usually poor, and boundary condition assumptions, used in various analyses, are usually over-idealized and do not correspond to actual laboratory measurement conditions.

By comparison, CAD and modeling of HTS microwave circuits postdate the discovery, by Bednorz and Muller, of superconductors with transition temperatures above the 77 K temperature of liquid nitrogen. These promise many practical applications of

superconductor microwave circuits in today's communications, given the abundance of nitrogen and the relatively cheap methods of its liquefaction. Superconductors have the property of zero DC resistance to currents. Hence at DC they are advantageous to use (less lossy) over regular conductors. This proves true also, as it turns out, at microwave frequencies (and even for some materials into the millimeter-wave frequencies). Since the use of HTS microwave circuits is not yet widespread in communications systems, there is comparatively less work in the area of modeling of these types of circuits.

HTS and conventional microwave circuits are similar in many ways, but certain critical differences cannot be neglected since they differentiate responses of identical looking circuits. With the aid of the plethora of CAD and modeling tools which exist today for conventional microwave circuits one can, however, model many HTS microwave circuits, taking care to properly modify relevant parameters.

This thesis first sets some upper bounds on expectations for the lossless behavior of HTSs and then presents a loss model, which exhibits good success in modeling the high-frequency electromagnetic behavior of HTSs, and further explains how to use it to model the behavior of different microwave circuits. Three applications are presented by way of examples of real HTS circuits for which measurements are compared with theory. The idea of HTS waveguides is also explored, showing some of the possibilities in this area.

A wide variety of CAD software packages have been used in writing this thesis. Whenever I could, I avoided writing my own programs and preferred to modify existing programs and CAD tools in order to use them in my application. Wherever I use a CAD software package I try to explain why I used that particular one and point out possible caveats for the use of alternatives (which in many cases I have tried to use). Most of these software packages are popular and well known either in the microwave modeling

community or in the mathematics community. I attempt a partial list, with a short description, of these in table 1:

Name	Company	Use
Touchstone	EEsof	Microwave CAD and modeling using "recipes."
EM	Sonnet	Planar Microwave Circuit Analysis using the method of moments.
MathCAD	MathSoft	Mathematical CAD.
Matlab	Mathworks	Matrix mathematical CAD.
Mathematica	Wolfram Research	Symbolic Mathematical CAD.
cc under UNICOS 7.0	CRAY Research	The standard C compiler 3.0 on a CRAY Y-MP2E main-frame computer system.
cc under UNICOS 7.C.3	CRAY Research	The standard C compiler 3.0 on a CRAY C98 main-frame computer system.

Table 1 Software used in this thesis.

1.2 An Outline of the Thesis

The areas discussed in this thesis are as follows. A mathematical statement of the implications of passivity is presented in chapter 2. Chapter 3 is devoted to the modeling of quasi-TEM transmission lines under different ratios of conductor thickness to field penetration depth. Chapter 4 is devoted to an experimental verification of the model presented in chapter 3. Chapter 5 presents the model of chapter 3 fit to the measured data from a real microwave low-pass filter (LPF). Chapter 6 presents the model of chapter 3 fit to the measured data from a real microwave band-pass filter (BPF). Chapter 7 presents some measurements of the non-linear behavior, with respect to input power, of the device

of chapter 5, and a possible extension of the model of chapter 3 into the non-linear regions. Chapter 8 presents a finite difference solution of Maxwell's equations in a HTS closed rectangular waveguide. The modeling is performed using a CRAY supercomputer and employs a finite difference approximation of the Helmholtz electromagnetic wave equations.

CHAPTER 2

SUPERCONDUCTIVITY AND PASSIVITY

2.1 Introduction

This chapter will attempt to clear up some misconceptions that the prefix "super" in the name of superconductors may have created. Frequently, the fallacious assumption is made that, by substituting normal conductors for superconductors in passive microwave circuits, all unwanted losses will magically disappear and the ideal minimum "noise figure" contribution for a given circuit can be achieved. While it is true that in the majority of cases the losses (of ohmic nature) in a given circuit decrease when superconductors are substituted for normal conductors, there are fundamental physical limitations imposed by passivity (i.e., the lack of active, energy-producing devices in the circuit) on the performance of a given circuit. These limitations will be quantified in the chapter below and a numerical example, of what these limitations mean for the case of a 3-port network will be furnished. All superconducting circuits considered in this thesis are passive. The following analysis will show that they are superconducting; yet not supernatural.

2.2 An Analytical Statement of Passivity

A network (superconducting or not) is considered passive when the power incident onto it is greater than or equal to the power reflected from it, for all possible excitations. A network described by the 'a' and 'b' wave parameters is shown in figure 1 below (using a 3-port network for depiction purposes).

The a-waves are the incident waves and the b-waves are the reflected waves, at each port. These are normalized so that, for example,

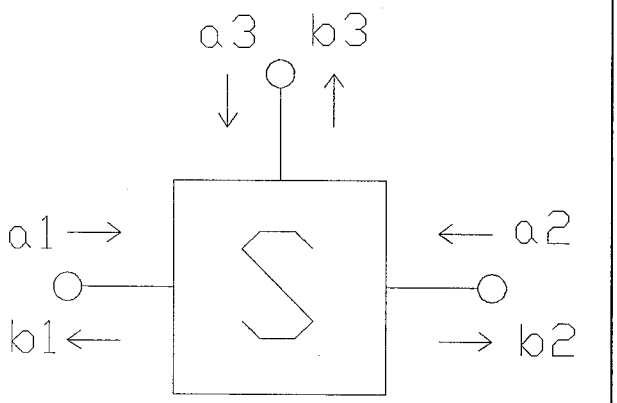

Figure 1 A 3-port network.

$$\frac{1}{2}|a_1^2| \qquad (1)$$

corresponds to the power carried by the wave incident at port 1. It is easy to see, then, that the total power incident to this network from all ports is

$$P_{inc} = \frac{1}{2}\sum_{i=1}^{N}|a_i|^2 \qquad (2)$$

where N is the total number of ports of the network.

Similarly, the total power scattered by the network is

$$P_{scat} = \frac{1}{2}\sum_{i=1}^{N}|b_i|^2 \quad . \qquad (3)$$

An alternate way of writing the above equations in matrix notation is

$$P_{inc} = \frac{1}{2}\mathbf{a}^{+}\mathbf{a} \qquad (4)$$

$$P_{scat} = \frac{1}{2}\mathbf{b}^{+}\mathbf{b} \qquad (5)$$

where $\mathbf{a}=(a_1,a_2,\ldots,a_N)^T$ and $\mathbf{b}=(b_1,b_2,\ldots,b_N)^T$ and the "dagger" notation is used to denote conjugate-transpose. By the definition of the S-matrix we have

$$\mathbf{b} = \mathbf{S}\mathbf{a} \qquad (6)$$

where **S** is an N by N matrix characteristic of the network.

Combining the last 3 equations gives the total dissipated power as

$$P_{dis} = P_{inc} - P_{scat} = \frac{1}{2}(\mathbf{a}^{+}\mathbf{a} - \mathbf{a}^{+}\mathbf{S}^{+}\mathbf{S}\mathbf{a}) = \frac{1}{2}\mathbf{a}^{+}(\mathbf{I} - \mathbf{S}^{+}\mathbf{S})\mathbf{a} = \frac{1}{2}\mathbf{a}^{+}\mathbf{Q}\mathbf{a} \qquad (7)$$

where I have defined the dissipation matrix, **Q**, of the network. For any passive network (superconducting or not) it must be

$$P_{dis} \geq 0, \quad \forall \mathbf{a} \ . \qquad (8)$$

Equations (8) and (7) imply that the matrix **Q** must be non-negative real (i.e., the quadratic form $\mathbf{a}^{+}\mathbf{Q}\mathbf{a}$ must be a non-negative real number $\forall \mathbf{a}$, or **Q** must be a positive semi-definite matrix). Let us examine the implications of this on **Q**. To draw our conclusions we will use the following theorems from matrix theory:

Theorem 1

Every hermitian matrix has real eigenvalues.

Theorem 2

A hermitian matrix has non-negative eigenvalues if and only if it is positive semi-definite.

Theorem 3

For every hermitian matrix there exists a complete set of orthonormal eigenvectors.

Clearly, $\mathbf{S}^{+}\mathbf{S}$ is a hermitian and positive semi-definite matrix (proof: $(\mathbf{S}^{+}\mathbf{S})^{+} = \mathbf{S}^{+}(\mathbf{S}^{+})^{+} = \mathbf{S}^{+}\mathbf{S}$ and $\mathbf{a}^{+}(\mathbf{S}^{+}\mathbf{S})\mathbf{a} = (\mathbf{a}^{+}\mathbf{S}^{+})(\mathbf{S}\mathbf{a}) = (\mathbf{S}\mathbf{a})^{+}(\mathbf{S}\mathbf{a}) = \mathbf{b}^{+}\mathbf{b} \geq \mathbf{0} \quad \forall \mathbf{a}$, since the last expression is the square of the norm of the vector **b** and therefore non-negative). Hence, by Theorems 1 and 2, the eigenvalues of $\mathbf{S}^{+}\mathbf{S}$ are all real and non-negative, i.e.,

$$\lambda_i^{S^+S} \geq 0, \quad \forall i \quad . \tag{9}$$

The matrix $\mathbf{Q}$ is also hermitian (proof: $\mathbf{Q}^+ = \left(\mathbf{I} - \mathbf{S}^+\mathbf{S}\right)^+ = \mathbf{I}^+ - \left(\mathbf{S}^+\mathbf{S}\right)^+ = \mathbf{I} - \mathbf{S}^+\mathbf{S} = \mathbf{Q}$) and its eigenvalues are given by

$$\lambda_i^Q = 1 - \lambda_i^{S^+S} \quad \forall i \quad . \tag{10}$$

Proof:

Assume λ_i^Q is an eigenvalue of $\mathbf{Q}$.

Hence it must be that

$$\det\left(\mathbf{Q} - \lambda_i^Q \mathbf{I}\right) = \det\left(\mathbf{I} - \mathbf{S}^+\mathbf{S} - \lambda_i^Q \mathbf{I}\right) = -\det\left[\mathbf{S}^+\mathbf{S} - \left(1 - \lambda_i^Q\right)\mathbf{I}\right] = 0$$

i.e., $1 - \lambda_i^Q$ is an eigenvalue of $\mathbf{S}^+\mathbf{S}$, q.e.d.

Using (9) and (10) we conclude that

$$\lambda_i^Q \leq 1, \quad \forall i \quad . \tag{11}$$

Hence, using Theorems 1 and 2, the hermiticity of $\mathbf{Q}$ and equation (11) we can state the necessary and sufficient condition of passivity (equation (7)) in the following theorem.

Theorem

$$\text{Passivity} \Leftrightarrow 0 \leq \lambda_i^Q \leq 1 \quad \forall i \quad . \tag{12}$$

(Actually the right part of the right-hand-side of equation (12) is guaranteed, as has been proven in equation (11), but it is a good check on any calculations).

Equation (12) states, in words, that the eigenvalues of $\mathbf{Q}$ (which are real since it is hermitian) must be between 0 and 1 (greater than or equal to zero because of passivity and less than or equal to one because of the positive-semi-definiteness of $\mathbf{S}^+\mathbf{S}$).

An alternate proof of the above theorem, which gives more insight into the physical significance of the eigenvalues and eigenvectors of $\mathbf{Q}$ is as follows:

Let us assume that we excite the network of figure 1 with an incident wave $\mathbf{a}_*$, an eigenvector of matrix $\mathbf{Q}$, of power P_{inc}, that corresponds to an eigenvalue λ_*^Q. By definition, $\mathbf{a}_*$ must obey the following two equations:

$$\frac{1}{2}\mathbf{a}_*^+\mathbf{a}_* = P_{inc} \tag{13}$$

and

$$\mathbf{Q}\mathbf{a}_* = \lambda_*^Q\mathbf{a}_* \ . \tag{14}$$

Substituting (13) and (14) into (7) we obtain

$$P_{dis} = \frac{1}{2}\mathbf{a}_*^+\mathbf{Q}\mathbf{a}_* = \frac{1}{2}\mathbf{a}_*^+\lambda_*^Q\mathbf{a}_* = \lambda_*^Q\left(\frac{1}{2}\mathbf{a}_*^+\mathbf{a}_*\right) = \lambda_*^Q P_{inc} \tag{15}$$

By the definition of dissipated power we have

$$0 \le P_{dis} \le P_{inc} \ . \tag{16}$$

Substituting (15) into (16) we obtain the desired result, as expressed in equation (12).

Equation (15) provides a good physical interpretation of the significance of the eigenvalues of matrix $\mathbf{Q}$. An eigenvalue of $\mathbf{Q}$ is the fraction of the incident power that is dissipated in the network, when the latter is excited by the eigenvector corresponding to that eigenvalue. Equation (15) also tells us how to minimize the power dissipated in the network: Excite the network with an incident wave that is an eigenvector of $\mathbf{Q}$ that corresponds to its minimum eigenvalue. In fact, if $\mathbf{Q}$ has a zero eigenvalue, i.e., it is singular, it is possible to excite the network in a way that no power is dissipated (with the eigenvector that corresponds to the zero eigenvalue).

2.3 Implications of Passivity. An Example.

2.3.1 The Circuit

This example is relevant to a current effort in industry to fabricate multi-way power dividers and combiners for array-antenna applications. The unit-cell of most of these dividers is a 3-port or a 4-port with one port terminated (branch-line, rat-race, Wilkinson couplers, etc.). As the size of the array-antenna increases, so do the required "levels" of power division (as the base-two logarithm of the size). Therefore, the insertion loss of these unit-cell devices, which are cascaded in "levels," becomes an important concern and design parameter. The examples of unit-cell devices mentioned above all provide isolated output ports which are matched to 50 Ohms. In other examples of corporate multi-port power dividers without isolation, the output ports are not matched to 50 Ohms. These work well with passive arrays, where the antennas have input impedances close to 50 Ohms, but are not suitable, say, for driving the amplifiers of active arrays, since the amplifiers want to "see" a 50 Ohm impedance at their input. Therefore, these devices, which are not 3-ports, will not be considered.

Following the trend, an idea which JPL is considering for reducing the size of the conical receiving horns in its Goldstone huge (34 m diameter) antennas, is using microstrip patch array antennas with superconducting beam forming networks at cryogenic temperatures. As calculations will show there is a minimum insertion loss, largely dictated by the geometry of the circuit used, below which a passive circuit cannot operate.

Let us consider, then, a 3-port network as an example. A branch-line coupler with its isolated port terminated with a 50 Ohm load (figure 2). One of the three

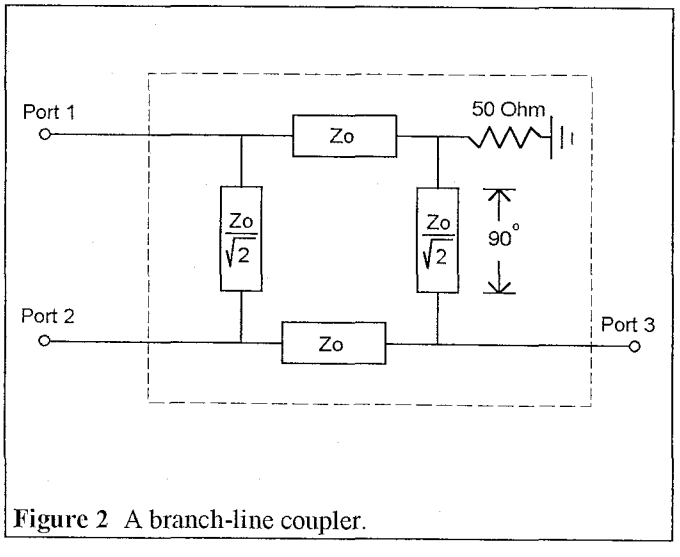

Figure 2 A branch-line coupler.

remaining ports (say port 1) is the input and the other two (say ports 2 and 3) the outputs. In an idealized model, where all the lines are exactly one quarter of a wavelength long at the design frequency and lossless (no ohmic losses), the isolation between ports 2 and 3 can be analytically shown to be infinite (i.e., S23=0). However, the realities of building the circuit on a substrate are different. On the actual mask which is used to fabricate the circuit one can see that, at the point where the (mutually) perpendicular quarter-wave lines join, there is a T-junction. This T-junction has dimensions itself and cannot be considered a lumped element. What this means is that the microwave current density is spread throughout the T-junction and does not go through it only at one point. There are an infinite number of linear paths along which the phase length of the current is 90 degrees and there are also an infinite number of linear paths along which the phase length is slightly different from 90 degrees. In the actual response of the circuit this effect shows up as a "broadening" and a "shallowing" of the infinite well that the graph of S23 ideally exhibits about the design frequency. This effect is independent of ohmic losses (i.e., occurs on both normal and superconducting circuits) and means that S23 is very small, not 0, at the design frequency. This rationale, which is geometry dependent but not material properties dependent, allows us to set a lower bound on S23. This bound, together with the passivity constraints on the **Q** matrix, yield constraints on the insertion loss of this circuit which are not material dependent. It does not matter how lossless the material is, the constraints will be there.

2.3.2 The Calculations

The software package Matlab, by Mathworks Inc., is used for the analysis. Matlab is preferred because it is optimized for matrix computations and quite accurate in eigenvalue problems. An initial attempt to use MathCAD, by MathSoft Inc., failed because the root-finding accuracy of the package, to solve the characteristic equation and obtain the

eigenvalues, was not good enough. Three different cases are analyzed. A sample Matlab file for the first case is included as appendix A of this chapter. The methodology is the same in all three cases:

1. Assume a form for the S-matrix of the network.

2. Compute the eigenvalues of the Q-matrix as a function of insertion loss and isolation.

3. Plot, in the two-dimensional space defined by the insertion loss and the isolation, the curve demarcating the region where the 3-port is passive (i.e., realizable with passive components) from the region where it is not. (i.e., plot the locus of points that lie where the minimum eigenvalue of **Q** crosses from positive to negative values).

An alternative method to determine the physically achievable region, where **Q** is passive, is to find the locus of points, in the isolation-insertion loss space, that make the matrix **Q** singular. This approach should, however, be taken with caution to avoid trivial roots of the characteristic polynomial of **Q**.

Case 1. Perfectly matched 3-dB coupler w/ finite isolation and insertion loss.

The (symmetric) S-matrix is assumed to have the form

$$S = \begin{bmatrix} 0 & \frac{\alpha}{\sqrt{2}} & \frac{\alpha}{\sqrt{2}} \\ \frac{\alpha}{\sqrt{2}} & 0 & x \\ \frac{\alpha}{\sqrt{2}} & x & 0 \end{bmatrix}$$

α: Insertion loss, x: isolation

The diagonal elements of the matrix (S11, S22 and S33) are assumed zero, (i.e., the device is perfectly matched). S21 and S31 would ideally have the value $1/\sqrt{2}$ (3 dB coupler) and α is the additional loss in excess of the ideal division loss (insertion loss).

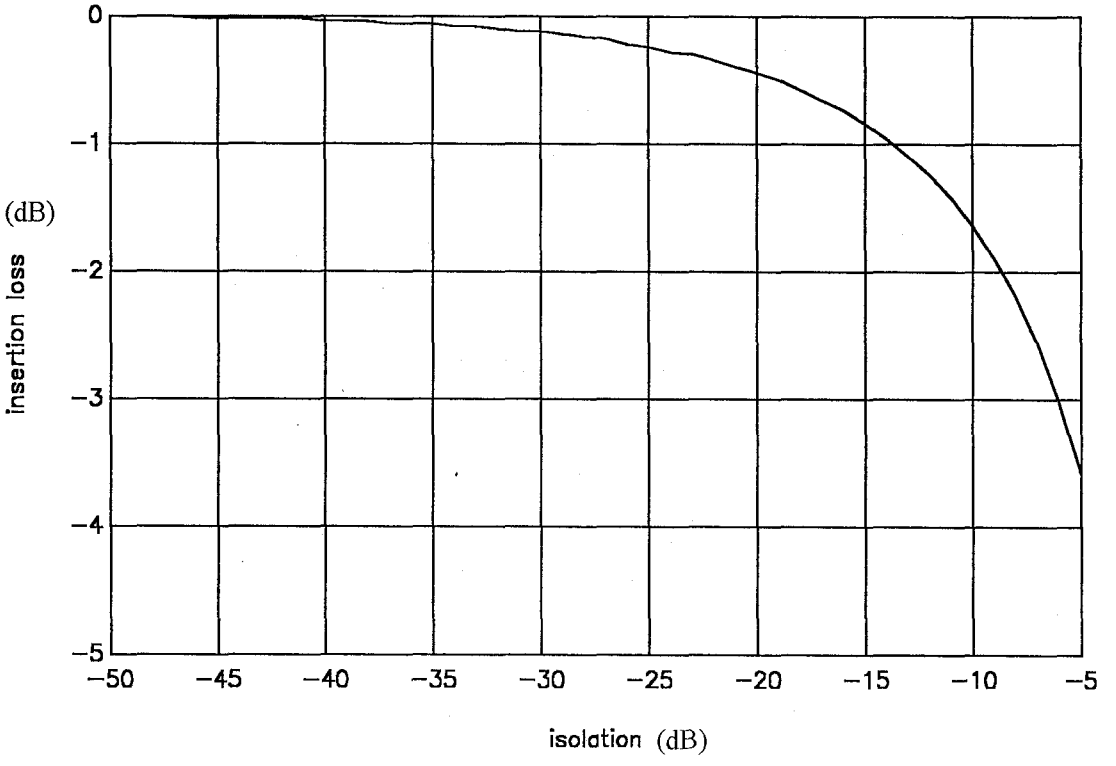

Figure 3 Trade-off between insertion loss & isolation.

The result of the analysis is shown in figure 3. The horizontal axis is the negative of the isolation (i.e., S32, since isolation is defined positive) in dB. The vertical axis is the negative of the insertion loss. On the plotted curve, the minimum eigenvalue of matrix **Q** is exactly zero. Therefore, the minimum possible dissipated power, for this network, may be achieved by exciting the network with an eigenvector of **Q** that corresponds to this zero eigenvalue. The equation of the zero-eigenvalue locus of points that make zero dissipation possible, for this form of S-matrix, is

$$\alpha = \sqrt{1 - x} \quad . \tag{17}$$

The corresponding normalized, unit-power eigenvector is

$$\begin{pmatrix} \sqrt{\frac{2-2x}{2-x}} \\ \frac{1}{\sqrt{2-x}} \\ \frac{1}{\sqrt{2-x}} \end{pmatrix} . \qquad (18)$$

The "achievable" region for a passive circuit is below the curve. A typical value of isolation to be expected by the circuits mentioned in above is about 20 dB (seldom more than 30 dB). Here I treat the isolation as the "known" and read what the achievable insertion loss is for this 3-port. The point of comparison will be 18 dB isolation. In this case, for 18 dB isolation, the minimum achievable insertion loss is 0.59 dB. As the isolation tends to infinity (i.e., x=0 in the S-matrix) the minimum insertion loss tends to 0 dB, as is to be expected for an ideal circuit.

Figure 4 is a plot of the power in each of the three components of the unit-power, zero-dissipation eigenvector (equation (16)) versus the isolation. Typically, in microwave

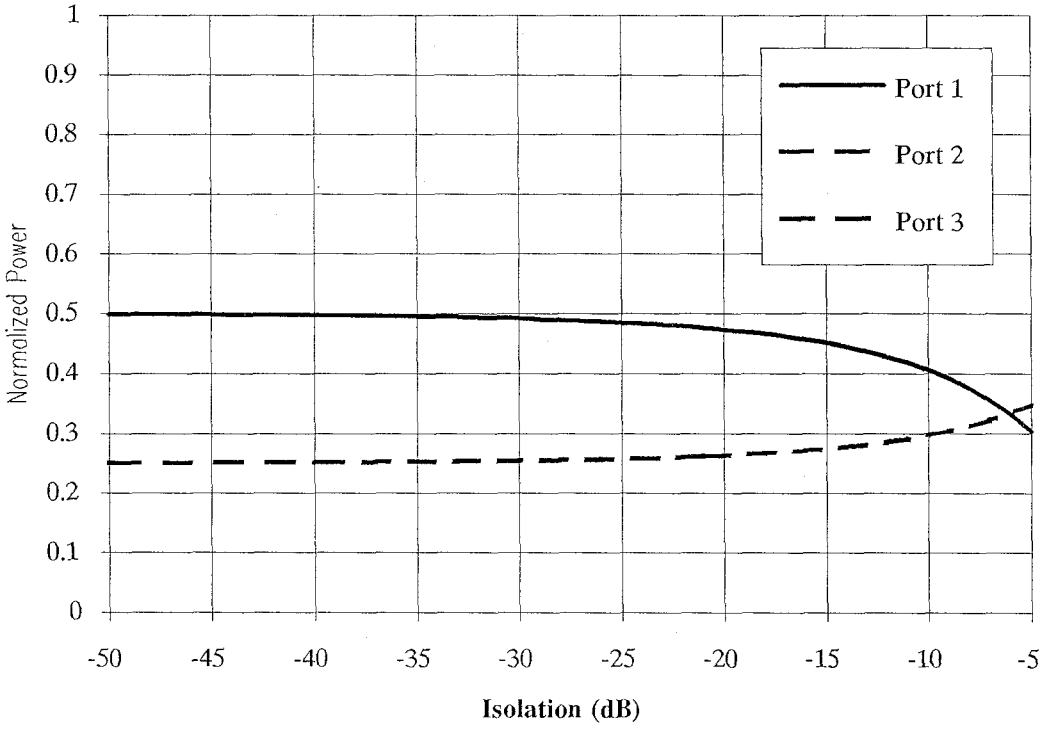

Figure 4 The power, in each of the ports, for zero dissipation.

circuits, the excitation to the network is a wave incident to port one, the input port. Hence, the closer the minimum-loss eigenvector (equation (16)) is to the vector $\left(\sqrt{2} \quad 0 \quad 0\right)$, the closer we can come to realizing the zero-dissipation condition.

Case 2. Imperfectly matched 3-dB coupler.

The S-matrix was assumed to have the form

$$\mathbf{S}=\begin{bmatrix} 0.1 & \frac{\alpha}{\sqrt{2}} & \frac{\alpha}{\sqrt{2}} \\ \frac{\alpha}{\sqrt{2}} & 0.1 & x \\ \frac{\alpha}{\sqrt{2}} & x & 0.1 \end{bmatrix}$$

α: Insertion loss, x: isolation

for sub-case i. and

$$\mathbf{S}=\begin{bmatrix} 0.1 & \frac{\alpha}{\sqrt{2}}\angle -90 & \frac{\alpha}{\sqrt{2}}\angle -90 \\ \frac{\alpha}{\sqrt{2}}\angle -90 & 0.1 & x\angle -180 \\ \frac{\alpha}{\sqrt{2}}\angle -90 & x\angle -180 & 0.1 \end{bmatrix}$$

α: Insertion loss, x: isolation

for sub-case ii.

In this case, a 20 dB return loss on all ports is assumed. Figure 5 shows the results of the analysis for these matrices. The lower and upper curves show the analysis results for sub-cases i. and ii. respectively.

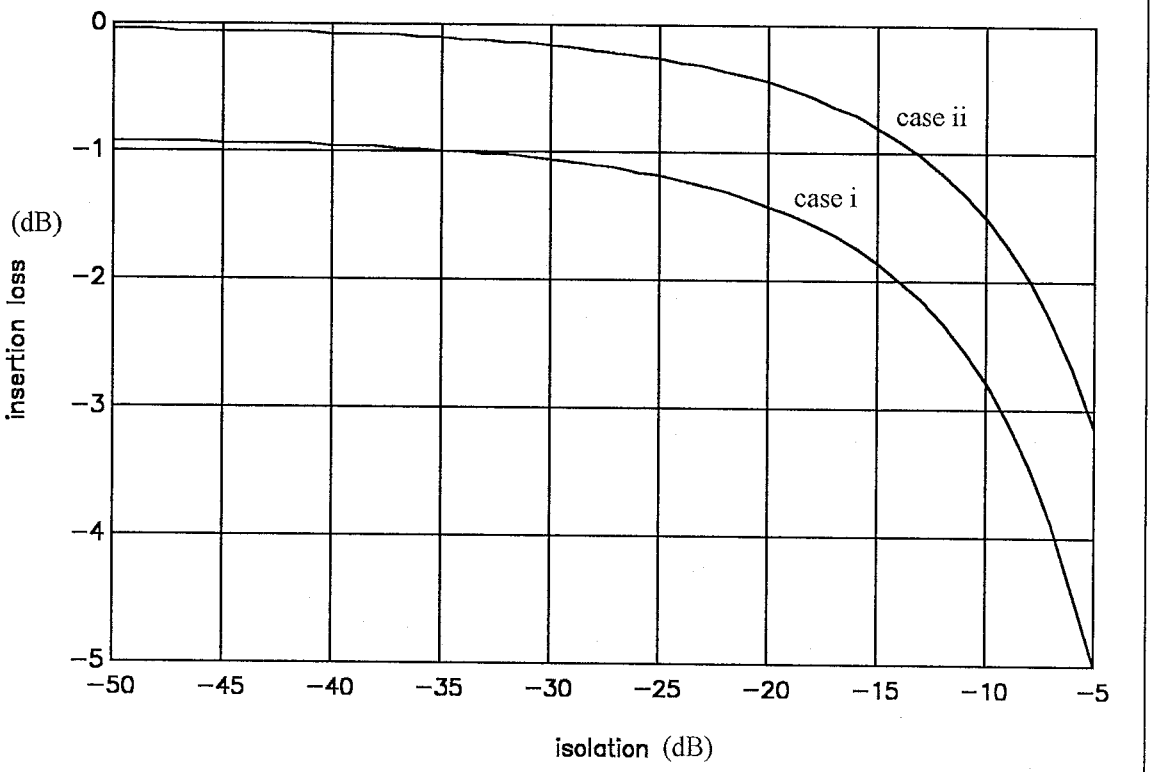

Figure 5 Trade-off between insertion loss & isolation.

Sub-case i.

The minimum achievable insertion loss at 18 dB isolation increases to 1.56 dB. However, this case is too restrictive as all the components of the S-matrix are "forced" to be in phase. It is instructive however to note that the trade-off between insertion loss and isolation also depends on the required phase through the circuit. In this case the minimum insertion loss tends to 0.92 dB.

The equation of the zero-eigenvalue locus of points plotted for this sub-case is

$$\alpha = \frac{1}{10}\sqrt{81 - 90x} \tag{19}$$

and the unit-power, zero-dissipation eigenvector is

$$\begin{pmatrix} \sqrt{\frac{18-20x}{18-10x}} \\ \frac{3}{\sqrt{18-10x}} \\ \frac{3}{\sqrt{18-10x}} \end{pmatrix} \quad (20)$$

Figure 6 is a plot of the power in each of the three components of the unit-power, zero-dissipation eigenvector (equation (20)) versus the isolation.

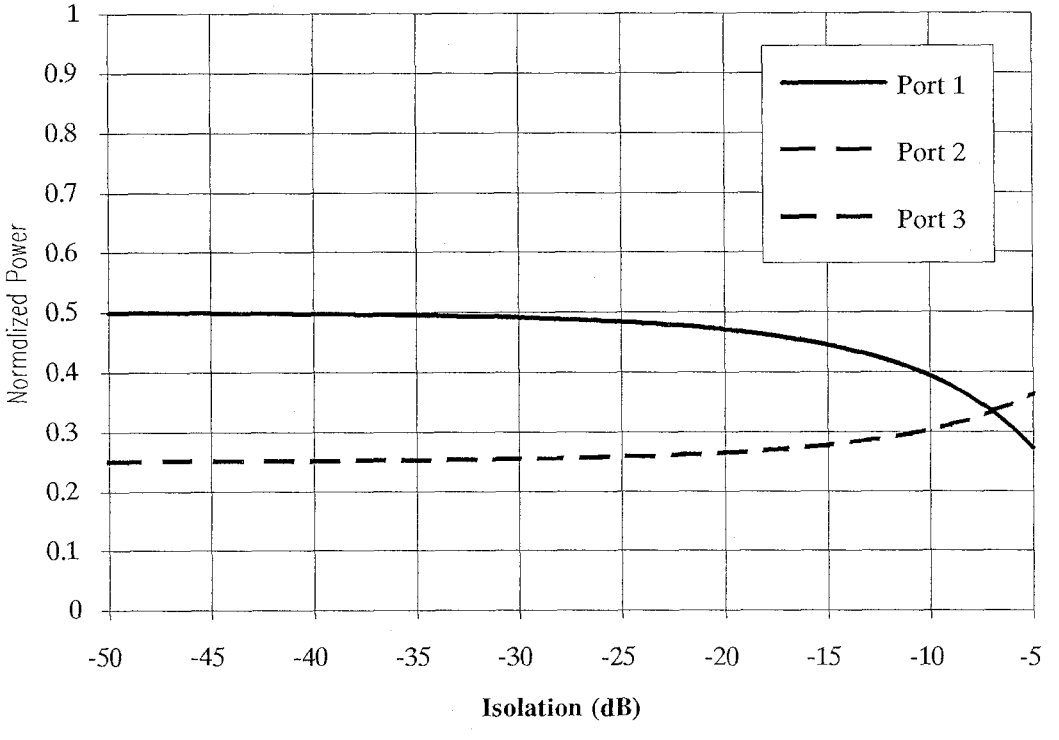

Figure 6 The power, in each of the ports, for zero dissipation.

Sub-case ii.

The phases of the S-matrix components are set to the values of a 0°/180° rat-race coupler. The minimum achievable insertion loss at 18 dB isolation is 0.56 dB. As the isolation tends to infinity (i.e., x=0 in the S-matrix) the minimum insertion loss tends to 0.04 dB

(which corresponds to the expected loss, in the ideal case, due to the reflected power $|S11|^2$). Hence, an imperfectly matched 3-port will always have some insertion loss higher than the ideal which corresponds to the reflection losses at the input.

The equation of the zero-eigenvalue locus of points plotted for this sub-case is

$$\alpha = \frac{1}{10}\sqrt{99-90x} \tag{21}$$

and the unit-power, zero-dissipation eigenvector is

$$\begin{pmatrix} -j\sqrt{\dfrac{11-10x}{10-5x}} \\ \dfrac{3}{\sqrt{20-10x}} \\ \dfrac{3}{\sqrt{20-10x}} \end{pmatrix} . \tag{22}$$

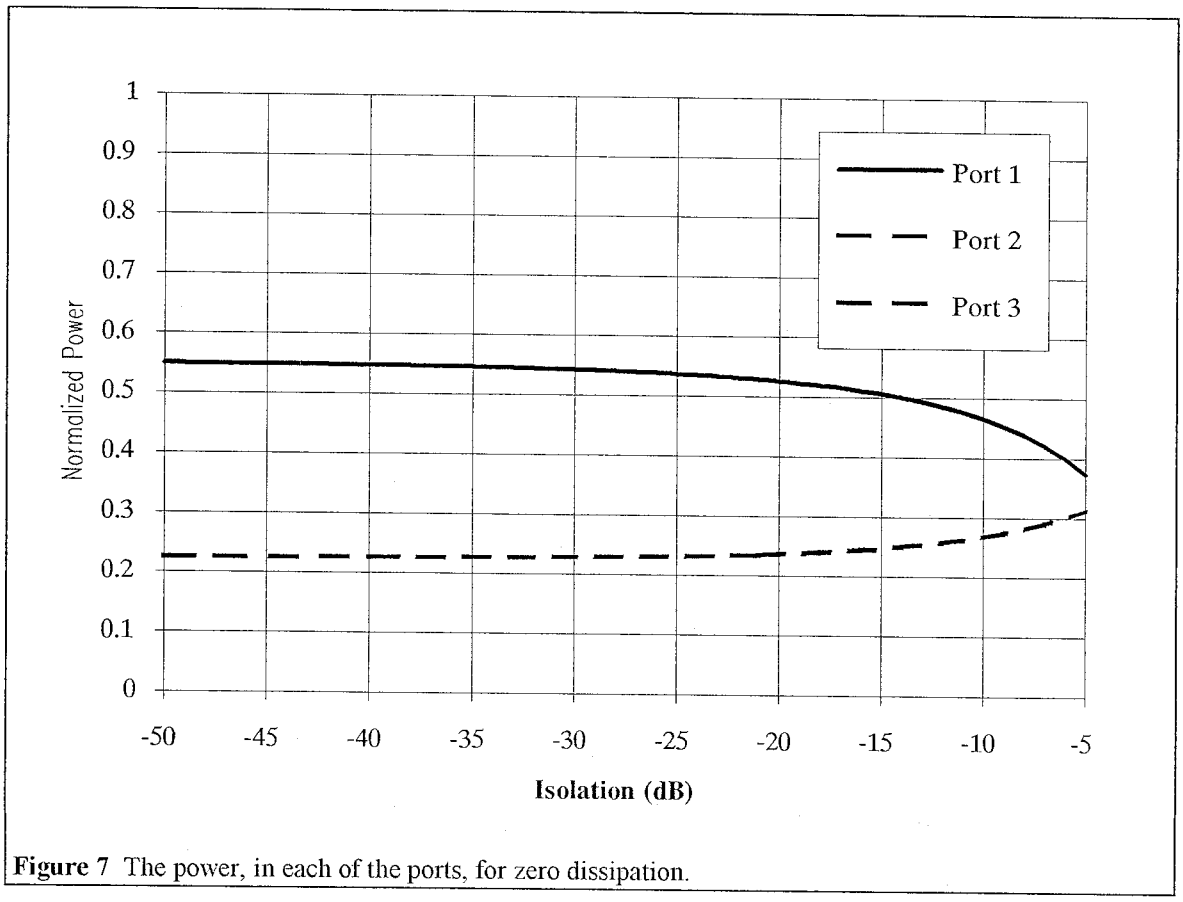

Figure 7 The power, in each of the ports, for zero dissipation.

Figure 7 is a plot of the power in each of the three components of the unit-power, zero-dissipation eigenvector (equation (22)) versus the isolation.

Case 3. 2:3 coupler w/ phases from a measured Wilkinson type coupler.

To relax the constraint that all the elements of the S-matrix are in phase, the measured phases of all the S-matrix components of an actual 2:3 Wilkinson power divider, centered at 30 GHz, are used. The assumed S-matrix is

$$\mathbf{S}=\begin{bmatrix} 0.1\angle -17 & \alpha\sqrt{\frac{3}{5}}\angle -55 & \alpha\sqrt{\frac{2}{5}}\angle -55 \\ \alpha\sqrt{\frac{3}{5}}\angle -55 & 0.1\angle -117 & x\angle -6 \\ \alpha\sqrt{\frac{2}{5}}\angle -55 & x\angle -6 & 0.1\angle -83 \end{bmatrix}$$

with the usual definitions of x and α. The results of the analysis are shown in figure 8, below

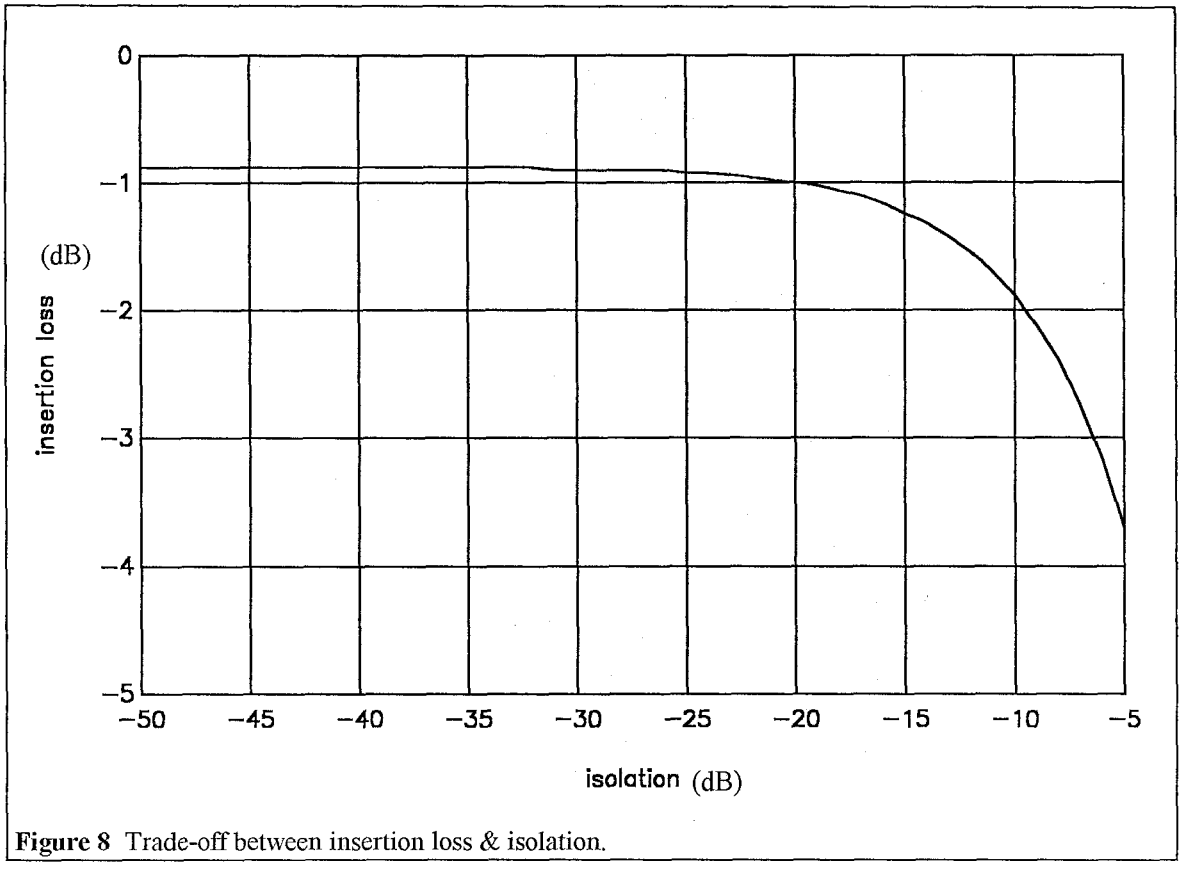

Figure 8 Trade-off between insertion loss & isolation.

The minimum insertion loss at 18 dB isolation is 1.1 dB. The minimum as isolation tends to infinity is 0.88 dB. The above results are not sensitive to "adding line lengths at the input and output ports."

The equation of the zero-eigenvalue locus of points plotted for this sub-case is

$$\alpha = \frac{\sqrt{9.99\cdot 10^4 - 813x - 1.00\cdot 10^5 x^2 - 513x^3 - \sqrt{\begin{matrix}3.73\cdot 10^8 - 1.47\cdot 10^8 x + 8.56\cdot 10^9 x^2 + 2.95\cdot 10^7 x^3 \\ -1.84\cdot 10^{10} x^4 + 1.20\cdot 10^8 x^5 + 9.50\cdot 10^9 x^6\end{matrix}}}}{\sqrt{99080 - 164.1x - 96000x^2}} \quad . \tag{23}$$

The algebraic expression for the zero-dissipation eigenvector is too complicated and is therefore not included. Figure 9 is a plot of the power in each of the three components of the unit-power, zero-dissipation eigenvector versus the isolation.

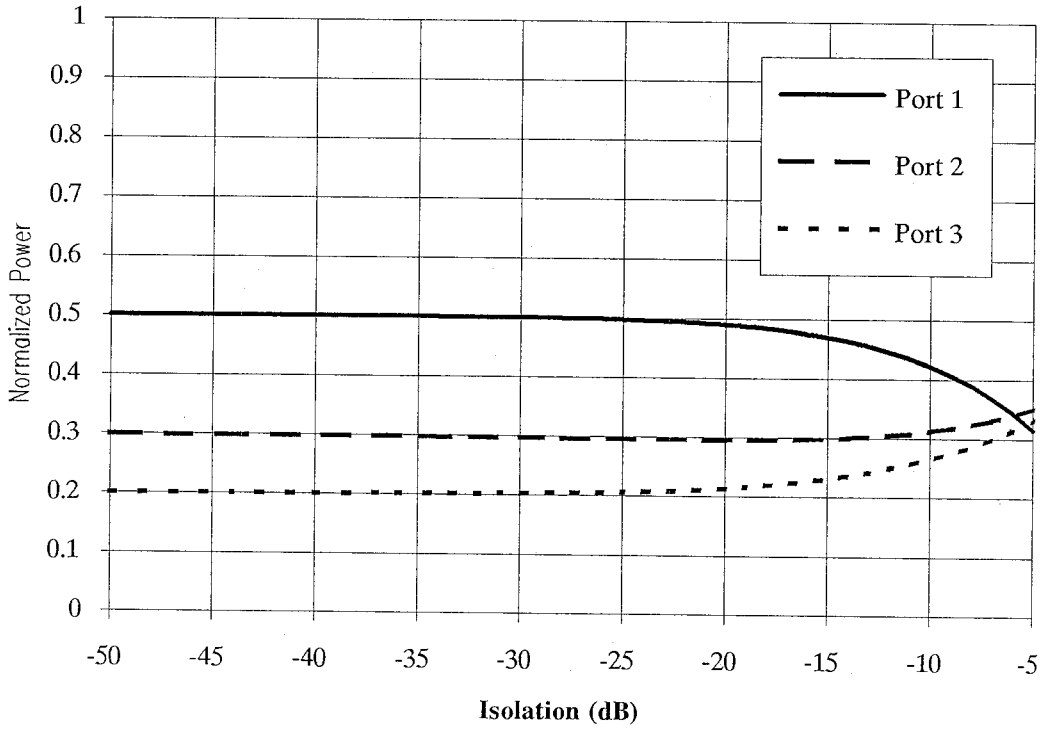

Figure 9 The power, in each of the ports, for zero dissipation.

2.4 Conclusions

This chapter has attempted to show that there exist more fundamental considerations than just dielectric loss tangent and conductivity of metallization limiting the performance of passive multi-port networks. The example of 3-port couplers was used. In cases where bounds or restrictions can be set on certain parameters as a result of considerations independent of ohmic losses, there are frequently additional restrictions on the performance of the network, imposed by passivity, that need to be considered. In the example above, insertion losses are imposed on matched 3-ports by passivity requirements and there is nothing that can be done about them. If they are unbearable to the design engineer, then other alternatives have to be considered. In particular the above results also show that a matched divider without isolation is very lossy (see figs. 2-4 @ 5 dB

isolation). The contra-positive of the above statement is that if a divider without isolation has low insertion loss, it cannot have low return loss on all ports.

Appendix A

Sample Matlab File

```
clear;
clg;
i=1;
S(1,1)=0;
S(2,2)=0;
S(3,3)=0;
for x=-50:1:-5
        for alpha=-5:0.02:0
        alpha_mag=10^(alpha/20);
        S(2,1)=alpha_mag/sqrt(2);
        S(3,1)=alpha_mag/sqrt(2);
        S(1,2)=S(2,1);
        S(1,3)=S(3,1);
        x_mag=10^(x/20);
        S(2,3)=x_mag;
        S(3,2)=S(2,3);
        Q=eye(3)-S'*S;
        l=eig(Q);
        if l(1) <=0 | l(2) <=0 | l(3) <=0
                g(i,1)=x;
                g(i,2)=alpha;
                break;
        end;
        end;
i=i+1;
end;
g
axis([-50 -5 -5 0]);
plot(g(:,1),g(:,2));
xlabel('isolation');
ylabel('insertion loss');
grid;
```

CHAPTER 3

LOW FIELD MODELING OF QUASI-TRANSVERSE ELECTRIC AND MAGNETIC (TEM) HTS MICROWAVE TRANSMISSION LINES

3.1 Introduction

Most commonly used types of microwave transmission line are of the TEM or quasi-TEM type. Examples are microstrip, stripline, coplanar waveguide (CPW), slotline and microshield. For all the above examples of transmission lines, the fundamental (lowest order) propagating electromagnetic mode has small field components along the direction of propagation of the wave. Two advantages of TEM modes are that they have good dispersion characteristics (i.e., they are suitable for distortionless broadband transmission) and they have no low frequency cut-off. This chapter presents a phenomenological mathematical model which permits effective modeling of HTS transmission lines using CAD tools designed for non-HTS circuits.

In usual microwave circuits the transmission line conductor thickness is large compared to the skin depth (or depth of penetration of the fields into the conductor) As an example, a common metallization thickness is 17.8 μm (0.0007 inches or 0.7 mils) and the skin depth of copper at 10 GHz is 0.66 μm. In this limit the surface resistance of the transmission line is proportional to the square root of frequency, a simple explicit function of frequency [1]. In a similar limit in HTS transmission lines, surface impedance is proportional to the square of frequency, again a simple explicit function of frequency, as will be shown in section 3.3. Unfortunately, typical film thicknesses of HTS circuits (e.g., 500 nm) are,

because of manufacturing process limitations, of the order of the penetration depth of the fields into the superconductor at cryogenic temperatures (e.g., for Yttrium Barium Copper Oxide (YBCO) with zero temperature penetration depth, λ_o, of 140 nm and critical temperature, T_c, of 85 K the penetration depth at 77 K, $\lambda(77)$, is 429 nm). In this case the range of integration of the integral in section 3.3 cannot cover the whole semi-plane and the dependence of surface resistance on frequency deviates from the square law and becomes more involved. The response of this typical type of HTS transmission line is addressed in section 3.4.

3.2 The Two-Fluid Model of a Superconductor

A simple, yet powerful and commonly used model of a superconductor is presented in this section. It is fundamental to an understanding of the rest of this thesis and will therefore be presented fully. In this model the superconductor is visualized as two fluids made up of two kinds of charge carriers. One fluid consists of the "normal" electrons, which will be denoted by the subscript *n*, and are the electrons found in a normal conductor. They are responsible for scattering and therefore for Ohmic losses. The second fluid consists of the "superconducting" electrons, which will be denoted by the subscript *s*, and are the lossless carriers responsible for superconductivity. They do not scatter but are accelerated by the electric field in the same way as normal electrons. The purpose of this section is to arrive at an expression for the conductivity of a two-fluid modeled superconductor.

Newton's law applied to the accelerating superelectrons due to the electric field **E** gives

$$m\frac{d\mathbf{v}_s}{dt} = -e\mathbf{E} \qquad (1)$$

where m is the mass of the super-electrons, e is the magnitude of their electric charge, $\boldsymbol{E}$ is the applied electric field, v_s is the velocity of the super-electrons and t is time.

The same law applied to the normal electrons can only be applied in an average sense,

(denoted by the <>), because of the randomly varying velocity of the electrons due to collisions, and has to include a "damping" term due to scattering:

$$m\frac{d<\mathbf{v}_n>}{dt}+m\frac{<\mathbf{v}_n>}{\tau}=-e\mathbf{E} \quad . \tag{2}$$

Here τ is the characteristic time between collisions.

Assuming a steady-state sinusoidal excitation, of the form $e^{j\omega t}$, where ω is the angular frequency of the excitation, the above equations become

$$jm\omega\mathbf{v}_s=-e\mathbf{E} \tag{3}$$

$$jm\omega<\mathbf{v}_n>+m\frac{<\mathbf{v}_n>}{\tau}=-e\mathbf{E} \quad . \tag{4}$$

By the definition of current density we have

$$\mathbf{J}_s=-n_s e\mathbf{v}_s \tag{5}$$

$$\mathbf{J}_n=-n_n e<\mathbf{v}_n> \tag{6}$$

where J is current density and n is carrier density (i.e., number per unit volume). Although superconducting electrons are paired (in Cooper pairs [2]), here we count two electrons per pair, i.e., we still consider the electron, and not the pair, to be the superconducting carrier.

The total current is, therefore, given by the sum of the super-current and the normal current, as calculated using equations (3), (5) and (4), (6) respectively.

$$\mathbf{J}=\mathbf{J}_n+\mathbf{J}_s=e\left(\frac{n_s e}{jm\omega}-\frac{n_n e}{m(j\omega+\tau^{-1})}\right)\mathbf{E} \quad . \tag{7}$$

Hence, the conductivity, which is by definition the ratio of current density to electric field, is given by

$$\sigma=\frac{\mathbf{J}}{\mathbf{E}}=\frac{n_n e^2\tau}{m(1+\omega^2\tau^2)}-j\frac{e^2}{m\omega}\left(n_s+\frac{\omega^2\tau^2}{(1+\omega^2\tau^2)}n_n\right) \tag{8}$$

where (7) was factored into its real and imaginary parts.

The collision characteristic time constant, τ, is of the order of 10^{-14} seconds so for frequencies below 100 GHz we have $(\omega\tau)^2 << 1$. Also, within the scope of the two-fluid model it will never be $n_s << n_n$ (although we may approach this condition in chapter 7). Hence, (8) may be simplified as

$$\sigma = \sigma_1 - j\sigma_2 = \frac{e^2 \tau n_n}{m} - j\frac{n_s e^2}{m\omega} \quad . \tag{9}$$

The normal bulk conductivity of a material is given by

$$\sigma_n = \frac{ne^2\tau}{m} \quad . \tag{10}$$

Hence, with the help of (10), we can rewrite the real part of (9) as

$$\sigma_1 = \sigma_n \frac{n_n}{n} \quad . \tag{11}$$

Here n is the total carrier density, so $n = n_s + n_n$. Experimentally, we know that [2]

$$\frac{n_n}{n} = \left(\frac{T}{T_c}\right)^4 \tag{12}$$

where "T" is the temperature and "T_C" is the critical temperature of the superconductor, i.e., that temperature above which superconducting phenomena disappear. Hence (11) can be expressed as

$$\sigma_1 = \sigma_n \left(\frac{T}{T_c}\right)^4 \quad . \tag{13}$$

The real part of the conductivity, σ_1, has now been expressed in "readily measurable" explicit physical parameters. In order to do the same for the imaginary part, σ_2, we need to do a little more work.

The starting point is London's first equation for superconductors [3].

$$\nabla \times \mathbf{J}_s = -\frac{1}{\mu_0 \lambda^2}\mathbf{B} \tag{14}$$

where

$$\lambda = \sqrt{\frac{m}{\mu_0 n_s e^2}} \tag{15}$$

and μ_o is the magnetic permeability of vacuum. Equation (15) may be used to substitute some of the parameters of the imaginary part of (9) that do not correspond to explicit physical parameters, provided λ itself has an intuitive physical interpretation. To show this we need Maxwell's curl B equation, assuming displacement and normal currents negligible.

$$\nabla \times \mathbf{B} = \mu_0 \mathbf{J}_s \ . \tag{16}$$

Taking the curl of (14) and using the vector identity $\nabla \times \nabla \times \mathbf{B} = \nabla(\nabla \cdot \mathbf{B}) - \nabla^2 \mathbf{B}$ and Maxwell's equation $\nabla \cdot \mathbf{B} = 0$ we obtain

$$-\nabla^2 \mathbf{B} = \mu_0 \nabla \times \mathbf{J} \ . \tag{17}$$

Substituting (14) into (17) gives

$$\nabla^2 \mathbf{B} = \mu_0 \left(\frac{1}{\mu_0 \lambda^2}\mathbf{B} \right) = \frac{1}{\lambda^2}\mathbf{B} \ . \tag{18}$$

Assuming a one-dimensional coordinate system where, say, $\nabla^2 \rightarrow \frac{d^2}{dz^2}$, the classic solutions to this second-degree equation are of the form $e^{\pm\frac{z}{\lambda}}$. Assuming $z > 0$, the solution corresponding to the plus sign does not make physical sense, and the solution corresponding to the minus sign describes an exponentially attenuating wave that attenuates to 1/e of its original value at depth λ. λ is called the penetration depth of a superconductor. It is a function of temperature, but not of field strength or frequency. It is important to distinguish between this penetration depth, which is a DC phenomenon and

persists even when $\omega = 0$, and the skin depth of a normal conductor. The skin depth of a superconductor, associated with AC fields, will be derived in the next section. Substituting now (15) into (9) we get

$$\sigma_2 = \frac{1}{\omega\mu_0\lambda^2} = \frac{1}{2\pi f\mu_0\lambda^2} \quad . \tag{19}$$

Experimentally, it has been shown [3] that λ has the following temperature dependence

$$\lambda(T) = \frac{\lambda_0}{\sqrt{1-\left(\frac{T}{T_c}\right)^4}} \tag{20}$$

where λ_0 is the zero temperature penetration depth. Finally substituting (20), (19) and (13) into (9) we have the sought after expression for the conductivity of a superconductor

$$\sigma = \sigma_n\left(\frac{T}{T_c}\right)^4 - j\frac{1-\left(\frac{T}{T_c}\right)^4}{2\pi f\mu_0\lambda_0^{\,2}} \tag{21}$$

which is only valid when $T < T_c$. (21) has to be qualified before being used. The model and theory used to derive it are linear, local and low field theories [3]. The validity of the expression should, therefore, not be pushed beyond these limits when accuracy is required, although, as will be shown in chapter 7, (21) can be stretched into these limits with some partial success.

To better understand what the significance of the complex conductivity postulated by (21) is, we take a look at Poynting's equation [1].

$$\nabla\cdot(\mathbf{e}\times\mathbf{h}) = -\frac{\partial}{\partial t}\left(\frac{\varepsilon}{2}|\mathbf{e}|^2\right) - \frac{\partial}{\partial t}\left(\frac{\mu}{2}|\mathbf{b}|^2\right) - \mathbf{e}\cdot\mathbf{j} \quad . \tag{22}$$

Here I have used lower case letters to represent real quantities (as opposed to phasors), with the usual field notation. The last term represents the power density converted to heat. When we switch to phasor quantities we can time average the quantity $\mathbf{e}\cdot\mathbf{j}$ by taking

$\frac{1}{2}\mathrm{Re}(\mathbf{E}\cdot\mathbf{J}^*)$. Hence, the average power density lost to heat becomes

$$\frac{1}{2}\mathrm{Re}\left[\mathbf{E}\cdot(\sigma_1 - j\sigma_2)^*\mathbf{E}^*\right] = \frac{1}{2}\sigma_1|\mathbf{E}|^2 \quad . \tag{23}$$

Hence, the smaller σ_1, the less power is dissipated into heat. For a given magnitude of conductivity, $|\sigma| = \sqrt{\sigma_1^2 + \sigma_2^2}$, the closer the phase to $-\frac{\pi}{2}$, the closer to lossless the circuit is. Examination of equation (21) reveals that a lossy transmission line has the dependencies listed in table 1. Equation (21) will be used in the next section to derive a result for the surface resistance of a bulk superconductor.

When this variable **increases**...	The circuit losses...
σ_n	Increase
T	Increase
T_c	Decrease
f	Increase
λ_0	Increase

Table 1 Dependencies of losses on physical variables.

3.3 Surface Impedance of a Bulk Superconductor

Let us consider a HTS material filling the half-space $z > 0$. Let a uniform x-directed current flow in the material, with the current density at the surface being J_0. Then the equation governing the distribution of J into the superconductor is [4]

$$\frac{\partial^2 J_x}{\partial z^2} = j\omega\mu\sigma J_x \tag{24}$$

The (bounded) solution to this equation is

$$J_x = J_{0x}e^{-\zeta z} \tag{25}$$

where

$$\zeta = \sqrt{j\omega\mu_0\sigma} = (1+j)\sqrt{\pi f\mu_0\sigma} \quad . \tag{26}$$

Substituting (9) into (26), after some algebraic manipulations we get

$$\zeta = \sqrt{\mu_0 \frac{e^2}{m}\left(n_s + j(\omega\tau)n_n\right)} = \sqrt{\mu_0 \frac{e^2}{m} n_s\left(1 + j\frac{(\omega\tau)n_n}{n_s}\right)} = \frac{1}{\lambda}\left(1 + j\frac{(\omega\tau)n_n}{2n_s} + \ldots\right) \tag{27}$$

where the rest of the terms of the Taylor expansion can be neglected since $(\omega\tau)^2 << 1$.

After algebraic manipulations and substitutions from (10), (11), (12) and (15) we get

$$\zeta = \frac{1}{\lambda} + j\frac{1}{2}\omega\mu_0\sigma_n\left(\frac{T}{T_c}\right)^4 \quad . \tag{28}$$

Inspection of (28) reveals that the skin depth of the superconductor is equal to the penetration depth, and is independent of frequency.

To find the surface impedance we need to integrate the current density in (25) from zero to infinity to find the total current per unit width, J_w, flowing in the region $z > 0$.

$$J_{wx} = \int_0^\infty J_{0x} e^{-\zeta z} dz = -\frac{J_{0x}}{\zeta} e^{-\zeta z}\Big|_0^\infty = \frac{J_{0x}}{\zeta} \quad . \tag{29}$$

But, by the definition of conductivity we have $J_{0x} = \sigma E_{0x}$, therefore

$$J_{wx} = \frac{\sigma E_{0x}}{\zeta} = \sqrt{\frac{\sigma}{j\omega\mu_0}} E_{0x} \tag{30}$$

and by the definition of surface impedance

$$Z_s = \frac{E_{0x}}{J_{wx}} = \sqrt{\frac{j\omega\mu_0}{\sigma}} = \sqrt{\frac{j\omega\mu_0}{\frac{e^2}{m\omega}\left(n_n\omega\tau - jn_s\right)}} = \sqrt{\frac{j\omega\mu}{-jn_s\frac{e^2}{m\omega}\left(1 + j\frac{n_n}{n_s}\omega\tau\right)}} \quad \therefore$$

$$Z_s = j\omega\mu_0\lambda\left(1 - j\frac{n_n}{2n_s}\omega\tau\right) = \frac{1}{2}\mu_0{}^2\omega^2\lambda^3\sigma_n\left(\frac{T}{T_c}\right)^4 + j\omega\mu_0\lambda \equiv R_s + j\omega L_s \qquad (31)$$

where a Taylor expansion has again been used and quadratic and higher terms discarded. As promised, the surface resistance is proportional to the square of the frequency. The surface inductance is proportional to the penetration depth.

Equation (31) holds true when two limits are satisfied. The first is obvious from the above analysis (equation (29)), and is that the thickness of the HTS film must be infinite. Effectively what this means is that, if d is the HTS film thickness, the ratio d/λ must be large (for example if d/λ=2, R_S is underestimated by 15.9% and L_S is underestimated by 3.7%). The second assumption that must hold is that the HTS film must lie on a semi-infinite dielectric material. If this is not the case, the presence of a ground plane (in the case of a two conductor quasi-TEM transmission line) on the bottom of the dielectric slab changes the effective surface impedance further [5], and leads to complicated expressions that are impractical for design use.

The next section presents a phenomenological loss equivalence model that solves this problem and can be used with any microwave CAD program.

3.4 A Phenomenological Loss Equivalence Model for Quasi-TEM HTS Microwave Transmission Lines

Due to the similarity between a normal conductor and a superconductor the lossless S-parameters of two identical circuits, one made with a "perfect" conductor, i.e., one that exhibits zero surface impedance, and the other with a superconductor, are analogous. This means that one may start to model an HTS transmission line and calculate its electrical length and impedance from its geometrical dimensions using the standard

formulas for perfect conductors [6]. This analogy breaks down because there are losses, resulting from the non-zero surface resistance of equation (31), which must be included in the calculation of the microwave S-parameters of the transmission line. Because the importance of HTS transmission lines lies in reducing losses relative to normal conductors, this is a very important difference. The surface resistance of a regular conductor is proportional to the square root of the frequency [1]. However, the surface resistance of a superconductor, according to equation (31), is proportional to the square of the frequency. The superconductor may be modeled as a "normal" conductor with a complex conductivity. The real and imaginary parts of the conductivity are the result of the normal electrons and superconducting electron pairs (Cooper pairs) respectively, as posed in the two-fluid theory. For convenience I reproduce here equation (21) for the complex conductivity.

$$\sigma = \sigma_n \left(\frac{T}{T_c}\right)^4 - j\frac{1-\left(\frac{T}{T_c}\right)^4}{2\pi f \mu_0 \lambda_0^{\,2}} \tag{21}$$

where σ_n is the normal part of the conductivity, T is the absolute temperature, T_c is the critical temperature of the superconductor, f is the frequency, μ_0 is the magnetic permeability of vacuum and λ_0 is the zero-temperature penetration depth of the magnetic and electric fields into the superconductor. Using this conductance one may use Lee & Itoh's phenomenological loss equivalence (PEM) method to calculate the additional distributed internal impedance Z_i, in Ohms/meter, due to the penetration of the fields into the superconductor and the related surface impedance [7] as follows.

$$Z_i = Z_s G \coth(\zeta G A) \tag{32}$$

where

$$\zeta = \sqrt{j\omega\mu_0\sigma} = (1+j)\sqrt{\pi f \mu_0 \sigma} \tag{26}$$

is the complex propagation constant of an electromagnetic wave propagating in a bulk superconductor (see above discussion in section 3.3),

$$Z_s = \sqrt{j\frac{2\pi f\mu_0}{\sigma}} \tag{33}$$

is the complex surface impedance of an electromagnetic wave propagating in a bulk superconductor (see equation (31) above), G is the incremental inductance geometric factor, i.e., the partial derivative of the inductance of the line with respect to the receding walls of the line and A is the cross-sectional area of the line under characterization. The exponential attenuation coefficient follows directly from the above, as [1]

$$\alpha_c = \frac{\mathrm{Re}(Z_i)}{2Z_0'} \tag{34}$$

in Nepers/meter, where Z_0' is the impedance corrected using Z_i.

This series of calculations is easy to perform numerically, with any mathematical CAD program for every different set of values of the parameters, but gives no insight into how each individual parameter affects the attenuation. Moreover they are impossible to enter into most popular microwave CAD software packages, which cannot handle complex algebra, for circuit design and optimization. The equations were, therefore, reduced algebraically to obtain the following explicit formulae for the additional distributed internal resistance R_i and reactance X_i.

$$R_i = \mathrm{Re}(Z_i) = \frac{B}{A|\sigma|\psi}\left[\cos\left(\frac{\pi}{4}+\frac{\phi}{2}-\chi\right)+e^{2B\cos\theta}\cos\left(2B\sin\theta+\frac{\pi}{4}+\frac{\phi}{2}-\chi\right)\right] \tag{35}$$

and

$$X_i = \mathrm{Im}(Z_i) = \frac{B}{A|\sigma|\psi}\left[\sin\left(\frac{\pi}{4}+\frac{\phi}{2}-\chi\right)+e^{2B\cos\theta}\sin\left(2B\sin\theta+\frac{\pi}{4}+\frac{\phi}{2}-\chi\right)\right] \tag{36}$$

where

$|\sigma| = \sqrt{\sigma_1^2 + \sigma_2^2}$ is the magnitude of the conductivity, $\phi = \arctan\left(\frac{\sigma_2}{\sigma_1}\right)$ is the phase of the conjugate of the conductivity,

$$\theta = \frac{5\pi}{4} - \frac{\phi}{2}$$

$$B = GA\sqrt{2\pi f \mu_0 |\sigma|}$$

$$\psi = \sqrt{\left[e^{2B\cos\theta}\cos(2B\sin\theta) - 1\right]^2 + \left[e^{2B\cos\theta}\sin(2B\sin\theta)\right]^2}$$

and

$$\chi = \arctan\left[\frac{e^{2B\cos\theta}\sin(2B\sin\theta)}{e^{2B\cos\theta}\cos(2B\sin\theta) - 1}\right].$$

To calculate Z_0', the corrected characteristic impedance of the transmission line, we proceed as follows. Let L' be the corrected distributed inductance of the transmission line. Then

$$Z_0' = \sqrt{\frac{L'}{C}}\ , \tag{37}$$

where C is the distributed capacitance of the transmission line, which remains unaffected by the field penetration into the superconductor. But,

$$L' = L + L_i = L + \frac{X_i}{2\pi f}\ , \tag{38}$$

where L is the distributed inductance of the transmission line, as calculated assuming a perfect conductor, before applying the PEM. Now, to calculate L we need to express them as

$$L = \sqrt{\frac{L}{C}}\sqrt{LC} = \frac{Z_0}{v_{ph}} = \frac{Z_0\sqrt{\varepsilon_{eff}}}{c} \tag{39}$$

and

$$C = \sqrt{\frac{C}{L}}\sqrt{LC} = \frac{1}{Z_0 v_{ph}} = \frac{\sqrt{\varepsilon_{eff}}}{Z_0 c} \quad , \tag{40}$$

where Z_O is the characteristic impedance of the perfect conductor transmission line, ε_{eff} is the effective relative dielectric constant of the perfect conductor transmission line and c is the velocity of light.

Substituting (38), (39) and (40) into (37) gives

$$Z_0' = Z_0\sqrt{1+\frac{c}{2\pi\sqrt{\varepsilon_{eff}}f}\frac{X_i}{Z_0}} \quad . \tag{41}$$

Likewise, using (38), (39) and (40), the corrected phase velocity may be calculated as

$$v_{ph}' = \frac{1}{\sqrt{L'C}} = \frac{c}{\sqrt{\varepsilon_{eff}}}\frac{1}{\sqrt{1+\frac{c}{2\pi\sqrt{\varepsilon_{eff}}f}\frac{X_i}{Z_0}}} \tag{42}$$

and the corrected effective relative dielectric constant as

$$\varepsilon_{eff}' = \left(\frac{c}{v_{ph}}\right)^2 = \varepsilon_{eff}\left(1+\frac{c}{2\pi\sqrt{\varepsilon_{eff}}f}\frac{X_i}{Z_0}\right) \quad . \tag{43}$$

From (42) the corrected propagation constant may be calculated as

$$\beta' = \frac{\omega}{v_{ph}'} = \frac{2\pi f\sqrt{\varepsilon_{eff}}}{c}\sqrt{1+\frac{c}{2\pi\sqrt{\varepsilon_{eff}}f}\frac{X_i}{Z_0}} = \beta\sqrt{1+\frac{c}{2\pi\sqrt{\varepsilon_{eff}}f}\frac{X_i}{Z_0}} \quad . \tag{44}$$

It is important to note that equations (34), (41), (42), (43) and (44) are only approximate equations that work well only when R_i is small relative to ωL. This is true of most HTS transmission lines in their low-power linear region. However, examples of some cases in which this condition may be violated are if $T \approx T_c$ or if, say due to high transfer currents, $\frac{n_n}{n} \approx 1$, or if the HTS film is so thin that $0 < \frac{d}{\lambda} << 1$. In such cases, it is worth using the more exact relations for TEM lines which will be presented in chapter 7.

The next chapter presents an experimental verification of the model presented in this

section.

3.5 Algebraic Verification of Equations (35) and (36)

Equations (35) and (36) are the key equations from which the loss and phase parameters of the transmission lines are calculated. They are derived from (26), (32) and (33) after algebraic manipulation. Of pivotal interest here is the proper choice of the phase plane of the square root of σ in (26) and (33), since equations (26) and (32) have a branch-cut that extends from zero to infinity on the σ-complex plane. To assure that this is properly done MathCAD is used. A test additional internal impedance calculation for three different line widths is performed using the MathCAD worksheet included in appendix A of this chapter. The chosen line widths, taken from the filter of chapter 5, are 6, 50 and 200 microns, with corresponding incremental inductance factors of 125500, 23500, 17340 and parameter values

$$T = 77\,K, \quad T_c = 85\,K, \quad f = 5\,GHz, \quad \lambda_o = 400\,nm, \quad \sigma_n = 1.6 \cdot 10^6\,S/m, \qquad (45)$$

where T is the absolute temperature, T_c is the critical temperature of the HTS line, f is the frequency, λ_o is the zero-temperature penetration depth and σ_n is the normal conductivity of the HTS line. The additional distributed internal resistance, R_i and reactance, X_i, are computed twice, for the same above parameters, once using (35) and (36) and again using the real and imaginary parts of (32). The results are identical, as shown in figure 1 and in appendix A of this chapter. This is a numerical verification of the algebraic manipulations leading to equations (35) and (36).

$\mathrm{Re}[Z_i]$	R_i	$\mathrm{Im}[Z_i]$	X_i
134.539	134.539	$7.055 \cdot 10^3$	$7.055 \cdot 10^3$
16.273	16.273	947.013	947.013
5.416	5.416	485.865	485.865

Figure 1 Identical results of equations (35), (36) and (32).

3.6 References

[1] S. Ramo, J. R. Whinnery and T. Van Duzer, *Fields and Waves in Communication Electronics*, Wiley, New York, 1965.

[2] T. Van Duzer and C. W. Turner, *Principles of Superconductive Devices and Circuits*, Elsevier, New York, 1981.

[3] A. C. Rose-Innes and E. H. Roderick, *Introduction to Superconductivity*, Pergamon, Oxford, 1969.

[4] S. E. Schwarz, *Electromagnetics for Engineers*, Saunders, Philadelphia, 1990.

[5] P. Hartemann, "Effective and Intrinsic Surface Impedances of High-Tc Superconducting Thin Films," IEEE Transactions on Applied Superconductivity, Vol. 2, pp. 228-235, December 1992.

[6] K. Gupta, R. Garg and I. Bahl, *Microstrip Lines and Slotlines*, Artech, Dedham, MA, 1979.

[7] H. Lee and T. Itoh, "Phenomenological Loss Equivalence Method for Planar Quasi-TEM Transmission Lines with a Thin Normal Conductor or Superconductor," IEEE Transactions on Microwave Theory and Techniques, Vol. 37, pp. 1904-1909, December 1989.

Appendix A

MathCAD File that Algebraically Verifies Equations (35) and (36)

$i := 1, 2 .. 3$

$w_i :=$

$6 \cdot 10^{-6}$
$50 \cdot 10^{-6}$
$200 \cdot 10^{-6}$

$t := 0.5 \cdot 10^{-6}$

$\mu_o := 4 \cdot \pi \cdot 10^{-7}$

$\varepsilon_o := 8.854 \cdot 10^{-12}$

$\eta_o := \sqrt{\frac{\mu_o}{\varepsilon_o}}$ $\eta_o = 376.734$

$c := \frac{1}{\sqrt{\mu_o \cdot \varepsilon_o}}$ $c = 2.998 \cdot 10^{8}$

$\lambda_o := 400 \cdot 10^{-9}$

$T := 77$

$T_c := 85$

$f := 5 \cdot 10^{9}$

$\sigma_v := 1.6 \cdot 10^{6}$

$$\sigma := \sigma_v \cdot \left[\frac{T}{T_c}\right]^4 - j \cdot \frac{1 - \left[\frac{T}{T_c}\right]^4}{2 \cdot \pi \cdot f \cdot \mu_o \cdot {\lambda_o}^2}$$

$\sigma = 1.077 \cdot 10^{6} - 5.17 \cdot 10^{7}\, i$

$G_i :=$

125500
23500
17340

$$Z_s := \sqrt{j \cdot 2 \cdot \pi \cdot f \cdot \frac{\mu_o}{\sigma}}$$

$$A_i := w_i \cdot t$$

$$\zeta := (1 + j) \cdot \sqrt{\pi \cdot f \cdot \mu_0 \cdot \sigma}$$

$$Z_{i_i} := Z_s \cdot G_i \cdot \coth\left[\zeta \cdot G_i \cdot A_i\right]$$

$$B_i := G_i \cdot A_i \cdot \sqrt{2 \cdot \pi \cdot f \cdot \mu_0 \cdot |\sigma|}$$

$$\phi := -\arg\left[\sigma\right]$$

$$\theta := \frac{5 \cdot \pi}{4} - \frac{\phi}{2}$$

$$\psi_i := \sqrt{\left[\exp\left[2 \cdot B_i \cdot \cos\left[\theta\right]\right] \cdot \cos\left[2 \cdot B_i \cdot \sin\left[\theta\right]\right] - 1\right]^2 + \exp\left[4 \cdot B_i \cdot \cos\left[\theta\right]\right] \cdot \sin\left[2 \cdot B_i \cdot \sin\left[\theta\right]\right]^2}$$

$$\chi_i := \operatorname{atan}\left[\frac{\exp\left[2 \cdot B_i \cdot \cos\left[\theta\right]\right] \cdot \sin\left[2 \cdot B_i \cdot \sin\left[\theta\right]\right]}{\exp\left[2 \cdot B_i \cdot \cos\left[\theta\right]\right] \cdot \cos\left[2 \cdot B_i \cdot \sin\left[\theta\right]\right] - 1}\right]$$

$$R_i := \frac{B_i}{A_i \cdot |\sigma| \cdot \psi_i} \cdot \left[\cos\left[\frac{\pi}{4} + \frac{\phi}{2} - \chi_i\right] + \exp\left[2 \cdot B_i \cdot \cos\left[\theta\right]\right] \cdot \cos\left[2 \cdot B_i \cdot \sin\left[\theta\right] + \frac{\pi}{4} + \frac{\phi}{2} - \chi_i\right]\right]$$

$$X_i := \frac{B_i}{A_i \cdot |\sigma| \cdot \psi_i} \cdot \left[\sin\left[\frac{\pi}{4} + \frac{\phi}{2} - \chi_i\right] + \exp\left[2 \cdot B_i \cdot \cos\left[\theta\right]\right] \cdot \sin\left[2 \cdot B_i \cdot \sin\left[\theta\right] + \frac{\pi}{4} + \frac{\phi}{2} - \chi_i\right]\right]$$

$\mathrm{Re}\left[Z_{i_i}\right]$
134.539
16.273
5.416

R_i
134.539
16.273
5.416

$\mathrm{Im}\left[Z_{i_i}\right]$
$7.055 \cdot 10^3$
947.013
485.865

X_i
$7.055 \cdot 10^3$
947.013
485.865

CHAPTER 4

VALIDATION AND APPLICATION OF THE PEM LOSS MODEL: AN HTS MICROSTRIP RING RESONATOR

4.1 Introduction

In this chapter the PEM loss model presented in the previous chapter is applied to an HTS microstrip ring resonator. A resonator is chosen because it is a simple structure, whose electrical behavior depends on a minimum number of physical parameters, yet yields a large amount of information.

4.2 The YBCO Microstrip Ring Resonator

The layout of the YBCO microstrip ring resonator is shown in figure 1 below. The dimensions are in millimeters (mm). It is purchased from Conductus Inc. at a very discounted "student" price, for which the author is grateful.

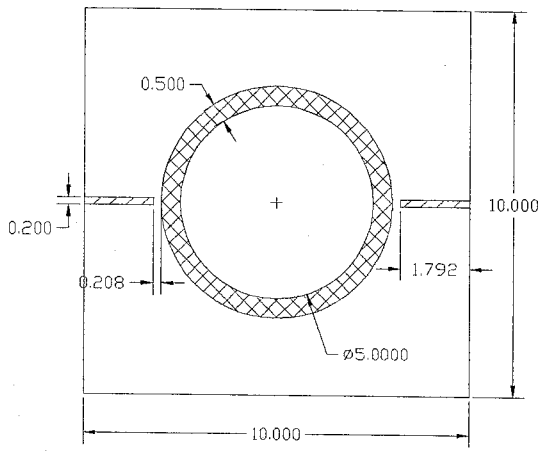

Figure 1 The layout of the YBCO microstrip ring resonator.

It consists of a YBCO microstrip ring, of 5 mm inner and 6 mm outer diameter (cross-hatched in figure 1) and an input and output gold microstrip straight-line section of length 1.792 mm (single hatched in figure 1). The substrate is lanthanum aluminate and measures 10x10x0.508 mm. The input and output lines are electromagnetically coupled to the ring via a 0.208 mm gap.

The characteristic impedance of the ring is 32 Ω and that of the input and output line sections is 47 Ω. The S-parameters of the circuit are measured using a Hewlett-Packard HP 8510 C Network Analyzer with the circuit dunked in liquid nitrogen (77 K).

4.3 The Model

4.3.1 The Modeling Methodology

The physical parameters of the resonator circuit, listed in table 1, are supplied by Conductus. These are the thickness and relative dielectric constant of the substrate, and the thickness and critical temperature of the YBCO film. These are used in conjunction with the various transmission line dimensions (i.e., width, w) to arrive at the electromagnetic parameters of each type of line used in the circuit.

Parameter	Value
Substrate Thickness	0.508 mm
Substrate Dielectric Constant	24
YBCO Film Thickness	0.4-0.6 μm
YBCO Film Critical Temperature	85 K

Table 1 The physical parameters of the microstrip.

There are two types of lines used in the resonator circuit, the input and output straight line sections and the ring line. The electromagnetic parameters of these lines, i.e., effective relative dielectric constant, ε_r^{eff} and characteristic impedance, Z_O, listed in table 1, are first calculated, using standard microstrip formulas [1]. These are entered into a MathCAD worksheet, included as appendix A of this chapter, to arrive at the parameters of table 2. Although the value given for the relative dielectric constant of the lanthanum aluminate by Conductus is 24.0, there is a range of values used in the literature, from 23.5 to 24.5.

Line...	w (mm)	ε_r^{eff}	Z_0 (Ω)
In/Out	0.2	14.7	47.0
Ring	0.5	15.7	32.1

Table 2 The electrical parameters of the two types of line.

layout as the one shown in figure 2, but made out of gold, are used.

Figure 2 is a plot of the dB-magnitude of S21 versus frequency of the gold ring resonator and also a simple model using Atwater's dispersion equation. Notice here how the peaks of the modeled and measured responses (resonance frequencies) match almost perfectly. With the rest of the dispersion models ([3]-[7]) this is not the case. Hence Atwater's [2] microstrip dispersion model is adopted in the rest of this thesis. It is applied to the effective relative dielectric constants, listed in column 1 of table 2, to add the appropriate frequency dependence and yield correct effective relative dielectric constants at each frequency.

The electromagnetic parameters listed in table 2, after compensation for dispersion as mentioned above, are then plugged into equations (3.34)-(3.43) to obtain the final "corrected" values, which include complex conductivity and field penetration effect. The necessary parameters to model the two types of transmission lines used in the ring resonator circuit are the exponential loss coefficient α_c (in dB/mm), the effective relative dielectric constant ε_r^{eff} and the characteristic impedance Z_o (in Ohms). Given these parameters and the physical length of each transmission line the circuit S-parameter response may be modeled by "connecting," via signal flow graphs, the S-parameters of each individual type of line and calculating the overall response using Mason's rule, or simply solving a system of linear equations.

4.3.2 Using Touchstone and Academy (TM) by EEsof Inc.

The process described above, of combining the modeled S-parameters of each type of transmission line at each frequency to arrive at an aggregate modeled response of a circuit, may be simply executed by a computer given the appropriate program. Using a program

that is customized to the particular circuit it models forces modification (if not re-write) for every different circuit. Most programming languages also have a "tenuous relationship" with the computer's graphics routines, and hence plotting the analysis results can add undesired hassle. In addition, changing the plotted parameters would require modifying and re-compiling the program every time such a change would be desired, a time consuming process.

The alternative is to use an existing microwave CAD software package to perform the algebraic combination of the S-parameters and the plotting of the results. In this thesis I have chosen to use two popular microwave CAD software packages by EEsof Inc. that are widely used in the industry: Touchstone (TM) and Academy (TM). Touchstone is a microwave computer-aided analysis and design software package analyzes linear microwave circuits. Its input is a *netlist* or circuit file which contains a number of microwave elements connected in a number of nodes. Touchstone includes its own element library which contains models of many commonly used linear elements.

The input netlist file is subdivided into several *blocks* each of which contains a different kind of information. The three most important blocks are the *CKT*, the *VAR* and the *EQN* block. The CKT block contains the nodal description of the circuit to be analyzed. The VAR block contains the definitions of constants used in the CKT block. The EQN block contains definitions of new variable related to the constants defined in the VAR block. The program sweeps the frequency variable over a specified (in the *FREQ* block) range of frequencies at specified increments and plots the calculated measurements versus frequency (as specified in the *OUT* block) in an output graphics window. Academy is a schematic capture and layout tool that does away with the need for an input netlist file. It uses Touchstone as its simulator and enables versatile plotting of many output parameters at a time, by the effective use of windowing environments in many platforms.

Within the EQN block of Touchstone there is a pre-defined variable called *FREQ* which always contains the instantaneous value of the sweep frequency. Using FREQ in the EQN block, frequency dependent calculations, like dispersion or the PEM model, may be implemented. One of the elements available in the libraries is the *TLINP* element. This element models a physical transmission line and takes the effective relative dielectric constant, the characteristic impedance, the loss per unit length and the physical length of the line as its inputs. Hence, it is ideally suited to our calculated variables (see previous section) and the circuit may be modeled by combining a number of such elements. Using Touchstone fast analysis and efficient plotting is possible.

Equations (3.34)-(3.43) are frequency dependent and therefore need to be calculated in the EQN block of the Touchstone circuit file. A sample circuit file is included as appendix B of this chapter. The EQN block of the YBCO microstrip ring resonator circuit file is separated into two sub-sections, each containing equations (3.34)-(3.43) for one of the narrow and wide lines respectively. Equations (3.35) and (3.36) are too long for Touchstone, so they are broken down into many smaller equations, in the circuit file. The VAR block contains the variables listed in table 2, with values calculated in the MathCAD sheet of appendix A. The convention employed for naming variables in the VAR and EQN blocks is last letter *n* for the narrow lines and *w* for the wide lines. The results of the calculations are the loss due to the surface resistance of the line, in dB/mm, the corrected characteristic impedance and the corrected effective dielectric constant, for each type of line. These are fed into a number of inter-connected TLINP elements in the circuit block.. Each

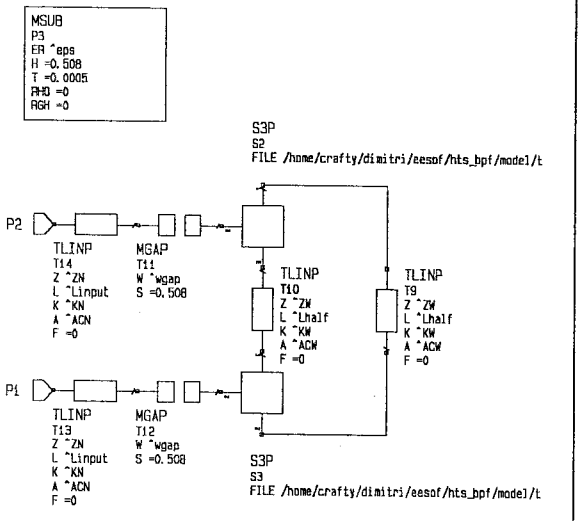

Figure 3 A schematic representation of the model.

TLINP element emulates a propagating mode of the form $e^{(-\alpha z - j\beta z)}$ of a given characteristic impedance. Four TLINP elements, each given the true length of the line it models, model the four lines of the ring resonator. The ring is modeled via two lines, each of half the true length of the ring. The two lines are interconnected via a 3-port S-parameter matrix which emulates a lumped (dimensionless) lossless T-junction (see section 6.2.2 for a more detailed discussion). This is done so that the *MGAP* Touchstone element, which models a gap in a microstrip line, may be connected to the third port of the T-matrix to model the coupling gap between the input and output lines and the ring. Figure 3 shows a schematic representation of the model circuit, as described above. It is plotted by the Academy schematic capture utility.

It is important to stress again that Touchstone is provided with all the pre-calculated parameters and models and hence its own built-in transmission line models are not used, with the exception of the model of the microstrip gap (MGAP) which is identical in the HTS and the normal circuits. The function of Touchstone is to perform the algebraic combination of the S-parameters of the different types of transmission lines of the filter and conveniently plot the results in formats familiar to microwave engineers.

4.3.3 The Modeling Strategy

The two most important unknowns used in modeling the YBCO HTS, are the normal conductivity, σ_n and the zero-temperature penetration depth, λ_o. Applied physics researchers who grow extra pure single crystal YBCO report a λ_o.of 140 nm and a σ_n of $1.14 \cdot 10^6$ S/m [8]. This is, however, the penetration depth in the very pure, single crystal limit. The YBCO crystal fabricated at Conductus to make the HTS microstrip ring resonator is not a single crystal and the controlled laboratory conditions under which it is deposited are not state-of-the-art. As a result the crystal grows in many separate grains

and there is a surface energy associated with the boundaries between different grains. The existence of grains and grain boundaries causes the penetration depth to be non-uniform over the surface of the circuit and larger than in the pure single crystal case [9]. Imperfections and contaminants in the crystal also increase the penetration depth. However, if the variations occur in an area that is spatially small compared to the wavelength, they can be averaged out and an overall effective penetration depth may be used. Polakos et al. from AT&T Bell Labs report an effective penetration depth of 450 nm for a similarly deposited HTS microstrip circuit [10].

In the initial modeling attempts the value of Polakos was used for the penetration depth and the value of reference [8] for the normal conductivity. The fit between modeled and measured response data was already very close, within 2.1 dB in magnitude of S21 and 0.2 radians in the angle of S21. Subsequently the optimizer feature of Touchstone was used. The optimizer performs a gradient search in the N-dimensional Euclidean space defined by the optimized variables for the optimum vector that minimizes the integrated squared error, over frequency, between the measured and the modeled S-parameters. The zero-temperature penetration depth and real part of the conductivity are permitted to optimize. The optimum extracted values for these parameters are

λ_o=438 nm

σ_n=5.67x10^6 S/m

(see appendix B, variables LD and Sn in the VAR block).

Both values are close to Polakos' values. Another parameter that is optimized for minimum integrated square error between the modeled and measured S-parameters is the line length of the 50 Ω input and output lines, for best phase of S21 match. This is because the Thru-Reflect-Line (TRL) calibration standards that are used to calibrate the HP 8510C network analyzer that is used to measure the resonator circuit have an

unknown phase reference plane. Also, because the electromagnetic coupling between the end of the input/output lines and the ring is greater than if the lines on both sides of the gap were the same width (due to the larger fringing capacitance at the end of the line) the width of the MGAP element is permitted to optimize. The resulting optimized value for the effective width is 0.34 mm, 1.7 times its real width of 0.2 mm.

4.4 Comparison of Model versus Measurement

The following figures contain a comparison of the results of the modeling and the measured data, using the optimum parameter values reported above. Figures 4-7 are plotted versus a wide frequency range of 4-13 GHz, whereas figures 8-11 are plotted against a 30 MHz frequency range centered about the lowest order resonance frequency (4.36088 GHz). Figure 4 shows a comparison of the insertion loss (magnitude of S21 plotted in a log vertical scale) of the two ring resonators of identical layout, one made of YBCO and the other of gold, as discussed above. In the same figure the modeled value of S21 is plotted. Obviously, in this case, the HTS circuit has much higher Q (i.e., lower loss) than the corresponding gold one.

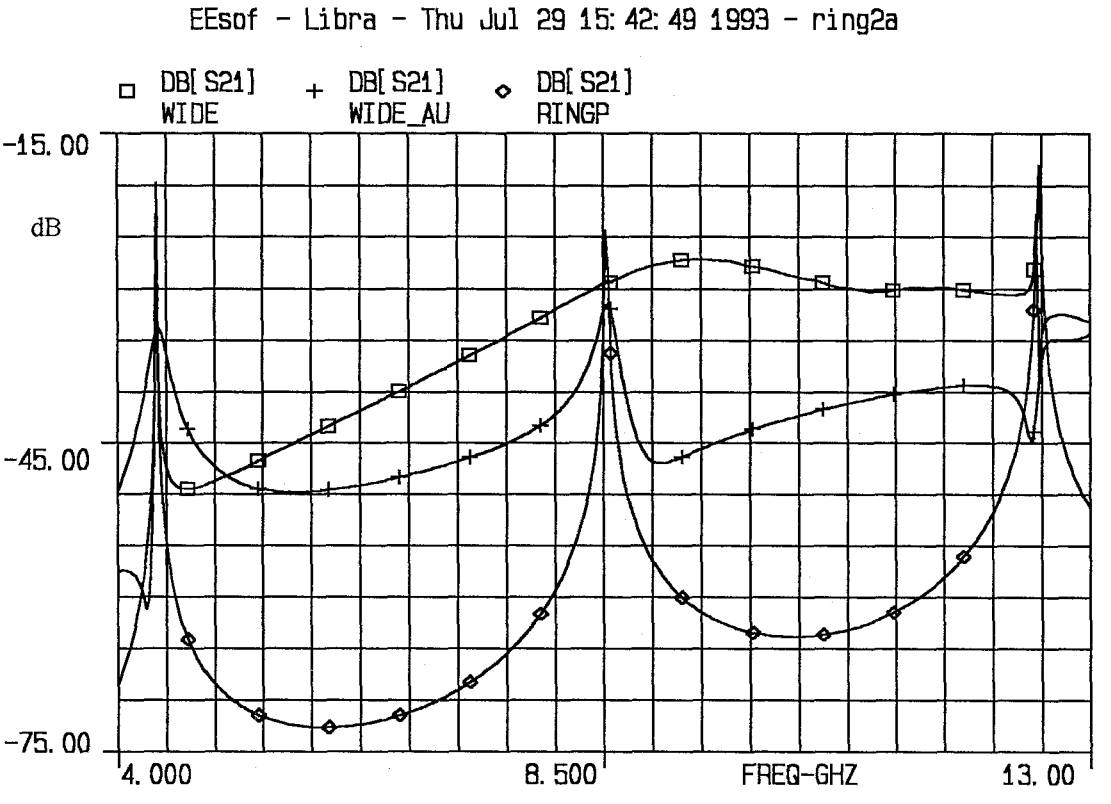

Figure 4 Measured (WIDE for HTS circuit, WIDE_AU for gold circuit) versus modeled (RINGP) magnitude of S21.

Figure 5 is a plot of the measured versus modeled angle of S21 of the HTS resonator and also, for comparison, the angle of S21 of the gold resonator.

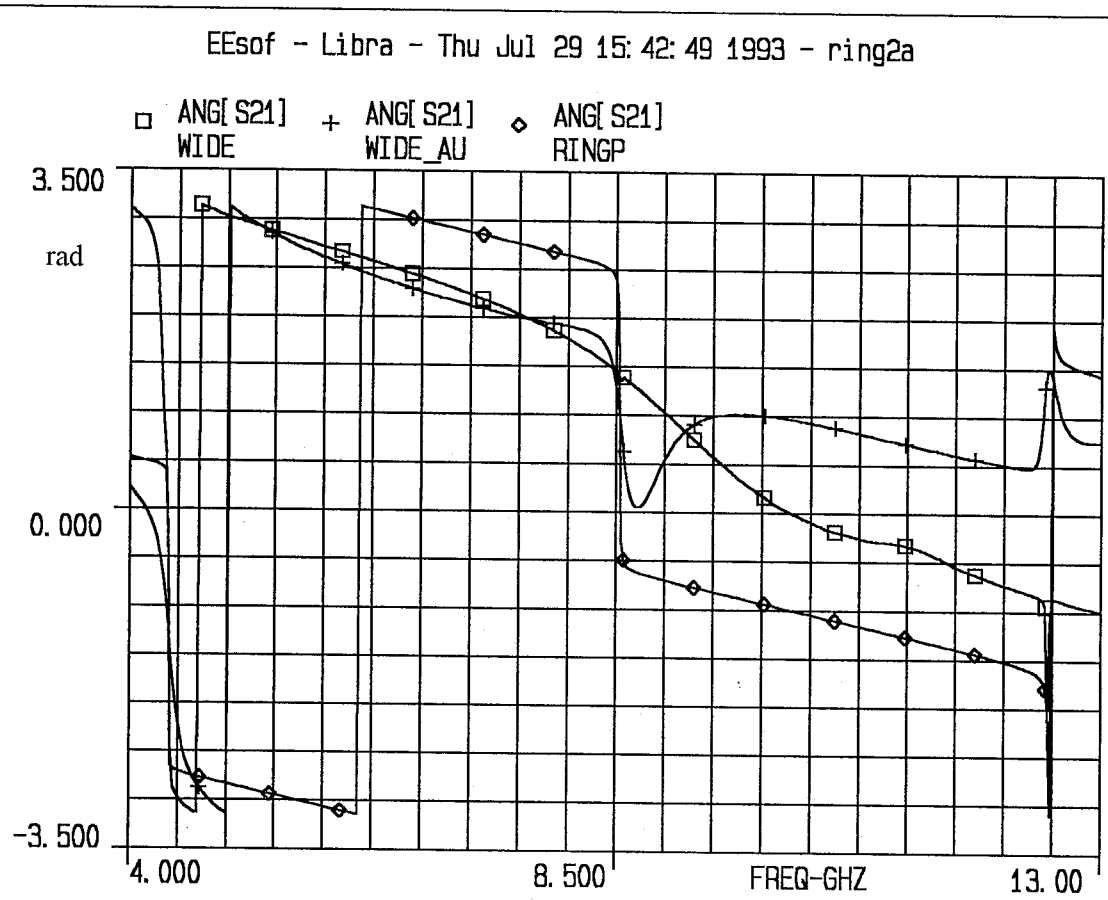

Figure 5 Measured (WIDE for HTS circuit, WIDE_AU for gold circuit) versus modeled (RINGP) angle of S21.

Figure 6 is a plot of the measured versus modeled magnitude of S11 of the HTS resonator, and also includes the measured magnitude of S11 of the gold resonator for comparison..

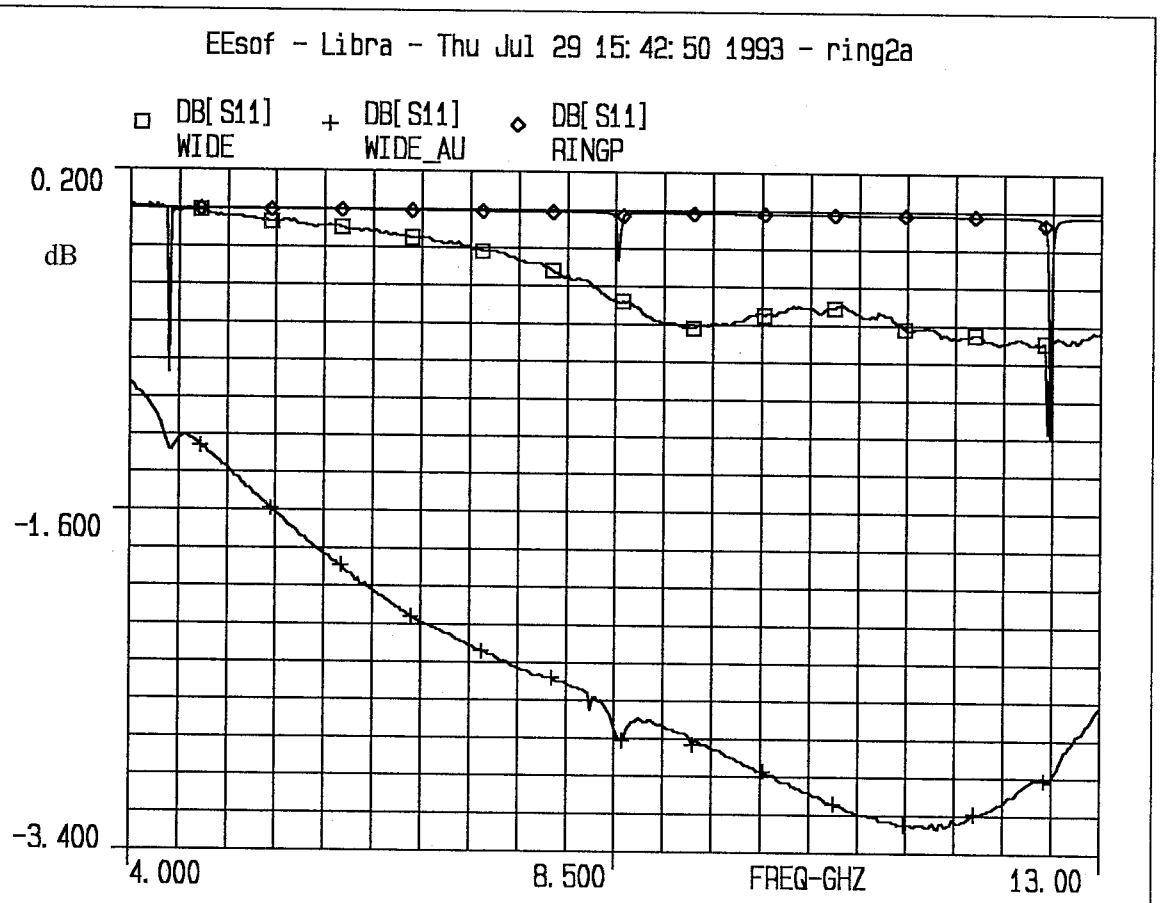

Figure 6 Measured (WIDE for HTS circuit, WIDE_AU for gold circuit) versus modeled (RINGP) magnitude of S11.

Figure 7 is a plot of the measured versus modeled angle of S11 of the HTS resonator and also, for comparison, the angle of S21 of the gold resonator.

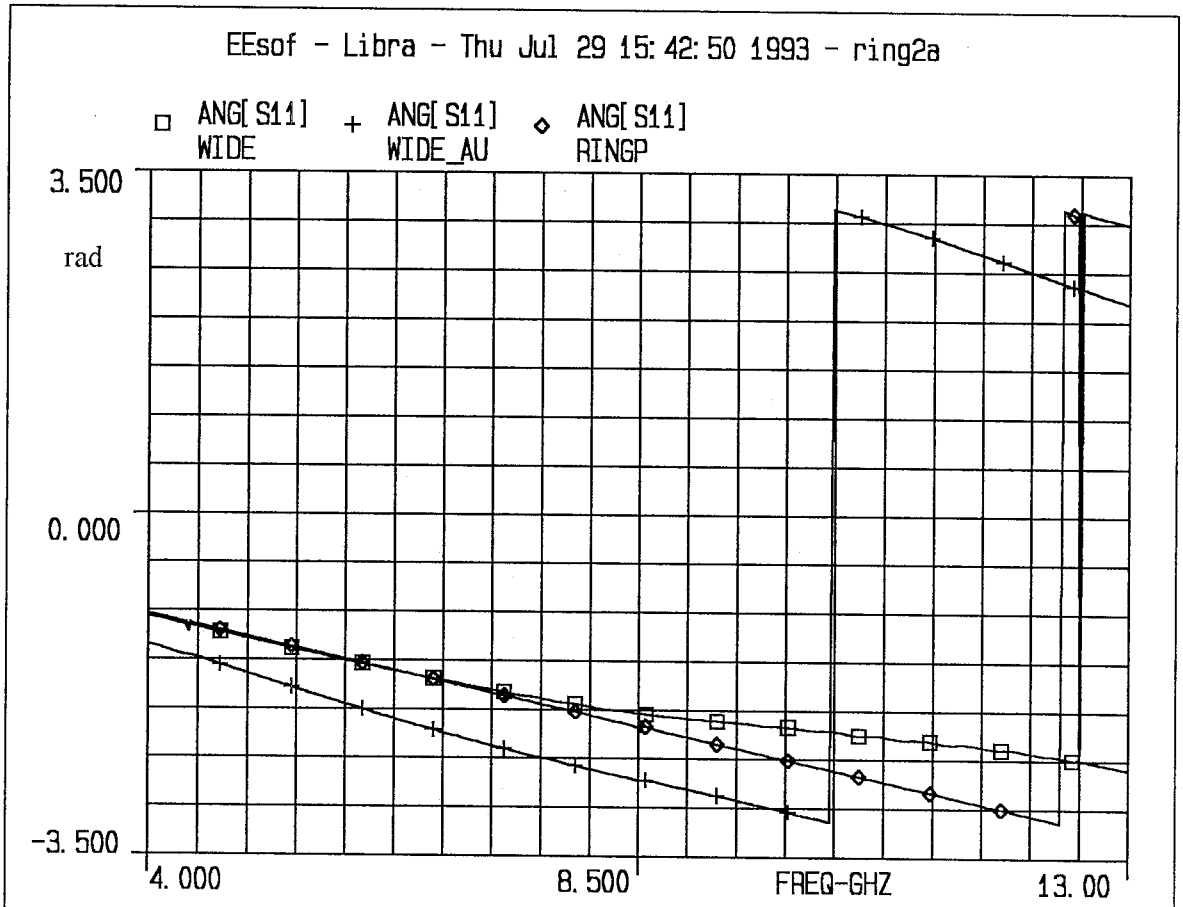

Figure 7 Measured (WIDE for HTS circuit, WIDE_AU for gold circuit) versus modeled (RINGP) angle of S11.

Figures 4-7 are plotted over a wide frequency range, from 4 to 13 GHz. The figures that follow, numbered 8 through 11, focus in a narrow interval (30 MHz) about the lowest order resonance frequency of the HTS resonator (4.361 GHz). Figure 8 is a plot of the measured versus modeled dB magnitude of S21. The agreement between model and measurement is good. The calculated loaded Q (Q_L) of the HTS resonator is 1697, while the model yields a value of 1707, an excellent agreement which verifies that the PEM model, presented in chapter 3, successfully accounts for surface "ohmic" losses in the HTS.

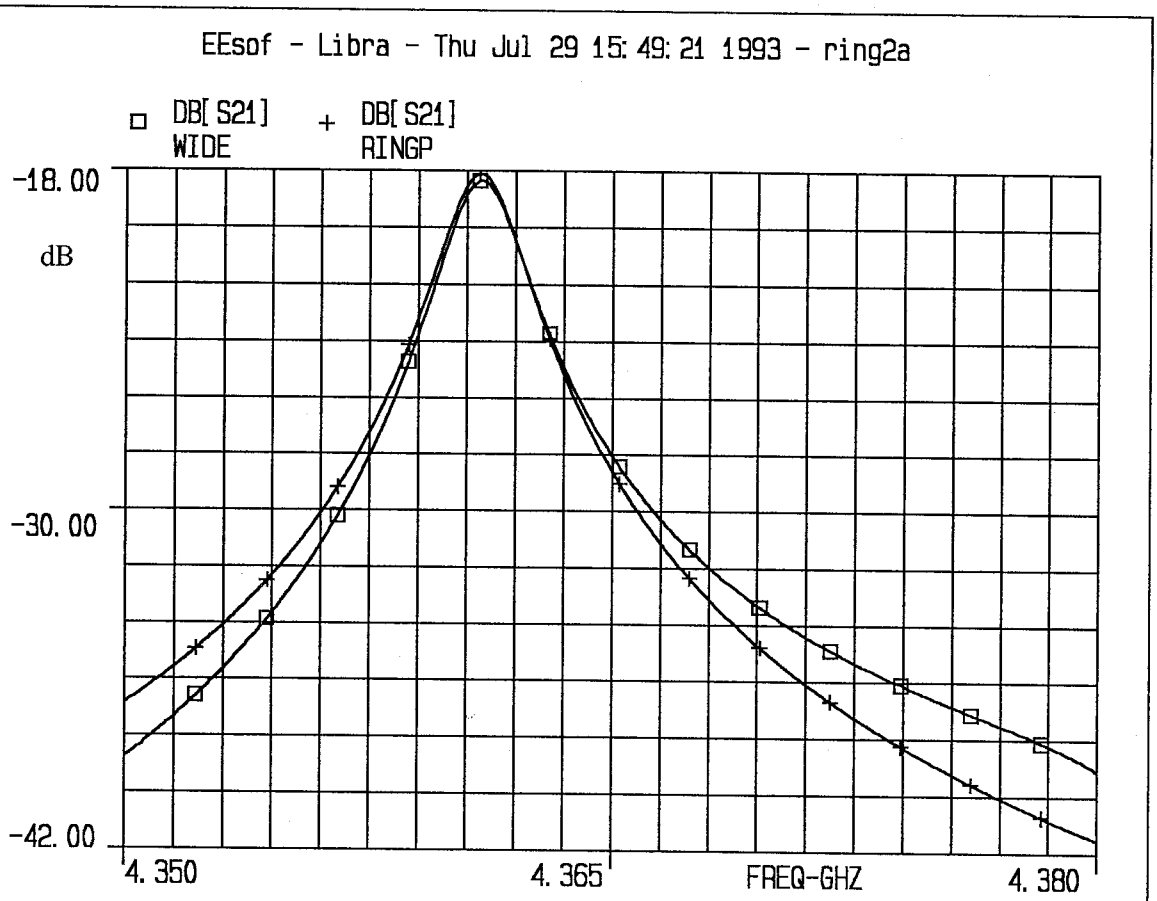

Figure 8 Measured (WIDE) versus modeled (RINGP) magnitude of S21.

Figure 9 is a plot of the measured versus modeled angle of S21 of the HTS resonator.

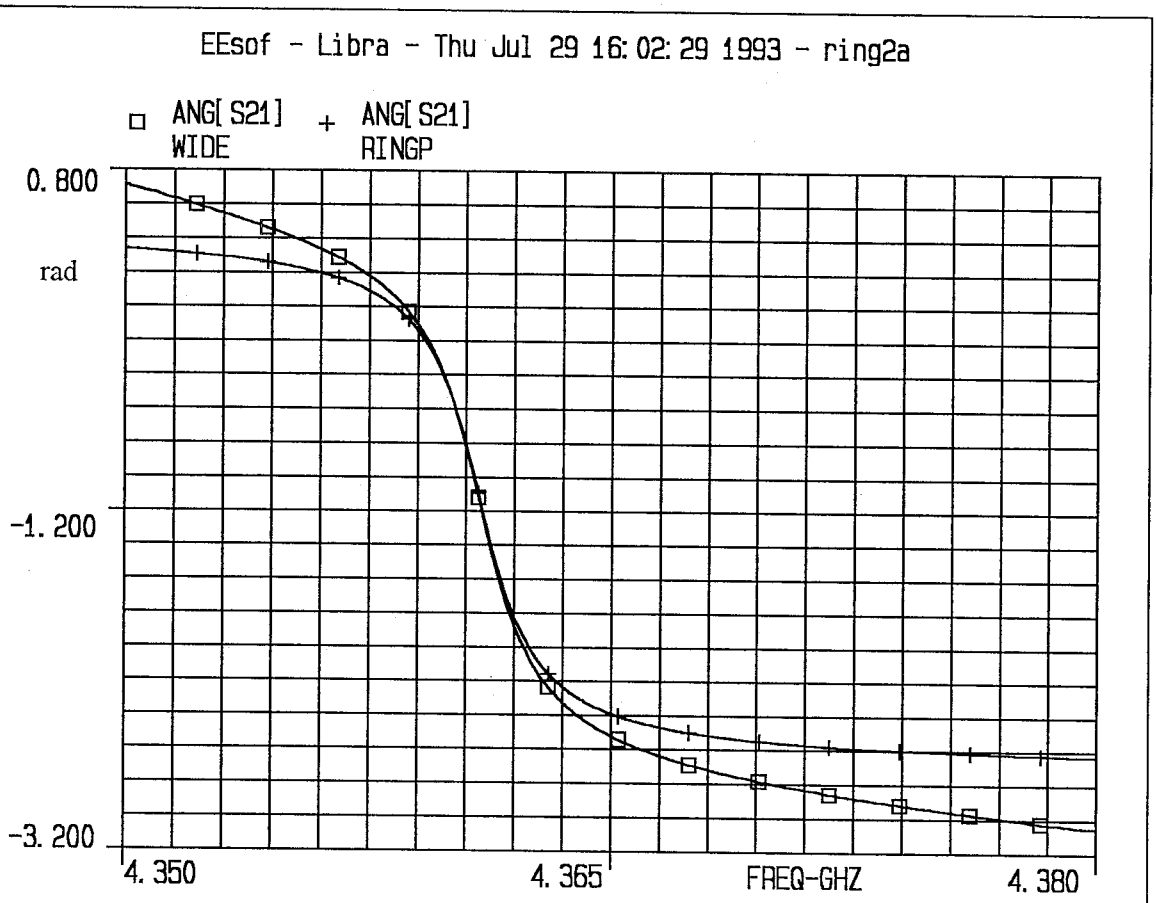

Figure 9 Measured (WIDE) versus modeled (RINGP) angle of S21.

Figure 10 is a plot of the measured versus modeled magnitude of S11 of the HTS resonator.

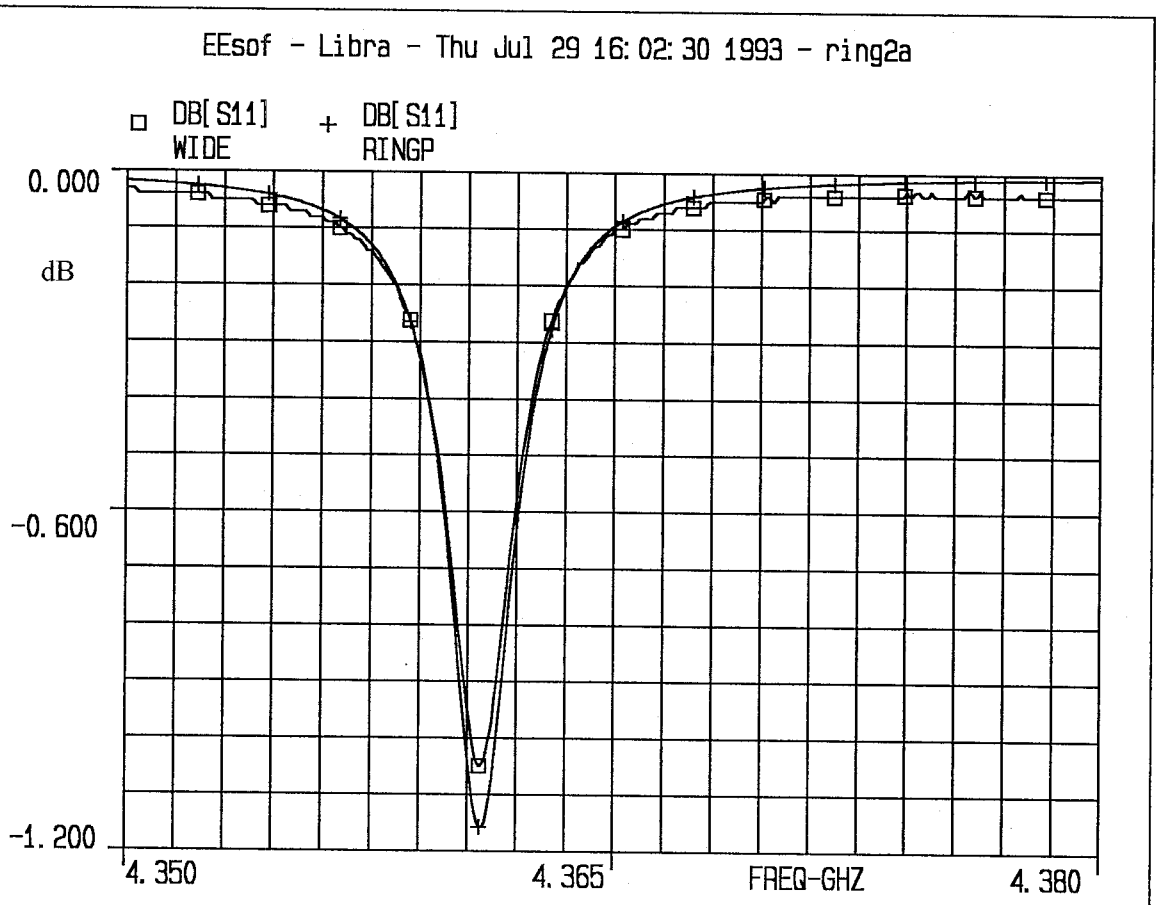

Figure 10 Measured (WIDE) vs. modeled (RINGP) magnitude of S11.

Figure 11 is a plot of the measured versus modeled angle of S11.

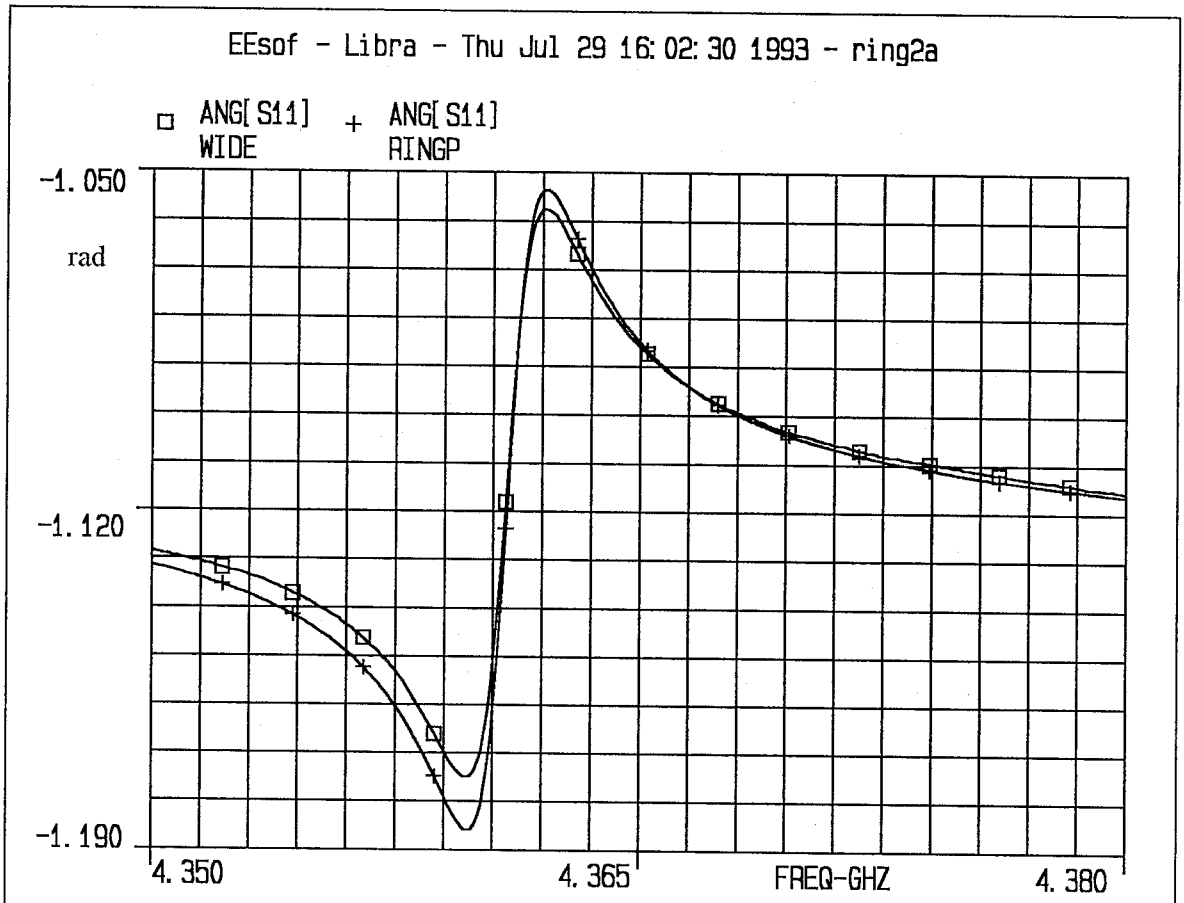

Figure 11 Measured (WIDE) versus modeled (RINGP) angle of S11.

4.5 References

[1] K. Gupta, R. Garg and I. Bahl, *Microstrip Lines and Slotlines*, Artech, Dedham, MA, 1979.

[2] H. A. Atwater, *Introduction to Microwave Theory*, McGraw-Hill, New York, 1962.

[3] T. G. Bryant and J. A. Weiss, "Parameters of Microstrip Transmission Lines and Coupled Pairs of Microstrip Lines," IEEE Transactions on Microwave Theory and Techniques, Vol. MTT-16, pp.1021-1027, December 1968.

[4] M. V. Schneider, "Microstrip Lines for Microwave Integrated Circuits," The Bell System Technical Journal, Vol. 48, No. 5, pp. 1421-1444, May/June 1969.

[5] E. O. Hammerstad, "Equations for Microstrip Circuit Design," Proceedings of the European Microwave Conference, Hamburg, W. Germany, pp. 268-272, September 1975.

[6] H. A. Wheeler, "Transmission Line Properties of a Strip on a Dielectric Sheet on a Plane," IEEE Transactions on Microwave Theory and Techniques, Vol. MTT-25, Mo. 8, pp. 631-647, August 1977.

[7] E. O. Hammerstad and O. Jensen, "Accurate Models for Microstrip Computer-Aided Design," IEEE MTT-S Symposium Digest, pp. 407-409, June 1980.

[8] D. R. Harshman et al., "Magnetic Penetration Depth in Single Crystal $YBa_7Cu_3O_7$," Physical Review, Vol. B39, p. 2596.

[9] T. L. Hylton and M. R. Beasley "Effect of Grain Boundaries on Magnetic Field Penetration in Polycrystalline Superconductors," Physical Review, Vol B39, pp. 9042-9048, May 1989.

[10] P. A. Polakos, C. E. Rice, M. V. Schneider and R. Trambarulo, "Electrical Characteristics of Thin-Film Ba2YCu3O7 Superconducting Ring Resonators," Microwave & Guided Wave Letters, Vol. 1, 1991.

Appendix A

MathCAD File Used to Calculate the Parameters of the Two Types of Transmission Line Used in the Resonator Circuit

Physical Constants

$$\varepsilon_0 := 8.854 \cdot 10^{-12}$$

$$\mu_0 := 4 \cdot \pi \cdot 10^{-7}$$

$$c := \frac{1}{\sqrt{\varepsilon_0 \cdot \mu_0}} \qquad \eta := \sqrt{\frac{\mu_0}{\varepsilon_0}}$$

Microstrip Parameters

$$h := 20 \cdot 10^{-3} \cdot 2.54 \cdot 10^{-2}$$

$$h = 5.08 \cdot 10^{-4}$$

$$t := 5 \cdot 10^{-7}$$

$$i := 1, 2 .. 20$$

$$er_i := 22.9 + i \cdot 0.1$$

Microstrip Design Equations

Ring

$$W := 0.5 \cdot 10^{-3}$$

$$W_{em} := if\left[\frac{W}{h} > \frac{1}{\left[2 \cdot \pi\right]}, W + \frac{1.25}{\pi} \cdot t \cdot \left[1 + ln\left[2 \cdot \frac{h}{t}\right]\right], W + \frac{1.25}{\pi} \cdot t \cdot \left[1 + ln\left[4 \cdot \pi \cdot \frac{W}{t}\right]\right]\right]$$

$$F := if\left[\frac{W}{h} > 1, \left[1 + 12 \cdot \frac{h}{W}\right]^{-\left[\frac{1}{2}\right]}, \left[1 + 12 \cdot \frac{h}{W}\right]^{-\left[\frac{1}{2}\right]} + 0.04 \cdot \left[1 - \frac{W}{h}\right]^2\right]$$

$$ere_i := \frac{\left[er_i + 1\right]}{2} + \frac{\left[er_i - 1\right]}{2} \cdot F - \frac{\left[er_i - 1\right]}{4.6} \cdot \frac{\left[\frac{t}{h}\right]}{\sqrt{\frac{W}{h}}} \qquad W_{em} = 5.017 \cdot 10^{-4}$$

$$Z_{om_i} := if\left[\frac{W}{h} > 1, \frac{\eta}{\sqrt{ere_i}} \cdot \left[\frac{W_{em}}{h} + 1.393 + 0.667 \cdot ln\left[\frac{W_{em}}{h} + 1.444\right]\right]^{-1}, \frac{\eta}{\left[2 \cdot \pi \cdot \sqrt{ere_i}\right]} \cdot ln\left[8 \cdot \frac{h}{W_{em}} + 0.25 \cdot \frac{W_{em}}{h}\right]\right]$$

Calculate new impedances under recession of walls by dnormal:

$$dnormal := \frac{t}{1000}$$

$$t := t - 2 \cdot dnormal \qquad t = 4.99 \cdot 10^{-7}$$

$$W := W - 2 \cdot dnormal \qquad W = 5 \cdot 10^{-4}$$

$$F := if\left[\frac{W}{h} > 1, \left[1 + 12 \cdot \frac{h}{W}\right]^{-\left[\frac{1}{2}\right]}, \left[1 + 12 \cdot \frac{h}{W}\right]^{-\left[\frac{1}{2}\right]} + 0.04 \cdot \left[1 - \frac{W}{h}\right]^{2}\right]$$

$$ered_i := \frac{\left[er_i + 1\right]}{2} + \frac{\left[er_i - 1\right]}{2} \cdot F - \frac{\left[er_i - 1\right]}{4.6} \cdot \frac{\left[\frac{t}{h}\right]}{\sqrt{\frac{W}{h}}}$$

$$W_{em} := if\left[\frac{W}{h} > \frac{1}{\left[2 \cdot \pi\right]}, W + \frac{1.25}{\pi} \cdot t \cdot \left[1 + \ln\left[2 \cdot \frac{h}{t}\right]\right], W + \frac{1.25}{\pi} \cdot t \cdot \left[1 + \ln\left[4 \cdot \pi \cdot \frac{W}{t}\right]\right]\right]$$

$$W_{em} = 5.017 \cdot 10^{-4}$$

$$Z_{omd_i} := if\left[\frac{W}{h} > 1, \frac{\eta}{\sqrt{ered_i}} \cdot \left[\frac{W_{em}}{h} + 1.393 + 0.667 \cdot \ln\left[\frac{W_{em}}{h} + 1.444\right]\right]^{-1}, \frac{\eta}{\left[2 \cdot \pi \cdot \sqrt{ered_i}\right]} \cdot \ln\left[8 \cdot \frac{h}{W_{em}} + 0.25 \cdot \frac{W_{em}}{h}\right]\right]$$

$$G_{m_i} := \frac{1}{\left[\mu_0 \cdot c\right]} \cdot \frac{\left[\sqrt{ered_i} \cdot Z_{omd_i} - \sqrt{ere_i} \cdot Z_{om_i}\right]}{dnormal}$$

er_i	ere_i	Z_{om_i}	G_{m_i}
23	15.024	32.824	2406.1695
23.1	15.088	32.755	2406.1695
23.2	15.151	32.686	2406.1695
23.3	15.215	32.617	2406.1695
23.4	15.279	32.549	2406.1695
23.5	15.343	32.481	2406.1695
23.6	15.406	32.414	2406.1695
23.7	15.47	32.347	2406.1695
23.8	15.534	32.281	2406.1695
23.9	15.598	32.215	2406.1695
24	15.661	32.149	2406.1695
24.1	15.725	32.084	2406.1695
24.2	15.789	32.019	2406.1695
24.3	15.853	31.955	2406.1695
24.4	15.916	31.891	2406.1695
24.5	15.98	31.827	2406.1695
24.6	16.044	31.764	2406.1695
24.7	16.108	31.701	2406.1695
24.8	16.171	31.638	2406.1695
24.9	16.235	31.576	2406.1695

Input/Output Lines

$$W := 0.2 \cdot 10^{-3}$$

$$W_{em} := \text{if}\left[\frac{W}{h} > \frac{1}{\left[2 \cdot \pi\right]}, W + \frac{1.25}{\pi} \cdot t \cdot \left[1 + \ln\left[2 \cdot \frac{h}{t}\right]\right], W + \frac{1.25}{\pi} \cdot t \cdot \left[1 + \ln\left[4 \cdot \pi \cdot \frac{W}{t}\right]\right]\right]$$

$$F := \text{if}\left[\frac{W}{h} > 1, \left[1 + 12 \cdot \frac{h}{W}\right]^{-\left[\frac{1}{2}\right]}, \left[1 + 12 \cdot \frac{h}{W}\right]^{-\left[\frac{1}{2}\right]} + 0.04 \cdot \left[1 - \frac{W}{h}\right]^2\right]$$

$$ere_i := \frac{\left[er_i + 1\right]}{2} + \frac{\left[er_i - 1\right]}{2} \cdot F - \frac{\left[er_i - 1\right]}{4.6} \cdot \frac{\left[\frac{t}{h}\right]}{\sqrt{\frac{W}{h}}} \qquad W_{em} = 2.017 \cdot 10^{-4}$$

$$Z_{om_i} := \text{if}\left[\frac{W}{h} > 1, \frac{\eta}{\sqrt{ere_i}} \cdot \left[\frac{W_{em}}{h} + 1.393 + 0.667 \cdot \ln\left[\frac{W_{em}}{h} + 1.444\right]\right]^{-1}, \frac{\eta}{\left[2 \cdot \pi \cdot \sqrt{ere_i}\right]} \cdot \ln\left[8 \cdot \frac{h}{W_{em}} + 0.25 \cdot \frac{W_{em}}{h}\right]\right]$$

Calculate new impedances under recession of walls by dnormal:

$$dnormal := \frac{t}{1000}$$

$$t := t - 2 \cdot dnormal \qquad t = 4.98 \cdot 10^{-7}$$

$$W := W - 2 \cdot dnormal \qquad W = 2 \cdot 10^{-4}$$

$$F := if\left[\frac{W}{h} > 1, \left[1 + 12 \cdot \frac{h}{W}\right]^{-\left[\frac{1}{2}\right]}, \left[1 + 12 \cdot \frac{h}{W}\right]^{-\left[\frac{1}{2}\right]} + 0.04 \cdot \left[1 - \frac{W}{h}\right]^2\right]$$

$$ered_i := \frac{\left[er_i + 1\right]}{2} + \frac{\left[er_i - 1\right]}{2} \cdot F - \frac{\left[er_i - 1\right] \cdot \left[\frac{t}{h}\right]}{\sqrt{\frac{W}{h}}}$$

$$W_{em} := if\left[\frac{W}{h} > \frac{1}{\left[2 \cdot \pi\right]}, W + \frac{1.25}{\pi} \cdot t \cdot \left[1 + \ln\left[2 \cdot \frac{h}{t}\right]\right], W + \frac{1.25}{\pi} \cdot t \cdot \left[1 + \ln\left[4 \cdot \pi \cdot \frac{W}{t}\right]\right]\right]$$

$$W_{em} = 2.017 \cdot 10^{-4}$$

$$Z_{omd_i} := if\left[\frac{W}{h} > 1, \frac{\eta}{\sqrt{ered_i}} \cdot \left[\frac{W_{em}}{h} + 1.393 + 0.667 \cdot \ln\left[\frac{W_{em}}{h} + 1.444\right]\right]^{-1}, \frac{\eta}{\left[2 \cdot \pi \cdot \sqrt{ered_i}\right]} \cdot \ln\left[8 \cdot \frac{h}{W_{em}} + 0.25 \cdot \frac{W_{em}}{h}\right]\right]$$

$$G_{m_i} := \frac{1}{\left[\mu_0 \cdot c\right]} \cdot \frac{\left[\sqrt{ered_i} \cdot Z_{omd_i} - \sqrt{ere_i} \cdot Z_{om_i}\right]}{dnormal}$$

er_i	ere_i	Z_{om_i}	G_{m_i}
23	14.115	48.006	6300.0696
23.1	14.174	47.905	6300.0696
23.2	14.234	47.805	6300.0696
23.3	14.294	47.705	6300.0696
23.4	14.353	47.606	6300.0696
23.5	14.413	47.507	6300.0696
23.6	14.472	47.409	6300.0696
23.7	14.532	47.312	6300.0696
23.8	14.592	47.215	6300.0696
23.9	14.651	47.119	6300.0696
24	14.711	47.023	6300.0696
24.1	14.771	46.928	6300.0696
24.2	14.83	46.834	6300.0696
24.3	14.89	46.74	6300.0696
24.4	14.949	46.647	6300.0696
24.5	15.009	46.554	6300.0696
24.6	15.069	46.462	6300.0696
24.7	15.128	46.37	6300.0696
24.8	15.188	46.279	6300.0696
24.9	15.247	46.189	6300.0696

Appendix B

Touchstone Circuit File that Models the HTS Resonator

```
!8-4-93
!FINAL VERSION
!WITH ER=24.0
!
!
!
DIM
FREQ        GHZ
RES         OH
COND        /OH
IND         NH
CAP         PF
LNG         MM
TIME        PS
ANG         RAD
VOL         V
CUR         MA
PWR         DBM
VAR

LD0 =437.524700000
T = 77                    !TEMPERATURE OF MEASUREMENT
Tc = 85                   !Critical Temperture of Sample
Sn =5668582.00000

! CONSTANTS
e0 = 8.854E-12            !Permittivity of free space


eps =24.0000000000
KN00 =14.7100000000
ZN0 =47.0200000000
KW00 =15.6600000000
ZW0 =32.1500000000
AGN = 1e-10
AGW = 2.5E-10
GN = 6300
GW = 2406.2

wgap =0.34256800000
Lhalf =8.40539300000
Linput =1.33346500000

SigAu =200000000.000

EQN

FDN =4*0.508*FREQ/300*sqrt(eps-1)*(0.5+sqr(1+2*LOG(1+0.2/0.508)))
FDW =4*0.508*FREQ/300*sqrt(eps-1)*(0.5+sqr(1+2*LOG(1+0.5/0.508)))
KN0 =KN00*SQR(1+(SQRT(eps/KN00)-1)/(1+4*FDN**(-1.5)))
KW0=KW00*SQR(1+(SQRT(eps/KW00)-1)/(1+4*FDW**(-1.5)))


LD=LD0*1e-9
```

```
! Computation of losses for first, narrow spaced, coupled lines
!      Constants

 U0 = 4*PI*1e-7              !Magnetic Permeability of vacuum
 c = 1/sqrt(e0*U0)           !Velocity of light
 h0=sqrt(U0/e0)              !Impedance of free space

 f = FREQ*1e9                !Frequency in Hz
 Sr = Sn*(T/Tc)**4           !Real Part of conductivity of YBCO (Sigma1)
 Si = (1-(T/Tc)**4)/(2*PI*f*U0*LD**2)  !Imaginary Part of conductivity (Sigma2)
 P = ATAN(Si/Sr)             !Angle of conductivity  (Phi)
 Th= 5*PI/4-P/2              !Auxiliary angle definition (Theta)
 Sigmag= SQRT(SQR(Sr)+SQR(Si)) !Norm of conductivity

! MICROSTRIP LINE PARAMETERS

! WIDE RING LINE

 BW= GW*AGW*SQRT(2*PI*f*U0*sigmag)          !B
 CW= EXP(2*BW*COS(Th))
 DW= COS(2*BW*SIN(Th))
 EW= SIN(2*BW*SIN(Th))
 UW= SQRT(SQR(CW*DW-1)+SQR(CW*EW))          !Psi
 WW= ATAN(CW*EW/(CW*DW-1))                  !Chi
 FW= BW/(AGW*sigmag*UW)                     !Prefactor of Ri and Xi
 MW= 2*BW*SIN(Th)
 NW= COS(PI/4+P/2-WW)
 RPW= COS(MW+PI/4+P/2-WW)

 RiW= FW*(NW+CW*RPW)                        !Internal Resistance  / Meter

 NIW= SIN(PI/4+P/2-WW)
 RDW= SIN(MW+PI/4+P/2-WW)

 LiW = 1/(2*PI*f)*FW*(NIW+CW*RDW)           !Internal Inductance / Meter

 CORRW = 1+(c/sqrt(KW0))*(LiW/ZW0)          !Correction Factor (3.41)

 ZW = ZW0*sqrt(CORRW)                       !Corrected Char Impedance

 KW = KW0*CORRW                             !Corrected  Dielectric Const (3.43)

ACW =(8.686e-3) * RiW/(2*ZW)


! NARROW INPUT/OUTPUT LINE

 Th2= 5*PI/4                !Auxiliary angle definition (Theta) for Gold

 BN =GN*AGN*SQRT(2*PI*f*U0*SigAu)
 CN= EXP(2*BN*COS(Th2))
 DN= COS(2*BN*SIN(Th2))
 EN= SIN(2*BN*SIN(Th2))
```

```
UN= SQRT(SQR(CN*DN-1)+SQR(CN*EN))          !Psi
WN= ATAN(CN*EN/(CN*DN-1))                  !Chi
FN =BN/(AGN*SigAu*UN)
MN= 2*BN*SIN(Th2)
NN= COS(PI/4-WN)
RPN= COS(MN+PI/4-WN)

RiN = FN*(NN+CN*RPN)              !Internal Resistance  / Meter

NIN= SIN(PI/4-WN)
RDN= SIN(MN+PI/4-WN)

LiN = 1/(2*PI*f)*FN*(NIN+CN*RDN)     !Internal Inductance / Meter

CORRN = 1+(c/sqrt(KN0))*(LiN/ZN0)     !Correction Factor (3.41)

ZN  = ZN0*sqrt(CORRN)              !Corrected Char Impedance

KN  = KN0*CORRN                   !Corrected  Dielectric Const (3.43)

ACN  = (8.686e-3) * RiN/(2*ZN)      !Loss Coefficient, in [dB/mm]


CKT

S2P_S1 1 2 0 /home/crafty/dimitri/eesof/hts_ring/ringl2
DEF2P 1 2 WIDE
MSUB_P3 ER^eps H=0.50800000000 T=0.00050000000 RHO=0.00000000000 &
RGH=0.00000000000
S3P_S2 2 13 3 /home/crafty/dimitri/eesof/hts_bpf/model/t MTEE W1=1.00000000000 &
W2=1.00000000000 W3=1.00000000000
S3P_S3 12 11 6 /home/crafty/dimitri/eesof/hts_bpf/model/t MTEE &
W1=1.00000000000 W2=1.00000000000 W3=1.00000000000
MGAP_T11 3 7 W^wgap S=0.50800000000
MGAP_T12 6 8 W^wgap S=0.50800000000
TLINP_T9 11 2 Z^ZW L^Lhalf K^KW A^ACW F=0.00000000000 MLIN W=1.00000000000 &
L=5.00000000000
TLINP_T10 13 12 Z^ZW L^Lhalf K^KW A^ACW F=0.00000000000 MLIN W=1.00000000000 &
L=5.00000000000
TLINP_T13 8 10 Z^ZN L^Linput K^KN A^ACN F=0.00000000000 MLIN W=1.00000000000 &
L=5.00000000000
TLINP_T14 7 9 Z^ZN L^Linput K^KN A^ACN F=0.00000000000 MLIN W=1.00000000000 &
L=5.00000000000
DEF2P 10 9 RINGP
RES_R1 1 0 R^KW
DEF1P 1 TEST
S2P_S1 1 2 0 /home/crafty/dimitri/eesof/hts_ring/rngau_w4
DEF2P 1 2 WIDE_AU
TERM

PROC

MODEL
```

```
SOURCE

DCTR

FREQ
 SWEEP 4.35 4.38 7.50E-5
!SWEEP 4 13 0.0225
POWER

FILEOUT

OUTVAR

OUTEQN

OUT

 wide DB[s21] gr1
!wide_au DB[s21] gr1
 ringp DB[s21] gr1

 wide ANG[s21] gr2
!wide_au ANG[s21] gr2
 ringp ANG[s21] gr2

 wide DB[s11] gr3
!wide_au DB[s11] gr3
 ringp DB[s11] gr3

 wide ANG[s11] gr4
!wide_au ANG[s11] gr4
 ringp ANG[s11] gr4

TEST RE[Z11] SCN

GRID

HBCNTL

OPT
 RANGE 4.3575 4.365
 RINGP MODEL WIDE

YIELD

TOL
```

CHAPTER 5

AN APPLICATION OF THE PEM LOSS MODEL: AN HTS CPW LOW PASS FILTER (LPF)

5.1 The YBCO CPW LPF

In this chapter the model described in Chapter 3 is applied to an HTS CPW LPF. The layout of the filter is shown in figure 1 below. The dimensions are in microns (μm). The YBCO HTS is laid on a lanthanum aluminate substrate which measures 10x10x0.508 mm. The large enclosed areas around the narrow winding line represent the coplanar ground-plane.

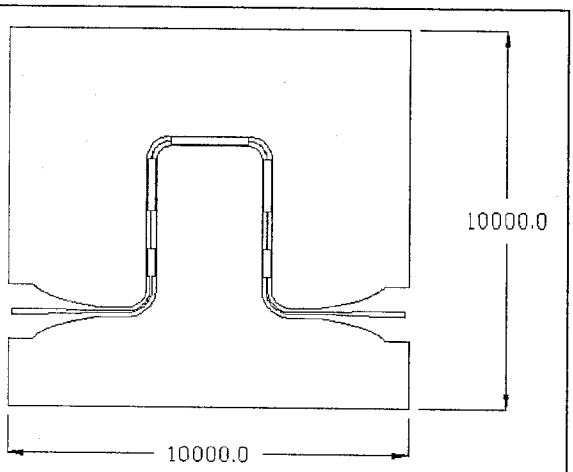

Figure 1 The layout of the HTS CPW LPF.

The narrow winding line consists of alternating high and low impedance sections of HTS CPW transmission line (narrow and wide line sections respectively), the sum of the electrical lengths of which is an odd multiple of one quarter of a wavelength, at the stop band of the filter. The CPW has a lower ground plane (i.e., the bottom face of the substrate is metalized and serves as an additional RF ground). The input and output width-tapered lines are designed to maintain a 50 Ω impedance and act as a transition from a K-connector coax-to-microstrip launch to coplanar waveguide. The CPW transmission line is meandered to minimize the area required for the circuit (since most commercially available lanthanum aluminate substrates are of this standard size and growing large uniform YBCO crystals presents a manufacturing problem). This filter was designed by W. Chew and A. L. Riley of the Spacecraft RF Development Group and the

HTS was deposited by B. D. Hunt, L. J. Bajuk and M. C. Foote of the Thin Film Physics Group at JPL for Phase I of the Naval Research Laboratory (NRL) High Temperature Superconductor Space Experiment (HTSSE). Several filters, of the same design, were fabricated. The filter 3 dB cutoff frequency varies from 7 to 9.5 GHz and the maximum stop band rejection from 40 to 50 dB, between different devices, depending on the quality of the YBCO film.

5.2 The Model

5.2.1 The Modeling Methodology

The model of the HTS CPW LPF includes several effects, for each of which material is drawn from CPW-related papers, cited in the references of this chapter. These are combined with the complex-conductivity PEM model to arrive at physical parameters that fully describe each type of CPW line used in the filter (four different types according to cross-sectional dimensions). The relevant physical parameters are the effective dielectric constant, the characteristic impedance and the exponential loss coefficient per unit length. Because of the TEM nature of the fundamental propagating mode of CPW, the first two are constant with respect to frequency, whereas the last is a function of frequency. From these physical parameters the S-parameter matrix of each type of line is derived. All of these are combined to produce an S-parameter matrix that models the overall response of the filter. The latter is done using Touchstone (TM), by EEsof Inc., a widely-used microwave CAD software package. It is important to stress that Touchstone is provided with all the pre-calculated parameters and models and its own built-in CPW models are not used. The function of Touchstone is to perform the algebraic combination of the S-parameters of the different types of transmission lines of the filter and conveniently plot the results in formats familiar to microwave designers. There are four types of CPW lines

used in the filter (the fourth type is an average of the dimensions of the 50 Ω input/output taper). The dimension variables are defined in figure 2 and the four line types and their dimensions and physical properties are listed in table 1, where Z_o is the characteristic impedance of the line, G is the incremental inductance geometric factor, as defined in chapter 3 and ε_{eff} is the effective dielectric constant of the line. The results listed in table 1 can also be found, in more detail, in appendix A of this chapter. Appendix A is a MathCAD file which calculates the characteristics of each type of line, given the physical parameters of the line (i.e., width, gap, substrate thickness, substrate dielectric constant and frequency).

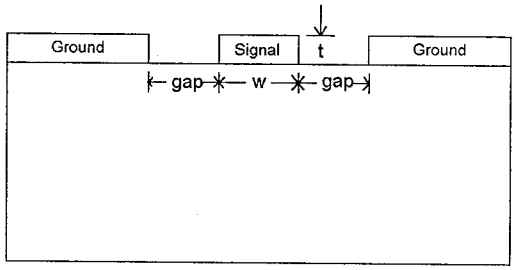

Figure 2 Definitions of CPW dimension variables.

Line Type	w (μm)	gap (μm)	Z_0 (Ω)	G	ε_{eff}
Narrow	6	122	83.4	125500	12.46
50 Ω	50	100	49.6	23500	12.52
Wide	200	25	22.6	17340	12.49
Avg. of taper	96.3	219.6	49.7	12860	12.85

Table 1 The four types of line of the filter and their properties.

To arrive at the parameters listed in table 1, four effects are included. First the parameters of a lossless CPW line without a lower ground plane are calculated using equations from K. Gupta's book [1]. Then the existence of a lower ground plane is accounted for, using equations from G. Ghione's paper [2]. Subsequently the loss, corrected impedance and dielectric constant are calculated using equations (3.34)-(3.43). The final effect which is included is dielectric loss. This is calculated assuming a dielectric loss tangent of 0.0001 (an approximate value reported in literature). The effect of dielectric loss is, however, in this case, negligible and is only included for completeness of the model.

5.2.2 The Touchstone Circuit File

Equations (3.34)-(3.43) are frequency dependent and therefore need to be calculated internal to Touchstone. They are entered in the *EQN* block of the Touchstone circuit file. A sample circuit file (also called a *netlist*) is included as appendix B of this chapter. The EQN block is the part of the circuit file where the user can define variables using equations relating variables from the *VAR* block (the part of the circuit file where constant variables are defined) and constants. The EQN block has access to *FREQ*, the sweep frequency variable. Hence the frequency dependent variables are re-calculated for each frequency of the sweep, as Touchstone calculates and plots the frequency response of the circuit under analysis. The EQN block of the HTS CPW LPF circuit file is separated into three sections, each containing equations (3.34)-(3.43) for one of the narrow, wide and 50 Ω lines respectively. Equations (3.35) and (3.36) are too long for Touchstone, so they are broken down into many smaller equations, in the circuit file. The VAR block contains the variables listed in table 1, with values calculated in the MathCAD sheet of appendix A. The convention employed for naming variables in the VAR and EQN blocks is last letter *n* for the narrow lines, *w* for the wide lines and *5* or *50* for the 50 Ω lines. The calculations provide results of the loss due to the surface resistance of the line, in dB/μm, the corrected characteristic impedance and the corrected effective dielectric constant, for each type of line. These are fed into the *TLINP* Touchstone element, which models a physical transmission line of known impedance, effective dielectric constant, length and attenuation coefficient. The TLINP element emulates a propagating mode of the form $e^{(-\alpha z - j\beta z)}$ of a given characteristic impedance. Six TLINP elements, each given the true length of the line it models, model the six lines of half of the filter. They are connected via two-port S-parameter files that model the discontinuity that is presented to the propagating wave by the changes of the line widths. These two-port S-parameter files where calculated using *EM* by Sonnet Software Inc [3]. EM is an electromagnetic analysis software package

which uses an analytical full-wave numerical approach to analyze stratified planar enclosed microwave circuits. This analytical full-wave numerical approach invokes a Galerkin method of moments technique which develops the dyadic Green's function operator as a bi-dimensional infinite vectorial summation of homogeneous rectangular waveguide eigenfunctions, resulting in a subsectional technique making use of roof-top expansion and testing functions that are closely related to spectral domain techniques. A similar analysis, using EM, is performed for the input and output 50 Ω tapers, and they are included as S-parameter files as well. However, since the EM analysis assumes perfect conductors (or loss proportional to the square root of frequency, which would be inappropriate in this case), the input and output tapers contribute some loss which would be ignored. To model this unaccounted-for loss two extra TLINP elements are included at the input; one has the negative length of the other. One of the TLINP elements contributes the calculated loss while the other is made lossless, but one cancels the phase of the other so that the total phase of the two is zero. The total filter is modeled by a cascade of the half filter model back-to-back with itself. This is possible because the filter is symmetric about an axis through its mid-point.

5.2.3 The Modeling Strategy

The two most important unknowns used in modeling the YBCO HTS, are the normal conductivity, σ_n and the zero temperature penetration depth, λ_o. Applied physics researchers who grow extra pure single crystal YBCO report a λ_o.of 140 nm and a σ_n of $1.14 \cdot 10^6$ S/m [4]. This is, however, the penetration depth in the very pure, single crystal limit. The YBCO crystal deposited at JPL to make the CPW LPF is not a single crystal and the controlled laboratory conditions under which it was deposited are not state-of-the-art. As a result the crystal grows in many separate grains and there is a surface energy associated with the boundaries between different grains. The existence of grains and grain

boundaries causes the penetration depth to be non-uniform over the surface of the circuit and larger than in the pure single crystal case [5]. Imperfections and contaminants in the crystal also increase the penetration depth. However, if the variations occur in an area that is spatially small compared to the wavelength, they can be averaged out and an overall effective penetration depth may be used. Polakos et al. from AT&T Bell Labs report an effective penetration depth of 450 nm for a similarly deposited HTS microstrip circuit [6].

In the initial modeling attempts the value of Polakos was used for the penetration depth and the value of reference [4] for the normal conductivity. The fit between modeled and measured response data was already very close, within 0.6 dB in magnitude of S21 and 0.5 radians in the angle of S21. However, the uncertainty of a precise value for T_c, the critical temperature of the YBCO, imposes a corresponding uncertainty window on the zero temperature penetration depth, λ_o and the normal conductivity, σ_n over which the response is optimized for a minimum integrated squared error best fit. More specifically, the critical temperature of the YBCO films was found to be in the range from 83 to 88 K, using DC measurements that were made before packaging. However the precise value for each film was not recorded. All measurements of the S-parameters of the HTS CPW LPFs, which are used for modeling and fitting, were made at liquid nitrogen (LN_2) temperature (77 K). For modeling, a value of 77 K is assumed for T and 85 K for T_c. The inaccuracy in the latter assumption is about an 4.9% difference in λ_o and 4.7% difference in σ_n per degree of difference of T_c from its true value. Hence the 5 K window of uncertainty in T_c corresponds to a 110 nm window of uncertainty in λ_o and a 270000 S/m window of uncertainty in σ_n. The optimum extracted values of these parameters, for one of the devices are

λ_o=483 nm

σ_n=1.8x10^6 S/m.

Both values are within their uncertainty window from Polakos' values. Another parameter that is optimized for minimum integrated square error between the modeled and measured S-parameters is the line length of the 50 Ω input and output tapers, for best phase match. It is important to point out that the qualities of the various YBCO films, as extracted by the above optimization method performed on the various devices, vary considerably. The zero-temperature penetration depth varies in the range from 400 to 700 nm and the normal conductivity in the range $0.5 \cdot 10^6$ to $4 \cdot 10^6$. These ranges are relatively large and point to the need for more repeatability in the YBCO deposition process, but they may be smaller than they seem, if variations in the critical temperature of the YBCO films are taken into account.

5.3 Comparison of Model versus Measurement

5.3.1 S-parameters versus Frequency

The following figures contain a comparison of the results of the modeling and the measured data, using the optimum values reported above. Figure 3 shows a comparison of the insertion loss (magnitude of S21) of two CPW LPFs of identical layout, one made of YBCO and the other of silver. To make the comparison fair, both the silver and the YBCO are at the LN_2 temperature of 77 K. Obviously, in this case, the best efforts of the normal metal do not match the performance of the HTS. The difference in cutoff frequency is due to the kinetic inductance of the HTS, which is successfully modeled by equation (3.36).

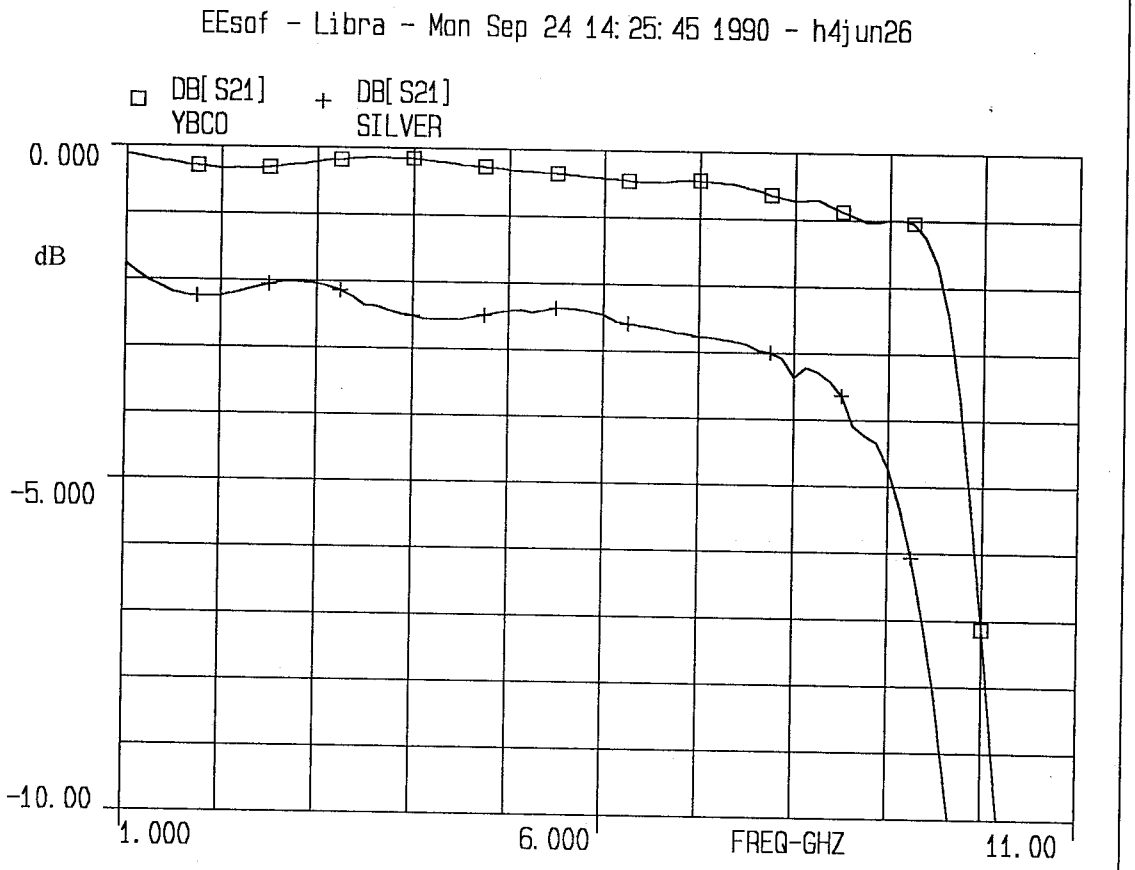

Figure 3 Comparison of insertion loss of silver and YBCO filters.

Figure 4 shows a comparison of the measured versus modeled magnitude of the insertion loss (S21) plotted on a vertical dB scale.

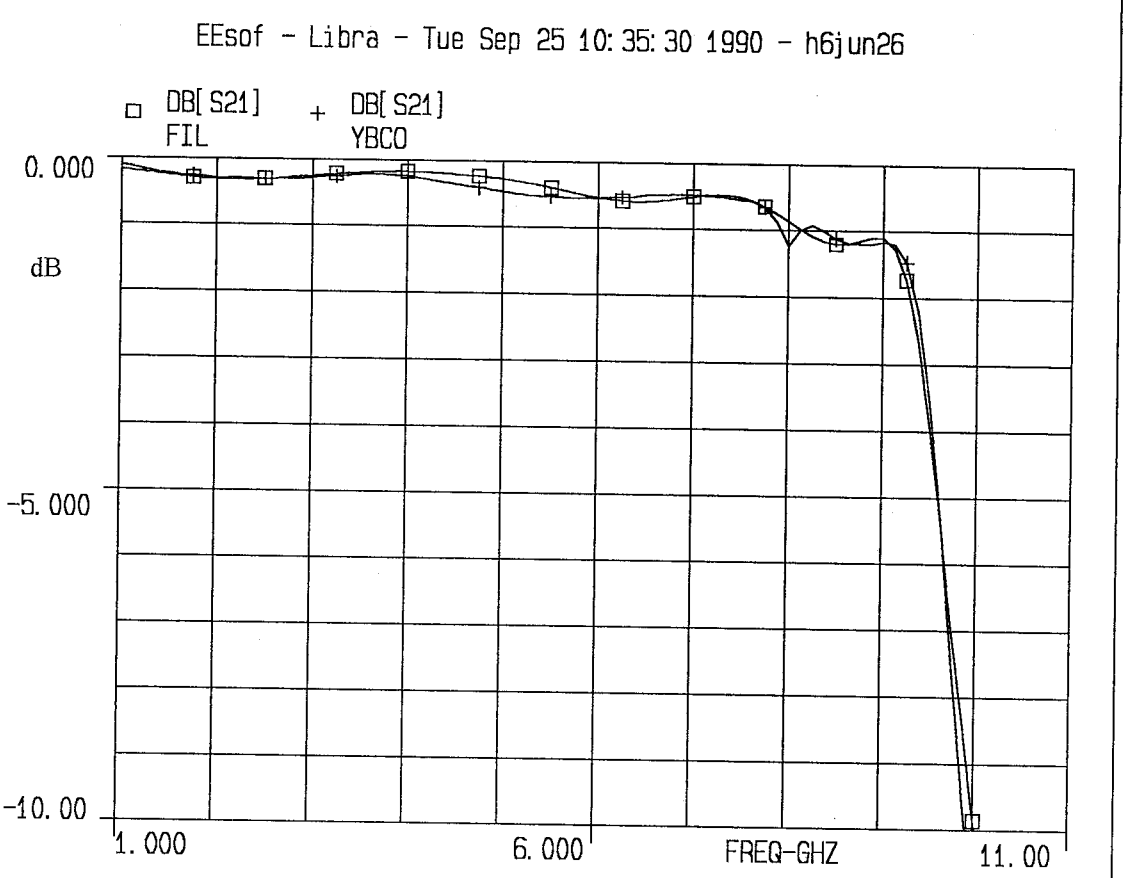

Figure 4 Measured (YBCO) versus modeled (FIL) magnitude of S21.

Figure 5 shows a comparison of the measured versus modeled phase (angle) of S21. The vertical scale is in radians.

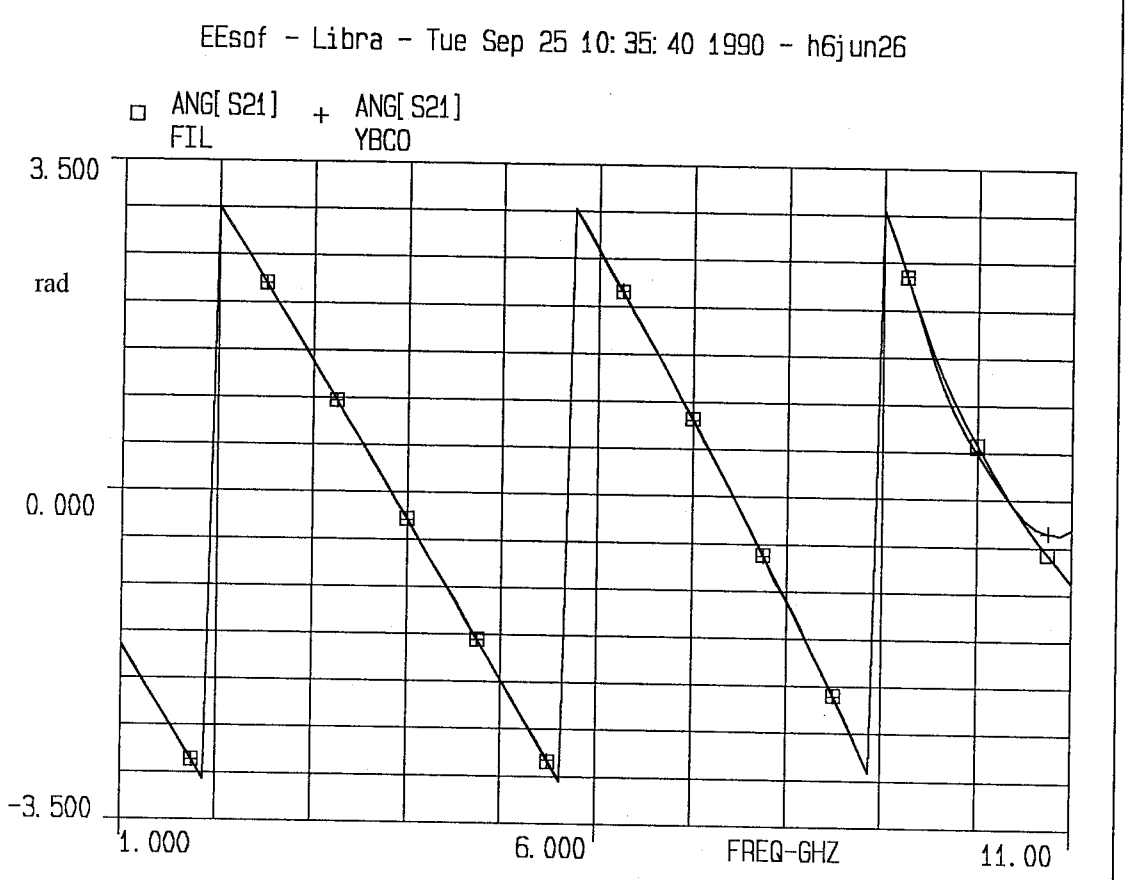

Figure 5 Measured (YBCO) versus modeled (FIL) angle of S21.

Figure 6 shows a comparison of the measured versus modeled magnitude of the return loss (S11) plotted on a vertical dB scale.

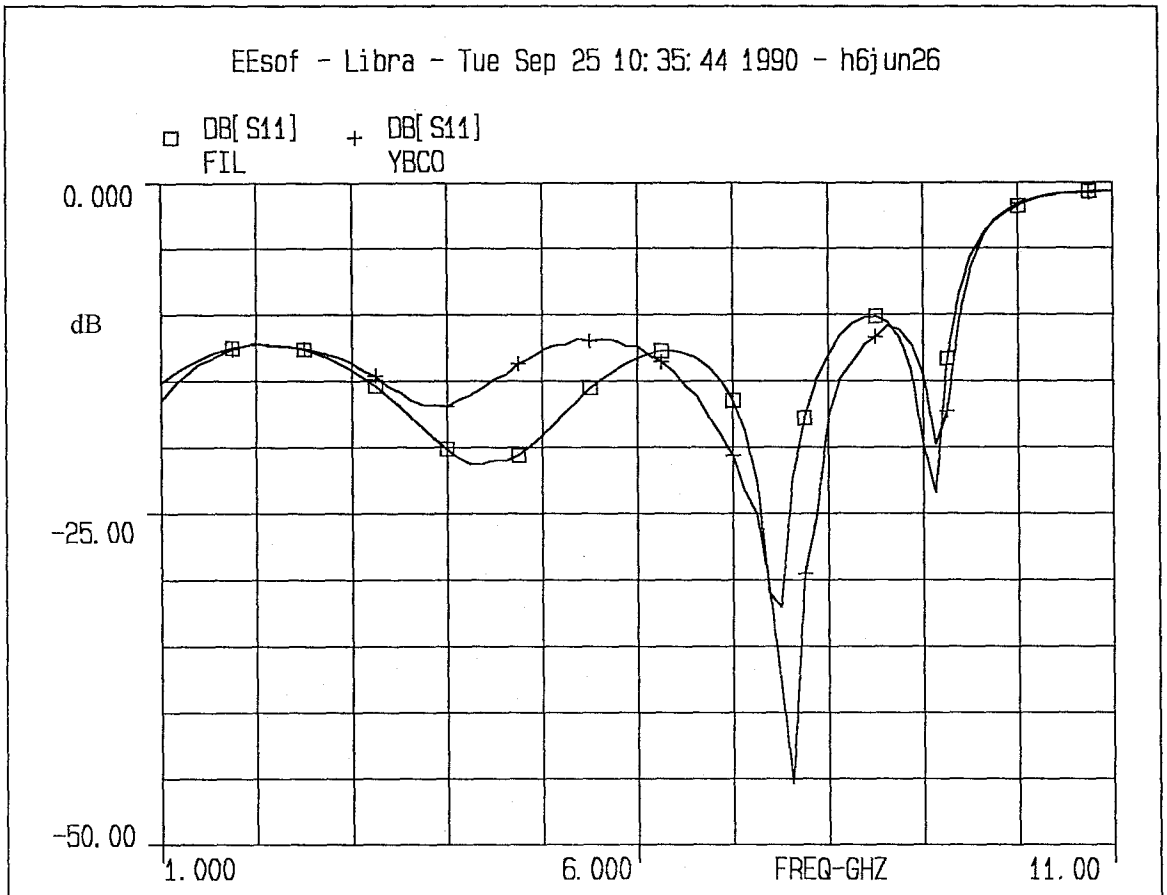

Figure 6 Measured (YBCO) versus modeled (FIL) magnitude of S11.

Figure 7 shows a comparison of the measured versus modeled angle of S11. The vertical scale is in radians.

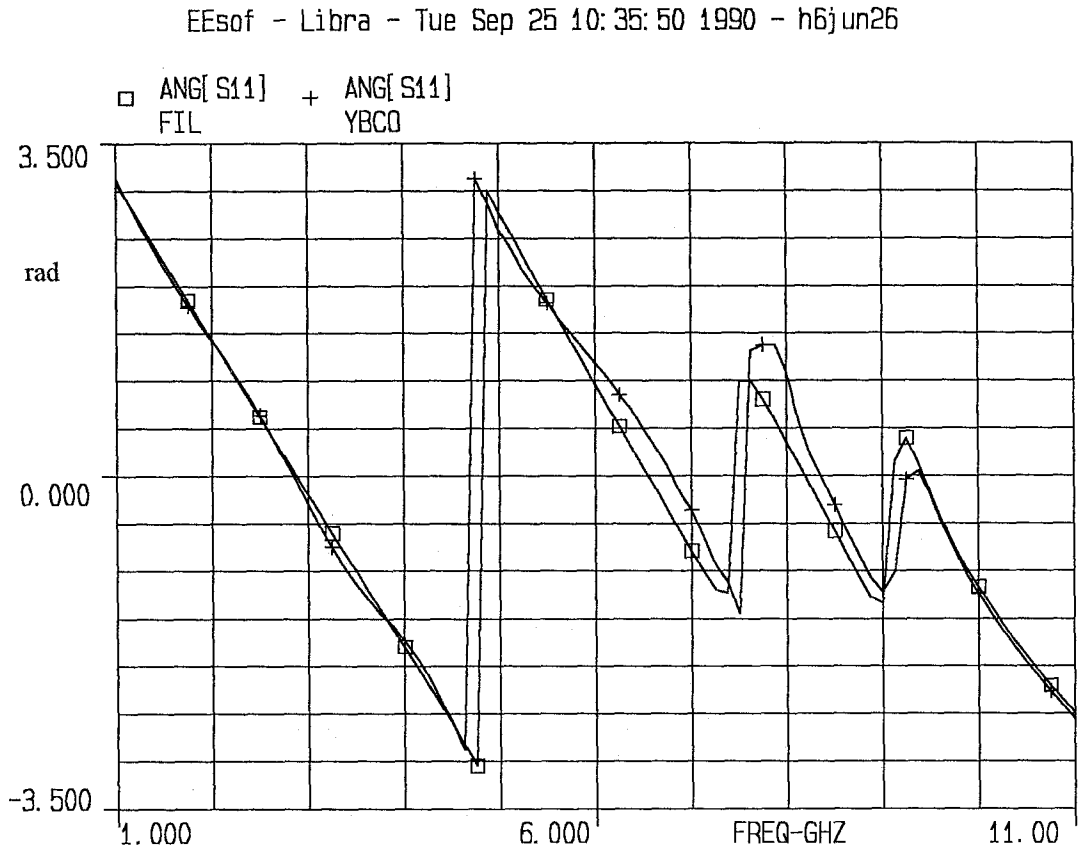

Figure 7 Measured (YBCO) versus modeled (FIL) angle of S11.

Figure 8 shows a comparison of the measured versus modeled S21, plotted on a Smith chart of radius 1.

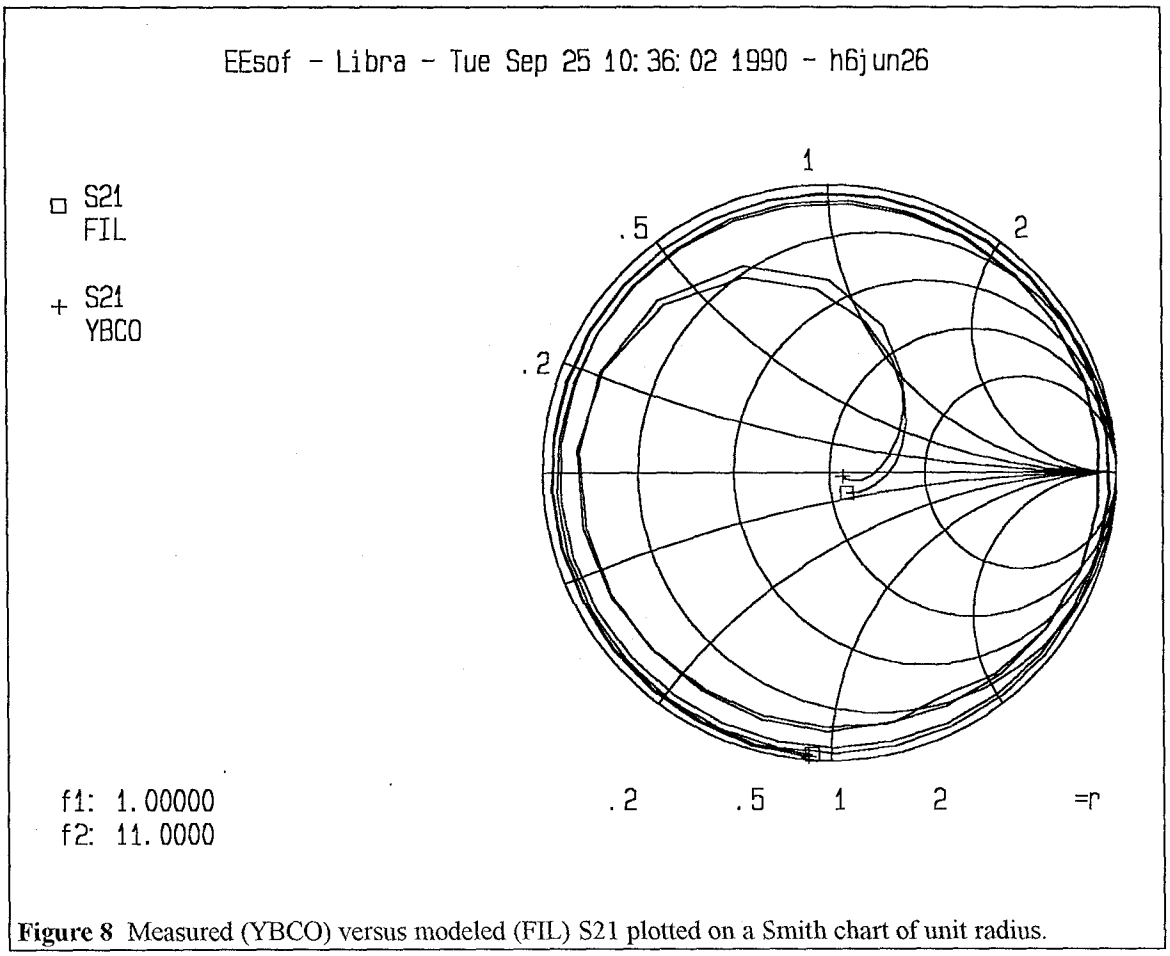

Figure 8 Measured (YBCO) versus modeled (FIL) S21 plotted on a Smith chart of unit radius.

5.3.2 Temperature Dependence of the Insertion Loss

In addition to measurements taken at a constant 77 K temperature, with the hermetically packaged HTS CPW LPFs immersed in LN_2, another set of measurements was taken at different temperatures in the range from 15 to 95 K, in the vacuum jacket of a closed cycle refrigerator. However, in these measurements the connecting cables inside the refrigerator and the air-tight connectors could not be calibrated out, so their insertion loss and insertion phase is included in the measured S-parameters. This insertion loss, which is about 4 dB and increases slowly with frequency, may be neglected at frequencies where the insertion loss of the HTS CPW LPF is itself sufficiently greater than 4 dB. Therefore, this measured data should only be used beyond the pass band of the filter (say 9.5-11

GHz). The data is used for a comparison of the measured versus predicted temperature dependence of the insertion loss of the filter, with the understanding that because of the lack of an accurate calibration, the comparison is qualitative only. For this reason the measured and predicted insertion losses are not superimposed, as is done hitherto, but are plotted in two separate figures. It is important to stress that no optimization is performed in this case. The extracted optimized parameters from section 5.2.3 are used and the only variable that is varied is T. Figures 9 and 10 show the measured and predicted insertion losses of the same filter respectively, at temperature 50, 60, 70 and 80 K.

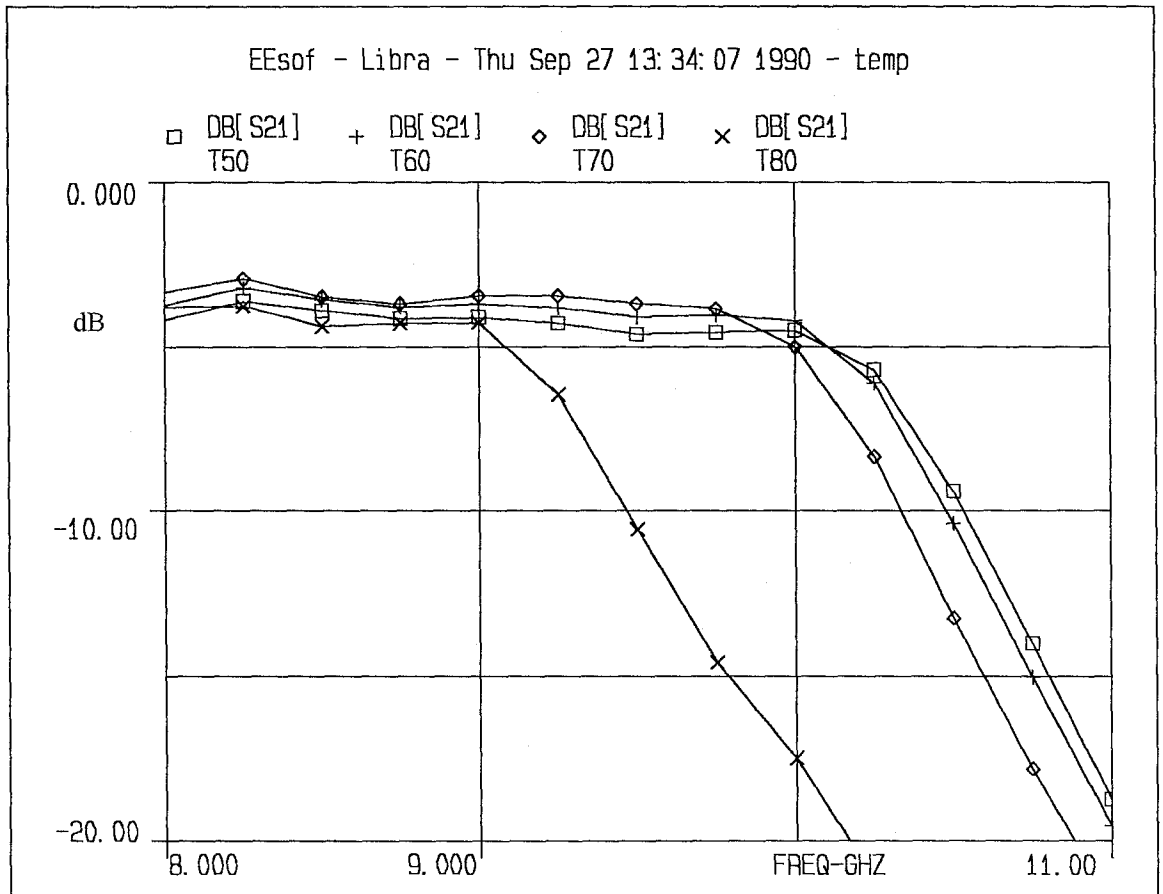

Figure 9 Measured magnitude of the insertion loss at 50, 60, 70 and 80 K.

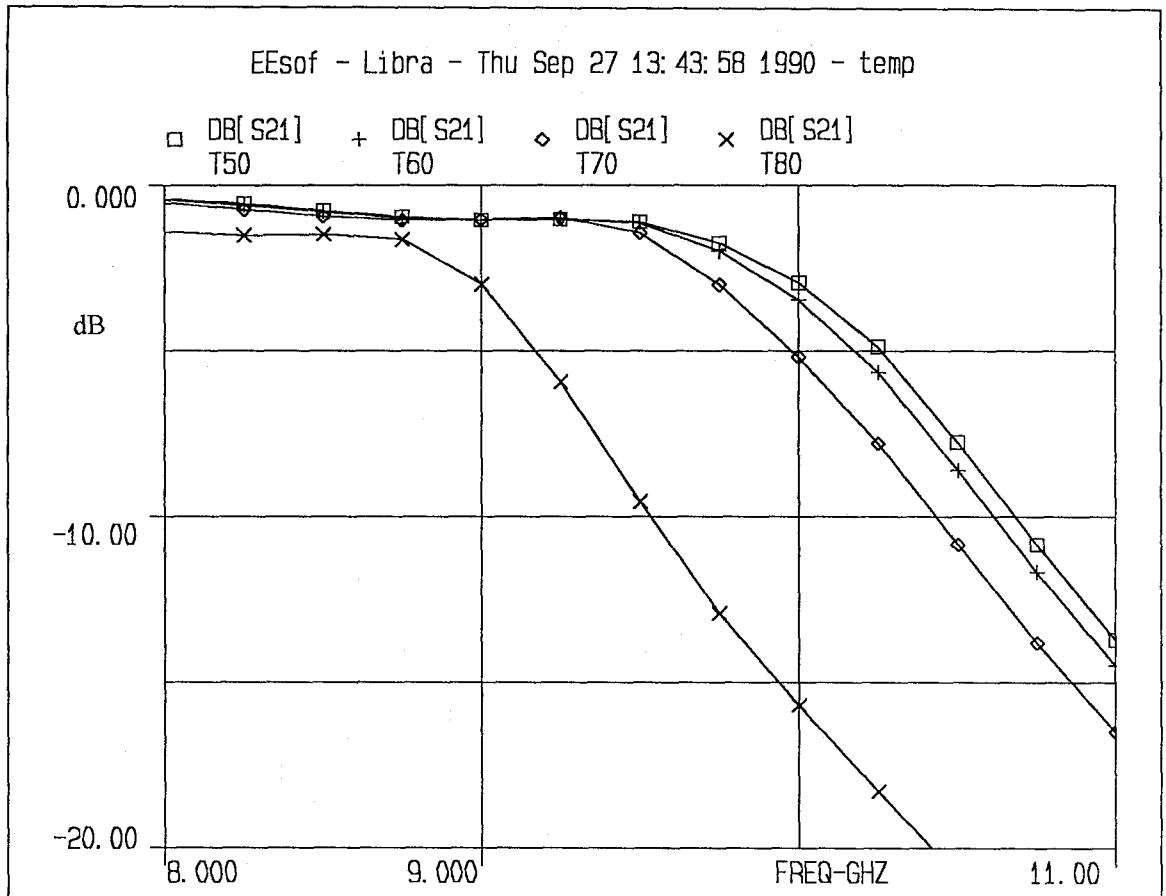

Figure 10 Predicted magnitude of the insertion loss at 50, 60 70 and 80 K.

The essential features of figure 9 are captured in figure 10. The non-uniform shift of the cut-off frequencies with respect to temperature and the almost parallel slopes of the response in the stop band are similar in the two figures. The slopes in figure 9 are a little steeper than those in figure 10, but this is to be expected since the cable and connector losses, which are not calibrated out of the data of figure 9, are an increasing function of frequency.

5.4 References

[1] K. Gupta, R. Garg and I. Bahl, *Microstrip Lines and Slotlines*, Artech, Dedham, MA, 1979.

[2] G. Ghione and C. Naldi, "Parameters of Coplanar Waveguides with Lower Ground Plane," Electronics Letters, Vol. 19, pp. 179-181, September 1983.

[3] J. C. Rautio and R. F. Harrington, "An Electromagnetic Time-Harmonic Analysis of Shielded Microstrip Circuits," IEEE Transactions on Microwave Theory and Techniques, Vol. MTT-35, pp. 726-730, Aug. 1987.

[4] D. R. Harshman et al., "Magnetic Penetration Depth in Single Crystal $YBa_7Cu_3O_7$," Physical Review, Vol. B39, p. 2596.

[5] T. L. Hylton and M. R. Beasley "Effect of Grain Boundaries on Magnetic Field Penetration in Polycrystalline Superconductors," Physical Review, Vol B39, pp. 9042-9048, May 1989.

[6] P. A. Polakos, C. E. Rice, M. V. Schneider and R. Trambarulo, "Electrical Characteristics of Thin-Film $Ba_2YCu_3O_7$ Superconducting Ring Resonators," Microwave & Guided Wave Letters, Vol. 1, 1991.

[7] D. Antsos, "Modeling of Planar Quasi-TEM Superconducting Transmission Lines," JPL New Technology Report, NASA Case No. NPO-D-18418, JPL Case No. 7950, January 1991.

[8] D. Antsos, "Equations for Designing Superconducting Transmission Lines," NASA Tech Briefs Journal, Vol. 16, No. 8, p. 30, August 1992.

[9] D. Antsos, W. Chew et al., "Modeling of Planar Quasi-TEM Superconducting Transmission Lines," IEEE Transactions on Microwave Theory and Techniques, Vol. 40, No. 6, pp. 1128-1132, June 1992.

[10] W. Chew, A. L. Riley et al., "Design and Performance of a High-T_c Superconductor Coplanar Waveguide Filter," IEEE Transactions on Microwave Theory and Techniques, Vol. 39, No. 9, pp. 1455-1461, September 1991.

Appendix A

Sample MathCAD File Used to Calculate the Parameters of the CPW Lines of the LPF

Coplanar waveguide parameters with losses for thin conductor
20 Sept 1990

The following effects are included:

EFFECT:	REFERENCE:
CPW (No loss, no ground plane)	K. C Gupta
Lower Ground Plane	G. Ghione
Loss for cond thickness of order of penetration depth	H. Lee

Define the elliptic integral:

$$K(k) := \int_0^{\frac{\pi}{2}} \frac{1}{\sqrt{1 - k^2 \cdot \sin[\phi]^2}} \, d\phi$$

$$K'(k) := K\left[\sqrt{1 - k^2}\right]$$

$$KK'(k) := \frac{K(k)}{K'(k)}$$

Parameters to use:

Substrate permittivity

$\varepsilon\rho := 24$ $\quad i := 1..4$

CPW Line Widths of Center Conductor

$w_i :=$

$6 \cdot 10^{-6}$	Narrow, high imp line
$50 \cdot 10^{-6}$	50 Ohm line
$200 \cdot 10^{-6}$	Wide, lo imp line
$96.29 \cdot 10^{-6}$	Average of 50 Ohm taper

Substrate thickness

$h := 0.500 \cdot 10^{-3}$

Conductor thickness

$t := 0.5 \cdot 10^{-6}$

Size of differential for calculating
the incremental inductance geometric factor G

$$\delta\text{νορμαλ} := \frac{t}{1000}$$

$$\eta\delta := h + \delta\text{νορμαλ}$$

$$\tau\delta := t - 2 \cdot \delta\text{νορμαλ}$$

$$\tau\delta = 4.99 \cdot 10^{-7}$$

Thickness effect

$$Delta_i := \left[\frac{1.25 \cdot t}{\pi}\right] \cdot \left[1 + \ln\left[\frac{4 \cdot \pi \cdot w_i}{t}\right]\right]$$

$$\Delta\varepsilon\lambda\tau\alpha\delta_i := \left[\frac{1.25 \cdot \tau\delta}{\pi}\right] \cdot \left[1 + \ln\left[\frac{4 \cdot \pi \cdot \left[w_i - 2 \cdot \delta\text{νορμαλ}\right]}{\tau\delta}\right]\right]$$

$$aeff_i := \frac{w_i + Delta_i}{2} \qquad gap_i := \frac{250 \cdot 10^{-6} - w_i}{2}$$

$$beff_i := \frac{w_i}{2} + gap_i - \frac{Delta_i}{2} \qquad gap_4 := 219.55 \cdot 10^{-6}$$

$$k_i := \frac{aeff_i}{beff_i} \qquad k'_i := \sqrt{1 - \left[k_i\right]^2}$$

$$k1_i := \frac{\tanh\left[\frac{\pi \cdot aeff_i}{2 \cdot h}\right]}{\tanh\left[\frac{\pi \cdot beff_i}{2 \cdot h}\right]}$$

$$\alpha\varepsilon\phi\phi\delta_i := \frac{w_i + \Delta\varepsilon\lambda\tau\alpha\delta_i}{2} - \delta\text{νορμαλ}$$

$$\beta\varepsilon\phi\phi\delta_i := \frac{w_i}{2} + gap_i - \frac{\Delta\varepsilon\lambda\tau\alpha\delta_i}{2} + \delta\text{νορμαλ}$$

$$\kappa\delta_i := \frac{\alpha\varepsilon\phi\phi\delta_i}{\beta\varepsilon\phi\phi\delta_i} \qquad \gamma\alpha\pi\delta_i := gap_i + 2 \cdot \delta\text{νορμαλ}$$

$$\kappa 1\delta_i := \frac{\tanh\left[\frac{\pi \cdot \alpha\varepsilon\phi\phi\delta_i}{2 \cdot h}\right]}{\tanh\left[\frac{\pi \cdot \beta\varepsilon\phi\phi\delta_i}{2 \cdot h}\right]}$$

Constants

$\sigma_{A\gamma} := 6.17 \cdot 10^{7}$ Conductivity of Silver

$\sigma_{X\upsilon} := 5.8 \cdot 10^{7}$ Conductivity of Copper

$\mu 0 := 4 \cdot \pi \cdot 10^{-7}$

$\varepsilon 0 := 8.854 \cdot 10^{-12}$

$c := \frac{1}{\sqrt{\mu 0 \cdot \varepsilon 0}}$ $c = 2.998 \cdot 10^{8}$

$\eta 0 := \sqrt{\frac{\mu 0}{\varepsilon 0}}$ $\eta 0 = 376.734$

$\lambda 0_{\Psi BXO} := 5660 \cdot 10^{-10}$

$T := 77$

$T_c := 85$

$f := 1 \cdot 10^{9}$

$\sigma v := 1.14 \cdot 10^{6}$

$$\sigma_{\Psi BXO} := \sigma v \cdot \left[\frac{T}{T_c}\right]^4 - j \cdot \frac{1 - \left[\frac{T}{T_c}\right]^4}{2 \cdot \pi \cdot f \cdot \mu 0 \cdot \lambda 0_{\Psi BXO}{}^2}$$

$\sigma := \sigma_{\Psi BXO}$ $\sigma = 7.677 \cdot 10^{5} - 1.291 \cdot 10^{8}\, i$

$$Zs := \sqrt{j \cdot 2 \cdot \pi \cdot f \cdot \frac{\mu 0}{\sigma}}$$

$Rs := Re(Zs)$

$Zs = 2.325 \cdot 10^{-5} + 0.008i$

Find effective permittivity and impedance

$$\varepsilon\varepsilon\phi\phi\chi\pi\omega_i := \frac{1 + \frac{\varepsilon\rho}{KK'[k_i]} \cdot KK'[k1_i]}{1 + \frac{KK'[k1_i]}{KK'[k_i]}}$$

$\varepsilon\varepsilon\phi\phi\chi\pi\omega_i$

12.558
12.594
12.627
12.884

$$\varepsilon\varepsilon\phi\phi\tau_i := \varepsilon\varepsilon\phi\phi\chi\pi\omega_i - \frac{0.7 \cdot [\varepsilon\varepsilon\phi\phi\chi\pi\omega_i - 1] \cdot \left[\frac{t}{gap_i}\right]}{KK'[k_i] + 0.7 \cdot \left[\frac{t}{gap_i}\right]}$$

$$\varepsilon\varepsilon\phi\phi\tau\delta_i := \varepsilon\varepsilon\phi\phi\chi\pi\omega_i - \frac{0.7 \cdot [\varepsilon\varepsilon\phi\phi\chi\pi\omega_i - 1] \cdot \left[\frac{\tau\delta}{\gamma\alpha\pi\delta_i}\right]}{KK'[\kappa\delta_i] + 0.7 \cdot \left[\frac{\tau\delta}{\gamma\alpha\pi\delta_i}\right]}$$

$$Zcpw_i := \left[\frac{60 \cdot \pi}{\sqrt{\varepsilon\varepsilon\phi\phi\tau_i}}\right] \cdot \frac{1}{KK'[k_i] + KK'[k1_i]}$$

$$Z\chi\pi\omega\delta_i := \left[\frac{60 \cdot \pi}{\sqrt{\varepsilon\varepsilon\phi\phi\tau\delta_i}}\right] \cdot \frac{1}{KK'[\kappa\delta_i] + KK'[\kappa1\delta_i]}$$

$$G_i := \left[\frac{1}{\eta 0}\right] \cdot \frac{\sqrt{\varepsilon\varepsilon\phi\phi\tau_i} \cdot [Z\chi\pi\omega\delta_i - Zcpw_i]}{\delta\nu o\rho\mu\alpha\lambda}$$

$A_i := w_i \cdot t$

$\zeta := (1 + j) \cdot \sqrt{\pi \cdot f \cdot \mu 0 \cdot \sigma}$

$$Zi_i := Zs \cdot G_i \cdot \coth\left[\zeta \cdot G_i \cdot A_i\right]$$

w_i	$Zcpw_i$	$\varepsilon\varepsilon\phi\phi\tau_i$	Zi_i	G_i
$6 \cdot 10^{-6}$	83.382	12.455	$15.358 + 2.705i \cdot 10^3$	$1.255 \cdot 10^5$
$5 \cdot 10^{-5}$	49.555	12.519	$1.847 + 345.315i$	$2.35 \cdot 10^4$
$2 \cdot 10^{-4}$	22.642	12.488	$0.519 + 144i$	$1.734 \cdot 10^4$
$9.629 \cdot 10^{-5}$	49.711	12.847	$0.96 + 181.307i$	$1.286 \cdot 10^4$

$$L_i := Zcpw_i \cdot \left[\frac{\sqrt{\varepsilon\varepsilon\phi\phi\tau_i}}{c}\right] + \left[\frac{Im\left[Zi_i\right]}{2 \cdot \pi \cdot f}\right]$$

$$C_i := \left[\frac{\sqrt{\varepsilon\varepsilon\phi\phi\tau_i}}{c}\right] \cdot \left[\frac{1}{Zcpw_i}\right]$$

$$R_i := Re\left[Zi_i\right]$$

$Im\left[Zi_i\right]$	R_i
$2.705 \cdot 10^3$	15.358
345.315	1.847
144	0.519
181.307	0.96

$$Z0_i := \sqrt{\frac{L_i}{C_i}}$$

$Z0_i$
100.01
51.831
23.594
50.904

Ohmic, penetration depth-induced losses

$$\alpha\chi_i := \frac{Re\left[Zi_i\right]}{2 \cdot \sqrt{\frac{L_i}{C_i}}}$$

$\alpha\chi_i$
0.077
0.018
0.011
0.009

$$\alpha\chi\delta B_i := 8.686 \cdot \alpha\chi_i$$

$$\lambda := \frac{c}{f}$$

$$\tau\alpha\nu\delta := 0.0001$$

Dielectric Losses

$$\alpha\delta\delta B_i := \frac{27.3 \cdot \varepsilon\rho \cdot \left[\varepsilon\varepsilon\phi\phi\tau_i - 1 \right] \cdot \tau\alpha\nu\delta}{\sqrt{\varepsilon\varepsilon\phi\phi\tau_i} \cdot \left[\varepsilon\rho - 1 \right] \cdot \lambda}$$

$$\alpha\delta\delta B\_\upsilon\mu_i := 10^{-6} \cdot \alpha\delta\delta B_i$$

$$\alpha\chi\delta B\_\upsilon\mu_i := 10^{-6} \cdot \alpha\chi\delta B_i$$

$$\alpha\delta\delta B\_\upsilon\mu = \begin{bmatrix} 0 \\ 3.084 \cdot 10^{-8} \\ 3.093 \cdot 10^{-8} \\ 3.089 \cdot 10^{-8} \\ 3.141 \cdot 10^{-8} \end{bmatrix} \cdot \left[\frac{f}{10^9} \right] \qquad \alpha\chi\delta B\_\upsilon\mu = \begin{bmatrix} 0 \\ 6.669 \cdot 10^{-7} \\ 1.547 \cdot 10^{-7} \\ 9.547 \cdot 10^{-8} \\ 8.187 \cdot 10^{-8} \end{bmatrix} \cdot \left[\frac{f}{10^9} \right]^2$$

$$Li_i := \frac{\mathrm{Im}\left[Zi_i \right]}{2 \cdot \pi \cdot f}$$

Li_i

$4.305 \cdot 10^{-7}$
$5.496 \cdot 10^{-8}$
$2.292 \cdot 10^{-8}$
$2.886 \cdot 10^{-8}$

$$EFF_i := \sqrt{\frac{L_i}{L_i - Li_i}}$$

EFF_i

1.199
1.046
1.042
1.024

$$\varepsilon\varepsilon\phi\phi\tau\nu\varepsilon\omega_i := \varepsilon\varepsilon\phi\phi\tau_i \cdot \left[EFF_i \right]^2$$

$\varepsilon\varepsilon\phi\phi\tau\sigma\kappa\iota\nu_i := c^2 \cdot L_i \cdot C_i$

$\varepsilon\varepsilon\phi\phi\tau\nu\varepsilon\omega_i$
17.917
13.695
13.561
13.47

$\varepsilon\varepsilon\phi\phi\tau\sigma\kappa\iota\nu_i$
17.917
13.695
13.561
13.47

$Zcpwskin_i := \sqrt{\frac{R_i + j \cdot 2 \cdot \pi \cdot f \cdot L_i}{j \cdot 2 \cdot \pi \cdot f \cdot C_i}}$

$Zcpwskin_i$
100.01 - 0.087i
51.831 - 0.012i
23.594 - 0.003i
50.904 - 0.006i

Appendix B

Sample Touchstone Circuit file

```
! MODEL OF THE YBCO FILTER FIT TO DATA USING LOSS AND LOSS TANGENT
! ALSO USING S2P FILE FOR 50 OHM TAPER K-CONNECTOR TO CPWG INTERFACE
! USING EXACT EQUATIONS FOR ALL ATTENUATIONS AS A FUNCTION OF LD AND Sn
! BY DIMITRIOS ANTSOS ( SEPTEMBER 20,1990 )


DIM
 LNG UM
 ANG RAD
VAR
 LD# 1000E-10 4.83e-07 10000E-10      !PENETRATION DEPTH FOR YBCO
 T = 77                          !TEMPERATURE OF MEASUREMENT
 Tc = 85                         !Critical Temperture of Sample
 Sn #1E4  1791776. 1E8             !Normal Conductivity of Sample
 LI  # 2000 3730.566 3800          ! Does not affect phase, only taper loss
 L50 # 1800 2241.989 2400           ! = 2006.4 on circuit
 ACI0 =  8.30e-08                 ! COPPER LOSS OF INPUT TAPER (8.3e-8)
 ADI00 =  0.000500                 ! = 3.14e-4

        ! CONSTANTS
 e0 = 8.854E-12                  !Permittivity of free space
 AGn = 5e-12                     !Dimension Variable ( Narrow Line )
 Gn = 8.43479e4                   !Incremental Inductance Rule Var (Narr
 AGw = 1e-10
 Gw = 1.7336e4
 AG5 = 2.5e-11
 G5 = 2.3501e4

 Z500 = 49.56
 ZN0  = 83.38
 ZW0  = 22.64

 KI = 12.847

 K500 = 12.52
 KN0  = 12.455
 KW0  = 12.49

 L1  = 720.8
 L2  = 997.0
 L3  = 1369.7
 L4  = 761.3
 L5H = 924.0

 TAND =  0.000100

EQN

 ADN0 = 3.086E-4*TAND
 AD500 = 3.093E-4*TAND
 ADW0 = 3.089E-4*TAND

 ADI0 = ADI00*TAND       ! DIELECTRIC LOSS OF INPUT CPW 50 OHM TAPER
```

```
LI1 = -LI

AI  = ACI0  * FREQ**2 + ADI0 * FREQ


! Computation of exact loss for narrow line
!      Constants

U0 = 4*PI*1e-7              !Magnetic Permeability of vacuum
f = FREQ*1e9                !Frequency in Hz
Sr = Sn*(T/Tc)**4           !Real Part of conductivity of YBCO
Si = (1-(T/Tc)**4)/(2*PI*f*U0*LD**2)  !Imaginary Part of conductivity
P = ATAN(Si/Sr)-2*PI        !Angle of conductivity
Th= PI/4-P/2                !Auxiliary angle definition
r = SQRT(SQR(Sr)+SQR(Si))   !Norm of conductivity
c = 1/sqrt(e0*U0)           !Velocity of light

!      Narrow Line Parameters
Bn= Gn*AGn*SQRT(2*PI*f*U0*r)  !Fudge Factors
Cn= EXP(2*Bn*COS(Th))
Dn= COS(2*Bn*SIN(Th))
En= SIN(2*Bn*SIN(Th))
Un= SQRT(SQR(Cn*Dn-1)+SQR(Cn*En))
Wn= ATAN(Cn*En/(Cn*Dn-1))
Fn= Bn/(AGn*r*Un)
Mn= 2*Bn*SIN(Th)
Nn= COS(PI/4+P/2-Wn)
Rn= COS(Mn+PI/4+P/2-Wn)

ReZn = Fn*(Nn+Cn*Rn)        !Real Part of Internal Impedance / Meter
NIn= SIN(PI/4+P/2-Wn)
RIn= SIN(Mn+PI/4+P/2-Wn)
ImZn = Fn*(NIn+Cn*RIn)
Zn = SQRT(SQR(ZN0)-(c*ZN0)/(2*PI*SQRT(KN0)*f)*ImZn)
ACN = -(8.686e-6) * ReZn/(2*Zn)

EFFN = ZN / ZN0

!      Wide Line Parameters
Bw= Gw*AGw*SQRT(2*PI*f*U0*r)  !Fudge Factors
Cw= EXP(2*Bw*COS(Th))
Dw= COS(2*Bw*SIN(Th))
Ew= SIN(2*Bw*SIN(Th))
Uw= SQRT(SQR(Cw*Dw-1)+SQR(Cw*Ew))
Ww= ATAN(Cw*Ew/(Cw*Dw-1))
Fw= Bw/(AGw*r*Uw)
Mw= 2*Bw*SIN(Th)
Nw= COS(PI/4+P/2-Ww)
Rw= COS(Mw+PI/4+P/2-Ww)

ReZw = Fw*(Nw+Cw*Rw)        !Real Part of Internal Impedance / Meter
NIw= SIN(PI/4+P/2-Ww)
```

```
  RIw= SIN(Mw+PI/4+P/2-Ww)
  ImZw = Fw*(NIw+Cw*RIw)
  Zw = SQRT(SQR(Zw0)-(c*Zw0)/(2*PI*SQRT(Kw0)*f)*ImZw)
  ACw = -(8.686e-6) * ReZw/(2*Zw)

  EFFw = Zw / Zw0

!     50 Ohm Line Parameters
  B5= G5*AG5*SQRT(2*PI*f*U0*r)   !Fudge Factors
  C5= EXP(2*B5*COS(Th))
  D5= COS(2*B5*SIN(Th))
  E5= SIN(2*B5*SIN(Th))
  U5= SQRT(SQR(C5*D5-1)+SQR(C5*E5))
  W5= ATAN(C5*E5/(C5*D5-1))
  F5= B5/(AG5*r*U5)
  M5= 2*B5*SIN(Th)
  N5= COS(PI/4+P/2-W5)
  R5= COS(M5+PI/4+P/2-W5)

  ReZ5 = F5*(N5+C5*R5)          !Real Part of Internal Impedance / Meter
  NI5= SIN(PI/4+P/2-W5)
  RI5= SIN(M5+PI/4+P/2-W5)
  ImZ5 = F5*(NI5+C5*RI5)
  Z50= SQRT(SQR(Z500)-(c*Z500)/(2*PI*SQRT(K500)*f)*ImZ5)
  AC50 = -(8.686e-6) * ReZ5/(2*Z50)

  EFF50 = Z50 / Z500

  K50  = K500 * EFF50 * EFF50
  KN   = KN0  * EFFN * EFFN
  KW   = KW0  * EFFW * EFFW


  A50  = AC50 + AD500 * FREQ
  AN   = ACN + ADN0 * FREQ
  AW   = ACW + ADW0 * FREQ

CKT
S2PA 1 2 0 /user/dimitri/em/hts/costep1.s2p
DEF2P 1 2  BIG_STEP

S2PB 1 2 0 /user/dimitri/em/hts/hts1/costep2.s2p
DEF2P 1 2 SML_STEP

S2PC 1 2 0 ./h4jun26.s2p
DEF2P 1 2 YBCO

!S2PD 1 2 0 /user/dimitri/ckt/hts/silver/wc0523a.s2p
!DEF2P 1 2 SILVER

S2PE 1 2 0 /user/dimitri/em/hts/hts_50.s2p
DEF2P 1 2 FIFTY
```

```
 TLINP 1 2 Z=50 L^LI K^KI A^AI F=0
 TLINP 2 3 Z=50 L^LI1 K^KI  A=0 F=0
 FIFTY 3 4
 TLINP_T1 4 5  Z^Z50 L^L50 K^K50 A^A50 F=0.0000000
 SML_STEP   5 6
 TLINP_T2 6 7  Z^ZW L^L1 K^KW A^AW F=0.0000000
 BIG_STEP   7 8
 TLINP_T3 8 9 Z^ZN L^L2 K^KN A^AN F=0
 BIG_STEP 9 10
 TLINP_T4 10 11 Z^ZW L^L3 K^KW A^AW F=0.0000000
 BIG_STEP   11 12
 TLINP_T5 12 13 Z^ZN L^L4 K^KN A^AN F=0.0000000
 BIG_STEP  13 14
 TLINP_T6 14 15 Z^ZW L^L5H K^KW A^AW F=0.0000000
 DEF2P 1 15 HALF

 HALF 1 2
 HALF 3 2
 DEF2P 1 3 FIL


 !RES 1 0 R^rez5
 !DEF1P 1 TEST

FREQ
  SWEEP 1 11 .125
OUT
 FIL DB[S21] GR1
 YBCO DB[S21] GR1

 FIL DB[S11] GR3
 YBCO DB[S11] GR3

 FIL ANG[S21] GR2
 YBCO ANG[S21] GR2

 FIL ANG[S11] GR4
 YBCO ANG[S11] GR4

  FIL S21 SC2
  YBCO S21 SC2
! TEST RE[Z11] GR5

! FIL DB[S21] GR6
! YBCO DB[S21] GR6
GRID
 RANGE 1 11 1
 GR1 -10 0 1
 GR5 .001 .003 .0001

!RANGE 7 9 .2
! GR6 -2 0 .5
OPT
RANGE 2 11
```

YBCO MODEL FIL

CHAPTER 6

AN APPLICATION OF THE PEM LOSS MODEL: AN HTS MICROSTRIP BAND PASS FILTER (BPF)

6.1 The YBCO Microstrip BPF

In this chapter the model described in Chapter 3 is applied to an HTS microstrip BPF. The layout of the filter is shown in figure 1 below. The dimensions of the mask shown in figure 1 are 10x10 mm. The YBCO HTS is laid on a lanthanum aluminate substrate which measures 10x10x0.508 mm. The design is a combination of a parallel coupled resonator filter and a stub filter. There are three parallel coupled line resonators, two of them symmetric about a center axis of symmetry that is the perpendicular bisector of the middle coupled line resonator. There is also an open stub line connected to the input and output of the filter. The line is actually connected to the filter via a smoothly width-tapered line section (which improves the sharpness of the skirts of the filter). At the frequency that the electrical length of the open stub line is 90 degrees the line acts as a transformer and transforms the open circuit at its end to a short circuit at the input of the filter, thus providing a zero, or null to the thru response. This zero is at a frequency higher than the pass band of the filter and improves the sharpness of the roll-off of the latter. There are, scattered beyond the end of the stub line, small squares of metal

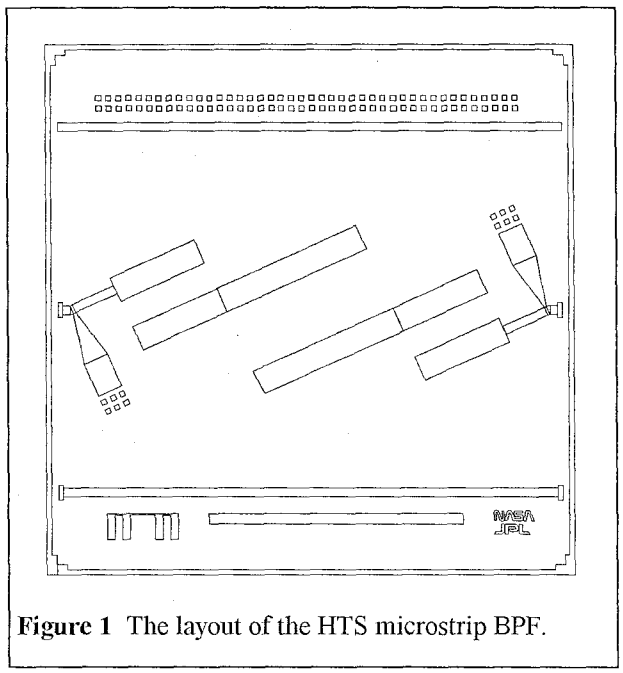

Figure 1 The layout of the HTS microstrip BPF.

which are meant to provide a degree of tunability of this response null (if the frequency of the null needs to be reduced, the little pieces of metal may be shorted to the main stub). This filter was designed by W. Chew of the Spacecraft RF Development Group and the HTS was deposited by B. D. Hunt and M. C. Foote of the Thin Film Physics Group of JPL for Phase II of the NRL HTSSE.

6.2 The Model

6.2.1 The Modeling Methodology

There are three main challenges in modeling this HTS microstrip BPF: The model of the tapered line which connects the stub to the input of the filter, the model of the coupled lines and the inclusion of dispersion (in contrast to the type of transmission line employed in the design of the filter presented in chapter 5, microstrip supports a quasi-TEM propagation mode which exhibits measurable distortion). In the particular case of this design the modeling frequency range of interest (6-8.5 GHz) has a fractional bandwidth of 34%, and it is arguable that dispersion may be neglected. However, in my opinion, it is a borderline case and therefore both analyses with and without dispersion will be included.

6.2.2 The Model of the Input/Output Stub Resonator

The stub resonator, which is connected to the input of the filter via a tapered-width line is shown in figure 2.

The reason for the tapered width line is that Touchstone, which was used to design the filter, does not model large 'T'-elements accurately. By tapering the width of the line from 0.5 mm down to 0.05 mm the size of the T is reduced and the accuracy of the modeling is increased. However, the tapered line presents a modeling problem because of its non-constant cross-section. Its parameters vary continuously along its length. Such a line cannot be modeled using the PEM model of chapter 3, which assumes a constant cross-section. The solution for modeling the filter is shown in figure 3.

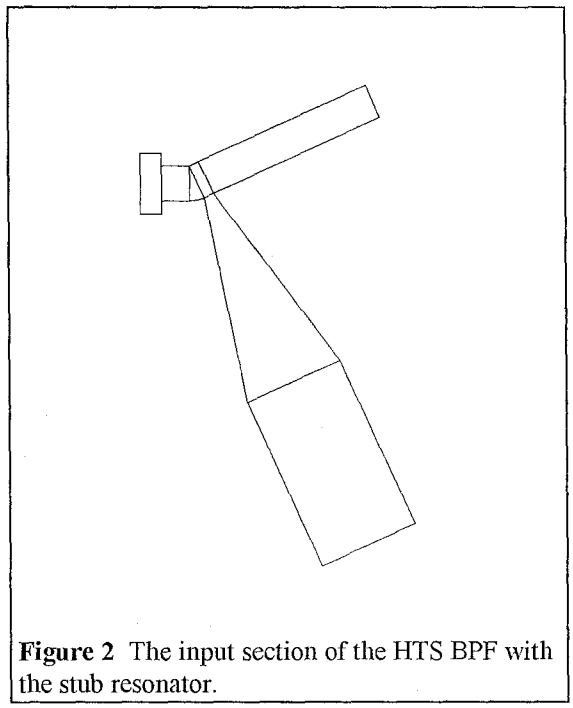

Figure 2 The input section of the HTS BPF with the stub resonator.

The stub line is made of constant width (and can now be modeled) and a normal large T is employed to connect it to the input of the filter. Figure 3 is only a representation of the concept of the solution. In the actual model, an ideal, lumped T element is used, in the form of a 3 by 3 S-parameter matrix, and the lengths of the stub and the 50 Ω connecting lines are increased to compensate. The 3 by 3 S-parameter matrix of an ideal, lumped T can be easily derived using four properties: The equipotential character of the T ($1+S_{11}=S_{21}$ because it is assumed dimensionless), the energy conservation principle ($\mathbf{S}^{+}\mathbf{S}=\mathbf{I}$, see chapter 2), the symmetry

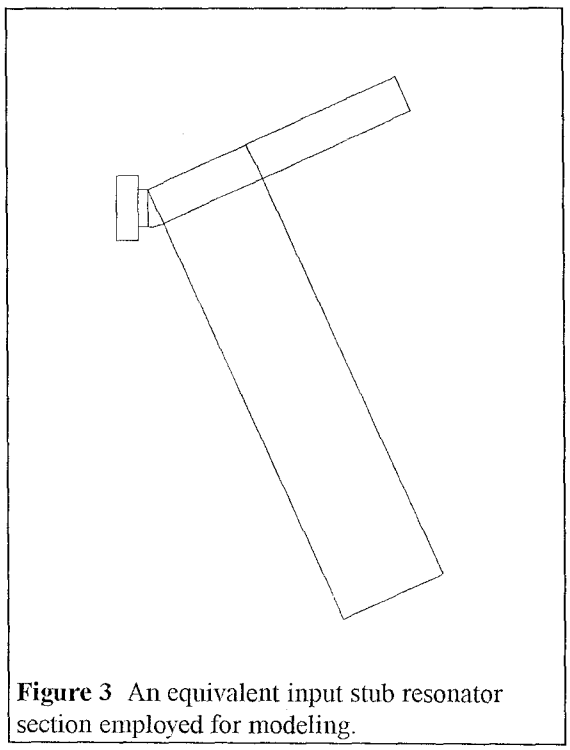

Figure 3 An equivalent input stub resonator section employed for modeling.

of the S-matrix ($S_{21} = S_{12}$, $S_{31} = S_{13}$ and $S_{32} = S_{23}$) and the 3 way symmetry of a T ($S_{11} = S_{22} = S_{33}$ and $S_{21} = S_{31} = S_{32}$). It is included here because of its general usefulness.

$$\mathbf{S} = \begin{bmatrix} -\frac{1}{3} & \frac{2}{3} & \frac{2}{3} \\ \frac{2}{3} & -\frac{1}{3} & \frac{2}{3} \\ \frac{2}{3} & \frac{2}{3} & -\frac{1}{3} \end{bmatrix} . \qquad (1)$$

Figure 4 shows a schematic representation of the actual input/output stub resonator section that is used in the HTS BPF model. This schematic representation is produced by Academy (TM), another software package by EEsof, which integrates Touchstone's analysis capabilities with a schematic and layout capture and entry utility.

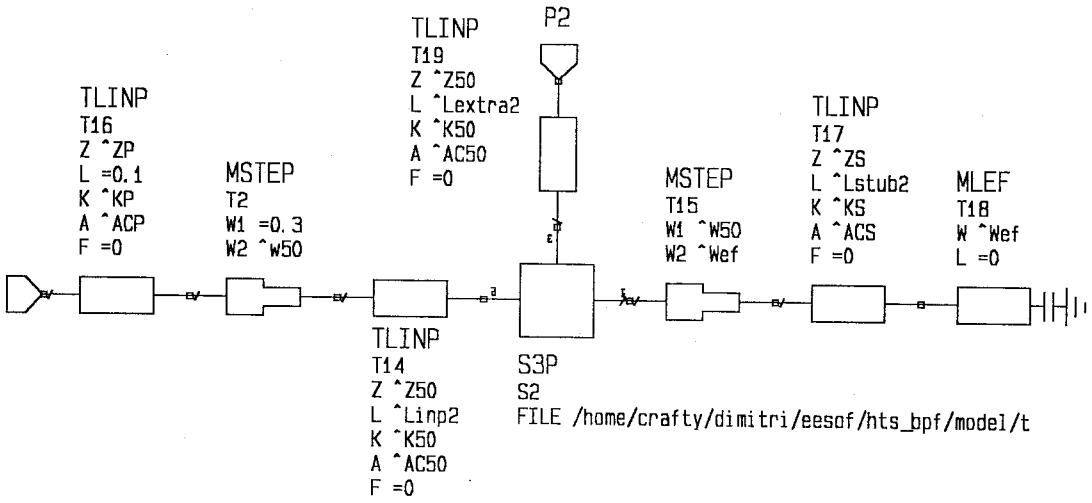

Figure 4 A schematic representation of the input/output stub resonator section

Each of the elements in figure 4 can be seen in the layout of figure 3, although the rectangular T seen in figure 3 is represented as a lumped T, by an S-parameter matrix (S3P), in figure 4. To compensate for the dimensions of the T, the lengths of TLINP (physical transmission lines, see chapter 5 for explanation) elements T19, T14 and T15 (see figure 4) are optimized for best match (minimum integrated square error) between the

S-parameters of the input/output resonator sections of figures 2 and 4. The optimization is performed assuming the ideal case of perfect conductors. The compensated line lengths are *Lextra2*, *Linp2* and *Lstub2* (see figure 4). Once the appropriate line lengths are chosen, the new input/output stub resonator section (figure 4) comprises only straight, constant-width microstrip lines of known length and can therefore be modeled using the theory developed in chapter 3. The low frequency physical parameters of the microstrip lines are calculated from their dimensions and the characteristics of the substrate, using formulas from Gupta's book [1] and dispersion is accounted for with formulas from Atwater's book [2]. There are several microstrip dispersion models proposed in the literature ([3]-[7]) but Atwater's model is found to be simple and yet of adequate accuracy.

There are three types of microstrip lines used in the input/output stub resonator section and in the filter as a whole. These, together with their dimensions and physical properties, are listed in table 1, as calculated in a MathCAD file, included as appendix A of this chapter.

Line Type	w (μm)	Z_0 (Ω)	G	ε_{eff}
50 Ω	172	49.0	7333	14.89
Wide	500	31.8	2406	15.98
Input Pad	300	39.9	4160	15.37

Table 1 The three line types of the filter and their properties.

The *wide* line is the open stub line, the 50 Ω line is the thin line that connects the stub to the coupled line part of the filter and the *input pad* is the little rectangular input line that is used for contact purposes. W here is the width of the line, Z_o is the characteristic impedance of the line, G is the incremental inductance geometric factor and ε_{eff} is the effective dielectric constant of the line. In this analysis dielectric loss is negligible and is therefore neglected.

6.2.3 The Coupled Microstrip Resonators Section

The layout of the coupled microstrip resonators section of the YBCO HTS BPF is shown in figure 5.

It consists of three coupled line resonators in cascade. The first and last are identical while the middle one is longer in length than the other two. Hence there are two types of coupled lines in the filter. The dimension variables of the coupled line pairs are shown in figure 6. Table 2

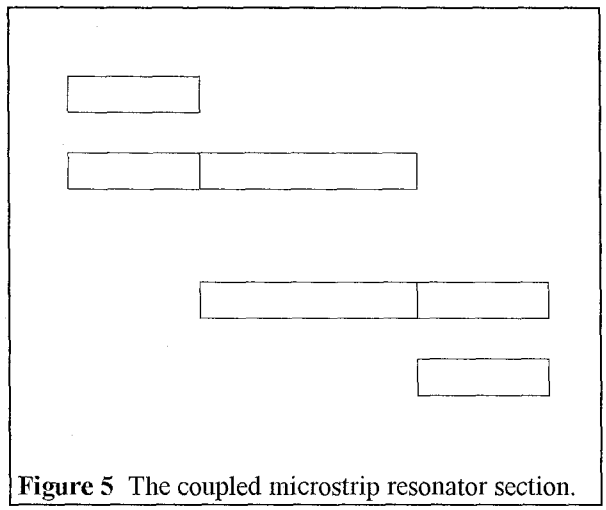

Figure 5 The coupled microstrip resonator section.

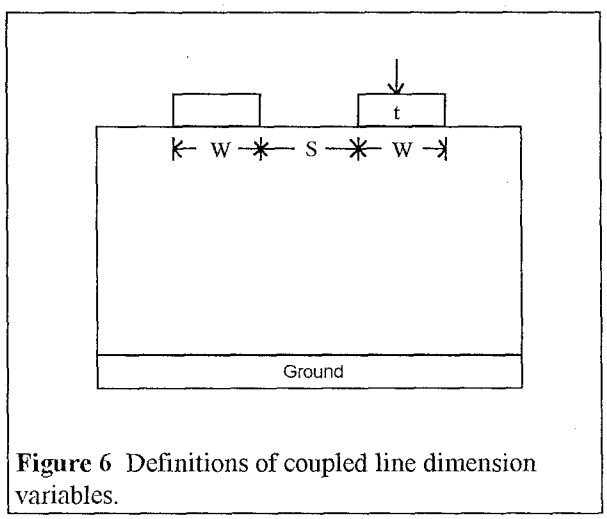

Figure 6 Definitions of coupled line dimension variables.

contains their dimensions and physical properties.

W and S are dimensions shown in figure 6, G is the incremental inductance geometric factor of the mode, Z is the zero-frequency characteristic impedance of the mode, ε^{eff} is the zero-frequency effective relative dielectric constant of the mode, Z_t

Coupled Line	W (μm)	S (μm)	G_e	G_o	Z_e (Ω)	Z_o (Ω)	ε_e^{eff}	ε_o^{eff}	Z_{te} (Ω)	Z_{to} (Ω)	f_{pe} (GHz)	f_{po} (GHz)
Narrow	500	559	2554	1827	36.0	28.5	17.34	13.35	43.3	38.5	14.1	44.7
Wide	500	1267	2522	1743	33.8	31.4	17.15	14.14	41.2	40.7	13.2	49.3

Table 2 The two types of coupled lines and their properties.

is the infinite-frequency characteristic impedance of the mode and f_p is the frequency at which the characteristic impedance of the mode is approximately equal to the average of its zero and infinite-frequency values and also the frequency at which the effective relative dielectric constant of the mode is approximately equal to the average of its zero and infinite-frequency values (the infinite frequency value being equal to the relative dielectric

constant of the substrate). In the previous notation the subscript 'e' denotes a parameter of the even mode and the subscript 'o' denotes a parameter of the odd mode. Examination of the last two columns of table 2 shows that odd mode dispersion can be neglected at the frequency of modeling (6-8.5 GHz). Appendix A includes a hard copy of the MathCAD file that is used to calculate the parameters listed in table 2. Equations from Gupta's book [1] and Garg's paper [8] are used for the calculations.

A word of caution to the reader is in order here. Some equations of references [1] and [8], for microstrip coupled line calculations, are found to be wrong and are corrected in appendix A. Specifically, equations (8.85), p. 338 of [1] and (7a), p. 701 of [8] for C_{ga} are wrong by a factor of 2. They are shown corrected in appendix A. Equations (8.86) and (8.87), p. 338 of [1] for C_{ga}, which use an approximation to the elliptic integral, are correct. However, the corresponding approximation in [8] (equation (7b), p. 701) is incorrect. Also, equation (18), p. 702 of [8] for Z_t is incorrect; the numerator and denominator of its fraction should be interchanged. This is also corrected in appendix A.

6.2.4 The Touchstone Circuit File

The Touchstone circuit files used for the analysis of the HTS BPF are included as appendices B and C of this chapter. In the circuit file of appendix B dispersion is neglected whereas in appendix C it is included. As in chapter 5, equations (3.34)-(3.43) are included in the EQN block of the Touchstone circuit file. (3.35) and (3.36) are broken down in smaller sub-equations because they are too long for Touchstone. The EQN block is sub-divided into five logical sections, each corresponding to one of the two types of coupled lines and three types of microstrip lines, respectively (see tables 1 and 2). The parameters of tables 1 and 2 are also included in the Touchstone file as constants in the VAR block. The resulting parameters, which are re-calculated for each individual

frequency of the sweep, are three: the loss due to the surface resistance of the line, in dB/μm, the corrected characteristic impedance and the corrected effective dielectric constant, for each type of line. Each of these is calculated for both the even and the odd mode. These are fed into a combination of TLINP elements, which are described in section 5.2.2, and *CLINP* elements. The CLINP element models a pair of coupled physical transmission lines of known odd and even mode impedance, effective relative dielectric constant, length and attenuation coefficient. The CLINP and TLINP elements are interconnected via *MSTEP* elements. These model the step discontinuity in the width of the microstrip transmission line. Since these elements are lumped, dimensionless elements, they are perfectly conducting and do not contribute to the loss of the circuit. Hence they can be used without modifications in modeling HTS circuits.

Four TLINP and two MSTEP elements are used in modeling the input/output stub resonator section, as shown in figure 4. A zero-length *MLEF* element, which models the open end capacitance of stub lines, is used for terminating the TLINP element which models the stub line of the input/output stub resonator section. Because it is zero-length, it may be used in HTS modeling, for the same reason as the MSTEP elements. Figure 7 shows the schematic representation generated by Academy for the coupled line resonator section of the filter.

Three CLINP, two MSTEP and six MLEF elements are used in this main section of the HTS BPF. The MSTEP elements model the microstrip line width change

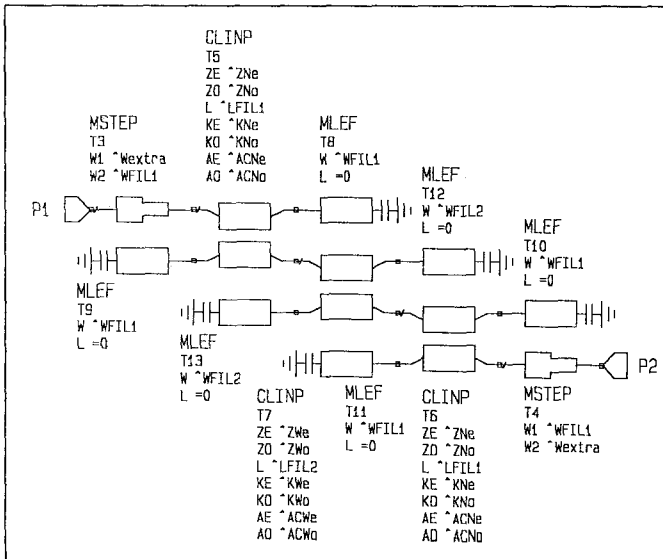

Figure 7 A schematic representation of the coupled line resonator section of the filter.

discontinuity from the 50 Ω line of the input/output stub resonator section to the coupled line resonator section. The MLEF elements are used to terminate the open end of the CLINP elements. The length of the first and last CLINP elements is 1815 μm and is stored in the variable *LFIL1* (in the VAR block) and the length of the middle CLINP element is 3004 μm, stored in *LFIL2*.

6.3 The Modeling Strategy

The strategy is to start the analysis with typical initial values for the zero-temperature penetration depth, λ_o, and the normal conductivity, σ_n. The same group that deposited the YBCO film of the LPF of chapter 5 deposited the YBCO film of the BPF of this chapter. Hence, it is reasonable to assume initial values in the range of values seen in the LPF of chapter 5. As in the latter case, the critical temperature, T_c of the YBCO film is again not known accurately (the uncertainty is 83 to 88 K), so a T_c of 85 K is assumed for the analysis. The assumed temperature of the measurements, T, is 77 K, the temperature of LN_2. The variables λ_o and σ_n.are then permitted to assume their optimum values, within a reasonable domain of values (see section 5.2.3), that minimizes the integrated square error between the measured and the modeled BPF S-parameters. Two cases are analyzed. In one case dispersion is neglected whereas in the other case it is included. The optimum values extracted for λ_o and σ_n.for the two cases are shown in table 3.

Case	λ_o (nm)	σ_n.(S/m)
No dispersion	756.9	$1.35 \cdot 10^6$
Dispersion	642.8	$6.00 \cdot 10^6$

Table 3 The optimum extracted values for the penetration depth and the normal conductivity.

6.4 Comparison of Measurement versus Model

6.4.1 The Case of No Dispersion

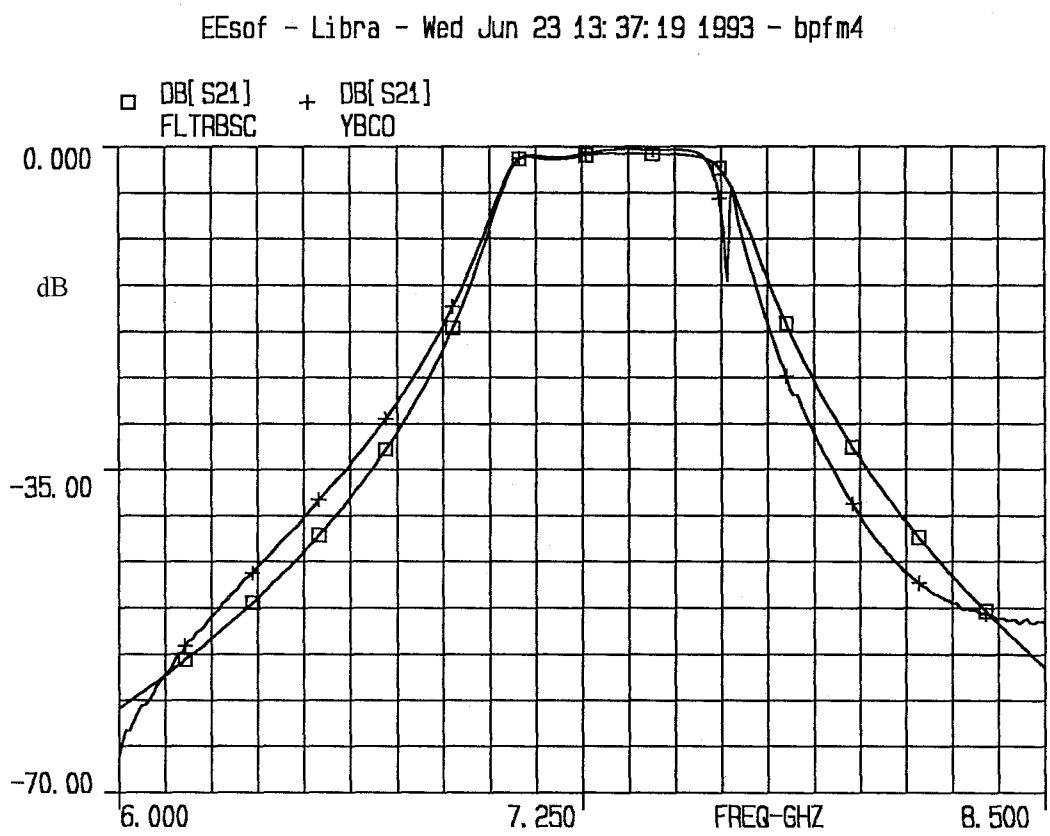

Figure 8 Measured (YBCO) versus modeled (FLTRBSC) magnitude of S21.

Figure 8 shows a comparison of the measured versus modeled magnitude of the insertion loss (S21) plotted on a vertical dB-scale.

The unexpected notch in the graph of S21 at 7.63 GHz is thought to be real and not a measurement error, but it could not be modeled. It is thought to be due to coupling between the input/output stub resonator and the first coupled line pair of the main section of the BPF (see figure 1). A similar notch appears in the measured phase of S21 at that same frequency, which is plotted in figure 9 together with the modeled phase of S21.

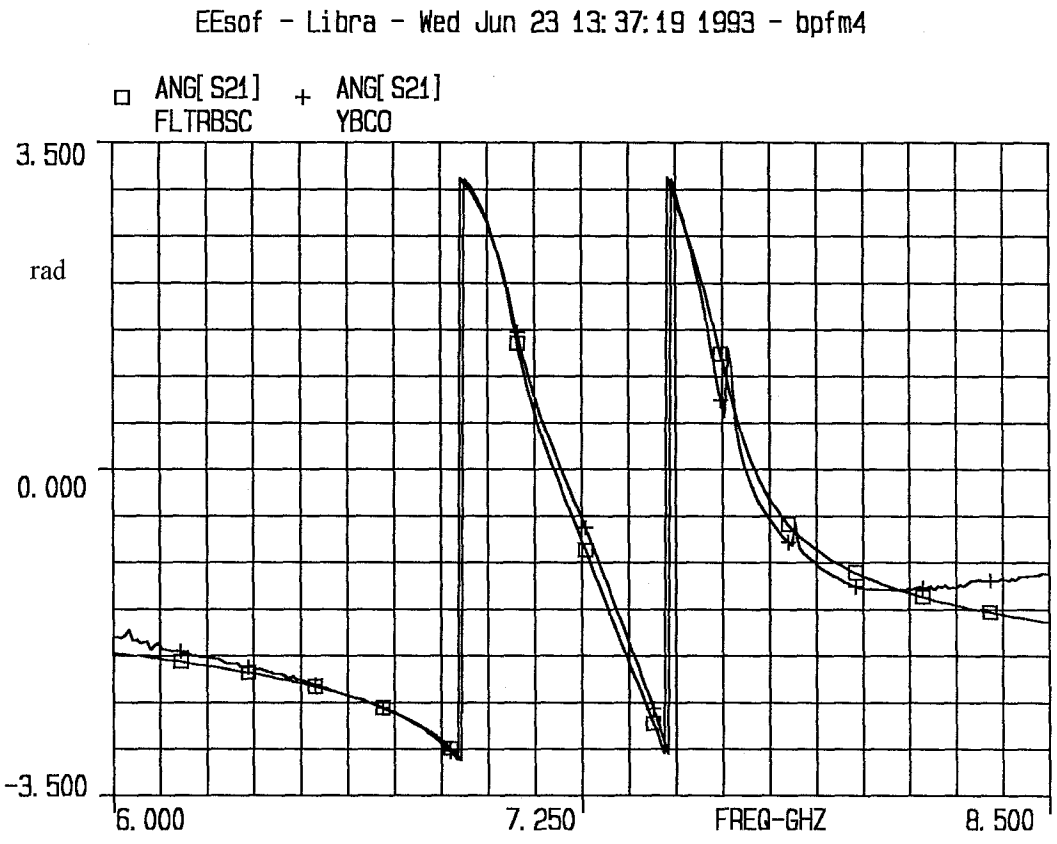

Figure 9 Measured (YBCO) versus modeled (FLTRBSC) angle of S21.

Figure 10 shows a comparison of the measured versus modeled magnitude of the return loss (S11) plotted on a vertical dB-scale.

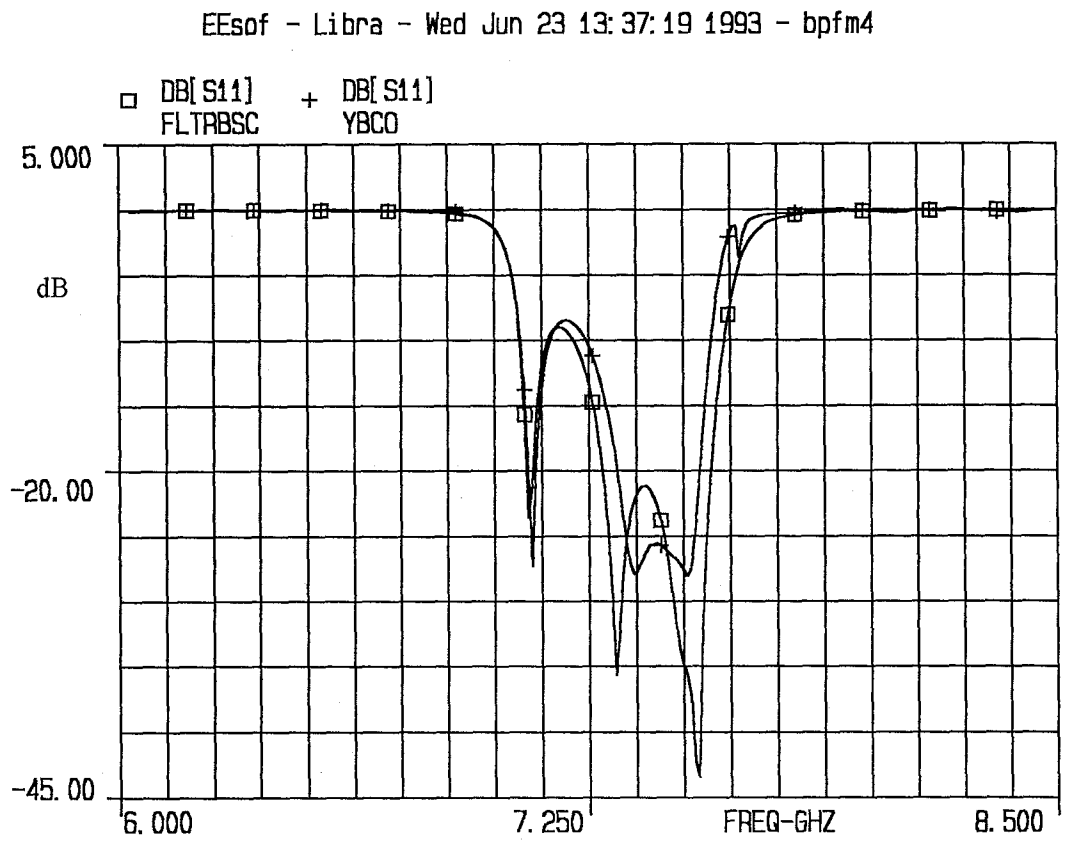

Figure 10 Measured (YBCO) versus modeled (FLTRBSC) magnitude of S11.

Figure 11 shows a comparison of the measured versus modeled angle of S11. The vertical scale is in radians.

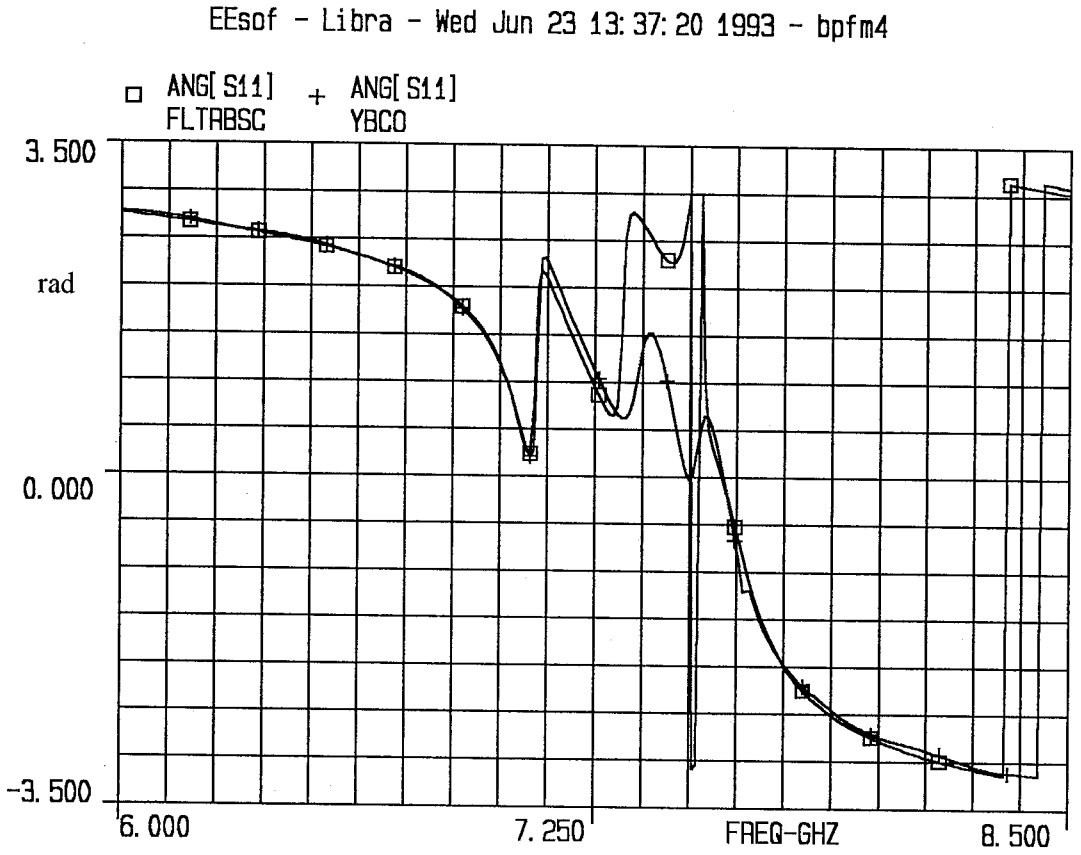

Figure 11 Measured (YBCO) versus modeled (FLTRBSC) angle of S11.

Figure 12 shows a comparison of the measured versus modeled S21, plotted on a Smith chart of unit radius.

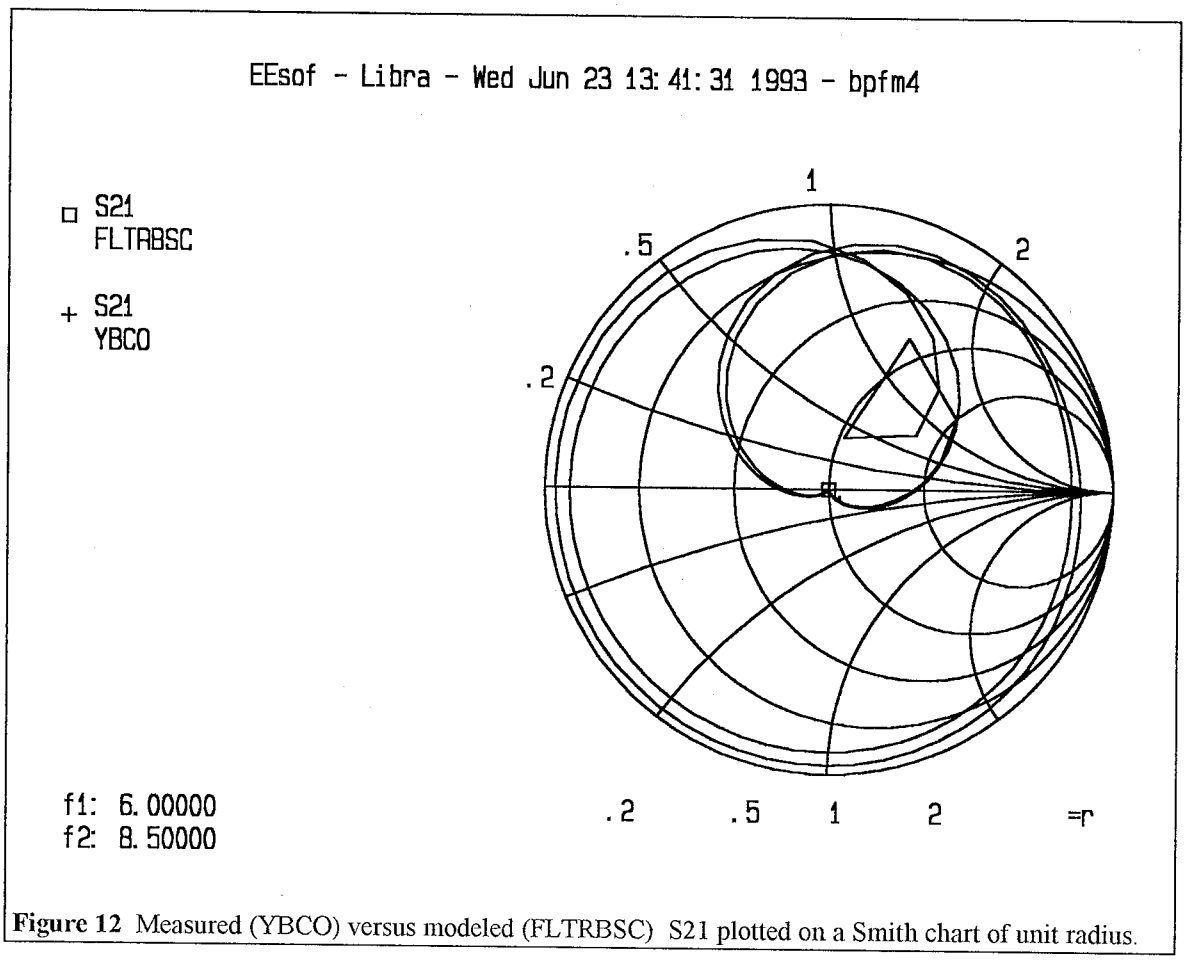

Figure 12 Measured (YBCO) versus modeled (FLTRBSC) S21 plotted on a Smith chart of unit radius.

6.4.2 The Case of Dispersion

Figure 13 shows a comparison of the measured versus modeled magnitude of the insertion loss (S21) plotted on a vertical dB-scale.

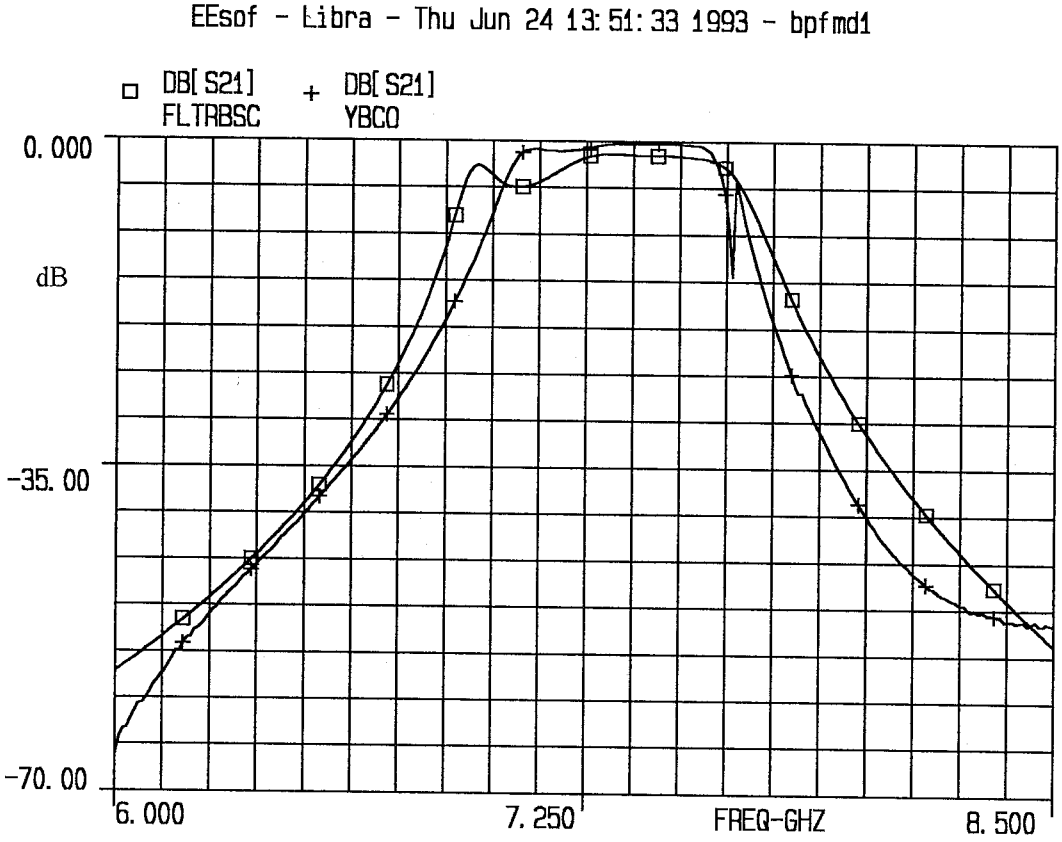

Figure 13 Measured (YBCO) versus modeled (FLTRBSC) magnitude of S21.

Figure 14 shows a comparison of the measured versus modeled phase (angle) of S21. The vertical scale is in radians.

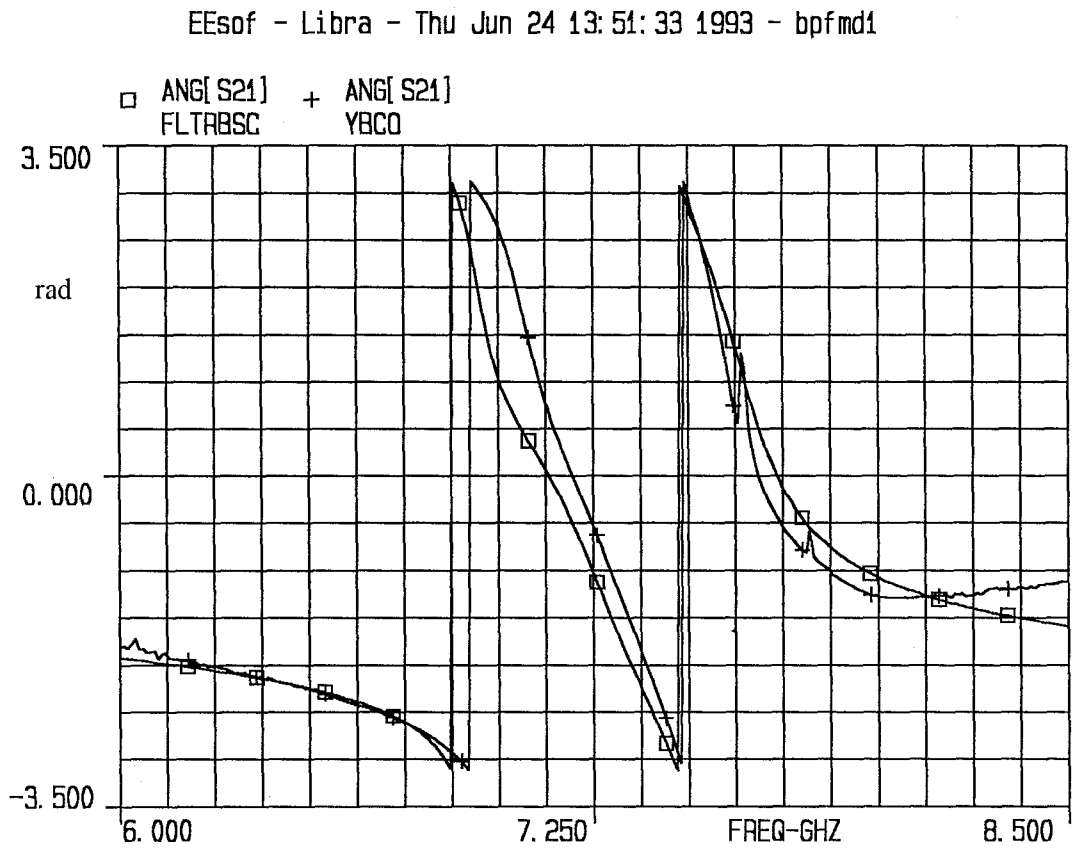

Figure 14 Measured (YBCO) versus modeled (FLTRBSC) angle of S21.

Figure 15 shows a comparison of the measured versus modeled magnitude of the return loss (S11) plotted on a vertical dB-scale.

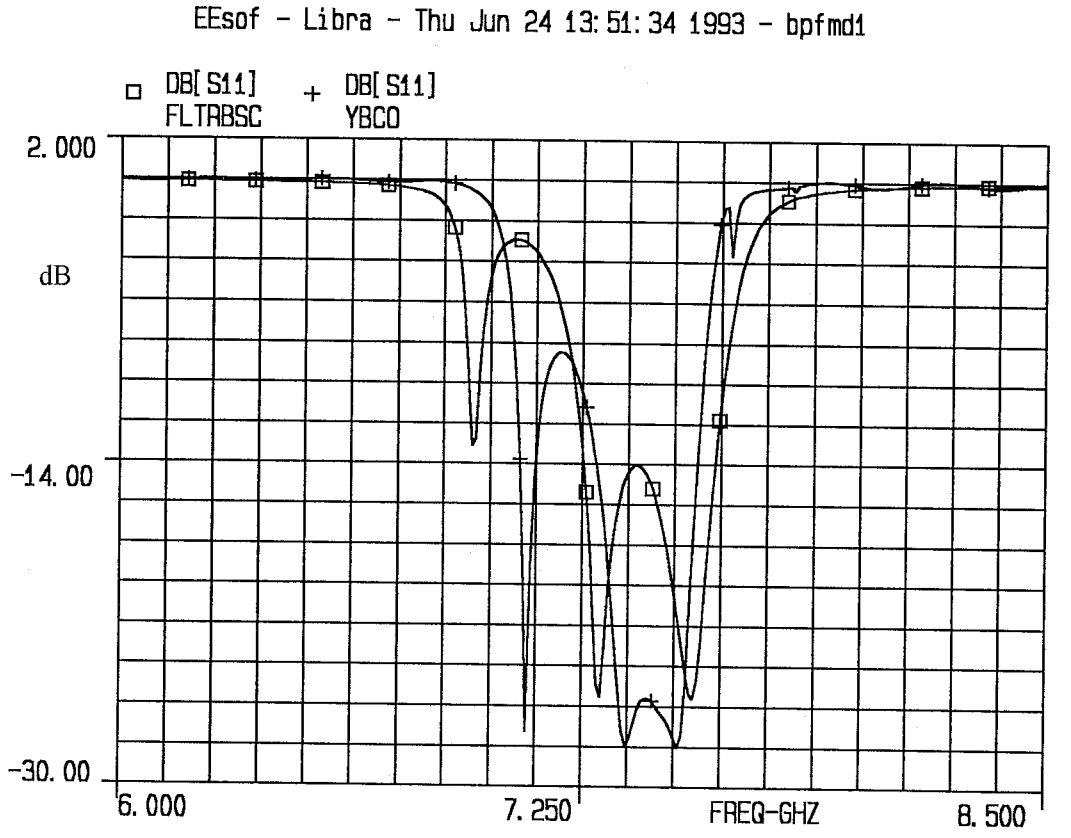

Figure 15 Measured (YBCO) versus modeled (FLTRBSC) magnitude of S11.

Figure 16 shows a comparison of the measured versus modeled angle of S11. The vertical scale is in radians.

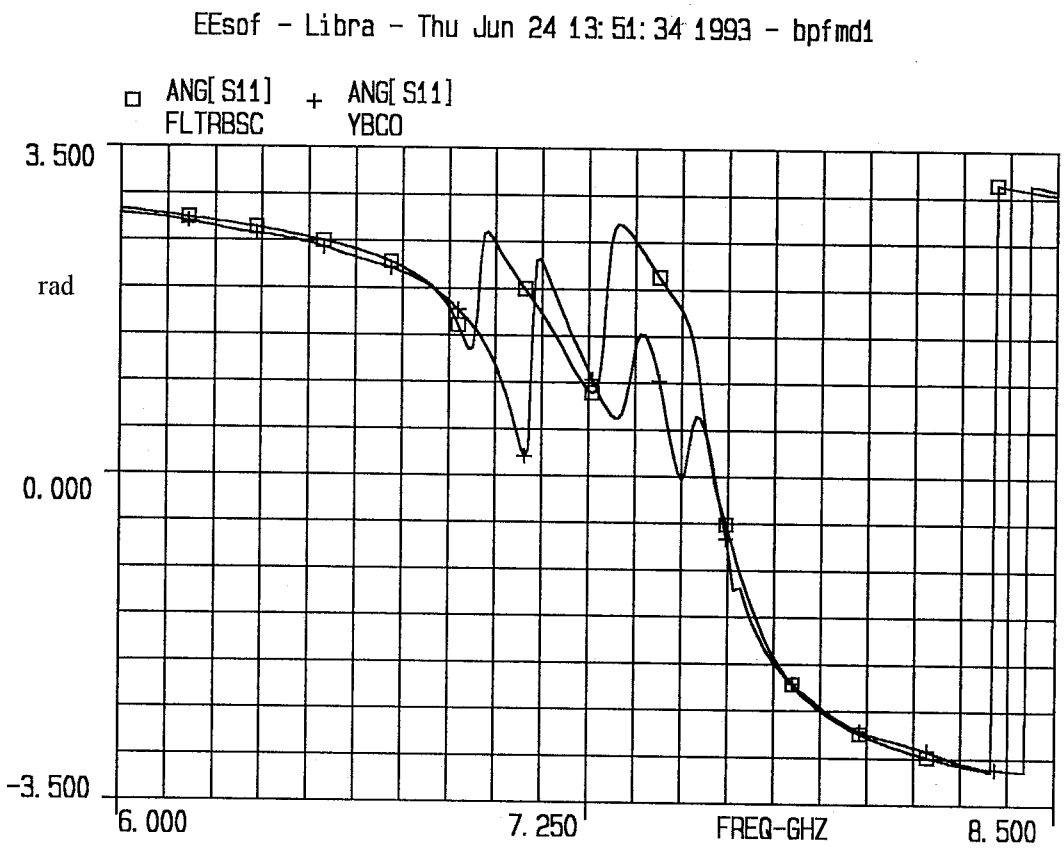

Figure 16 Measured (YBCO) versus modeled (FLTRBSC) angle of S11.

Figure 17 shows a comparison of the measured versus modeled S21, plotted on a Smith chart of unit radius.

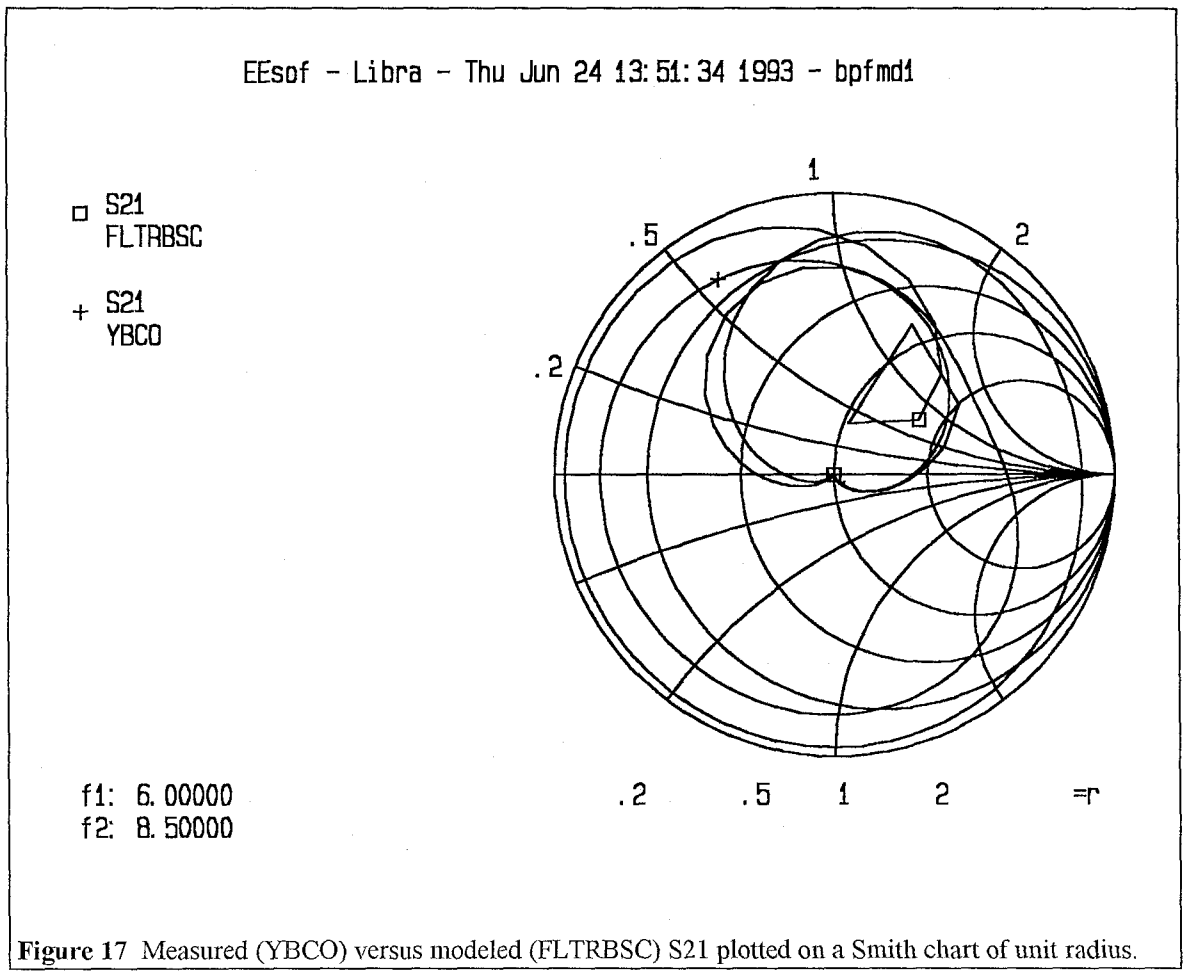

Figure 17 Measured (YBCO) versus modeled (FLTRBSC) S21 plotted on a Smith chart of unit radius.

6.4.3 Dispersion or No Dispersion? This is the Question

In the low fractional band width of this model, dispersion could be neglected. However, it does add some verisimilitude to some of the S-parameter curves, compared to the no-dispersion case. It is important to point out that most dispersion models (including the one used in this analysis, which is not perfect) incorporate an error on the order of a few per cent. Hence, if the correction that the PEM model itself applies to the line parameters is of the same order (i.e., a few per cent), then it does not make sense to incorporate any dispersion model in calculating these parameters. The correction that the PEM model applies is the factor in parenthesis multiplying ε_{eff} in equation (3.43)

(i.e., $\left(1+\frac{c}{2\pi\sqrt{\varepsilon_{eff}}f}\frac{X_i}{Z_0}\right)$). In the case of the BPF of this chapter, the correction factors are slightly, but not much, greater than this "noise floor" of the dispersion model. There may, therefore, be incosistencies, although some improvements are expected, by the application of the distortion model.

One such inconsistency is observed in table 3. The analysis with the dispersion model yields a more believable value for the zero-temperature penetration depth (in the range observed for the various LPFs described in chapter 5 and closer to values reported in the literature), yet an excessively large value for the normal conductivity. Figures 8 and 13, 9 and 14, and 10 and 15 show the no-dispersion model is slightly closer to the measured data, yet in figures 11 and 16 the dispersion model is significantly closer to the measured phase of S11 than the no-dispersion model. Both analyses are useful, each for different purposes, but for larger bandwidth modeling a dispersion model should be included.

6.5 References

[1] K. Gupta, R. Garg and I. Bahl, *Microstrip Lines and Slotlines*, Artech, Dedham, MA, 1979.

[2] H. A. Atwater, *Introduction to Microwave Theory*, McGraw-Hill, New York, 1962.

[3] T. G. Bryant and J. A. Weiss, "Parameters of Microstrip Transmission Lines and Coupled Pairs of Microstrip Lines," IEEE Transactions on Microwave Theory and Techniques, Vol. MTT-16, pp.1021-1027, December 1968.

[4] M. V. Schneider, "Microstrip Lines for Microwave Integrated Circuits," The Bell System Technical Journal, Vol. 48, No. 5, pp. 1421-1444, May/June 1969.

[5] E. O. Hammerstad, "Equations for Microstrip Circuit Design," Proceedings of the European Microwave Conference, Hamburg, W. Germany, pp. 268-272, September 1975.

[6] H. A. Wheeler, "Transmission Line Properties of a Strip on a Dielectric Sheet on a Plane," IEEE Transactions on Microwave Theory and Techniques, Vol. MTT-25, Mo. 8, pp. 631-647, August 1977.

[7] E. O. Hammerstad and O. Jensen, "Accurate Models for Microstrip Computer-Aided Design," IEEE MTT-S Symposium Digest, pp. 407-409, June 1980.

[8] R. Garg and I. J. Bahl, "Characteristics of Coupled Microstriplines," IEEE Transactions on Microwave Theory and Techniques, Vol. MTT-27, No. 7, pp. 700-705, July 1979.

Appendix A

Sample MathCAD File Used to Calculate the Parameters of the Microstrip Lines of the BPF

Microstrip Coupled Lines Parameters

Define the elliptic integral: $TOL := 10^{-5}$

$$K(k) := \int_0^{\frac{\pi}{2}} \frac{1}{\sqrt{1 - k^2 \cdot \sin[\phi]^2}} d\phi$$

$$K'(k) := K\left[\sqrt{1 - k^2}\right]$$

Physical Constants

$\varepsilon_o := 8.854 \cdot 10^{-12}$ $\mu_o := 4 \cdot \pi \cdot 10^{-7}$

$c := \frac{1}{\sqrt{\varepsilon_o \cdot \mu_o}}$ $\eta := \sqrt{\frac{\mu_o}{\varepsilon_o}}$

$f := 8 \cdot 10^9$

Microstrip Parameters

$h := 20 \cdot 10^{-3} \cdot 2.54 \cdot 10^{-2}$

$h = 5.08 \cdot 10^{-4}$

$W := 0.5 \cdot 10^{-3}$

$S := 0.559 \cdot 10^{-3}$

$L := 1.815 \cdot 10^{-3}$

$t := 5 \cdot 10^{-7}$

$er := 24.5$

Capacitances of coupled Lines

$$W_{em} := if\left[\frac{W}{h} > \frac{1}{[2 \cdot \pi]}, W + \frac{1.25}{\pi} \cdot t \cdot \left[1 + \ln\left[2 \cdot \frac{h}{t}\right]\right], W + \frac{1.25}{\pi} \cdot t \cdot \left[1 + \ln\left[4 \cdot \pi \cdot \frac{W}{t}\right]\right]\right]$$

$$F := if\left[\frac{W}{h} > 1, \left[1 + 12 \cdot \frac{h}{W}\right]^{-\left[\frac{1}{2}\right]}, \left[1 + 12 \cdot \frac{h}{W}\right]^{-\left[\frac{1}{2}\right]} + 0.04 \cdot \left[1 - \frac{W}{h}\right]^2\right]$$

$$ere := \frac{(er+1)}{2} + \frac{(er-1)}{2} \cdot F - \frac{(er-1)}{4.6} \cdot \frac{\left[\frac{t}{h}\right]}{\sqrt{\frac{W}{h}}} \qquad W_{em} = 5.0171425 \cdot 10^{-4}$$

$$ere = 15.9801098$$

$$Z_{om} := if\left[\frac{W}{h} > 1, \frac{\eta}{\sqrt{ere}} \cdot \left[\frac{W_{em}}{h} + 1.393 + 0.667 \cdot \ln\left[\frac{W_{em}}{h} + 1.444\right]\right]^{-1}, \frac{\eta}{\left[2 \cdot \pi \cdot \sqrt{ere}\right]} \cdot \ln\left[8 \cdot \frac{h}{W_{em}} + 0.25 \cdot \frac{W_{em}}{h}\right]\right]$$

$$Z_{om} = 31.8268821$$

$$C_p := \varepsilon_o \cdot er \cdot \frac{W}{h}$$

$$C_f := 0.5 \cdot \left[\frac{\sqrt{ere}}{\left[c \cdot Z_{om}\right]} - \varepsilon_o \cdot er \cdot \frac{W}{h}\right]$$

$$A := \exp\left[-0.1 \cdot \exp\left[2.33 - 2.53 \cdot \frac{W}{h}\right]\right]$$

$$C'_f := \frac{C_f}{\left[1 + A \cdot \frac{h}{S} \cdot \tanh\left[10 \cdot \frac{S}{h}\right]\right]} \cdot \sqrt{\frac{er}{ere}}$$

$$C_e := C_p + C_f + C'_f$$

$$C_e = 3.8556597 \cdot 10^{-10}$$

$$k := \frac{S}{(S + 2 \cdot W)} \qquad k = 0.3585632$$

$$\frac{K'(k)}{K(k)} = 1.5138718$$

$$C_{ga} := \varepsilon_o \cdot \frac{K'(k)}{K(k)} \qquad C_{ga} = 1.3403821 \cdot 10^{-11}$$

$$C_{gd} := \frac{\left[\varepsilon_o \cdot er\right]}{\pi} \cdot \ln\left[\coth\left[\pi \cdot \frac{S}{(4 \cdot h)}\right]\right] + 0.65 \cdot C_f \cdot \left[\frac{0.02}{\left[\frac{S}{h}\right]} \cdot \sqrt{er} + \left[1 - \frac{1}{er^2}\right]\right] \quad C_{gt} := 2 \cdot \varepsilon_o \cdot \frac{t}{S}$$

$$C_o := C_f + C_p + C_{gd} + C_{ga} + C_{gt}$$

$C_o = 4.2710151 \cdot 10^{-10}$

$er := 1$

$$ere := \frac{(er+1)}{2} + \frac{(er-1)}{2} \cdot F - \frac{(er-1)}{4.6} \cdot \frac{\left[\frac{t}{h}\right]}{\sqrt{\frac{W}{h}}} \qquad ere = 1$$

$$Z_{om} := if\left[\frac{W}{h} > 1, \frac{\eta}{\sqrt{ere}} \cdot \left[\frac{W_{em}}{h} + 1.393 + 0.667 \cdot \ln\left[\frac{W_{em}}{h} + 1.444\right]\right]^{-1}, \frac{\eta}{\left[2 \cdot \pi \cdot \sqrt{ere}\right]} \cdot \ln\left[8 \cdot \frac{h}{W_{em}} + 0.25 \cdot \frac{W_{em}}{h}\right]\right]$$

$Z_{om} = 127.2283735$

$$C_p := \varepsilon_o \cdot er \cdot \frac{W}{h}$$

$$C_f := 0.5 \cdot \left[\left[\frac{\sqrt{ere}}{\left[c \cdot Z_{om}\right]}\right] - \varepsilon_o \cdot er \cdot \frac{W}{h}\right]$$

$$C'_f := \frac{C_f}{\left[1 + A \cdot \frac{h}{S} \cdot \tanh\left[10 \cdot \frac{S}{h}\right]\right]} \cdot \frac{\sqrt{er}}{\sqrt{ere}}$$

$$C'_e := C_p + C_f + C'_f$$

$C'_e = 2.2236383 \cdot 10^{-11}$

$$C_{gd} := \frac{\left[\varepsilon_o \cdot er\right]}{\pi} \cdot \ln\left[\coth\left[\pi \cdot \frac{S}{(4 \cdot h)}\right]\right] + 0.65 \cdot C_f \cdot \left[\frac{0.02}{\left[\frac{S}{h}\right]} \cdot \sqrt{er} + \left[1 - \frac{1}{er^2}\right]\right]$$

$$C'_o := C_f + C_p + C_{gd} + C_{ga} + C_{gt}$$

$C'_o = 3.2000579 \cdot 10^{-11}$

"Zero frequency" results:

$$Zoe := \frac{1}{\left[c \cdot \sqrt{C'_e \cdot C_e}\right]} \qquad eere := \frac{C_e}{C'_e}$$

$$Zoo := \frac{1}{\left[c \cdot \sqrt{C'_o \cdot C_o}\right]} \qquad eore := \frac{C_o}{C'_o}$$

$Zoe = 36.0241111$ $\quad eere = 17.3394198$

$Zoo = 28.531869$ $\quad eore = 13.3466809$

$$f_{pe} := \frac{Zoe}{\left[4 \cdot \mu_o \cdot h\right]} \qquad f_{pe} = 14.1078134 \cdot 10^9$$

$$f_{po} := \frac{Zoo}{\left[\mu_o \cdot h\right]} \qquad f_{po} = 44.6947636 \cdot 10^9$$

$G_{de} := 0.6 + 0.0045 \cdot Zoe$ $\quad G_{de} = 0.7621085$

$G_{do} := 0.6 + 0.018 \cdot Zoo$ $\quad G_{do} = 1.1135736$

$$k_e := \tanh\left[\frac{\pi}{4} \cdot \frac{W}{h}\right] \cdot \tanh\left[\frac{\pi}{4} \cdot \frac{(W+S)}{h}\right]$$

$$k_o := \frac{\tanh\left[\frac{\pi}{4} \cdot \frac{W}{h}\right]}{\tanh\left[\frac{\pi}{4} \cdot \frac{(W+S)}{h}\right]}$$

$er := 24.5$

$$Z_{te} := 60 \cdot \frac{\pi}{\sqrt{er}} \cdot \frac{K'\left[k_e\right]}{K\left[k_e\right]} \qquad Z_{te} = 43.3304705$$

$$Ze := Z_{te} - \frac{\left[Z_{te} - Zoe\right]}{\left[1 + G_{de} \cdot \left[\frac{f}{f_{pe}}\right]^{1.6}\right]}$$

$Ze = 37.7423726$ $\quad Zoe = 36.0241111$

$$Z_{to} := 60 \cdot \frac{\pi}{\sqrt{er}} \cdot \frac{K'\left[k_o\right]}{K\left[k_o\right]} \qquad Z_{to} = 38.4461539$$

$$Zo := Z_{to} - \frac{\left[Z_{to} - Zoo\right]}{\left[1 + G_{do} \cdot \left[\frac{f}{f_{po}}\right]^{1.6}\right]}$$

Zo = 29.1891099 Zoo = 28.531869

$$ere := er - \frac{(er - eere)}{\left[1 + G_{de} \cdot \left[\frac{f}{f_{pe}}\right]^2\right]}$$

eere = 17.3394198 ere = 18.74882

$$ero := er - \frac{(er - eore)}{\left[1 + G_{do} \cdot \left[\frac{f}{f_{po}}\right]^2\right]}$$

eore = 13.3466809 ero = 13.7308881

Calculate new impedances under recession of walls by dnormal:

$$dnormal := \frac{t}{1000}$$

$t := t - 2 \cdot dnormal$ $t = 4.99 \cdot 10^{-7}$

$W := W - 2 \cdot dnormal$ $W = 4.99999 \cdot 10^{-4}$

$S := S + 2 \cdot dnormal$ $S = 5.59001 \cdot 10^{-4}$

Capacitances of coupled Lines

$$W_{em} := if\left[\frac{W}{h} > \frac{1}{[2 \cdot \pi]}, W + \frac{1.25}{\pi} \cdot t \cdot \left[1 + \ln\left[2 \cdot \frac{h}{t}\right]\right], W + \frac{1.25}{\pi} \cdot t \cdot \left[1 + \ln\left[4 \cdot \pi \cdot \frac{W}{t}\right]\right]\right]$$

$$F := if\left[\frac{W}{h} > 1, \left[1 + 12 \cdot \frac{h}{W}\right]^{-\left[\frac{1}{2}\right]}, \left[1 + 12 \cdot \frac{h}{W}\right]^{-\left[\frac{1}{2}\right]} + 0.04 \cdot \left[1 - \frac{W}{h}\right]^2\right]$$

$W_{em} = 5.0171022 \cdot 10^{-4}$

$$ere := \frac{(er+1)}{2} + \frac{(er-1)}{2} \cdot F - \frac{(er-1)}{4.6} \cdot \frac{\left[\frac{t}{h}\right]}{\sqrt{\frac{W}{h}}}$$

ere = 15.980117

$$Z_{om} := if\left[\frac{W}{h} > 1, \frac{\eta}{\sqrt{ere}} \cdot \left[\frac{W_{em}}{h} + 1.393 + 0.667 \cdot \ln\left[\frac{W_{em}}{h} + 1.444\right]\right]^{-1}, \frac{\eta}{\left[2 \cdot \pi \cdot \sqrt{ere}\right]} \cdot \ln\left[8 \cdot \frac{h}{W_{em}} + 0.25 \cdot \frac{W_{em}}{h}\right]\right]$$

$Z_{om} = 31.8269884$

$$C_p := \varepsilon_0 \cdot er \cdot \frac{W}{h}$$

$$C_f := 0.5 \cdot \left[\frac{\sqrt{ere}}{\left[c \cdot Z_{om} \right]} - \varepsilon_0 \cdot er \cdot \frac{W}{h} \right]$$

$$A := \exp\left[-0.1 \cdot \exp\left[2.33 - 2.53 \cdot \frac{W}{h} \right] \right]$$

$$C'_f := \frac{C_f}{\left[1 + A \cdot \frac{h}{S} \cdot \tanh\left[10 \cdot \frac{S}{h} \right] \right]} \cdot \sqrt{\frac{er}{ere}}$$

$$C_e := C_p + C_f + C'_f$$

$$C_e = 3.8556486 \cdot 10^{-10}$$

$$k := \frac{S}{(S + 2 \cdot W)} \qquad k = 0.3585641$$

$$C_{ga} := \varepsilon_0 \cdot \frac{K'(k)}{K(k)} \qquad C_{ga} = 1.3403807 \cdot 10^{-11} \qquad \frac{K'(k)}{K(k)} = 1.5138702$$

$$C_{gd} := \frac{\left[\varepsilon_0 \cdot er \right]}{\pi} \cdot \ln\left[\coth\left[\pi \cdot \frac{S}{(4 \cdot h)} \right] \right] + 0.65 \cdot C_f \cdot \left[\frac{0.02}{\left[\frac{S}{h} \right]} \cdot \sqrt{er} + \left[1 - \frac{1}{er^2} \right] \right]$$

$$C_{gt} := 2 \cdot \varepsilon_0 \cdot \frac{t}{S}$$

$$C_o := C_f + C_p + C_{gd} + C_{ga} + C_{gt}$$

$$C_o = 4.271002 \cdot 10^{-10}$$

$$er := 1$$

$$ere := \frac{(er + 1)}{2} + \frac{(er - 1)}{2} \cdot F - \frac{(er - 1)}{4.6} \cdot \frac{\left[\frac{t}{h} \right]}{\sqrt{\frac{W}{h}}} \qquad ere = 15.980117$$

$$Z_{om} := \text{if}\left[\frac{W}{h} > 1, \frac{\eta}{\sqrt{ere}} \cdot \left[\frac{W_{em}}{h} + 1.393 + 0.667 \cdot \ln\left[\frac{W_{em}}{h} + 1.444 \right] \right]^{-1}, \frac{\eta}{\left[2 \cdot \pi \cdot \sqrt{ere} \right]} \cdot \ln\left[8 \cdot \frac{h}{W_{em}} + 0.25 \cdot \frac{W_{em}}{h} \right] \right]$$

$$Z_{om} = 127.2288267$$

$$C_p := \varepsilon_o \cdot er \cdot \frac{W}{h}$$

$$C_f := 0.5 \cdot \left[\frac{\sqrt{ere}}{\left[c \cdot Z_{om} \right]} - \varepsilon_o \cdot er \cdot \frac{W}{h} \right]$$

$$C'_f := \frac{C_f}{\left[1 + A \cdot \frac{h}{S} \cdot \tanh\left[10 \cdot \frac{S}{h} \right] \right]} \cdot \sqrt{\frac{er}{ere}}$$

$$C'_e := C_p + C_f + C'_f \qquad C'_e = 2.2236311 \cdot 10^{-11}$$

$$C_{gd} := \frac{\left[\varepsilon_o \cdot er \right]}{\pi} \cdot \ln\left[\coth\left[\pi \cdot \frac{S}{(4 \cdot h)} \right] \right] + 0.65 \cdot C_f \cdot \left[\frac{0.02}{\left[\frac{S}{h} \right]} \cdot \sqrt{er} + \left[1 - \frac{1}{er^2} \right] \right]$$

$$C'_o := C_f + C_p + C_{gd} + C_{ga} + C_{gt}$$

$$C'_o = 3.2000473 \cdot 10^{-11}$$

"Zero frequency" results:

$$Zoed := \frac{1}{\left[c \cdot \sqrt{C'_e \cdot C_e} \right]} \qquad eered := \frac{C_e}{C'_e}$$

$$Zood := \frac{1}{\left[c \cdot \sqrt{C'_o \cdot C_o} \right]} \qquad eored := \frac{C_o}{C'_o}$$

$Zoed = 36.0242206$ $\quad eered = 17.3394256$

$Zood = 28.5319599$ $\quad eored = 13.346684$

Calculate the incremental inductance factor:

$$G_e := \frac{1}{\left[\mu_o \cdot c \right]} \cdot \frac{\left[\sqrt{eered} \cdot Zoed - \sqrt{eere} \cdot Zoe \right]}{dnormal} \qquad G_e = 2.554039 \cdot 10^3$$

$$G_o := \frac{1}{\left[\mu_o \cdot c \right]} \cdot \frac{\left[\sqrt{eored} \cdot Zood - \sqrt{eore} \cdot Zoo \right]}{dnormal} \qquad G_o = 1.8266337 \cdot 10^3$$

2nd TYPE OF COUPLED LINE

Microstrip Parameters

$h = 5.08 \cdot 10^{-4}$

$W := 0.5 \cdot 10^{-3}$

$S := 1.267 \cdot 10^{-3}$

$L := 3.004 \cdot 10^{-3}$

$t := 5 \cdot 10^{-7}$

$er := 24.5$

Capacitances of coupled Lines

$$W_{em} := if\left[\frac{W}{h} > \frac{1}{\left[2 \cdot \pi\right]}, W + \frac{1.25}{\pi} \cdot t \cdot \left[1 + ln\left[2 \cdot \frac{h}{t}\right]\right], W + \frac{1.25}{\pi} \cdot t \cdot \left[1 + ln\left[4 \cdot \pi \cdot \frac{W}{t}\right]\right]\right]$$

$$F := if\left[\frac{W}{h} > 1, \left[1 + 12 \cdot \frac{h}{W}\right]^{-\left[\frac{1}{2}\right]}, \left[1 + 12 \cdot \frac{h}{W}\right]^{-\left[\frac{1}{2}\right]} + 0.04 \cdot \left[1 - \frac{W}{h}\right]^2\right]$$

$$ere := \frac{(er+1)}{2} + \frac{(er-1)}{2} \cdot F - \frac{(er-1)}{4.6} \cdot \frac{\left[\frac{t}{h}\right]}{\sqrt{\frac{W}{h}}}$$

$W_{em} = 5.0171425 \cdot 10^{-4}$

$ere = 15.9801098$

$$Z_{om} := if\left[\frac{W}{h} > 1, \frac{\eta}{\sqrt{ere}} \cdot \left[\frac{W_{em}}{h} + 1.393 + 0.667 \cdot ln\left[\frac{W_{em}}{h} + 1.444\right]\right]^{-1}, \frac{\eta}{\left[2 \cdot \pi \cdot \sqrt{ere}\right]} \cdot ln\left[8 \cdot \frac{h}{W_{em}} + 0.25 \cdot \frac{W_{em}}{h}\right]\right]$$

$Z_{om} = 31.8268821$

$C_p := \varepsilon_0 \cdot er \cdot \frac{W}{h}$

$C_f := 0.5 \cdot \left[\frac{\sqrt{ere}}{\left[c \cdot Z_{om}\right]} - \varepsilon_0 \cdot er \cdot \frac{W}{h}\right]$

$A := \exp\left[-0.1 \cdot \exp\left[2.33 - 2.53 \cdot \frac{W}{h}\right]\right]$

$$C'_f := \frac{C_f}{\left[1 + A \cdot \frac{h}{S} \cdot \tanh\left[10 \cdot \frac{S}{h}\right]\right]} \cdot \frac{\sqrt{er}}{\sqrt{ere}}$$

$$C_e := C_p + C_f + C'_f$$

$$C_e = 4.0919793 \cdot 10^{-10}$$

$$k := \frac{S}{(S + 2 \cdot W)} \qquad k = 0.5588884$$

$$\frac{K'(k)}{K(k)} = 1.1954202$$

$$C_{ga} := \varepsilon_o \cdot \frac{K'(k)}{K(k)} \qquad C_{ga} = 1.0584251 \cdot 10^{-11}$$

$$C_{gd} := \frac{[\varepsilon_o \cdot er]}{\pi} \cdot \ln\left[\coth\left[\pi \cdot \frac{S}{(4 \cdot h)}\right]\right] + 0.65 \cdot C_f \cdot \left[\frac{0.02}{\left[\frac{S}{h}\right]} \cdot \sqrt{er} + \left[1 - \frac{1}{er^2}\right]\right]$$

$$C_{gt} := 2 \cdot \varepsilon_o \cdot \frac{t}{S}$$

$$C_o := C_f + C_p + C_{gd} + C_{ga} + C_{gt}$$

$$C_o = 3.9888096 \cdot 10^{-10}$$

$er := 1$

$$ere := \frac{(er+1)}{2} + \frac{(er-1)}{2} \cdot F - \frac{(er-1)}{4.6} \cdot \frac{\left[\frac{t}{h}\right]}{\sqrt{\frac{W}{h}}} \qquad ere = 1$$

$$Z_{om} := if\left[\frac{W}{h} > 1, \frac{\eta}{\sqrt{ere}} \cdot \left[\frac{W_{em}}{h} + 1.393 + 0.667 \cdot \ln\left[\frac{W_{em}}{h} + 1.444\right]\right]^{-1}, \frac{\eta}{\left[2 \cdot \pi \cdot \sqrt{ere}\right]} \cdot \ln\left[8 \cdot \frac{h}{W_{em}} + 0.25 \cdot \frac{W_{em}}{h}\right]\right]$$

$$Z_{om} = 127.2283735$$

$$C_p := \varepsilon_o \cdot er \cdot \frac{W}{h}$$

$$C_f := 0.5 \cdot \left[\frac{\sqrt{ere}}{\left[c \cdot Z_{om}\right]} - \varepsilon_o \cdot er \cdot \frac{W}{h}\right]$$

$$C'_f := \frac{C_f}{\left[1 + A \cdot \frac{h}{S} \cdot \tanh\left[10 \cdot \frac{S}{h}\right]\right]} \cdot \sqrt{\frac{er}{ere}}$$

$$C'_e := C_p + C_f + C'_f$$

$$C'_e = 2.3862336 \cdot 10^{-11}$$

$$C_{gd} := \frac{\left[\varepsilon_o \cdot er\right]}{\pi} \cdot \ln\left[\coth\left[\pi \cdot \frac{S}{(4 \cdot h)}\right]\right] + 0.65 \cdot C_f \cdot \left[\frac{0.02}{\left[\frac{S}{h}\right]} \cdot \sqrt{er} + \left[1 - \frac{1}{er^2}\right]\right]$$

$$C'_o := C_f + C_p + C_{gd} + C_{ga} + C_{gt}$$

$$C'_o = 2.8214978 \cdot 10^{-11}$$

"Zero frequency" results:

$$Zoe := \frac{1}{\left[c \cdot \sqrt{C'_e \cdot C_e}\right]} \qquad eere := \frac{C_e}{C'_e}$$

$$Zoo := \frac{1}{\left[c \cdot \sqrt{C'_o \cdot C_o}\right]} \qquad eore := \frac{C_o}{C'_o}$$

$Zoe = 33.7560405$ $\quad eere = 17.1482764$

$Zoo = 31.4422182$ $\quad eore = 14.1372061$

$$f_{pe} := \frac{Zoe}{\left[4 \cdot \mu_o \cdot h\right]} \qquad f_{pe} = 13.2195883 \cdot 10^9$$

$$f_{po} := \frac{Zoo}{\left[\mu_o \cdot h\right]} \qquad f_{po} = 49.2537839 \cdot 10^9$$

$G_{de} := 0.6 + 0.0045 \cdot Zoe$ $\quad G_{de} = 0.7519022$

$G_{do} := 0.6 + 0.018 \cdot Zoo$ $\quad G_{do} = 1.1659599$

$$k_e := \tanh\left[\frac{\pi}{4} \cdot \frac{W}{h}\right] \cdot \tanh\left[\frac{\pi}{4} \cdot \frac{(W+S)}{h}\right]$$

$$k_o := \frac{\tanh\left[\frac{\pi}{4}\cdot\frac{W}{h}\right]}{\tanh\left[\frac{\pi}{4}\cdot\frac{(W+S)}{h}\right]} \qquad er := 24.5$$

$$Z_{te} := 60\cdot\frac{\pi}{\sqrt{er}}\cdot\frac{K'[k_e]}{K[k_e]} \qquad Z_{te} = 41.2323794$$

$$Ze := Z_{te} - \frac{[Z_{te} - Zoe]}{\left[1+G_{de}\cdot\left[\frac{f}{f_{pe}}\right]^{1.6}\right]}$$

$Ze = 35.6389673$ $Zoe = 33.7560405$

$$Z_{to} := 60\cdot\frac{\pi}{\sqrt{er}}\cdot\frac{K'[k_o]}{K[k_o]} \qquad Z_{to} = 40.6873556$$

$$Zo := Z_{to} - \frac{[Z_{to} - Zoo]}{\left[1+G_{do}\cdot\left[\frac{f}{f_{po}}\right]^{1.6}\right]}$$

$Zo = 31.9953687$ $Zoo = 31.4422182$

$$ere := er - \frac{(er - eere)}{\left[1+G_{de}\cdot\left[\frac{f}{f_{pe}}\right]^{2}\right]}$$

$eere = 17.1482764$ $ere = 18.7355831$

$$ero := er - \frac{(er - eore)}{\left[1+G_{do}\cdot\left[\frac{f}{f_{po}}\right]^{2}\right]}$$

$eore = 14.1372061$ $ero = 14.4464519$

Calculate new impedances under recession of walls by dnormal:

$$dnormal := \frac{t}{1000}$$

$t := t - 2\cdot dnormal$ $t = 4.99\cdot10^{-7}$

$W := W - 2 \cdot dnormal \qquad W = 4.99999 \cdot 10^{-4}$

$S := S + 2 \cdot dnormal \qquad S = 0.001267001$

$er := 24.5$

Capacitances of coupled Lines

$$W_{em} := if\left[\frac{W}{h} > \frac{1}{\left[2 \cdot \pi\right]}, W + \frac{1.25}{\pi} \cdot t \cdot \left[1 + ln\left[2 \cdot \frac{h}{t}\right]\right], W + \frac{1.25}{\pi} \cdot t \cdot \left[1 + ln\left[4 \cdot \pi \cdot \frac{W}{t}\right]\right]\right]$$

$$F := if\left[\frac{W}{h} > 1, \left[1 + 12 \cdot \frac{h}{W}\right]^{-\left[\frac{1}{2}\right]}, \left[1 + 12 \cdot \frac{h}{W}\right]^{-\left[\frac{1}{2}\right]} + 0.04 \cdot \left[1 - \frac{W}{h}\right]^2\right] \qquad W_{em} = 5.0171022 \cdot 10^{-4}$$

$$ere := \frac{(er+1)}{2} + \frac{(er-1)}{2} \cdot F - \frac{(er-1)}{4.6} \cdot \frac{\left[\frac{t}{h}\right]}{\sqrt{\frac{W}{h}}} \qquad ere = 15.980117$$

$$Z_{om} := if\left[\frac{W}{h} > 1, \frac{\eta}{\sqrt{ere}} \cdot \left[\frac{W_{em}}{h} + 1.393 + 0.667 \cdot ln\left[\frac{W_{em}}{h} + 1.444\right]\right]^{-1}, \frac{\eta}{\left[2 \cdot \pi \cdot \sqrt{ere}\right]} \cdot ln\left[8 \cdot \frac{h}{W_{em}} + 0.25 \cdot \frac{W_{em}}{h}\right]\right]$$

$Z_{om} = 31.8269884$

$$C_p := \varepsilon_0 \cdot er \cdot \frac{W}{h}$$

$$C_f := 0.5 \cdot \left[\frac{\sqrt{ere}}{\left[c \cdot Z_{om}\right]} - \varepsilon_0 \cdot er \cdot \frac{W}{h}\right]$$

$$A := \exp\left[-0.1 \cdot \exp\left[2.33 - 2.53 \cdot \frac{W}{h}\right]\right]$$

$$C'_f := \frac{C_f}{\left[1 + A \cdot \frac{h}{S} \cdot \tanh\left[10 \cdot \frac{S}{h}\right]\right]} \cdot \sqrt{\frac{er}{ere}}$$

$$C_e := C_p + C_f + C'_f$$

$C_e = 4.0919668 \cdot 10^{-10}$

$k := \frac{S}{(S+2 \cdot W)}$ $\quad k = 0.5588891$

$\frac{K'(k)}{K(k)} = 1.1954193$

$C_{ga} := \varepsilon_o \cdot \frac{K'(k)}{K(k)}$ $\quad C_{ga} = 1.0584242 \cdot 10^{-11}$

$C_{gd} := \frac{[\varepsilon_o \cdot er]}{\pi} \cdot \ln\left[\coth\left[\pi \cdot \frac{S}{(4 \cdot h)}\right]\right] + 0.65 \cdot C_f \cdot \left[\frac{0.02}{\left[\frac{S}{h}\right]} \cdot \sqrt{er} + \left[1 - \frac{1}{er^2}\right]\right]$

$C_{gt} := 2 \cdot \varepsilon_o \cdot \frac{t}{S}$

$C_o := C_f + C_p + C_{gd} + C_{ga} + C_{gt}$

$C_o = 3.9887977 \cdot 10^{-10}$

$er := 1$

$ere := \frac{(er+1)}{2} + \frac{(er-1)}{2} \cdot F - \frac{(er-1)}{4.6} \cdot \frac{\left[\frac{t}{h}\right]}{\sqrt{\frac{W}{h}}}$ $\quad ere = 1$

$Z_{om} := if\left[\frac{W}{h} > 1, \frac{\eta}{\sqrt{ere}} \cdot \left[\frac{W_{em}}{h} + 1.393 + 0.667 \cdot \ln\left[\frac{W_{em}}{h} + 1.444\right]\right]^{-1}, \frac{\eta}{\left[2 \cdot \pi \cdot \sqrt{ere}\right]} \cdot \ln\left[8 \cdot \frac{h}{W_{em}} + 0.25 \cdot \frac{W_{em}}{h}\right]\right]$

$Z_{om} = 127.2288267$

$C_p := \varepsilon_o \cdot er \cdot \frac{W}{h}$

$C_f := 0.5 \cdot \left[\frac{\sqrt{ere}}{\left[c \cdot Z_{om}\right]} - \varepsilon_o \cdot er \cdot \frac{W}{h}\right]$

$C'_f := \frac{C_f}{\left[1 + A \cdot \frac{h}{S} \cdot \tanh\left[10 \cdot \frac{S}{h}\right]\right]} \cdot \frac{\sqrt{er}}{\sqrt{ere}}$

$C'_e = C_p + C_f + C'_f$ $\quad C'_e = 2.3862336 \cdot 10^{-11}$

$$C_{gd} := \frac{[\varepsilon_0 \cdot er]}{\pi} \cdot \ln\left[\coth\left[\pi \cdot \frac{S}{(4 \cdot h)}\right]\right] + 0.65 \cdot C_f \cdot \left[\frac{0.02}{\left[\frac{S}{h}\right]} \cdot \sqrt{er} + \left[1 - \frac{1}{er^2}\right]\right]$$

$$C'_o := C_f + C_p + C_{gd} + C_{ga} + C_{gt}$$

$$C'_o = 2.82149 \cdot 10^{-11}$$

"Zero frequency" results:

$$Zoed := \frac{1}{\left[c \cdot \sqrt{C'_e \cdot C_e}\right]} \qquad eered := \frac{C_e}{C'_e}$$

$$Zood := \frac{1}{\left[c \cdot \sqrt{C'_o \cdot C_o}\right]} \qquad eored := \frac{C_o}{C'_o}$$

$Zoed = 33.7561495$ $eered = 17.1482821$

$Zood = 31.4423089$ $eored = 14.137203$

Calculate the incremental inductance factor:

$$G_e := \frac{1}{[\mu_0 \cdot c]} \cdot \frac{\left[\sqrt{eered} \cdot Zoed - \sqrt{eere} \cdot Zoe\right]}{dnormal} \qquad G_e = 2.521708 \cdot 10^3$$

$$G_o := \frac{1}{[\mu_0 \cdot c]} \cdot \frac{\left[\sqrt{eored} \cdot Zood - \sqrt{eore} \cdot Zoo\right]}{dnormal} \qquad G_o = 1.7433891 \cdot 10^3$$

Microstrip Line Calculations

50 Ohm Microstrip Parameters

$W := 0.172 \cdot 10^{-3}$

$t := 5 \cdot 10^{-7}$

$er := 24.5$

$$F := if\left[\frac{W}{h} > 1, \left[1 + 12 \cdot \frac{h}{W}\right]^{-\left[\frac{1}{2}\right]}, \left[1 + 12 \cdot \frac{h}{W}\right]^{-\left[\frac{1}{2}\right]} + 0.04 \cdot \left[1 - \frac{W}{h}\right]^2\right]$$

$$ere := \frac{(er+1)}{2} + \frac{(er-1)}{2}\cdot F - \frac{(er-1)}{4.6}\cdot\frac{\left[\frac{t}{h}\right]}{\sqrt{\frac{W}{h}}} \qquad ere = 14.8933955$$

$$W_{em} := if\left[\frac{W}{h} > \frac{1}{\left[2\cdot\pi\right]}, W + \frac{1.25}{\pi}\cdot t\cdot\left[1 + ln\left[2\cdot\frac{h}{t}\right]\right], W + \frac{1.25}{\pi}\cdot t\cdot\left[1 + ln\left[4\cdot\pi\cdot\frac{W}{t}\right]\right]\right]$$

$$W_{em} = 1.7371425\cdot10^{-4}$$

$$Z_{om} := if\left[\frac{W}{h} > 1, \frac{\eta}{\sqrt{ere}}\cdot\left[\frac{W_{em}}{h} + 1.393 + 0.667\cdot ln\left[\frac{W_{em}}{h} + 1.444\right]\right]^{-1}, \frac{\eta}{\left[2\cdot\pi\cdot\sqrt{ere}\right]}\cdot ln\left[8\cdot\frac{h}{W_{em}} + 0.25\cdot\frac{W_{em}}{h}\right]\right]$$

$$Z_{om} = 49.0362546$$

Calculate new impedances under recession of walls by dnormal:

$$dnormal := \frac{t}{1000}$$

$$t := t - 2\cdot dnormal \qquad t = 4.99\cdot10^{-7}$$

$$W := W - 2\cdot dnormal \qquad W = 1.71999\cdot10^{-4}$$

$$F := if\left[\frac{W}{h} > 1, \left[1 + 12\cdot\frac{h}{W}\right]^{-\left[\frac{1}{2}\right]}, \left[1 + 12\cdot\frac{h}{W}\right]^{-\left[\frac{1}{2}\right]} + 0.04\cdot\left[1 - \frac{W}{h}\right]^{2}\right]$$

$$ered := \frac{(er+1)}{2} + \frac{(er-1)}{2}\cdot F - \frac{(er-1)}{4.6}\cdot\frac{\left[\frac{t}{h}\right]}{\sqrt{\frac{W}{h}}} \qquad ered = 14.8934085$$

$$W_{em} := if\left[\frac{W}{h} > \frac{1}{\left[2\cdot\pi\right]}, W + \frac{1.25}{\pi}\cdot t\cdot\left[1 + ln\left[2\cdot\frac{h}{t}\right]\right], W + \frac{1.25}{\pi}\cdot t\cdot\left[1 + ln\left[4\cdot\pi\cdot\frac{W}{t}\right]\right]\right]$$

$$W_{em} = 1.7371022\cdot10^{-4}$$

$$Z_{omd} := if\left[\frac{W}{h} > 1, \frac{\eta}{\sqrt{ered}}\cdot\left[\frac{W_{em}}{h} + 1.393 + 0.667\cdot ln\left[\frac{W_{em}}{h} + 1.444\right]\right]^{-1}, \frac{\eta}{\left[2\cdot\pi\cdot\sqrt{ered}\right]}\cdot ln\left[8\cdot\frac{h}{W_{em}} + 0.25\cdot\frac{W_{em}}{h}\right]\right]$$

$$Z_{omd} = 49.0365912$$

$$G_m := \frac{1}{[\mu_0 \cdot c]} \cdot \frac{\left[\sqrt{ered} \cdot Z_{omd} - \sqrt{ere} \cdot Z_{om}\right]}{dnormal}$$

$$G_m = 7.3326405 \cdot 10^{3}$$

Microstrip Line Calculations

Wide Microstrip Parameters

$$W := 0.5 \cdot 10^{-3}$$

$$t := 5 \cdot 10^{-7}$$

$$er := 24.5$$

$$F := if\left[\frac{W}{h} > 1, \left[1 + 12 \cdot \frac{h}{W}\right]^{-\left[\frac{1}{2}\right]}, \left[1 + 12 \cdot \frac{h}{W}\right]^{-\left[\frac{1}{2}\right]} + 0.04 \cdot \left[1 - \frac{W}{h}\right]^{2}\right]$$

$$ere := \frac{(er+1)}{2} + \frac{(er-1)}{2} \cdot F - \frac{(er-1)}{4.6} \cdot \frac{\left[\frac{t}{h}\right]}{\sqrt{\frac{W}{h}}} \qquad ere = 15.9801098$$

$$W_{em} := if\left[\frac{W}{h} > \frac{1}{[2 \cdot \pi]}, W + \frac{1.25}{\pi} \cdot t \cdot \left[1 + \ln\left[2 \cdot \frac{h}{t}\right]\right], W + \frac{1.25}{\pi} \cdot t \cdot \left[1 + \ln\left[4 \cdot \pi \cdot \frac{W}{t}\right]\right]\right]$$

$$W_{em} = 5.0171425 \cdot 10^{-4}$$

$$Z_{om} := if\left[\frac{W}{h} > 1, \frac{\eta}{\sqrt{ere}} \cdot \left[\frac{W_{em}}{h} + 1.393 + 0.667 \cdot \ln\left[\frac{W_{em}}{h} + 1.444\right]\right]^{-1}, \frac{\eta}{[2 \cdot \pi \cdot \sqrt{ere}]} \cdot \ln\left[8 \cdot \frac{h}{W_{em}} + 0.25 \cdot \frac{W_{em}}{h}\right]\right]$$

$$Z_{om} = 31.8268821$$

Calculate new impedances under recession of walls by dnormal:

$$dnormal := \frac{t}{1000}$$

$$t := t - 2 \cdot dnormal \qquad t = 4.99 \cdot 10^{-7}$$

$$W := W - 2 \cdot dnormal \qquad W = 4.99999 \cdot 10^{-4}$$

$$F := \text{if}\left[\frac{W}{h} > 1, \left[1 + 12\cdot\frac{h}{W}\right]^{-\left[\frac{1}{2}\right]}, \left[1 + 12\cdot\frac{h}{W}\right]^{-\left[\frac{1}{2}\right]} + 0.04\cdot\left[1 - \frac{W}{h}\right]^2\right]$$

$$ered := \frac{(er+1)}{2} + \frac{(er-1)}{2}\cdot F - \frac{(er-1)}{4.6}\cdot\frac{\left[\frac{t}{h}\right]}{\sqrt{\frac{W}{h}}}$$

ered = 15.980117

$$W_{em} := \text{if}\left[\frac{W}{h} > \frac{1}{[2\cdot\pi]}, W + \frac{1.25}{\pi}\cdot t\cdot\left[1 + \ln\left[2\cdot\frac{h}{t}\right]\right], W + \frac{1.25}{\pi}\cdot t\cdot\left[1 + \ln\left[4\cdot\pi\cdot\frac{W}{t}\right]\right]\right]$$

$W_{em} = 5.0171022\cdot10^{-4}$

$$Z_{omd} := \text{if}\left[\frac{W}{h} > 1, \frac{\eta}{\sqrt{ered}}\cdot\left[\frac{W_{em}}{h} + 1.393 + 0.667\cdot\ln\left[\frac{W_{em}}{h} + 1.444\right]\right]^{-1}, \frac{\eta}{\left[2\cdot\pi\cdot\sqrt{ered}\right]}\cdot\ln\left[8\cdot\frac{h}{W_{em}} + 0.25\cdot\frac{W_{em}}{h}\right]\right]$$

$Z_{omd} = 31.8269884$

$$G_m := \frac{1}{[\mu_0\cdot c]}\cdot\frac{\left[\sqrt{ered}\cdot Z_{omd} - \sqrt{ere}\cdot Z_{om}\right]}{dnormal}$$

$G_m = 2.4061695\cdot10^{3}$

Microstrip Line Calculations

Input Pad Microstrip Parameters

$W := 0.3\cdot10^{-3}$

$t := 5\cdot10^{-7}$

$er := 24.5$

$$F := \text{if}\left[\frac{W}{h} > 1, \left[1 + 12\cdot\frac{h}{W}\right]^{-\left[\frac{1}{2}\right]}, \left[1 + 12\cdot\frac{h}{W}\right]^{-\left[\frac{1}{2}\right]} + 0.04\cdot\left[1 - \frac{W}{h}\right]^2\right]$$

$$ere := \frac{(er+1)}{2} + \frac{(er-1)}{2}\cdot F - \frac{(er-1)}{4.6}\cdot\frac{\left[\frac{t}{h}\right]}{\sqrt{\frac{W}{h}}}$$

ere = 15.3669965

$$W_{em} := \text{if}\left[\frac{W}{h} > \frac{1}{\left[2\cdot\pi\right]}, W + \frac{1.25}{\pi}\cdot t\cdot\left[1 + \ln\left[2\cdot\frac{h}{t}\right]\right], W + \frac{1.25}{\pi}\cdot t\cdot\left[1 + \ln\left[4\cdot\pi\cdot\frac{W}{t}\right]\right]\right]$$

$$W_{em} = 3.0171425\cdot10^{-4}$$

$$Z_{om} := \text{if}\left[\frac{W}{h} > 1, \frac{\eta}{\sqrt{ere}}\cdot\left[\frac{W_{em}}{h} + 1.393 + 0.667\cdot\ln\left[\frac{W_{em}}{h} + 1.444\right]\right]^{-1}, \frac{\eta}{\left[2\cdot\pi\cdot\sqrt{ere}\right]}\cdot\ln\left[8\cdot\frac{h}{W_{em}} + 0.25\cdot\frac{W_{em}}{h}\right]\right]$$

$$Z_{om} = 39.9424912$$

Calculate new impedances under recession of walls by dnormal:

$$dnormal := \frac{t}{1000}$$

$$t := t - 2\cdot dnormal \qquad t = 4.99\cdot10^{-7}$$

$$W := W - 2\cdot dnormal \qquad W = 2.99999\cdot10^{-4}$$

$$F := \text{if}\left[\frac{W}{h} > 1, \left[1 + 12\cdot\frac{h}{W}\right]^{-\left[\frac{1}{2}\right]}, \left[1 + 12\cdot\frac{h}{W}\right]^{-\left[\frac{1}{2}\right]} + 0.04\cdot\left[1 - \frac{W}{h}\right]^{2}\right]$$

$$ered := \frac{(er+1)}{2} + \frac{(er-1)}{2}\cdot F - \frac{(er-1)}{4.6}\cdot\frac{\left[\frac{t}{h}\right]}{\sqrt{\frac{W}{h}}} \qquad ered = 15.3670063$$

$$W_{em} := \text{if}\left[\frac{W}{h} > \frac{1}{\left[2\cdot\pi\right]}, W + \frac{1.25}{\pi}\cdot t\cdot\left[1 + \ln\left[2\cdot\frac{h}{t}\right]\right], W + \frac{1.25}{\pi}\cdot t\cdot\left[1 + \ln\left[4\cdot\pi\cdot\frac{W}{t}\right]\right]\right]$$

$$W_{em} = 3.0171022\cdot10^{-4}$$

$$Z_{omd} := \text{if}\left[\frac{W}{h} > 1, \frac{\eta}{\sqrt{ered}}\cdot\left[\frac{W_{em}}{h} + 1.393 + 0.667\cdot\ln\left[\frac{W_{em}}{h} + 1.444\right]\right]^{-1}, \frac{\eta}{\left[2\cdot\pi\cdot\sqrt{ered}\right]}\cdot\ln\left[8\cdot\frac{h}{W_{em}} + 0.25\cdot\frac{W_{em}}{h}\right]\right]$$

$$Z_{omd} = 39.9426784$$

$$G_m := \frac{1}{\left[\mu_0\cdot c\right]}\cdot\frac{\left[\sqrt{ered}\cdot Z_{omd} - \sqrt{ere}\cdot Z_{om}\right]}{dnormal} \qquad G_m = 2.4061695\cdot10^{3}$$

Appendix B

Sample Touchstone Circuit File:

The Case of No Dispersion

```
                                !MODEL OF YBCO BPF FILTER
!DIMITRIOS ANTSOS 5-4-93


DIM
FREQ      GHZ
RES       OH
COND      /OH
IND       NH
CAP       PF
LNG       MM
TIME      PS
ANG       RAD
VOL       V
CUR       MA
PWR       DBM
VAR
LD0 #140.000000000 756.8542 8000.00000000
 T = 77                    !TEMPERATURE OF MEASUREMENT
 Tc = 85                   !Critical Temperture of Sample
Sn #100000.000000 1351382. 8000000.00000

 ! CONSTANTS
 e0 = 8.854E-12          !Permittivity of free space

 !COUPLED LINE PARAMETERS

AGN =0.00000000025
 GNe = 2.55404e3          !Incremental Inductance (Narrow gap, even mode)
 GNo = 1.826634e3         !Incremental Inductance (Narrow gap, odd mode)
 ZN0e= 36.02             !Even Mode Characteristic Impedance
 ZN0o= 28.53             !Odd Mode Characteristic Impedance
 KN0e= 17.33             !Even Mode Effective Dielectric Constant
 KN0o= 13.35             !Odd Mode Effective Dielectric Constant

AGW =0.00000000025
 GWe = 2.52171e3          !Incremental Inductance (Wide gap, even mode)
 GWo = 1.743389e3         !Incremental Inductance (Wide gap, odd mode)
 ZW0e= 33.76             !Even Mode Characteristic Impedance
 ZW0o= 31.44             !Odd Mode Characteristic Impedance
 KW0e= 17.15             !Even Mode Effective Dielectric Constant
 KW0o= 14.13             !Odd Mode Effective Dielectric Constant

 !MICROSTRIP LINE PARAMETERS

 !50 Ohm Line

AG5 =0.00000000009
 G5 = 7.33264e3           !Incremental Inductance
 Z5 = 49.03              !Characteristic Impedance
 K5 = 14.89              !Effective Dielectric Constant

 !Stub Line
```

```
AGS =0.00000000025
 GS = 2.40617e3          !Incremental Inductance
 ZS0 = 31.83             !Characteristic Impedance
 KS0 = 15.98             !Effective Dielectric Constant

 !Iput Pad Line

AGP =1.5e-10
 GP = 4160.03            !Incremental Inductance
 ZP0 = 39.94             !Characteristic Impedance
 KP0 = 15.37             !Effective Dielectric Constant

Lextra2 #0.30000000000 0.788364 1.50000000000
 LFIL1 =  1.815          !  1.815
 LFIL2 =  3.004          ! 3.004

 Wextra = 0.172
 WFIL1 = 0.5
 WFIL2 = 0.5

Lstub2 #1.00000000000 1.699751 3.50000000000
Linp2 #0.10000000000 0.294983 0.35000000000
W50 =0.17200000000
Wef =0.50000000000

eps =24.5000000000
EQN

LD=LD0*1e-9

! Computation of losses for first, narrow spaced, coupled lines
!      Constants

 U0 = 4*PI*1e-7          !Magnetic Permeability of vacuum
 c = 1/sqrt(e0*U0)       !Velocity of light
 h0=sqrt(U0/e0)          !Impedance of free space

 f = FREQ*1e9            !Frequency in Hz
 Sr = Sn*(T/Tc)**4       !Real Part of conductivity of YBCO (Sigma1)
 Si = (1-(T/Tc)**4)/(2*PI*f*U0*LD**2)  !Imaginary Part of conductivity (Sigma2)
 P = ATAN(Si/Sr)         !Angle of conductivity  (Phi)
 Th= 5*PI/4-P/2          !Auxiliary angle definition (Theta)
 Sigmag= SQRT(SQR(Sr)+SQR(Si)) !Norm of conductivity

! NARROW-GAP COUPLED-LINE EQUATIONS

! Even Mode

 BNe= GNe*AGN*SQRT(2*PI*f*U0*Sigmag)        !B
 CNe= EXP(2*BNe*COS(Th))
 DNe= COS(2*BNe*SIN(Th))
 ENe= SIN(2*BNe*SIN(Th))
 UNe= SQRT(SQR(CNe*DNe-1)+SQR(CNe*ENe))     !Psi
 WNe= ATAN(CNe*ENe/(CNe*DNe-1))             !Chi
```

```
FNe= BNe/(AGN*sigmag*UNe)                !Prefactor of Ri and Xi
MNe= 2*BNe*SIN(Th)
NNe= COS(PI/4+P/2-WNe)
RPNe= COS(MNe+PI/4+P/2-WNe)

RiNe = FNe*(NNe+CNe*RPNe)          !Internal Resistance  / Meter

NINe= SIN(PI/4+P/2-WNe)
RDNe= SIN(MNe+PI/4+P/2-WNe)

LiNe = 1/(2*PI*f)*FNe*(NINe+CNe*RDNe) !Internal Inductance / Meter

CORRNe = 1+(c/sqrt(KN0e))*(LiNe/ZN0e) !Correction Factor (3.41)

ZNe = ZN0e*sqrt(CORRNe)            !Corrected Char Impedance

KNe = KN0e*CORRNe                  !Corrected  Dielectric Const (3.43)

ACNe = (8.686e-3) * RiNe/(2*ZNe)     !Loss Coefficient, in [dB/mm]


! Odd Mode

BNo= GNo*AGN*SQRT(2*PI*f*U0*sigmag)          !B
CNo= EXP(2*BNo*COS(Th))
DNo= COS(2*BNo*SIN(Th))
ENo= SIN(2*BNo*SIN(Th))
UNo= SQRT(SQR(CNo*DNo-1)+SQR(CNo*ENo))       !Psi
WNo= ATAN(CNo*ENo/(CNo*DNo-1))               !Chi
FNo= BNo/(AGN*sigmag*UNo)                !Prefactor of Ri and Xi
MNo= 2*BNo*SIN(Th)
NNo= COS(PI/4+P/2-WNo)
RPNo= COS(MNo+PI/4+P/2-WNo)

RiNo = FNo*(NNo+CNo*RPNo)          !Internal Resistance  / Meter

NINo= SIN(PI/4+P/2-WNo)
RDNo= SIN(MNo+PI/4+P/2-WNo)

LiNo = 1/(2*PI*f)*FNo*(NINo+CNo*RDNo) !Internal Inductance / Meter

CORRNo = 1+(c/sqrt(KN0o))*(LiNo/ZN0o) !Correction Factor (3.41)

ZNo = ZN0o*sqrt(CORRNo)            !Corrected Char Impedance

KNo = KN0o*CORRNo                  !Corrected  Dielectric Const (3.43)

ACNo = (8.686e-3) * RiNo/(2*ZNo)     !Loss Coefficient, in [dB/mm]


! WIDE-GAP COUPLED-LINE EQUATIONS

! Even Mode
```

```
BWe= GWe*AGW*SQRT(2*PI*f*U0*sigmag)          !B
CWe= EXP(2*BWe*COS(Th))
DWe= COS(2*BWe*SIN(Th))
EWe= SIN(2*BWe*SIN(Th))
UWe= SQRT(SQR(CWe*DWe-1)+SQR(CWe*EWe))       !Psi
WWe= ATAN(CWe*EWe/(CWe*DWe-1))               !Chi
FWe= BWe/(AGW*sigmag*UWe)                    !Prefactor of Ri and Xi
MWe= 2*BWe*SIN(Th)
NWe= COS(PI/4+P/2-WWe)
RPWe= COS(MWe+PI/4+P/2-WWe)

RiWe = FWe*(NWe+CWe*RPWe)           !Internal Resistance  / Meter

NIWe= SIN(PI/4+P/2-WWe)
RDWe= SIN(MWe+PI/4+P/2-WWe)

LiWe = 1/(2*PI*f)*FWe*(NIWe+CWe*RDWe) !Internal Inductance / Meter

CORRWe = 1+(c/sqrt(KW0e))*(LiWe/ZW0e) !Correction Factor (3.41)

ZWe = ZW0e*sqrt(CORRWe)             !Corrected Char Impedance

KWe = KW0e*CORRWe                   !Corrected  Dielectric Const (3.43)

ACWe = (8.686e-3) * RiWe/(2*ZWe)     !Loss Coefficient, in [dB/mm]


! Odd Mode

BWo= GWo*AGW*SQRT(2*PI*f*U0*sigmag)          !B
CWo= EXP(2*BWo*COS(Th))
DWo= COS(2*BWo*SIN(Th))
EWo= SIN(2*BWo*SIN(Th))
UWo= SQRT(SQR(CWo*DWo-1)+SQR(CWo*EWo))       !Psi
WWo= ATAN(CWo*EWo/(CWo*DWo-1))               !Chi
FWo= BWo/(AGW*sigmag*UWo)                    !Prefactor of Ri and Xi
MWo= 2*BWo*SIN(Th)
NWo= COS(PI/4+P/2-WWo)
RPWo= COS(MWo+PI/4+P/2-WWo)

RiWo = FWo*(NWo+CWo*RPWo)           !Internal Resistance  / Meter

NIWo= SIN(PI/4+P/2-WWo)
RDWo= SIN(MWo+PI/4+P/2-WWo)

LiWo = 1/(2*PI*f)*FWo*(NIWo+CWo*RDWo) !Internal Inductance / Meter

CORRWo = 1+(c/sqrt(KW0o))*(LiWo/ZW0o) !Correction Factor (3.41)

ZWo = ZW0o*sqrt(CORRWo)             !Corrected Char Impedance

KWo = KW0o*CORRWo                   !Corrected  Dielectric Const (3.43)

ACWo = (8.686e-3) * RiWo/(2*ZWo)     !Loss Coefficient, in [dB/mm]
```

```
! MICROSTRIP LINE PARAMETERS

! 50 OHM LINE

 B5= G5*AG5*SQRT(2*PI*f*U0*sigmag)          !B
 C5= EXP(2*B5*COS(Th))
 D5= COS(2*B5*SIN(Th))
 E5= SIN(2*B5*SIN(Th))
 U5= SQRT(SQR(C5*D5-1)+SQR(C5*E5))          !Psi
 W5= ATAN(C5*E5/(C5*D5-1))                  !Chi
 F5= B5/(AG5*sigmag*U5)                     !Prefactor of Ri and Xi
 M5= 2*B5*SIN(Th)
 N5= COS(PI/4+P/2-W5)
 RP5= COS(M5+PI/4+P/2-W5)

 Ri5 = F5*(N5+C5*RP5)                       !Internal Resistance  / Meter

 NI5= SIN(PI/4+P/2-W5)
 RD5= SIN(M5+PI/4+P/2-W5)

 Li5 = 1/(2*PI*f)*F5*(NI5+C5*RD5)           !Internal Inductance / Meter

 CORR5 = 1+(c/sqrt(K5))*(Li5/Z5)            !Correction Factor (3.41)

 Z50 = Z5*sqrt(CORR5)                       !Corrected Char Impedance

 K50 = K5*CORR5                             !Corrected  Dielectric Const (3.43)

 AC50 = (8.686e-3) * Ri5/(2*Z50)            !Loss Coefficient, in [dB/mm]

! STUB LINE

 BS= GS*AGS*SQRT(2*PI*f*U0*sigmag)          !B
 CS= EXP(2*BS*COS(Th))
 DS= COS(2*BS*SIN(Th))
 ES= SIN(2*BS*SIN(Th))
 US= SQRT(SQR(CS*DS-1)+SQR(CS*ES))          !Psi
 WS= ATAN(CS*ES/(CS*DS-1))                  !Chi
 FS= BS/(AGS*sigmag*US)                     !Prefactor of Ri and Xi
 MS= 2*BS*SIN(Th)
 NS= COS(PI/4+P/2-WS)
 RPS= COS(MS+PI/4+P/2-WS)

 RiS= FS*(NS+CS*RPS)                        !Internal Resistance  / Meter

 NIS= SIN(PI/4+P/2-WS)
 RDS= SIN(MS+PI/4+P/2-WS)

 LiS = 1/(2*PI*f)*FS*(NIS+CS*RDS)           !Internal Inductance / Meter

 CORRS = 1+(c/sqrt(KS0))*(LiS/ZS0)          !Correction Factor (3.41)

 ZS = ZS0*sqrt(CORRS)                       !Corrected Char Impedance
```

```
 KS = KS0*CORRS                    !Corrected  Dielectric Const (3.43)

 ACS = (8.686e-3) * RiS/(2*ZS)     !Loss Coefficient, in [dB/mm]

! INPUT PAD LINE

 BP= GP*AGP*SQRT(2*PI*f*U0*sigmag)          !B
 CP= EXP(2*BP*COS(Th))
 DP= COS(2*BP*SIN(Th))
 EP= SIN(2*BP*SIN(Th))
 UP= SQRT(SQR(CP*DP-1)+SQR(CP*EP))          !Psi
 WP= ATAN(CP*EP/(CP*DP-1))                  !Chi
 FP= BP/(AGP*sigmag*UP)            !Prefactor of Ri and Xi
 MP= 2*BP*SIN(Th)
 NP= COS(PI/4+P/2-WP)
 RPP= COS(MP+PI/4+P/2-WP)

 RiP= FP*(NP+CP*RPP)               !Internal Resistance  / Meter

 NIP= SIN(PI/4+P/2-WP)
 RDP= SIN(MP+PI/4+P/2-WP)

 LiP = 1/(2*PI*f)*FP*(NIP+CP*RDP)  !Internal Inductance / Meter

 CORRP = 1+(c/sqrt(KP0))*(LiP/ZP0) !Correction Factor (3.41)

 ZP = ZP0*sqrt(CORRP)              !Corrected Char Impedance

 KP = KP0*CORRP                    !Corrected  Dielectric Const (3.43)

 ACP = (8.686e-3) * RiP/(2*ZP)     !Loss Coefficient, in [dB/mm]


Rbend =W50/2

CKT


!RES 1 0 R^rez5
!DEF1P 1 TEST

MSUB_P1 ER^eps H=0.50800000000 T=0.00050000000 RHO=0.00000000000 &
RGH=0.00000000000
MSTEP_T3 2 5 W1^Wextra W2^WFIL1
MSTEP_T4 6 3 W1^WFIL1 W2^Wextra MLIN W=2.00000000000 L=2.00000000000
CLINP_T5 5 7 8 9 ZE^ZNe ZO^ZNo L^LFIL1 KE^KNe KO^KNo AE^ACNe AO^ACNo MCFIL &
W=2.00000000000 S=3.00000000000 L=4.00000000000 W1=5.00000000000 &
W2=6.00000000000
CLINP_T6 14 11 6 12 ZE^ZNe ZO^ZNo L^LFIL1 KE^KNe KO^KNo AE^ACNe AO^ACNo MCFIL &
W=2.00000000000 S=2.00000000000 L=2.00000000000 W1=2.00000000000 &
W2=2.00000000000
```

```
CLINP_T7 8 13 14 15 ZE^ZWe ZO^ZWo L^LFIL2 KE^KWe KO^KWo AE^ACWe AO^ACWo MCFIL
&
W=2.00000000000 S=2.00000000000 L=2.00000000000 W1=2.00000000000 &
W2=2.00000000000
MLEF_T8 9 W^WFIL1 L=0.00000000000 CPWEGAP W=2.00000000000 G=2.00000000000 &
S=3.00000000000 L=4.00000000000
MLEF_T9 7 W^WFIL1 L=0.00000000000 CPWEGAP W=1.00000000000 G=2.00000000000 &
S=3.00000000000 L=4.00000000000
MLEF_T10 12 W^WFIL1 L=0.00000000000 CPWEGAP W=2.00000000000 G=2.00000000000 &
S=3.00000000000 L=4.00000000000
MLEF_T11 11 W^WFIL1 L=0.00000000000 CPWEGAP W=2.00000000000 G=2.00000000000 &
S=3.00000000000 L=4.00000000000
MLEF_T12 15 W^WFIL2 L=0.00000000000 CPWEGAP W=2.00000000000 G=2.00000000000 &
S=3.00000000000 L=4.00000000000
MLEF_T13 13 W^WFIL2 L=0.00000000000 CPWEGAP W=2.00000000000 G=2.00000000000 &
S=3.00000000000 L=4.00000000000
DEF2P 2 3 MAIN
MSTEP_T2 2 3 W1=0.30000000000 W2^w50
TLINP_T17 7 8 Z^ZS L^Lstub2 K^KS A^ACS F=0.00000000000 CONN_T15
MLEF_T18 8 W^Wef L=0.00000000000
TLINP_T19 10 9 Z^Z50 L^Lextra2 K^K50 A^AC50 F=0.00000000000 CONN_S2
TLINP_T14 3 4 Z^Z50 L^Linp2 K^K50 A^AC50 F=0.00000000000 CONN
S3P_S2 5 4 10 /home/crafty/dimitri/eesof/hts_bpf/model/t MTEE W1=0.50000000000 &
W2=0.50000000000 W3=0.50000000000
MSTEP_T15 5 7 W1^W50 W2^Wef
TLINP_T16 1 2 Z^ZP L=0.10000000000 K^KP A^ACP F=0.00000000000 MLIN W^w50 &
L^Lextra2
DEF2P 1 9 LEFTB
MAIN_X1 1 2
LEFTB_X2 3 1
LEFTB_X3 4 2
DEF2P 3 4 FLTRBSC
S2P_S1 1 2 0 /home/crafty/dimitri/eesof/hts_bpf/hts5c1dm MTEE W1=0.50000000000 &
W2=0.50000000000 W3=0.50000000000
DEF2P 1 2 YBCO
RES_R4 4 0 R^CORRWo MLIN W^W50 L^Lextra2
RES_R6 6 0 R^CORRS MLIN W^w50 L^Lextra2
RES_R5 5 0 R^CORR5 MLIN W^w50 L^Lextra2
DEF3P 4 5 6 TEST
TERM

PROC

MODEL


SOURCE

DCTR

FREQ
SWEEP 6 8.5 0.01
POWER
```

```
FILEOUT

OUTVAR

OUTEQN

OUT
fltrbsc DB[S21] GR1
 YBCO DB[S21] GR1

fltrbsc DB[S11] GR3
 YBCO DB[S11] GR3

fltrbsc ANG[S21] GR2
 YBCO ANG[S21] GR2

!fltrbsc ANG[S11] GR4
! YBCO ANG[S11] GR4

!MAIN S21 SC2
!YBCO S21 SC2
!TEST RE[Z11] GR5

!FIL DB[S21] GR6
!YBCO DB[S21] GR6
fltrbsc ANG[s11] gr4
YBCO ANG[s11] gr4
 TEST RE[Z11] SCN
 TEST RE[Z22] SCN
 TEST RE[Z33] SCN
!TEST RE[Z44] SCN
!TEST RE[Z55] SCN
!TEST RE[Z66] SCN
fltrbsc S21 sc2
YBCO S21 sc2
GRID
! RANGE 1 11 1
! GR1 -10 0 1
! GR5 .001 .003 .0001

!RANGE 7 9 .2
! GR6 -2 0 .5

!RANGE 6 8.5 .5
!gr4 -10 0 1

HBCNTL

OPT
 YBCO MODEL FLTRBSC

YIELD
```

Appendix C

Sample Touchstone Circuit File:
The Case of Dispersion

```
                                    !MODEL OF YBCO BPF FILTER
!DIMITRIOS ANTSOS 5-4-93


DIM
FREQ      GHZ
RES       OH
COND      /OH
IND       NH
CAP       PF
LNG       MM
TIME      PS
ANG       RAD
VOL       V
CUR       MA
PWR       DBM
VAR
LD0 #140.000000000 642.7823 1000.0000000
Sn #400000.000000 5999998. 6000000.00000
Lextra2 #0.30000000000 0.761918 1.50000000000
Lstub2 #1.00000000000 1.681639 3.50000000000
Linp2 #0.10000000000 0.259163 0.35000000000
 T = 77                    !TEMPERATURE OF MEASUREMENT
 Tc = 85                   !Critical Temperture of Sample

 ! CONSTANTS
 e0 = 8.854E-12            !Permittivity of free space

 !COUPLED LINE PARAMETERS

AGN =0.00000000025
 GNe = 2.55404e3           !Incremental Inductance (Narrow gap, even mode)
 GNo = 1.826634e3          !Incremental Inductance (Narrow gap, odd mode)
 ZN00e= 36.39              !Even Mode Characteristic Impedance
 ZN00o= 28.81              !Odd Mode Characteristic Impedance
 KN00e= 16.99              !Even Mode Effective Dielectric Constant
 KN00o= 13.08              !Odd Mode Effective Dielectric Constant
 ZTNe= 43.78               !Dispersive Impedance Correction
 ZTNo= 38.84


AGW =0.00000000025
 GWe = 2.52171e3           !Incremental Inductance (Wide gap, even mode)
 GWo = 1.743389e3          !Incremental Inductance (Wide gap, odd mode)
 ZW00e= 34.10              !Even Mode Characteristic Impedance
 ZW00o= 31.75              !Odd Mode Characteristic Impedance
 KW00e= 16.81              !Even Mode Effective Dielectric Constant
 KW00o= 13.86              !Odd Mode Effective Dielectric Constant
 ZTWe= 41.66               !Dispersive Impedance Correction
 ZTWo= 41.11

 !MICROSTRIP LINE PARAMETERS

 !50 Ohm Line
```

```
AG5 =0.00000000009
 G5 = 7.33264e3          !Incremental Inductance
 Z5 = 49.53             !Characteristic Impedance
 K500 = 14.60            !Effective Dielectric Constant

 !Stub Line

AGS =0.00000000025
 GS = 2.40617e3          !Incremental Inductance
 ZS0 = 32.15            !Characteristic Impedance
 KS00 = 15.66            !Effective Dielectric Constant

 !Iput Pad Line

AGP =1.5e-10
 GP = 4160.03            !Incremental Inductance
 ZP0 = 40.35            !Characteristic Impedance
 KP00 = 15.06            !Effective Dielectric Constant

 LFIL1 =  1.815          ! 1.815
 LFIL2 =  3.004          ! 3.004

 Wextra = 0.172
 WFIL1 = 0.5
 WFIL2 = 0.5

H=0.508

W50 =0.17200000000
Wef =0.50000000000
Wpad = 0.3

eps =24.0000000000
EQN

LD=LD0*1e-9

! Computation of losses for first, narrow spaced, coupled lines
!      Constants

 U0 = 4*PI*1e-7          !Magnetic Permeability of vacuum
 c = 1/sqrt(e0*U0)       !Velocity of light
 h0=sqrt(U0/e0)          !Impedance of free space

 f = FREQ*1e9            !Frequency in Hz
 Sr = Sn*(T/Tc)**4       !Real Part of conductivity of YBCO (Sigma1)
 Si = (1-(T/Tc)**4)/(2*PI*f*U0*LD**2)  !Imaginary Part of conductivity (Sigma2)
 P = ATAN(Si/Sr)         !Angle of conductivity  (Phi)
 Th= 5*PI/4-P/2          !Auxiliary angle definition (Theta)
 Sigmag= SQRT(SQR(Sr)+SQR(Si)) !Norm of conductivity

! NARROW-GAP COUPLED-LINE EQUATIONS
```

```
GDNe = 0.6+0.0045*ZN00e       !Even Mode Dispersion Correction Factor
GDNo = 0.6+0.018*ZN00o        !Odd Mode Dispersion Correction Factor
FPNe = 0.3915*ZN00e           !Dispersion Scaling Frequency, in GHz
FPNo = 1.566*ZN00o            !Dispersion Scaling Frequency, in GHz

KN0e=eps-(eps-KN00e)/(1+GDNe*sqr(FREQ/FPNe)) !Dispersive eff. diel. const.
KN0o=eps-(eps-KN00o)/(1+GDNo*sqr(FREQ/FPNo)) !Dispersive eff. diel. const.

ZN0e=ZTNe-(ZTNe-ZN00e)/(1+GDNe*((FREQ/FPNe)**1.6))
ZN0o=ZTNo-(ZTNo-ZN00o)/(1+GDNo*((FREQ/FPNo)**1.6))



! Even Mode

BNe= GNe*AGN*SQRT(2*PI*f*U0*Sigmag)          !B
CNe= EXP(2*BNe*COS(Th))
DNe= COS(2*BNe*SIN(Th))
ENe= SIN(2*BNe*SIN(Th))
UNe= SQRT(SQR(CNe*DNe-1)+SQR(CNe*ENe))       !Psi
WNe= ATAN(CNe*ENe/(CNe*DNe-1))               !Chi
FNe= BNe/(AGN*sigmag*UNe)                    !Prefactor of Ri and Xi
MNe= 2*BNe*SIN(Th)
NNe= COS(PI/4+P/2-WNe)
RPNe= COS(MNe+PI/4+P/2-WNe)

RiNe = FNe*(NNe+CNe*RPNe)          !Internal Resistance  / Meter

NINe= SIN(PI/4+P/2-WNe)
RDNe= SIN(MNe+PI/4+P/2-WNe)

LiNe = 1/(2*PI*f)*FNe*(NINe+CNe*RDNe) !Internal Inductance / Meter

CORRNe = 1+(c/sqrt(KN0e))*(LiNe/ZN0e) !Correction Factor (3.41)

ZNe = ZN0e*sqrt(CORRNe)            !Corrected Char Impedance

KNe = KN0e*CORRNe                  !Corrected  Dielectric Const (3.43)

ACNe = (8.686e-3) * RiNe/(2*ZNe)     !Loss Coefficient, in [dB/mm]


! Odd Mode

BNo= GNo*AGN*SQRT(2*PI*f*U0*sigmag)          !B
CNo= EXP(2*BNo*COS(Th))
DNo= COS(2*BNo*SIN(Th))
ENo= SIN(2*BNo*SIN(Th))
UNo= SQRT(SQR(CNo*DNo-1)+SQR(CNo*ENo))       !Psi
WNo= ATAN(CNo*ENo/(CNo*DNo-1))               !Chi
FNo= BNo/(AGN*sigmag*UNo)                    !Prefactor of Ri and Xi
MNo= 2*BNo*SIN(Th)
NNo= COS(PI/4+P/2-WNo)
RPNo= COS(MNo+PI/4+P/2-WNo)
```

```
RiNo = FNo*(NNo+CNo*RPNo)          !Internal Resistance  / Meter

NINo= SIN(PI/4+P/2-WNo)
RDNo= SIN(MNo+PI/4+P/2-WNo)

LiNo = 1/(2*PI*f)*FNo*(NINo+CNo*RDNo) !Internal Inductance / Meter

CORRNo = 1+(c/sqrt(KN0o))*(LiNo/ZN0o) !Correction Factor (3.41)

ZNo = ZN0o*sqrt(CORRNo)            !Corrected Char Impedance

KNo = KN0o*CORRNo                  !Corrected  Dielectric Const (3.43)

ACNo = (8.686e-3) * RiNo/(2*ZNo)   !Loss Coefficient, in [dB/mm]


! WIDE-GAP COUPLED-LINE EQUATIONS

GDWe = 0.6+0.0045*ZW00e       !Even Mode Dispersion Correction Factor
GDWo = 0.6+0.018*ZW00o        !Odd Mode Dispersion Correction Factor
FPWe = 0.3915*ZW00e           !Dispersion Scaling Frequency, in GHz
FPWo = 1.566*ZW00o            !Dispersion Scaling Frequency, in GHz

KW0e=eps-(eps-KW00e)/(1+GDWe*sqr(FREQ/FPWe)) !Dispersive eff. diel. const.
KW0o=eps-(eps-KW00o)/(1+GDWo*sqr(FREQ/FPWo)) !Dispersive eff. diel. const.

ZW0e=ZTWe-(ZTWe-ZW00e)/(1+GDWe*((FREQ/FPWe)**1.6))
ZW0o=ZTWo-(ZTWo-ZW00o)/(1+GDWo*((FREQ/FPWo)**1.6))

! Even Mode

BWe= GWe*AGW*SQRT(2*PI*f*U0*sigmag)          !B
CWe= EXP(2*BWe*COS(Th))
DWe= COS(2*BWe*SIN(Th))
EWe= SIN(2*BWe*SIN(Th))
UWe= SQRT(SQR(CWe*DWe-1)+SQR(CWe*EWe))       !Psi
WWe= ATAN(CWe*EWe/(CWe*DWe-1))               !Chi
FWe= BWe/(AGW*sigmag*UWe)                    !Prefactor of Ri and Xi
MWe= 2*BWe*SIN(Th)
NWe= COS(PI/4+P/2-WWe)
RPWe= COS(MWe+PI/4+P/2-WWe)

RiWe = FWe*(NWe+CWe*RPWe)          !Internal Resistance  / Meter

NIWe= SIN(PI/4+P/2-WWe)
RDWe= SIN(MWe+PI/4+P/2-WWe)

LiWe = 1/(2*PI*f)*FWe*(NIWe+CWe*RDWe) !Internal Inductance / Meter

CORRWe = 1+(c/sqrt(KW0e))*(LiWe/ZW0e) !Correction Factor (3.41)

ZWe = ZW0e*sqrt(CORRWe)            !Corrected Char Impedance
```

```
KWe = KW0e*CORRWe                !Corrected  Dielectric Const (3.43)

ACWe = (8.686e-3) * RiWe/(2*ZWe)      !Loss Coefficient, in [dB/mm]


! Odd Mode

BWo= GWo*AGW*SQRT(2*PI*f*U0*sigmag)          !B
CWo= EXP(2*BWo*COS(Th))
DWo= COS(2*BWo*SIN(Th))
EWo= SIN(2*BWo*SIN(Th))
UWo= SQRT(SQR(CWo*DWo-1)+SQR(CWo*EWo))       !Psi
WWo= ATAN(CWo*EWo/(CWo*DWo-1))               !Chi
FWo= BWo/(AGW*sigmag*UWo)                    !Prefactor of Ri and Xi
MWo= 2*BWo*SIN(Th)
NWo= COS(PI/4+P/2-WWo)
RPWo= COS(MWo+PI/4+P/2-WWo)

RiWo = FWo*(NWo+CWo*RPWo)           !Internal Resistance  / Meter

NIWo= SIN(PI/4+P/2-WWo)
RDWo= SIN(MWo+PI/4+P/2-WWo)

LiWo = 1/(2*PI*f)*FWo*(NIWo+CWo*RDWo) !Internal Inductance / Meter

CORRWo = 1+(c/sqrt(KW0o))*(LiWo/ZW0o) !Correction Factor (3.41)

ZWo = ZW0o*sqrt(CORRWo)              !Corrected Char Impedance

KWo = KW0o*CORRWo                !Corrected  Dielectric Const (3.43)

ACWo = (8.686e-3) * RiWo/(2*ZWo)      !Loss Coefficient, in [dB/mm]

!  MICROSTRIP LINE PARAMETERS

! 50 OHM LINE

! Dispersion

FD50=4*H*FREQ/300*sqrt(eps-1)*(0.5+sqr(1+2*LOG(1+W50/H)))
K5=K500*SQR(1+(SQRT(eps/K500)-1)/(1+4*FD50**(-1.5)))

!PEM Equations

B5= G5*AG5*SQRT(2*PI*f*U0*sigmag)            !B
C5= EXP(2*B5*COS(Th))
D5= COS(2*B5*SIN(Th))
E5= SIN(2*B5*SIN(Th))
U5= SQRT(SQR(C5*D5-1)+SQR(C5*E5))            !Psi
W5= ATAN(C5*E5/(C5*D5-1))                    !Chi
F5= B5/(AG5*sigmag*U5)                       !Prefactor of Ri and Xi
M5= 2*B5*SIN(Th)
N5= COS(PI/4+P/2-W5)
RP5= COS(M5+PI/4+P/2-W5)
```

```
 Ri5 = F5*(N5+C5*RP5)              !Internal Resistance  / Meter

 NI5= SIN(PI/4+P/2-W5)
 RD5= SIN(M5+PI/4+P/2-W5)

 Li5 = 1/(2*PI*f)*F5*(NI5+C5*RD5)     !Internal Inductance / Meter

 CORR5 = 1+(c/sqrt(K5))*(Li5/Z5)      !Correction Factor (3.41)

 Z50 = Z5*sqrt(CORR5)              !Corrected Char Impedance

 K50 = K5*CORR5                    !Corrected  Dielectric Const (3.43)

 AC50 = (8.686e-3) * Ri5/(2*Z50)      !Loss Coefficient, in [dB/mm]

! STUB LINE

!Dispersion

 FDS=4*H*FREQ/300*sqrt(eps-1)*(0.5+sqr(1+2*LOG(1+Wef/H)))
 KS0=KS00*SQR(1+(SQRT(eps/KS00)-1)/(1+4*FDS**(-1.5)))

! PEM Equations

 BS= GS*AGS*SQRT(2*PI*f*U0*sigmag)          !B
 CS= EXP(2*BS*COS(Th))
 DS= COS(2*BS*SIN(Th))
 ES= SIN(2*BS*SIN(Th))
 US= SQRT(SQR(CS*DS-1)+SQR(CS*ES))          !Psi
 WS= ATAN(CS*ES/(CS*DS-1))                  !Chi
 FS= BS/(AGS*sigmag*US)            !Prefactor of Ri and Xi
 MS= 2*BS*SIN(Th)
 NS= COS(PI/4+P/2-WS)
 RPS= COS(MS+PI/4+P/2-WS)

 RiS= FS*(NS+CS*RPS)               !Internal Resistance  / Meter

 NIS= SIN(PI/4+P/2-WS)
 RDS= SIN(MS+PI/4+P/2-WS)

 LiS = 1/(2*PI*f)*FS*(NIS+CS*RDS)     !Internal Inductance / Meter

 CORRS = 1+(c/sqrt(KS0))*(LiS/ZS0)    !Correction Factor (3.41)

 ZS = ZS0*sqrt(CORRS)              !Corrected Char Impedance

 KS = KS0*CORRS                    !Corrected  Dielectric Const (3.43)

 ACS = (8.686e-3) * RiS/(2*ZS)      !Loss Coefficient, in [dB/mm]

! INPUT PAD LINE

!Dispersion
```

```
  FDP=4*H*FREQ/300*sqrt(eps-1)*(0.5+sqr(1+2*LOG(1+Wpad/H)))
  KP0=KP00*SQR(1+(SQRT(eps/KP00)-1)/(1+4*FDP**(-1.5)))

! PEM Equations

  BP= GP*AGP*SQRT(2*PI*f*U0*sigmag)          !B
  CP= EXP(2*BP*COS(Th))
  DP= COS(2*BP*SIN(Th))
  EP= SIN(2*BP*SIN(Th))
  UP= SQRT(SQR(CP*DP-1)+SQR(CP*EP))          !Psi
  WP= ATAN(CP*EP/(CP*DP-1))                  !Chi
  FP= BP/(AGP*sigmag*UP)                     !Prefactor of Ri and Xi
  MP= 2*BP*SIN(Th)
  NP= COS(PI/4+P/2-WP)
  RPP= COS(MP+PI/4+P/2-WP)

  RiP= FP*(NP+CP*RPP)                        !Internal Resistance  / Meter

  NIP= SIN(PI/4+P/2-WP)
  RDP= SIN(MP+PI/4+P/2-WP)

  LiP = 1/(2*PI*f)*FP*(NIP+CP*RDP)           !Internal Inductance / Meter

  CORRP = 1+(c/sqrt(KP0))*(LiP/ZP0)          !Correction Factor (3.41)

  ZP = ZP0*sqrt(CORRP)                       !Corrected Char Impedance

  KP = KP0*CORRP                             !Corrected  Dielectric Const (3.43)

  ACP = (8.686e-3) * RiP/(2*ZP)              !Loss Coefficient, in [dB/mm]


Rbend =W50/2

CKT


!RES 1 0 R^rez5
!DEF1P 1 TEST

MSUB_P1 ER^eps H=0.50800000000 T=0.00050000000 RHO=0.00000000000 &
RGH=0.00000000000
MSTEP_T3 2 5 W1^Wextra W2^WFIL1
MSTEP_T4 6 3 W1^WFIL1 W2^Wextra
CLINP_T5 5 7 8 9 ZE^ZNe ZO^ZNo L^LFIL1 KE^KNe KO^KNo AE^ACNe AO^ACNo MCFIL &
W=2.00000000000 S=3.00000000000 L=4.00000000000 W1=5.00000000000 &
W2=6.00000000000
CLINP_T6 14 11 6 12 ZE^ZNe ZO^ZNo L^LFIL1 KE^KNe KO^KNo AE^ACNe AO^ACNo MCFIL &
W=2.00000000000 S=3.00000000000 L=4.00000000000 W1=5.00000000000 &
W2=6.00000000000
```

```
CLINP_T7 8 13 14 15 ZE^ZWe ZO^ZWo L^LFIL2 KE^KWe KO^KWo AE^ACWe AO^ACWo MCFIL
&
W=2.00000000000 S=3.00000000000 L=4.00000000000 W1=5.00000000000 &
W2=6.00000000000
MLEF_T8 9 W^WFIL1 L=0.00000000000 CPWEGAP W=1.00000000000 G=2.00000000000 &
S=3.00000000000 L=4.00000000000
MLEF_T9 7 W^WFIL1 L=0.00000000000 CPWEGAP W=1.00000000000 G=2.00000000000 &
S=3.00000000000 L=4.00000000000
MLEF_T10 12 W^WFIL1 L=0.00000000000 CPWEGAP W=1.00000000000 G=2.00000000000 &
S=3.00000000000 L=4.00000000000
MLEF_T11 11 W^WFIL1 L=0.00000000000 CPWEGAP W=1.00000000000 G=2.00000000000 &
S=3.00000000000 L=4.00000000000
MLEF_T12 15 W^WFIL2 L=0.00000000000 CPWEGAP W=1.00000000000 G=2.00000000000 &
S=3.00000000000 L=4.00000000000
MLEF_T13 13 W^WFIL2 L=0.00000000000 CPWEGAP W=1.00000000000 G=2.00000000000 &
S=3.00000000000 L=4.00000000000
DEF2P 2 3 MAIN
MSTEP_T2 2 3 W1=0.30000000000 W2^w50
TLINP_T17 7 8 Z^ZS L^Lstub2 K^KS A^ACS F=0.00000000000 CONN_T15
MLEF_T18 8 W^Wef L=0.00000000000
TLINP_T19 10 9 Z^Z50 L^Lextra2 K^K50 A^AC50 F=0.00000000000 CONN_S2
TLINP_T14 3 4 Z^Z50 L^Linp2 K^K50 A^AC50 F=0.00000000000 CONN
S3P_S2 5 4 10 /home/crafty/dimitri/eesof/hts_bpf/model/t MTEE W1=0.50000000000 &
W2=0.50000000000 W3=0.50000000000
MSTEP_T15 5 7 W1^W50 W2^Wef
TLINP_T16 1 2 Z^ZP L=0.10000000000 K^KP A^ACP F=0.00000000000 MLIN W^w50 &
L^Lextra2
DEF2P 1 9 LEFTB
MAIN_X1 1 2
LEFTB_X2 3 1
LEFTB_X3 4 2
DEF2P 3 4 FLTRBSC
S2P_S1 1 2 0 /home/crafty/dimitri/eesof/hts_bpf/hts5c1dm MTEE W1=0.50000000000 &
W2=0.50000000000 W3=0.50000000000
DEF2P 1 2 YBCO
RES_R4 4 0 R^KW0O MLIN W^W50 L^Lextra2
RES_R6 6 0 R^KW0E MLIN W^w50 L^Lextra2
RES_R5 5 0 R^KN0O MLIN W^w50 L^Lextra2
DEF3P 4 5 6 TEST
TERM

PROC

MODEL


SOURCE

DCTR

FREQ
SWEEP 6 8.5 0.01
!STEP 8
POWER
```

```
FILEOUT

OUTVAR

OUTEQN

OUT
fltrbsc DB[S21] GR1
 YBCO DB[S21] GR1

fltrbsc DB[S11] GR3
 YBCO DB[S11] GR3

fltrbsc ANG[S21] GR2
 YBCO ANG[S21] GR2

!fltrbsc ANG[S11] GR4
! YBCO ANG[S11] GR4

!MAIN S21 SC2
!YBCO S21 SC2
!TEST RE[Z11] GR5

!FIL DB[S21] GR6
!YBCO DB[S21] GR6
fltrbsc ANG[s11] gr4
YBCO ANG[s11] gr4
 TEST RE[Z11] SCN
 TEST RE[Z22] SCN
 TEST RE[Z33] SCN
!TEST RE[Z44] SCN
!TEST RE[Z55] SCN
!TEST RE[Z66] SCN
GRID
! RANGE 1 11 1
! GR1 -10 0 1
! GR5 .001 .003 .0001

!RANGE 7 9 .2
! GR6 -2 0 .5

!RANGE 6 8.5 .5
!gr4 -10 0 1

HBCNTL

OPT
 YBCO MODEL FLTRBSC

YIELD

TOL
```

CHAPTER 7

A MODIFICATION OF THE PEM LOSS MODEL FOR HIGH-LOSS MODELING. AN APPLICATION TO HIGH-POWER MODELING

7.1 A Modification of the PEM Loss Model. The High-Loss Case

Beyond the transmission line's inductance and capacitance per unit length the PEM model, presented in chapter 3, gives an additional impedance per unit length, Z_i, that is due to the field penetration into the conductors. It can be used with TEM and quasi-TEM (e.g., microstrip) lines. Equations (3.34) and (3.41)-(3.44) are, as was pointed out in chapter 3, only first-order approximations and work well when R_i, the additional distributed internal resistance due to the field penetration, is small relative to ωL. This is true of most HTS transmission lines in their low-power linear region. However, examples of some cases in which this condition may be violated are if $T \approx T_c$, or if, say due to high transfer currents, $\frac{n_n}{n} \approx 1$, or if the HTS film is so thin that $0 < \frac{d}{\lambda} << 1$, or if the width of the transmission line is very small. The last case is encountered in the HTS LPF presented in chapter 5, where the high-impedance lines are 33 times narrower than the low-impedance lines. One device of this design will be used in this chapter as a case-point for application of the improved PEM loss model. The chosen device has an HTS film with a particularly high-penetration depth to make the effect of the loss more pronounced.

The more accurate equations, to substitute (3.34) and (3.41)-(3.44), are derived using the following general equations that describe a wave propagating in a TEM medium [1]

$$\alpha'_c + j\beta'' = \sqrt{j\omega C(R_i + j\omega L')} \tag{1}$$

and

$$Z''_0 = \sqrt{\frac{R_i + j\omega L'}{j\omega C}} \ , \tag{2}$$

assuming G, the "leakage" conductance per unit length of the transmission line, to be zero. Here L' is the total distributed inductance of the transmission line (see equation 3.38), C is the distributed capacitance of the transmission line and ω is the angular frequency of the excitation. When (1) and (2) are used in conjunction with the model presented in chapter 3, the following more accurate equations are obtained for α'_c, the exponential attenuation per unit length, β'', the corrected propagation constant of the wave and Z''_o, the corrected characteristic impedance of the transmission line

$$\alpha'_c = \beta'\left[1+\left(\frac{1}{Q}\right)^2\right]^{\frac{1}{4}} \sin\left(\frac{\theta}{2}\right) \ , \tag{3}$$

$$\beta'' = \beta'\left[1+\left(\frac{1}{Q}\right)^2\right]^{\frac{1}{4}} \cos\left(\frac{\theta}{2}\right) \tag{4}$$

and

$$Z''_0 = Z'_0\left[1+\left(\frac{1}{Q}\right)^2\right]^{\frac{1}{4}} e^{j\frac{\theta}{2}} \ , \tag{5}$$

where

$$\theta = \arctan\left(\frac{1}{Q}\right) \tag{6}$$

and

$$Q = \frac{\omega L'}{R_i} \ . \tag{7}$$

From (4) and (5) corresponding expressions for v''_{ph}, the corrected phase velocity of the wave and ε''_{eff}, the corrected effective relative dielectric constant of the transmission line may also be derived as follows

$$v''_{ph} = v'_{ph}\left[1+\left(\frac{1}{Q}\right)^2\right]^{-\frac{1}{4}} \sec\left(\frac{\theta}{2}\right) \tag{8}$$

and

$$\varepsilon''_{eff} = \varepsilon'_{eff}\left[1+\left(\frac{1}{Q}\right)^2\right]^{\frac{1}{2}}\cos^2\left(\frac{\theta}{2}\right) . \qquad (9)$$

The variables β', Z'_o, L', R_i, v'_{ph} and ε'_{eff} in equations (3)-(9) are the first-order approximations for these physical quantities, as defined in equations (3.44), (3.41), (3.38), (3.35), (3.42) and (3.43) respectively. Clearly, as Q becomes large compared to unity, the double-primed variables of equations (4), (5), (8) and (9) tend to their single-primed counterparts of equations (3.41), (3.35), (3.42) and (3.43) respectively. This relationship is not as obvious in the case of α'_c and α_c (equations (3) and (3.34)) but it can be easily shown using first-order Taylor expansions to evaluate the square root and the sine of equation (3).

7.2 From a Complex to a Real Characteristic Impedance

The main difference between the primed and double-primed equations is that Z''_o in equation (5) is a complex quantity. This has the physical interpretation that the current and voltage are out of phase throughout the transmission line. The *TLINP* transmission line modeling element of Touchstone and the corresponding elements of most other commonly used microwave CAD software packages (DragonWave, SuperCompact, Puff), however, can only take a real impedance as an input. In the example of the HTS LPF of chapter 5, the narrow, high-impedance line has a corrected impedance, the real part and magnitude of which may be different by as much as 5%. Hence the question what is the best impedance to use for modeling the lossy transmission line arises. Candidates are the impedance as given by equation (3.41) and the

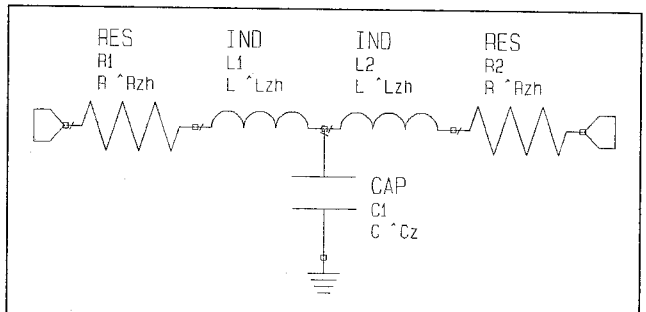

Figure 1 Unit cell of ladder network model

magnitude or the real part of the impedance as given by equation (5). To determine the best alternative the narrow transmission line used in the HTS CPW LPF of chapter 5 is modeled using a ladder RLC network of 128 elementary cells of length Dz. The CPW impedance of the line is 83 Ω and its length is 997 μm. The unit cell of the ladder network is shown in figure 1. Equation (3.35) is used to obtain R, the series resistance of a length Dz of the transmission line. Equations (3.36) and (3.38)-(3.40) together with the knowledge of the effective relative dielectric constant and characteristic impedance of the line are used to obtain L and C, the inductance and capacitance, respectively, of a length Dz of the transmission line. The calculated S-parameters of this model are compared to the S-parameters of the transmission line model with each of the three candidate real impedances mentioned above. Figures 2 and 3 show the plots of S11 and S21 for each of the 4 calculated responses respectively (LAD is the ladder network and LINE1, LINE2,

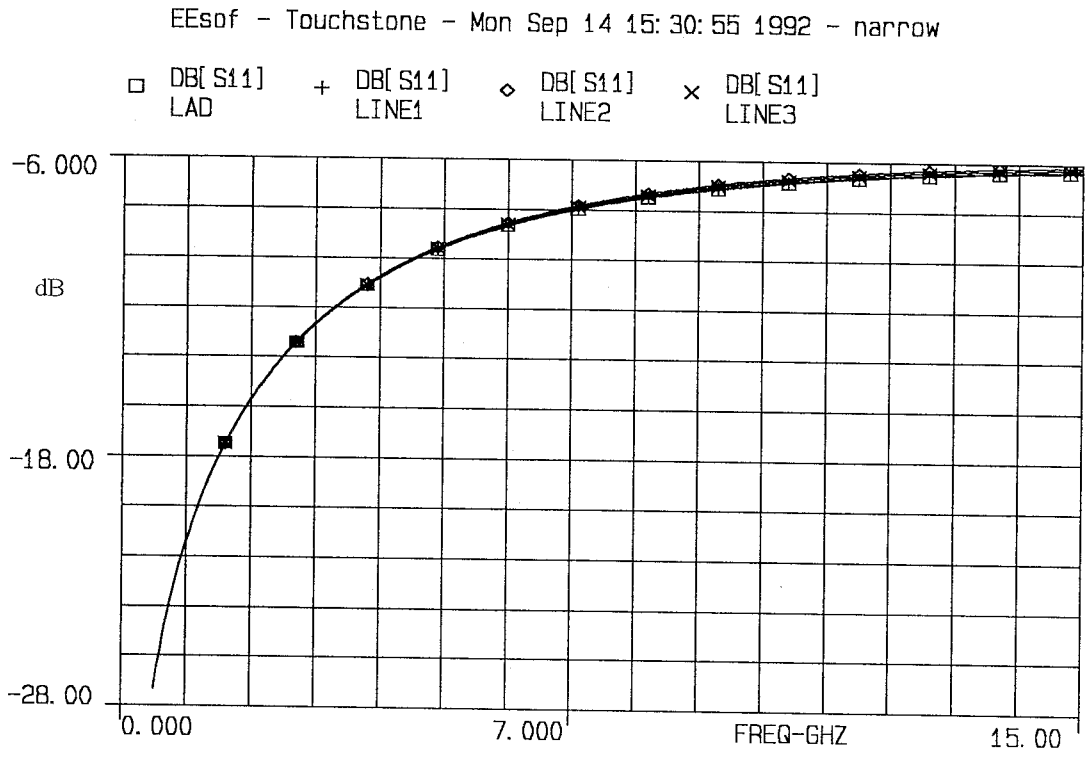

Figure 2 Magnitude of S11 of ladder and transmission lines.

LINE3 are the transmission line models with each of the candidate impedances mentioned above, respectively), plotted versus frequency.

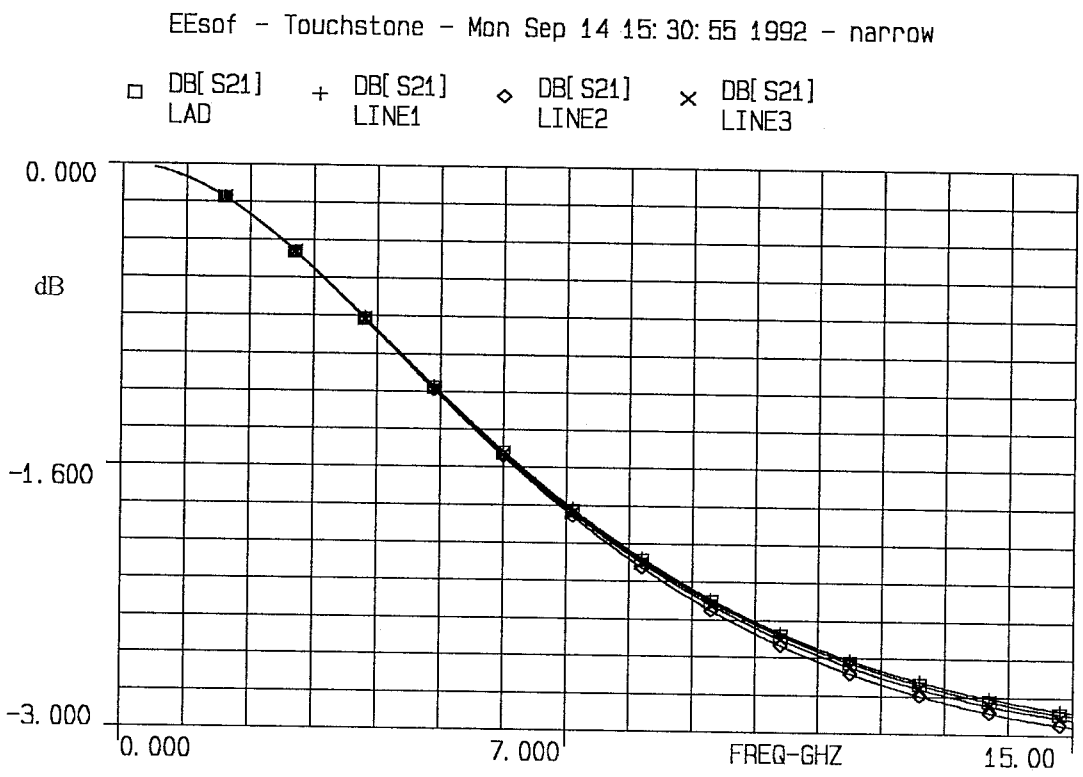

Figure 3 Magnitude of S21 of ladder and transmission lines.

Figures 4,5 and 6 show the difference in magnitude (left scale, dB) and phase (right scale, rad) of S11 and S21 of the ladder network from that of each of the three candidate transmission lines. As may be seen by comparison of figures 4-6, LINE1 best models the behavior of the ladder network (which faithfully emulates the complex impedance given by equation (6)). This corresponds to the impedance given by equation (3.41), which is used in all subsequent modeling.

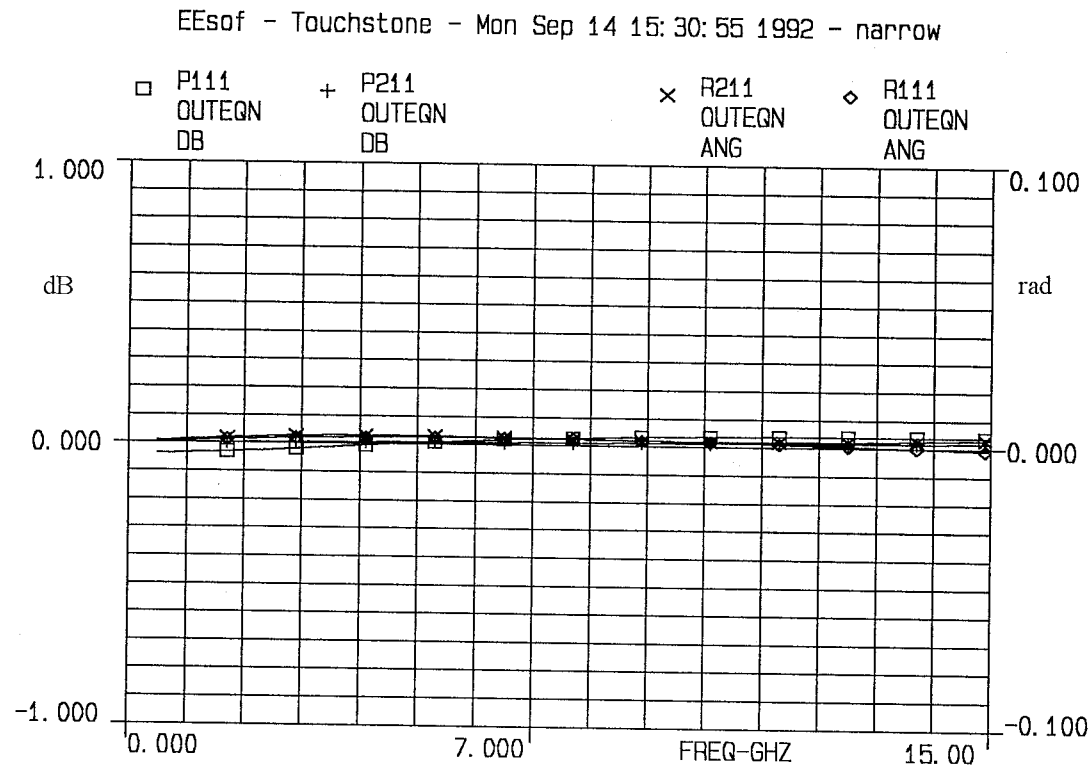

Figure 4 S-parameter differences between LAD and LINE1.

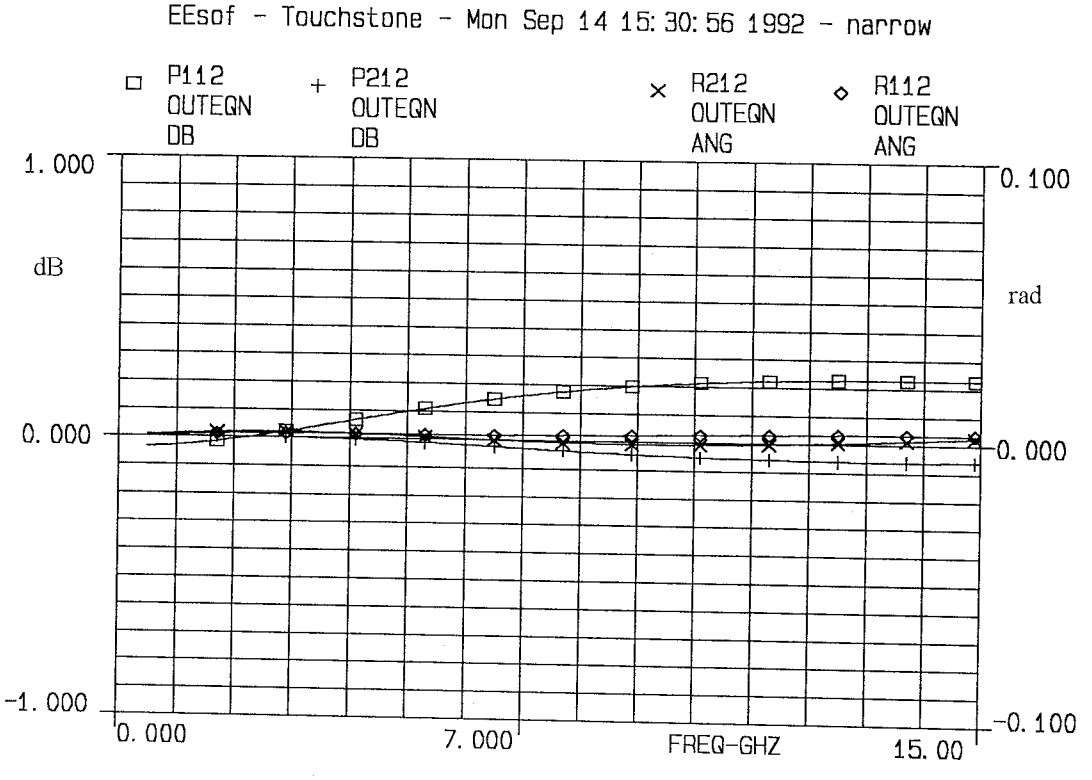

Figure 5 S-parameter differences between LAD and LINE2.

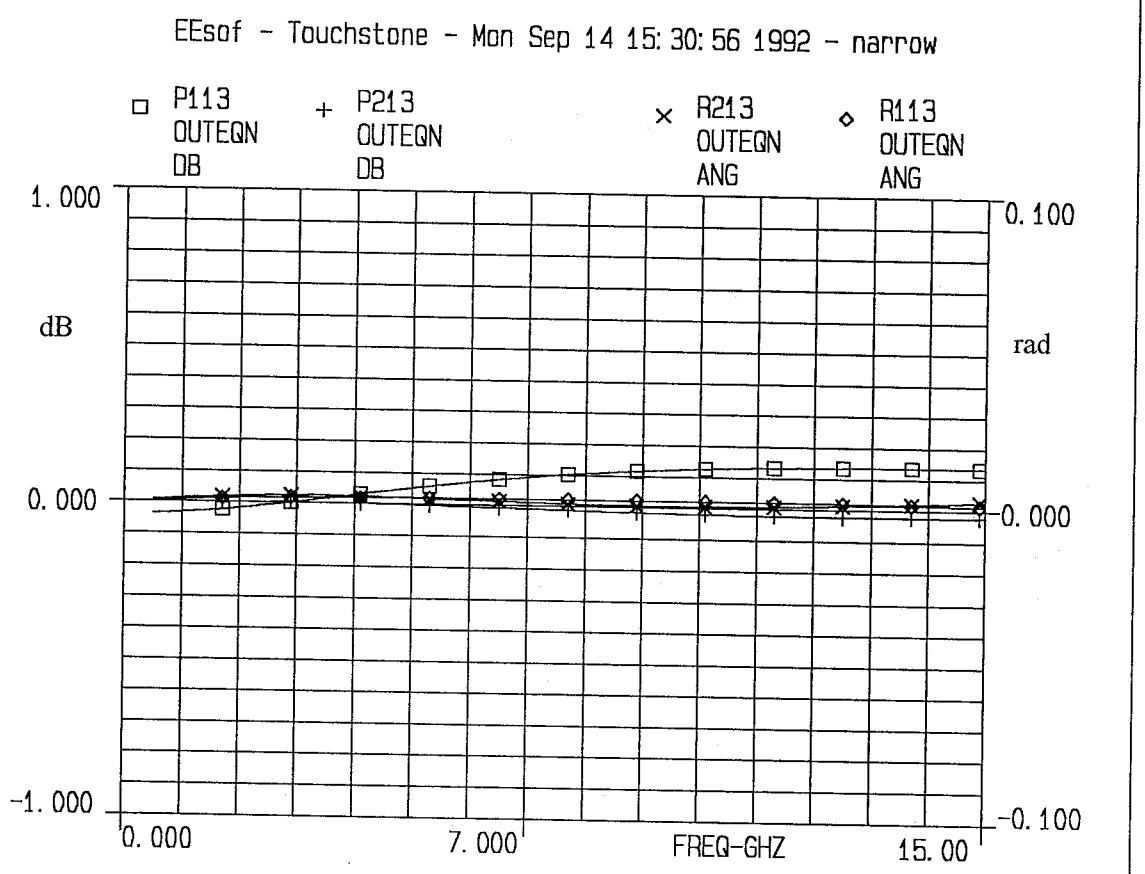

Figure 6 S-parameter differences between LAD and LINE3.

Figure 7 shows the three candidate impedances plotted versus frequency.

7.3 Application of the High Loss Model to a LPF of Chapter 5

When equations (3),(6),(7),(9) and (3.41) are incorporated into the loss model of the CPW LPF described in chapter 5, a better fit between measured and modeled data is achieved. Specifically, the integrated squared error between the modeled and the measured S-parameters decreases from 0.06710 to 0.06059, a 9.7 % decrease.

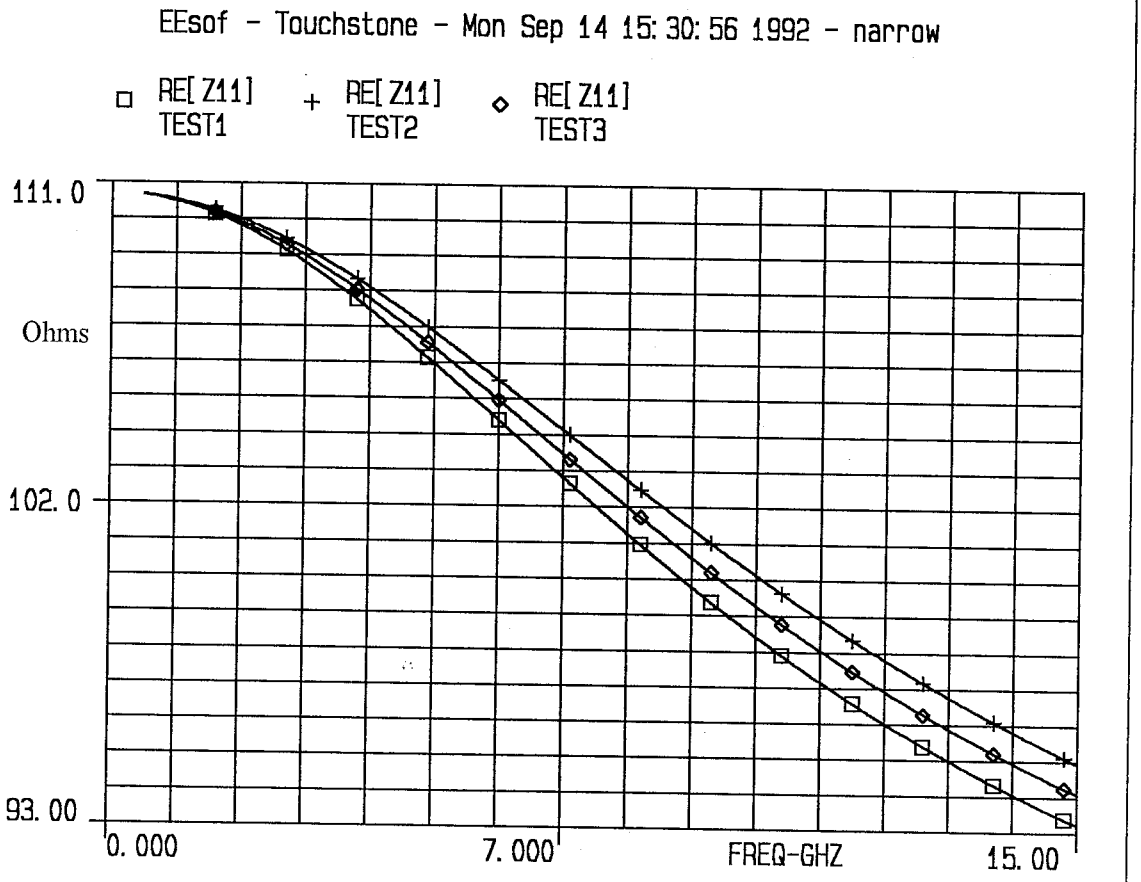

Figure 7 The three candidate impedances plotted versus frequency.

Figures 8-15 show the old and the new fit of the model to the measured S-parameters of the HTS CPW LPF of chapter 5. As mentioned above, a device with high penetration depth is chosen to accentuate the differences between the first-order and the high-loss model. As a result, the pass-band insertion-loss of the device of this chapter is larger than that of chapter 5 (compare figures 8 and 5.4).

Appendices A and B include the corresponding Touchstone circuit files. The greatest improvement is seen in the better modeling of the phase of S11 from 9 to 12 GHz (figures 14 and 15).

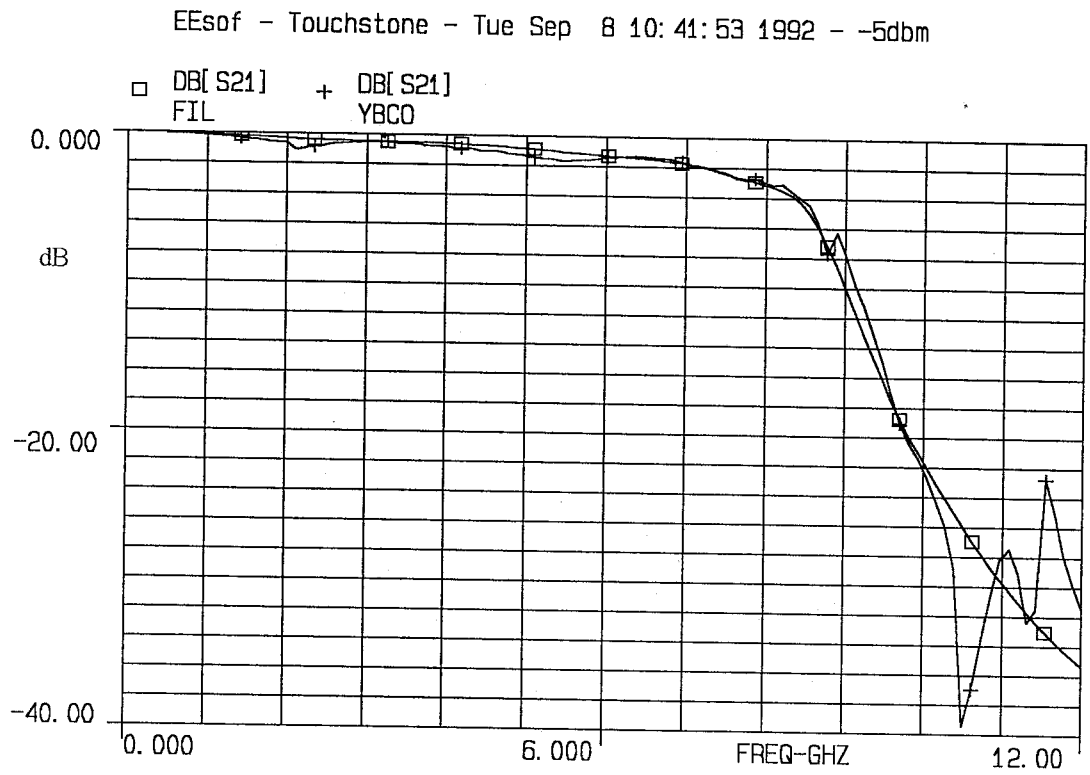

Figure 8 First-order model, magnitude of S21, measured (YBCO) versus modeled (FIL).

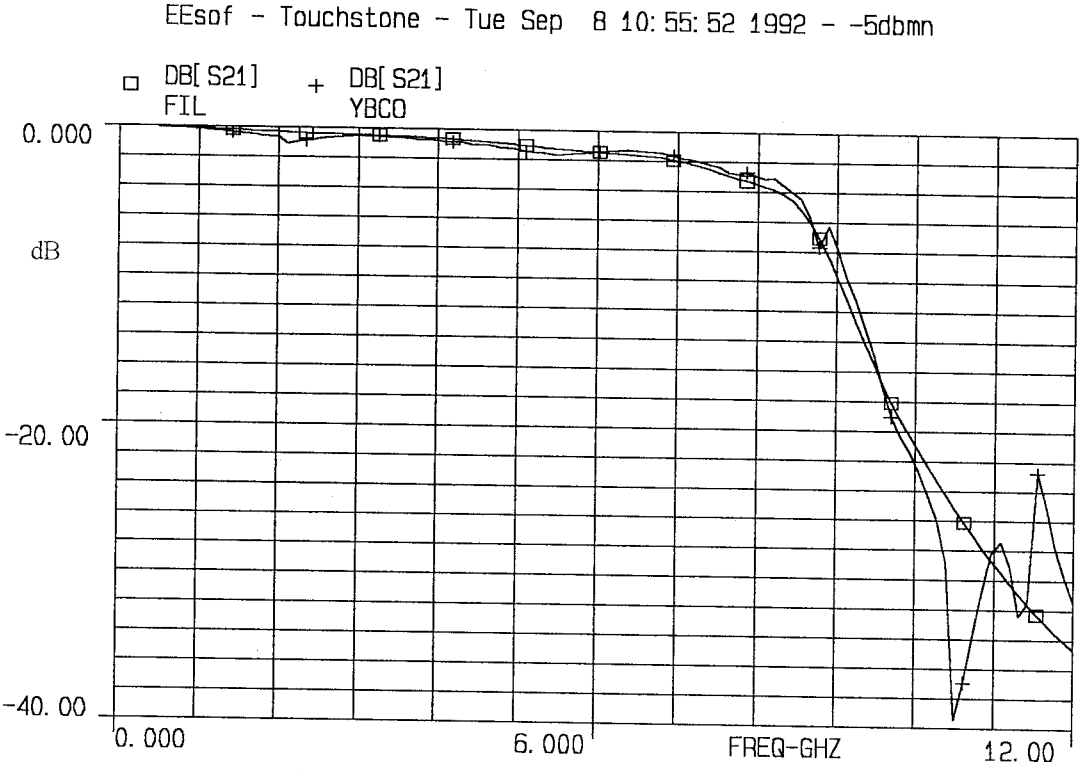

Figure 9 High-loss model, magnitude of S21, measured (YBCO) versus modeled (FIL).

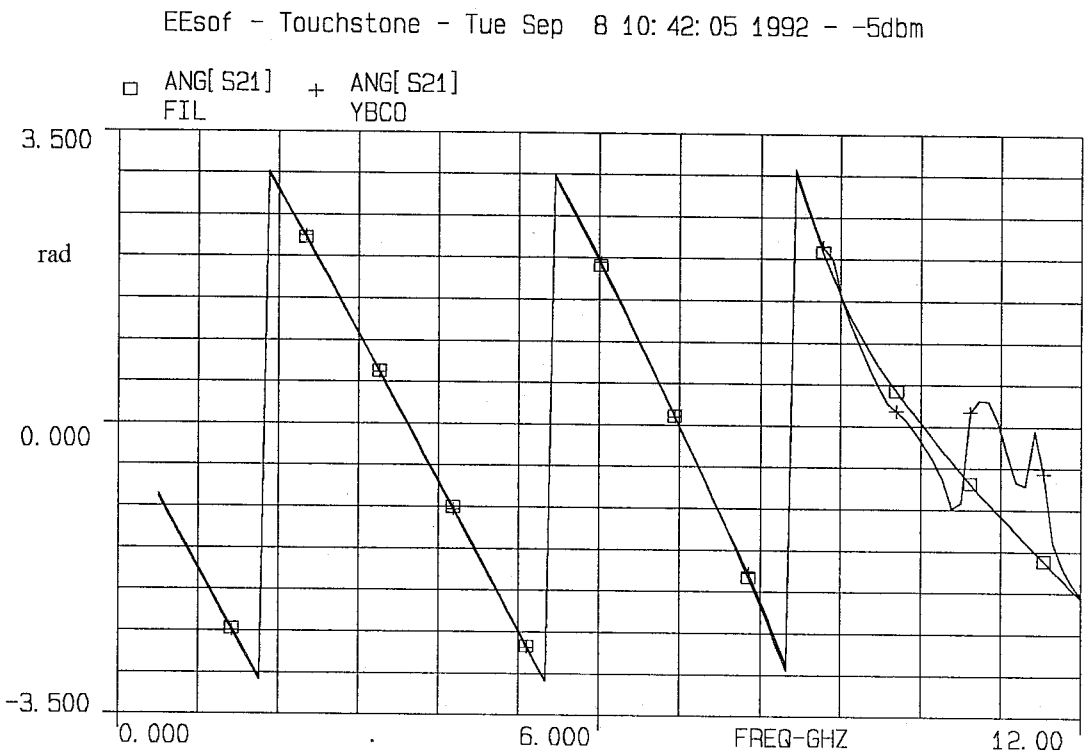

Figure 10 First-order model, phase of S21, measured (YBCO) versus modeled (FIL).

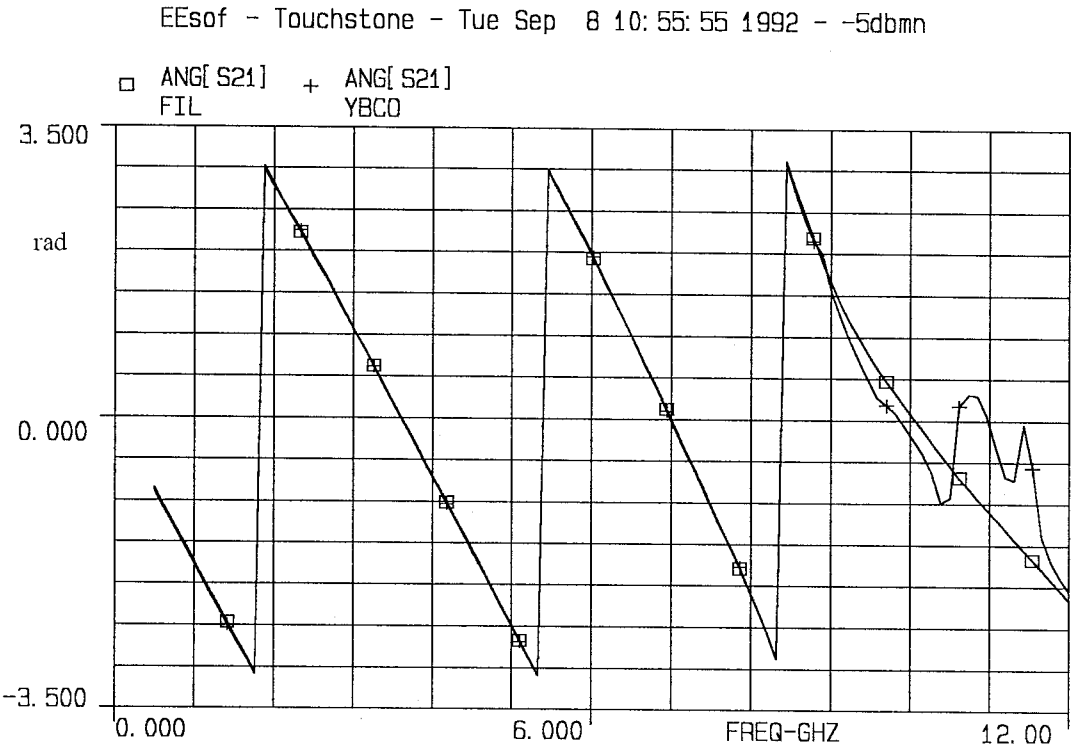

Figure 11 High-loss model, phase of S21, measured (YBCO) versus modeled (FIL).

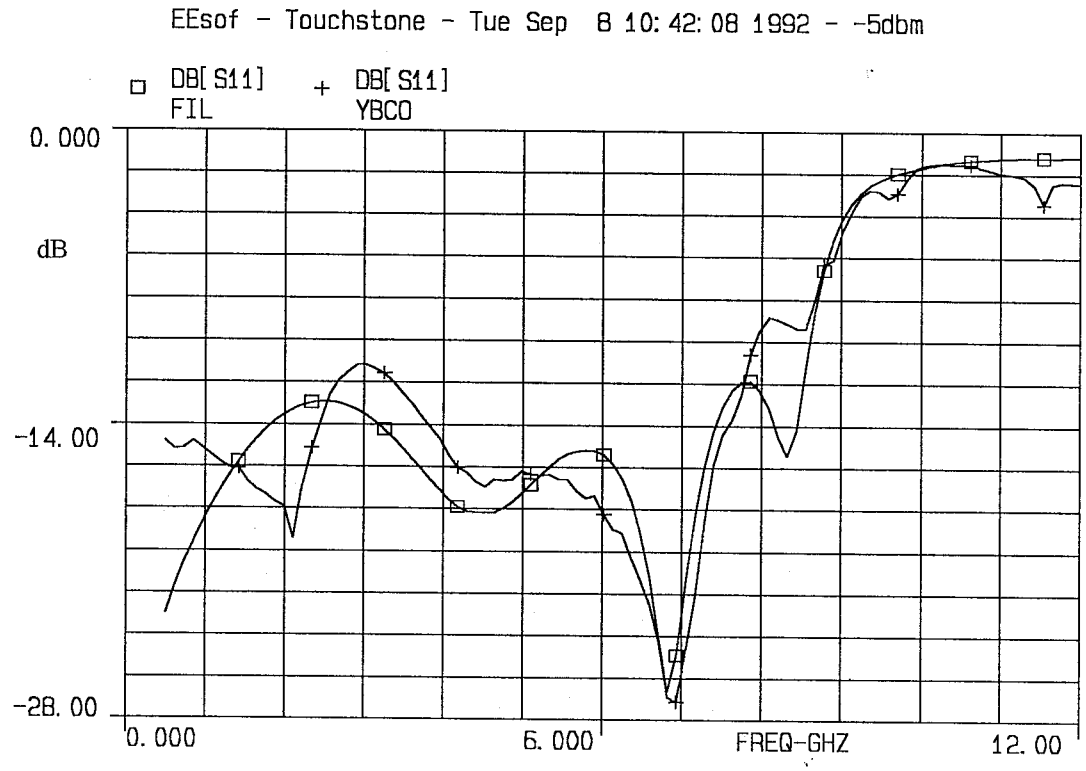

Figure 12 First-order model, magnitude of S11, measured (YBCO) versus modeled (FIL).

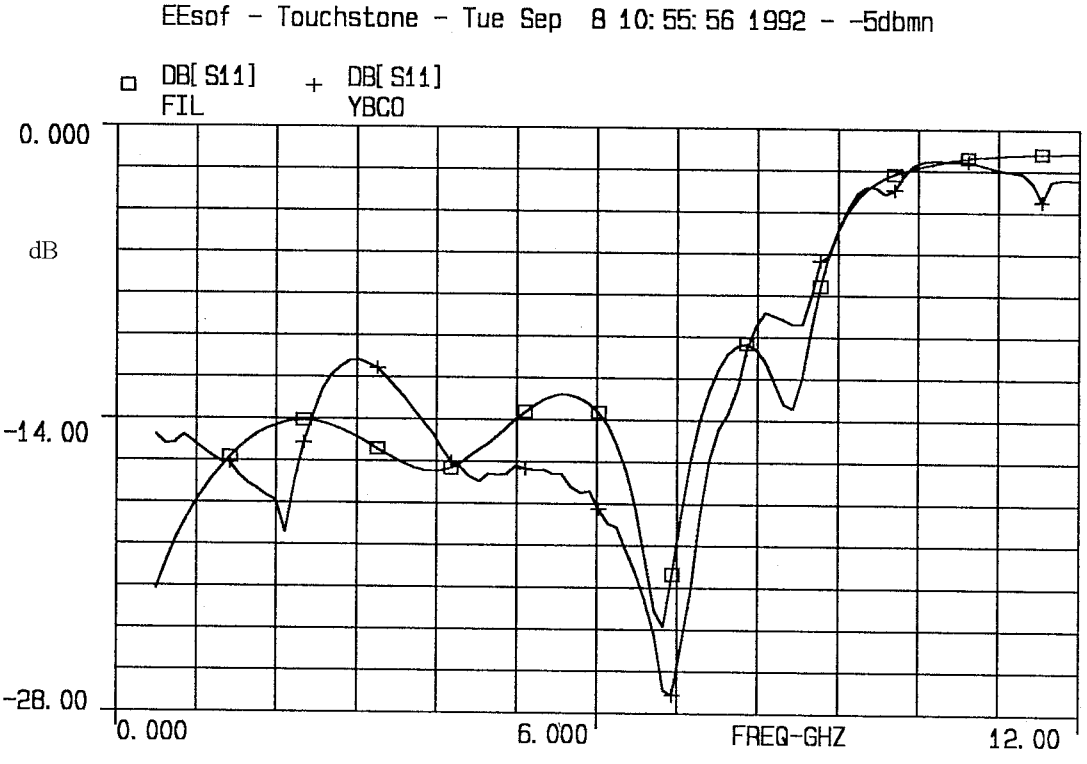

Figure 13 High-loss model, magnitude of S11, measured (YBCO) versus modeled (FIL).

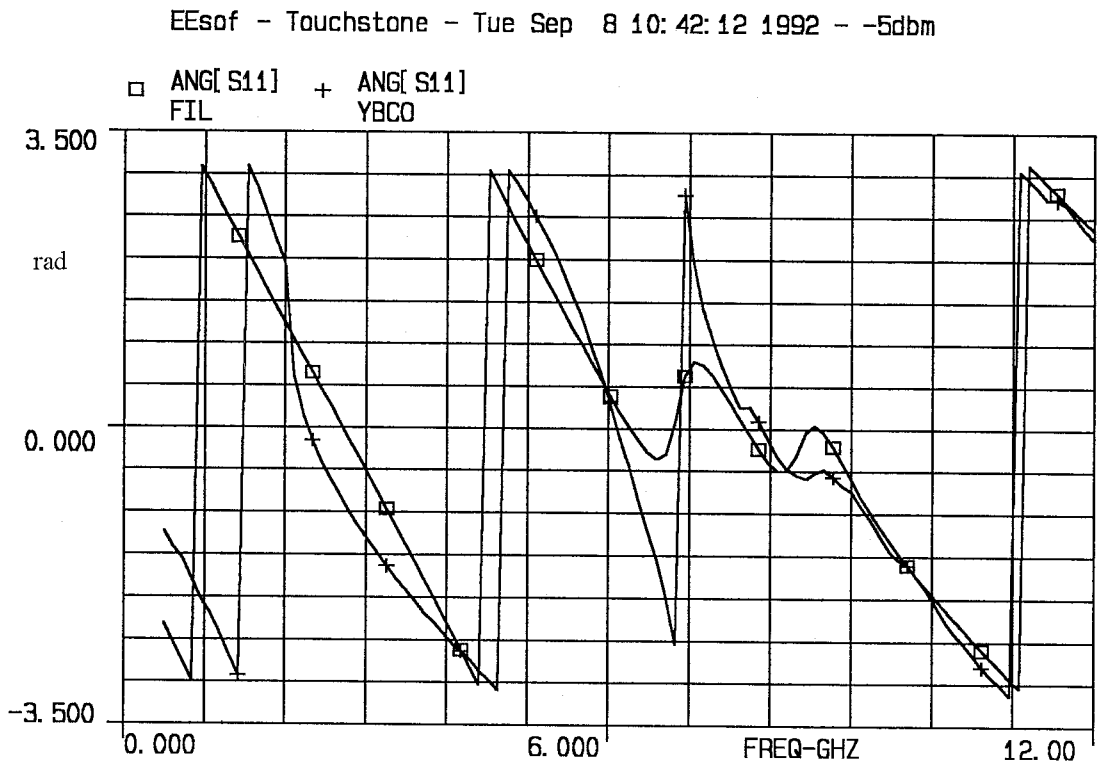

Figure 14 First-order model, phase of S11, measured (YBCO) versus modeled (FIL).

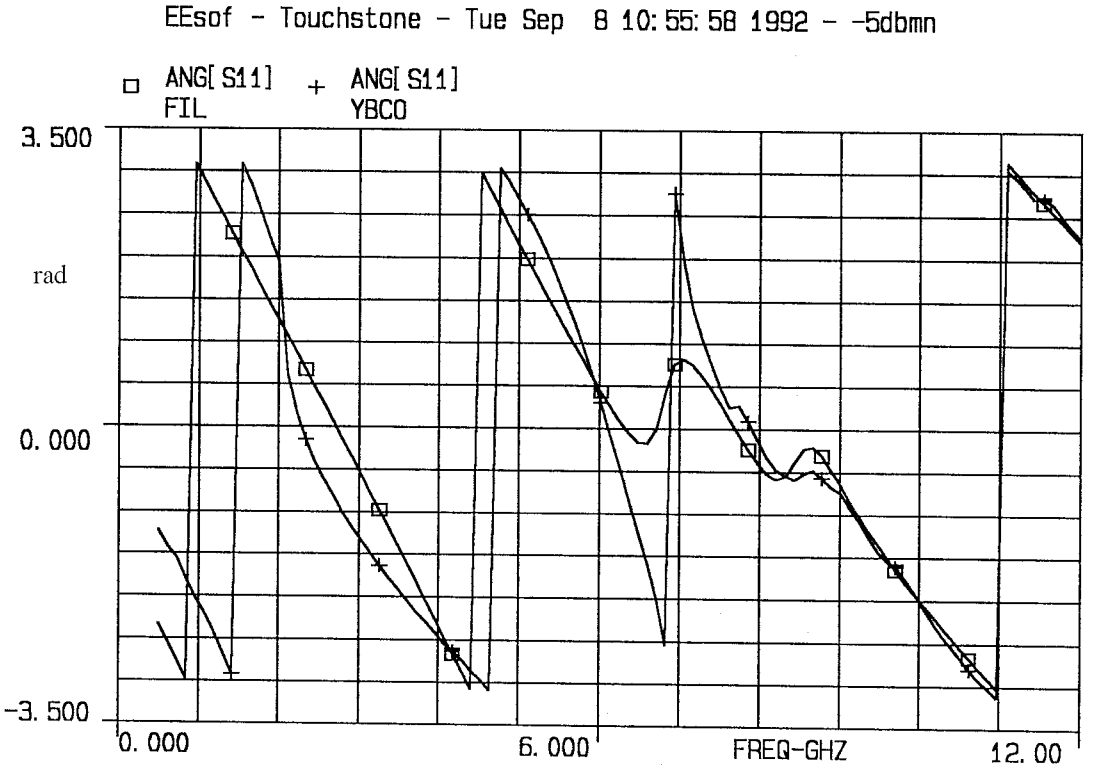

Figure 15 High-loss model, phase of S21, measured (YBCO) versus modeled (FIL).

7.4 Application of the High Loss Model to High Power Modeling

7.4.1 Introduction

The superconducting state is maintained in a superconductor as long as it is energetically favorable for electrons to be paired-up into Cooper pairs [2]. When a high magnetic field is applied to a superconductor (higher than a value called the critical field, H_c), the lower energy state for the electrons is not the paired state anymore. Hence the electron pairs are destroyed and with them the superconducting properties of the material. In Type I superconductors this transition is an abrupt one with respect to the applied magnetic field. In Type II superconductors and high temperature superconductors the transition is more gradual. It starts at the low critical field value H_{c1}, when the first electron pairs are broken up, and is complete at the high critical field value H_{c2}, when all electron pairs have been destroyed and the material is not superconducting anymore.

In the case of high-temperature superconductors, which, due to their crystalline nature, are insulators when non-superconducting, this is a very important effect, as it totally alters the material properties. When the applied magnetic field is in the range from H_{c1} to H_{c2}, the HTS appears lossy due to the deficiency in superconducting electron pairs. Associated with the critical magnetic fields are critical currents, which produce magnetic fields that can also drive the material non-superconducting. Hence the behavior of superconducting devices is non-linear with respect to input power. Proper modeling of this behavior may provide the capability for new innovative circuit designs (e.g., a power-sensitive, switching band-selection filter to protect the input of a sensitive receiver) and put bounds on the power-handling capability of superconducting devices. An attempt at first-order modeling of this behavior is presented below, using the high-loss PEM model presented in 7.1.

7.4.2 High Power Measurements

To model this power-dependent behavior of HTSs, measurements of devices at different input powers are required. One of the HTS YBCO CPW LPFs of chapter 5 is selected for these measurements. The experimental setup is shown in figure 16. An HP 8510C network analyzer is used in tandem with an HP 8349B solid-state amplifier and a 10 dB attenuator (to avoid overloading port 2 of the 8510). The 8510 is calibrated for power flatness, using an HP 8481B high-power sensor and an HP 437B power meter (i.e., the output power of port 1 is constant throughout the frequency sweep from 1 to 12 GHz).

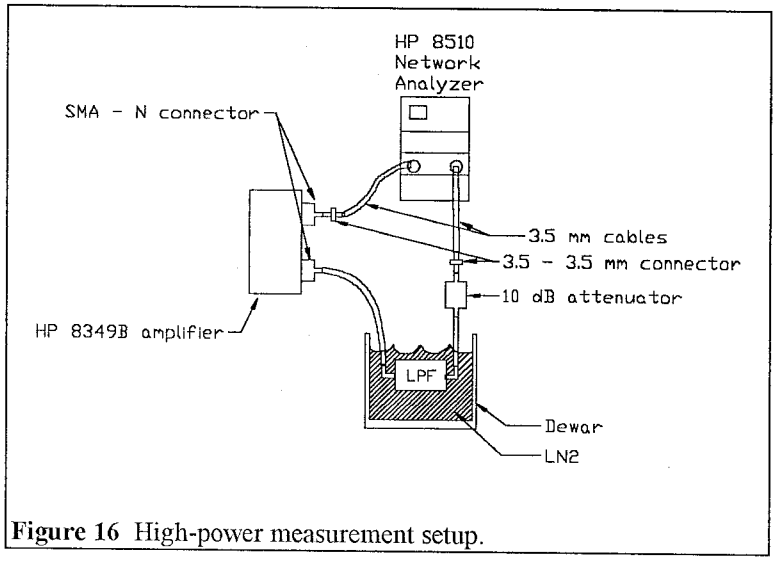

Figure 16 High-power measurement setup.

Unfortunately with this setup, which is necessary for input powers of 5 dBm and higher, only S21 can be measured (since a thru-calibration, the only one possible, does not correct for the return loss of the amplifier). Nine measurements are taken, at input powers of -20, -15, -10, -5, 0, 5, 10, 15 and 20 dBm respectively. For the first 6 measurements all four S-parameters are measured, while for the last 3 only S21 is measured. Figures 17 and 18 show the magnitude of S21, in dB, for the higher seven input power measurements (i.e., -10 to 20 dBm). The curve corresponding to 5 dBm has been plotted on both figures for reference and the scale is identical on both plots.

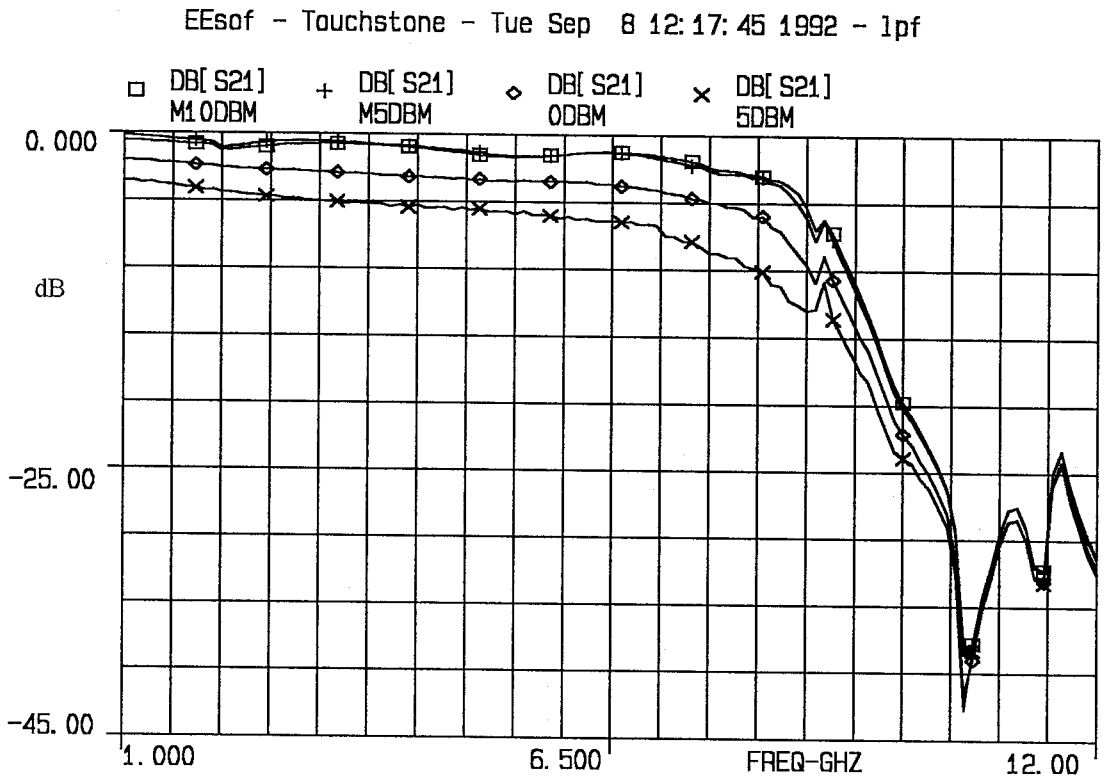

Figure 17 Measured magnitude of S21 at input powers -10, -5, 0 and 5 dBm.

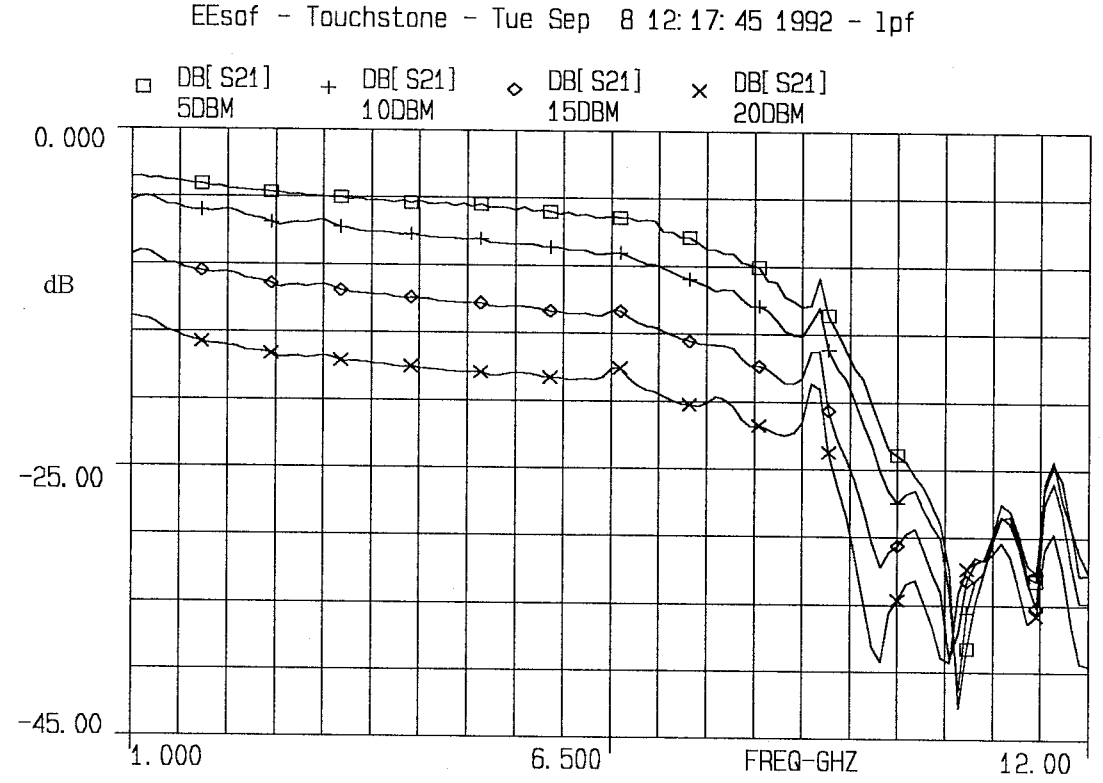

Figure 18 Measured magnitude of S21 at input powers 5, 10, 15 and 20 dBm.

The non-linear behavior of the circuit is evident. The curves at -10 and -5 dBm input powers are almost identical, but the one at 0 dBm is significantly different from these two which indicates that some component of the filter (probably the narrow lines) reaches its low critical field, H_{c1} ,at an input power between -5 and 0 dBm. As the power is further increased and the transmission lines of the filter become insulators, the low insertion loss pass-band of the filter disappears and the device becomes very lossy (over 15 dB insertion loss at 20 dBm input power).

7.4.3 The Power-Dependent Model

The first effort is to ascertain whether the model of chapter 3, with the enhancements of section 7.1, which enable more accurate modeling of high-loss lines, is sufficient for modeling the power-dependent behavior seen in figures 17 and 18. The parameters of the model are optimized for minimum integrated squared error relative to the measurements of the S-parameters of the filter at an input power of 5 dBm. The dependent variables of the optimization are the zero-temperature penetration depth, λ_o, and the normal part of the conductivity σ_n. This is equivalent to having optimized the density of superelectrons and normal electrons, because the real and imaginary parts of the complex conductivity are both optimized independently (see equation 3.9). The Touchstone file used to perform this analysis is included as appendix C and the resulting fit is shown in figures 19-22.

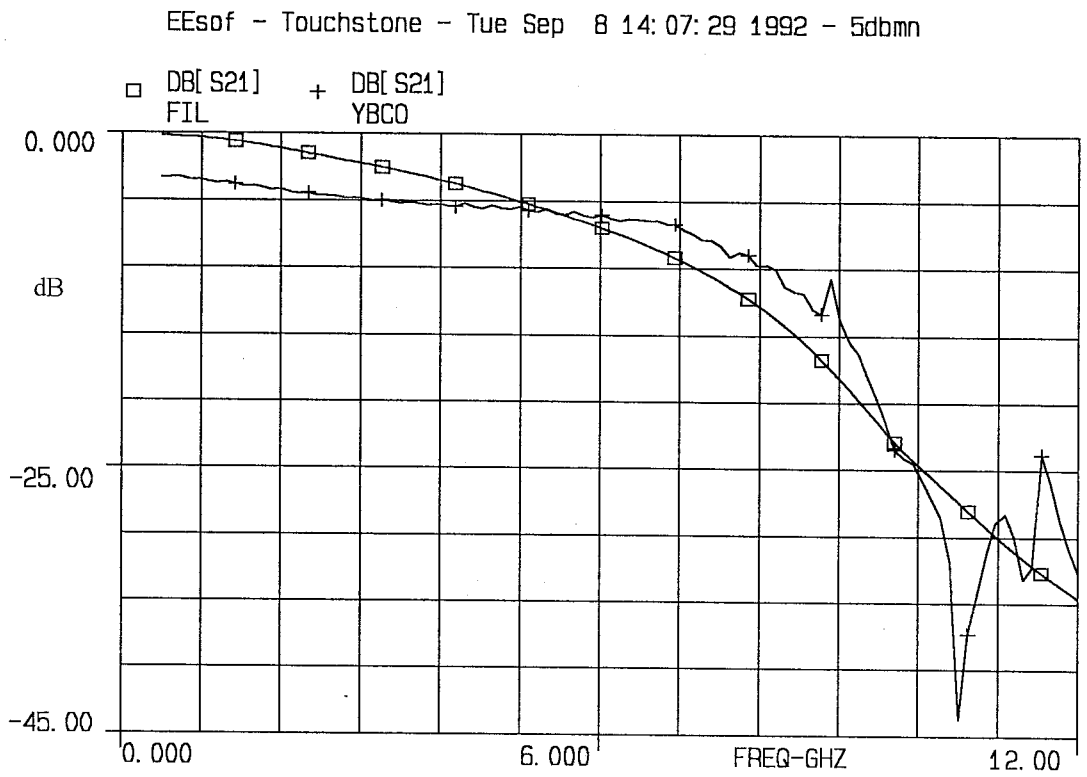

Figure 19 Magnitude of S21 of model versus measurement at 5 dBm input power.

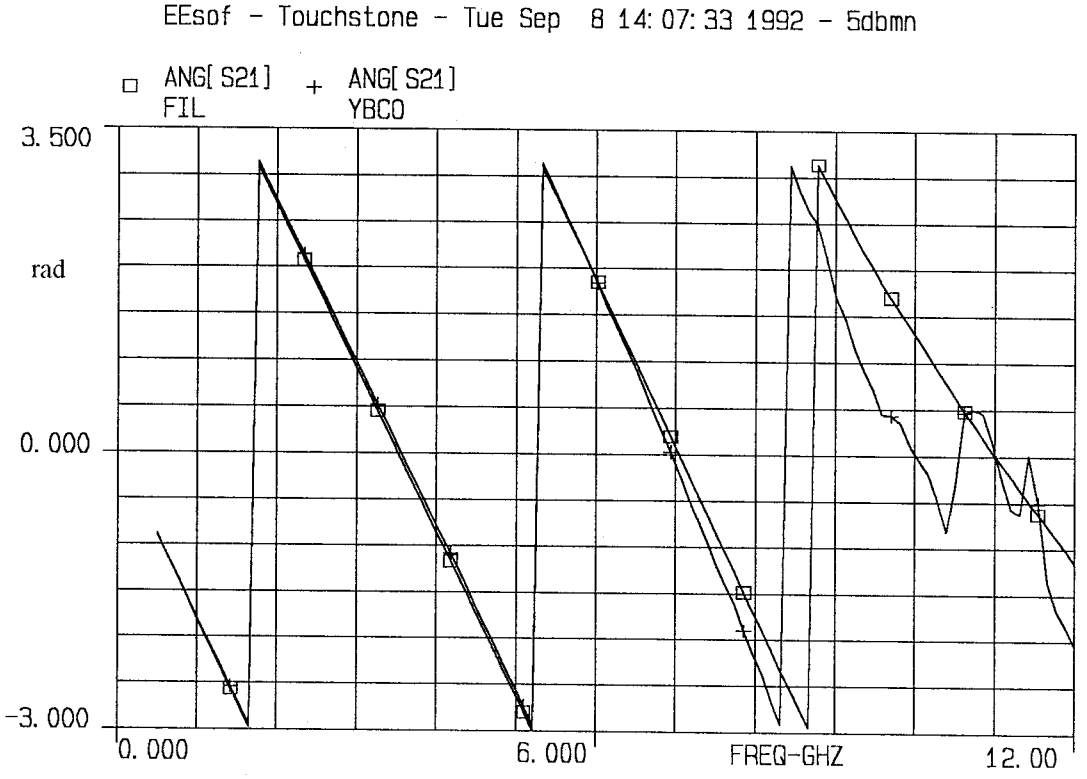

Figure 20 Phase of S21 of model versus measurement at 5 dBm input power.

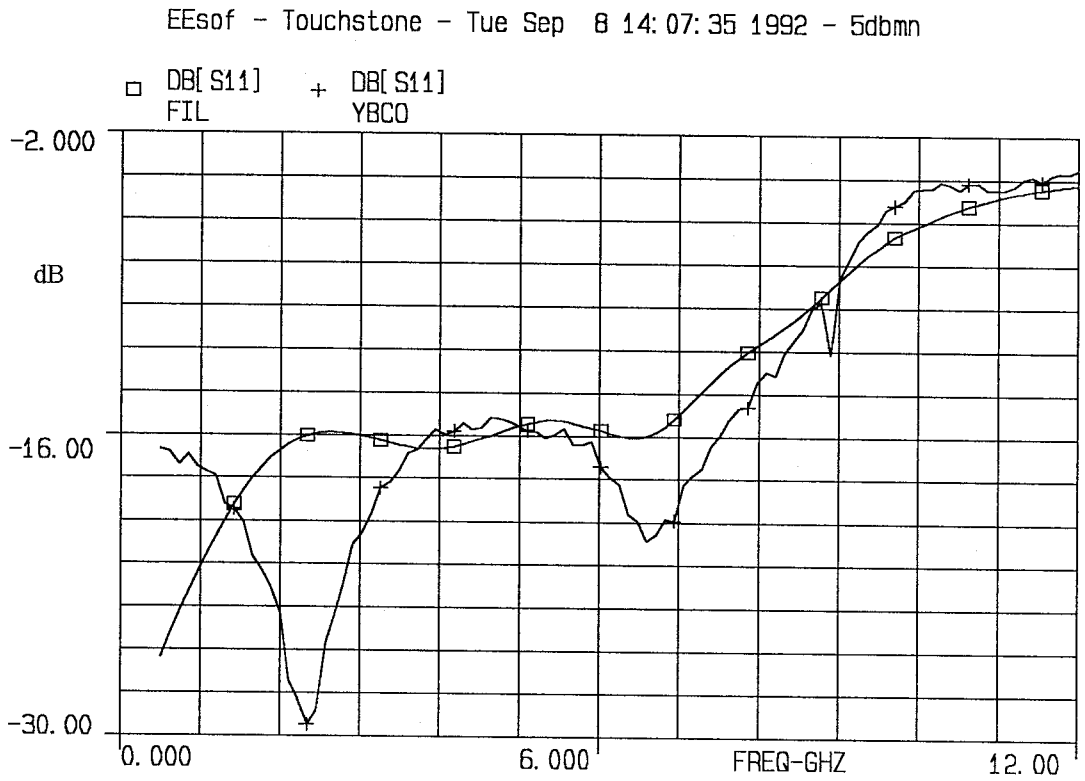

Figure 21 Magnitude of S11 of model versus measurement at 5 dBm input power.

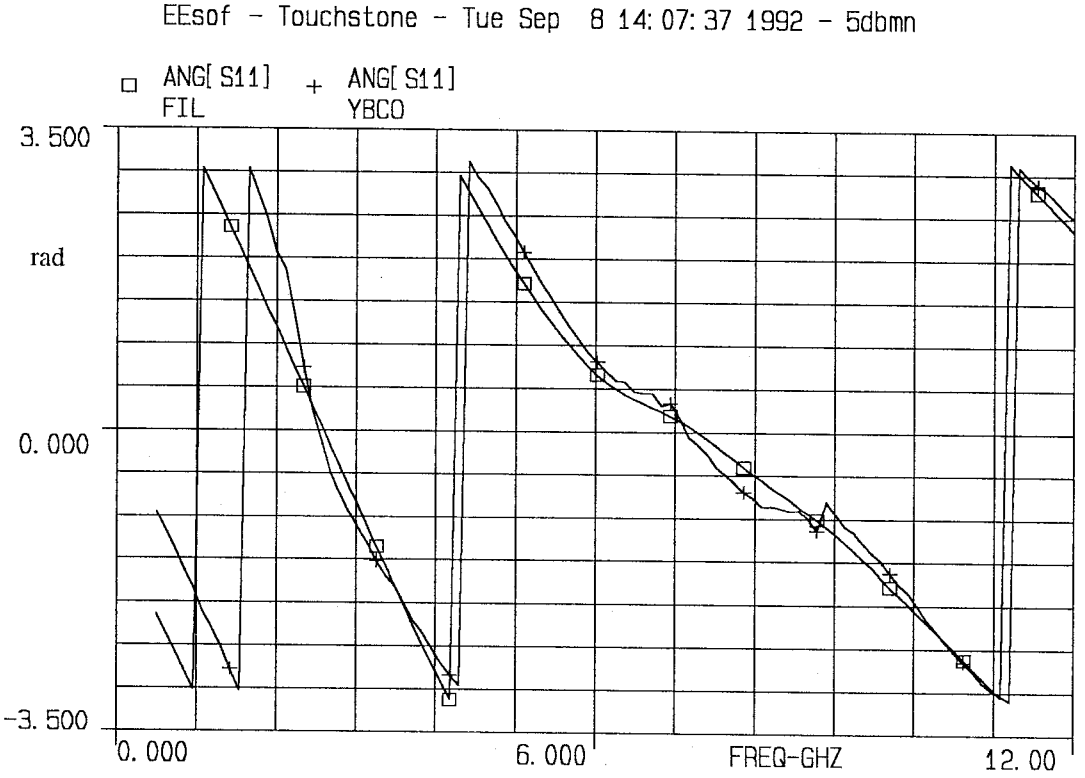

Figure 22 Phase of S11 of model versus measurement at 5 dBm input power.

7.4.4 Discussion of the Fit of the Model to the Measured Data

The integrated squared error between model and measurement is 0.09308, 53.6% more than for the low power case, as reported above. The higher error is partly due to the fact that the model doesn't pick up the locations of the poles of the filter (see figure 21 and compare to figure 13) and underestimates the insertion loss at the low end of the pass-band (see figure 19). These discrepancies may be due to inaccuracies in the impedance calculations (see discussion in section 7.4.1. above). The fit of the phases is quite good, however, which indicates that equation (4) for the corrected propagation constant correctly accounts for increased distributed internal inductance effects. The failure of the model to pinpoint the poles of the filter probably indicates that the model does not calculate impedance properly. This may be because the CPW LPF, which comprises narrow (high-impedance) and wide (low-impedance) lines, is operating in its non-linear power-dependent region. In the frequencies of the pass band of the filter, the forward-current (from the wave incident at the input port) goes through every line of the filter largely unscattered (without many reflections). The total current through every line must be almost the same. The current density is, therefore, higher in the narrow lines than in the wide lines. This means that the fields in the narrow lines are closer to the high-critical fields than in the wide lines and hence the number of superconducting electrons is higher in the wide than in the narrow lines. This points to the need for two improvements on the model:

1. The number of superelectrons must be dependent on the width of the modeled line.
2. The number of superelectrons and normal electrons should not be dependent only on temperature.

These improvements, together with the further refinement of considering the dependence of the model on the collision relaxation time τ, are built into the model using the following

derivation.

7.5 First-Order Effects due to Collision Relaxation

7.5.1 The Analysis

Let the variable $X(T,H;T_c,H_c)$ represent the fraction of the total electrons that are in normal state, i.e.,

$$\frac{n_n}{n} = X(T,H;T_c,H_c) \tag{10}$$

and

$$\frac{n_s}{n} = 1 - X \tag{11}$$

where n denotes electron volume density. From equation (3.8) we obtain

$$\sigma = \sigma_1 - j\sigma_2 = \frac{n_n}{n}\sigma_n - j\frac{e^2}{m\omega}\left[n_s + n_n(\omega\tau)^2\right] \tag{12}$$

where $(\omega\tau)^2 << 1$ has been assumed. However, this assumption cannot be used to simplify the imaginary part of (12) since, in high-power narrow lines, $n_n >> n_s$. Combining (10) and (12) we obtain

$$\sigma_1 = X\sigma_n \quad . \tag{13}$$

The corresponding expression for σ_2 is slightly more complicated. By the definition of the penetration depth we have

$$\lambda^2(T,H) = \frac{m}{\mu_0 n_s(T,H)e^2} \quad , \tag{14}$$

where μ_0 is the magnetic permeability of vacuum and m and e are the mass and charge of the electron, respectively. When T and H are zero all the electrons are superelectrons, i.e., $n_s = n$. Using these values and equation (11) to eleminate n_s from equation (14) we obtain

$$\frac{\lambda^2(0,0)}{\lambda^2(T,H)} = 1 - X \quad . \tag{15}$$

Combining (12), (14) and (15) gives

$$\sigma_2 = \frac{1-X}{\omega\mu_0\lambda^2(0,0)} + X\sigma_n\omega\tau \tag{16}$$

and the new expression for the conductivity becomes

$$\sigma = X\sigma_n - j\left[\frac{1-X}{\omega\mu_0\lambda^2(0,0)} + X\sigma_n\omega\tau\right] . \tag{18}$$

7.5.2 The Fit of the Model to Measurement

Equation (18) is incorporated into a new circuit file which is included as appendix D. An initial guess is used for τ and then it is permitted to optimize. A different X and corresponding σ is used for each of the line widths of the CPW LPF (hence three different X's are used, one for each of the narrow, the wide and the 50 Ω lines). The fit between model and measurements improves from 0.09308 integrated squared error (as reported above) to 0.06675, a 28.3% decrease. The improved fit is shown in figures 23-26.

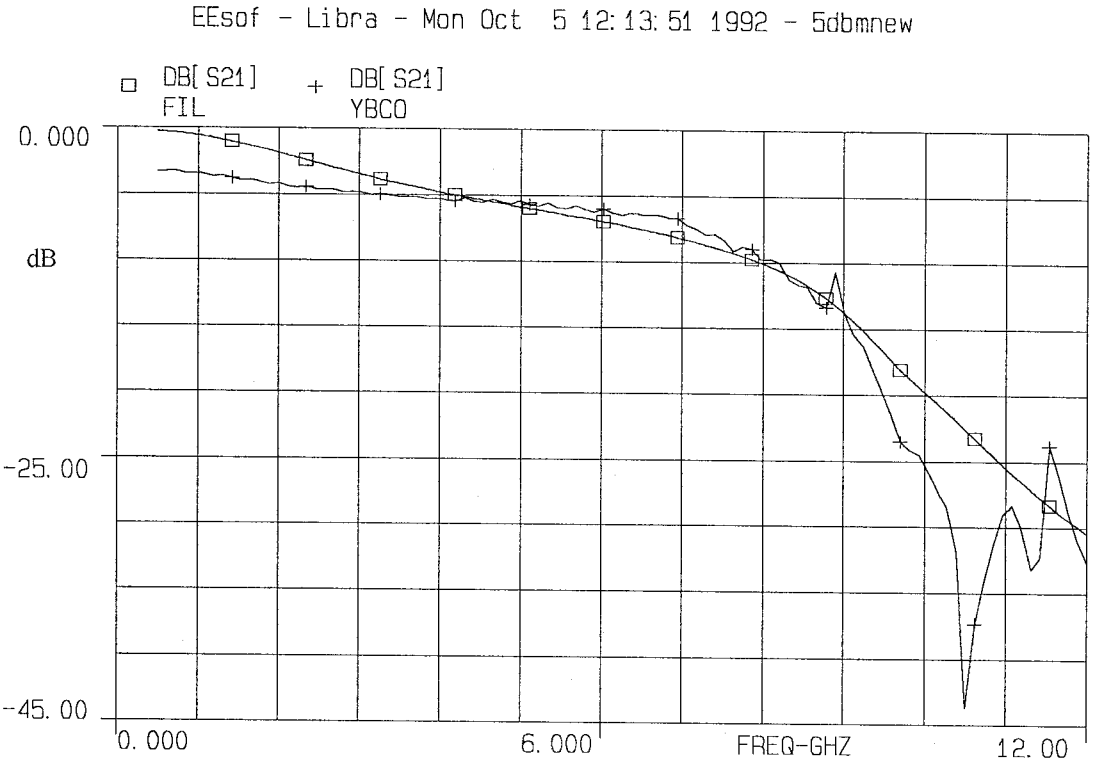

Figure 23 Magnitude of S21, model versus measured.

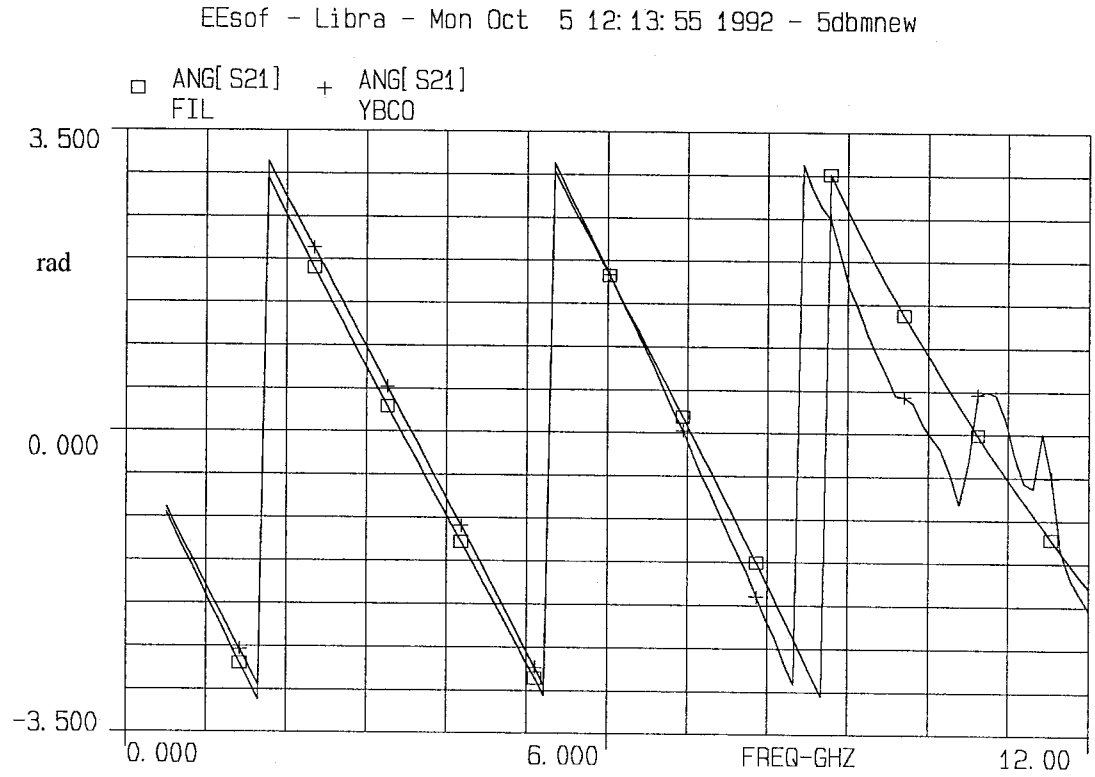

Figure 24 Phase of S21, model versus measured.

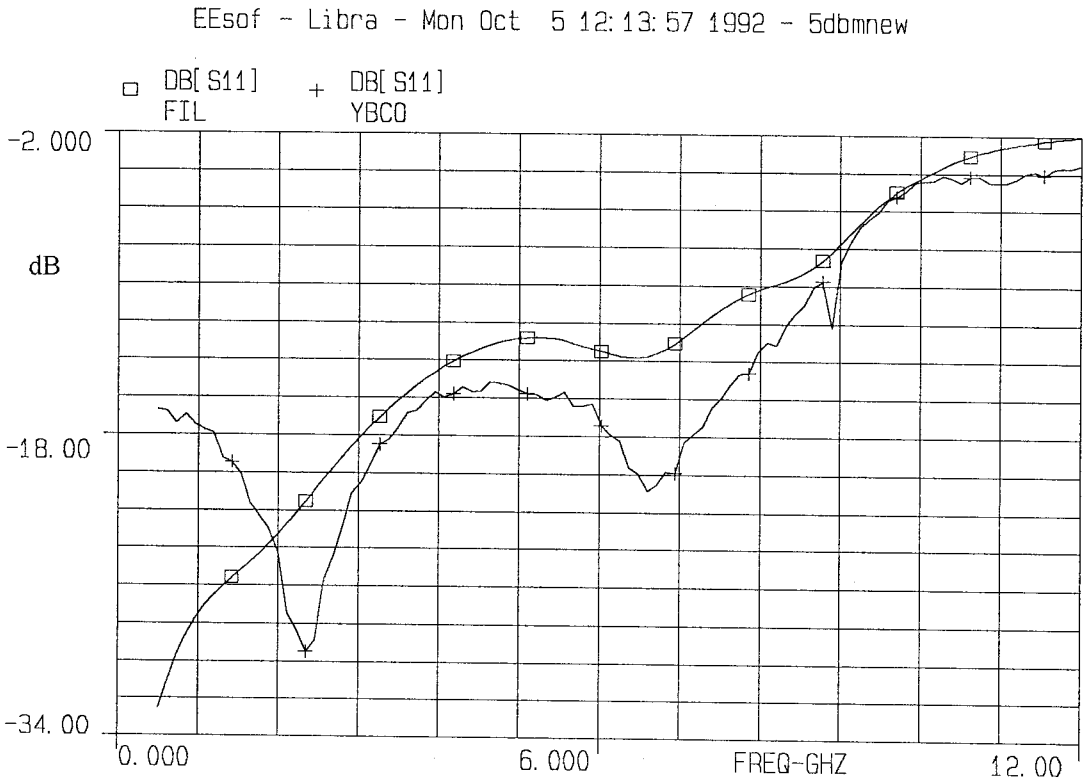

Figure 25 Magnitude of S11, model versus measured.

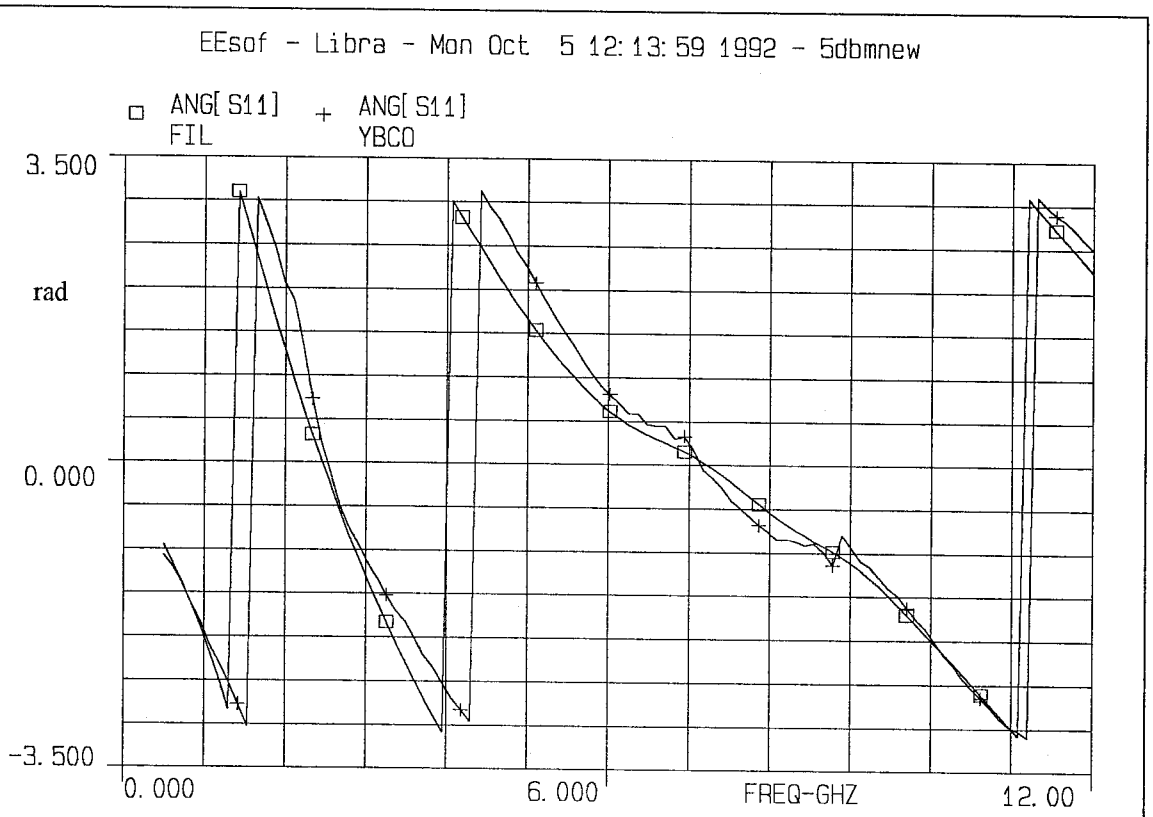

Figure 26 Phase of S11, model versus measured.

7.5.3 Discussion of the Results

Comparison of figures 23-26 to figures 19-22 reveals that the new model matches the measured location of the poles of the LPF better, although still not as accurately as in the low power case. It is encouraging that the optimized values of X for each of the narrow, 50 Ω and wide lines obey $X_{narrow}>X_{50\Omega}>X_{wide}$ (see appendix D). Indeed, by the rationale presented above, we would expect the narrow line to carry the most normal electrons and the wide the least. Although the fit of figures 23-26 is promising, the mismatch of the location of the poles between model and measurement indicates that there is something more going on in the physics that the model is not capturing. The reason for the discrepancy is thought to be a second-order effect of the non-linear behavior with respect to input power. As the input power increases the narrow lines "go normal" first,

due to the higher current density that they carry. The profile of the current density along the width of the line is expected to be a minimum at the midpoint and symmetric about it, peaking at the edges (the discontinuity). The same is true for the magnetic field. Hence the edges of the line must go normal at low input power and the middle at higher input power. Since YBCO is a crystalline substance, it becomes an insulator when it goes normal. This means that the line becomes effectively narrower when a strong enough input field is applied (with its edges having become insulating). This affects not only the cross-sectional area A and the incremental inductance factor G (equation (3.32)), but also the impedance of the line even before the PEM is applied for correction of the penetration depth effects, i.e., the impedance of the line as if it were made out of a normal conductor.

7.5.4 Testing the Variable Effective Line-Width Hypothesis

To test the above conjecture, a new circuit file is created, this time also optimizing A, G and Z for each type of line (see appendix E of this chapter). The integrated squared error between model and measurements is reduced to 0.02240, a 66.4% decrease relative to the previous model. This dramatic decrease in error confirms the conjecture put forth above. Examination of appendix E shows that, as expected, the parameters of the narrow lines are the ones most affected. While ZW0 and Z500, the impedances of the wide and 50 Ω lines respectively, do not change significantly as a result of optimization (from 22.64 to 23.93 Ω for the first and from 49.56 to 50.15 Ω for the second) ZN0, the impedance of the narrow line, increased from 83.38 to 114 Ω, which confirms the "narrowing" of the line due to high input power. The resulting fit is shown in figures 27-30.

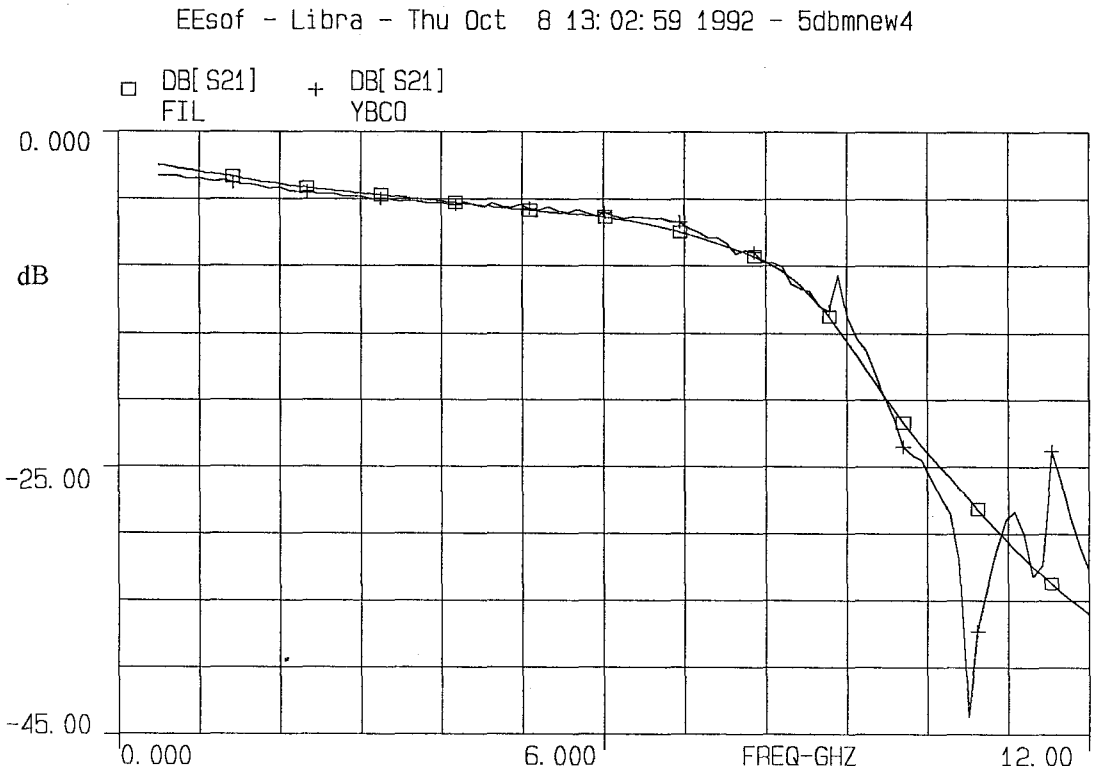

Figure 27 Magnitude of S21, model versus measured.

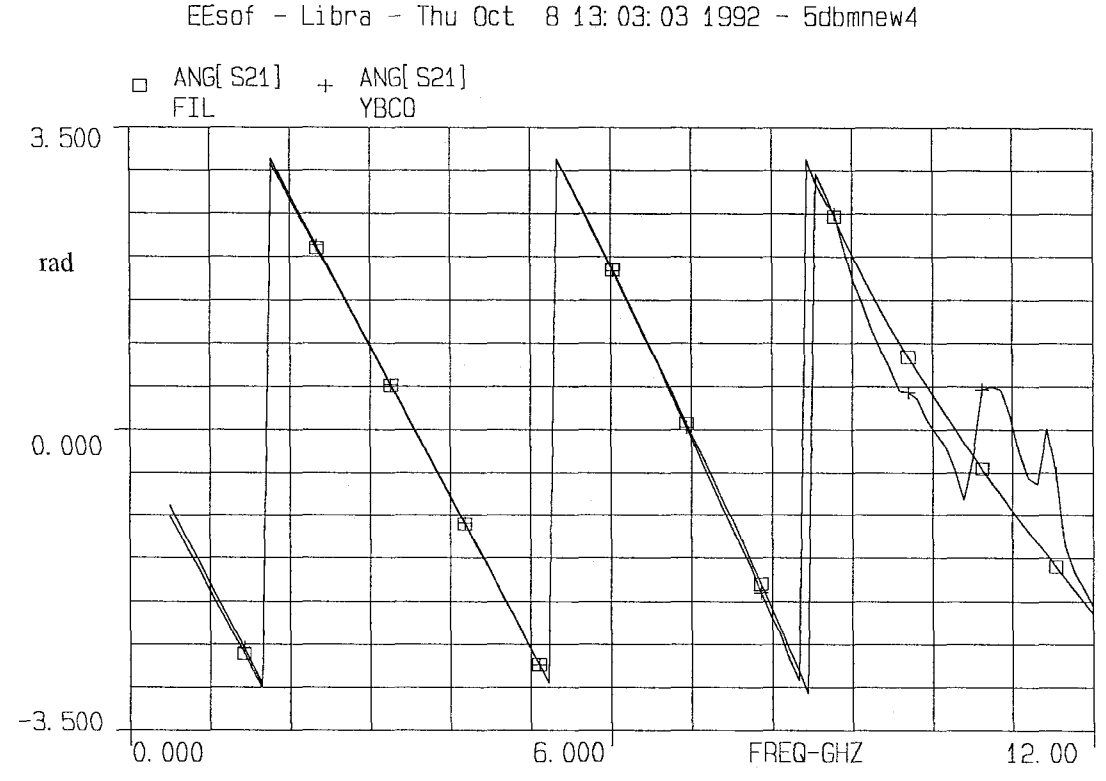

Figure 28 Phase of S21, model versus measured.

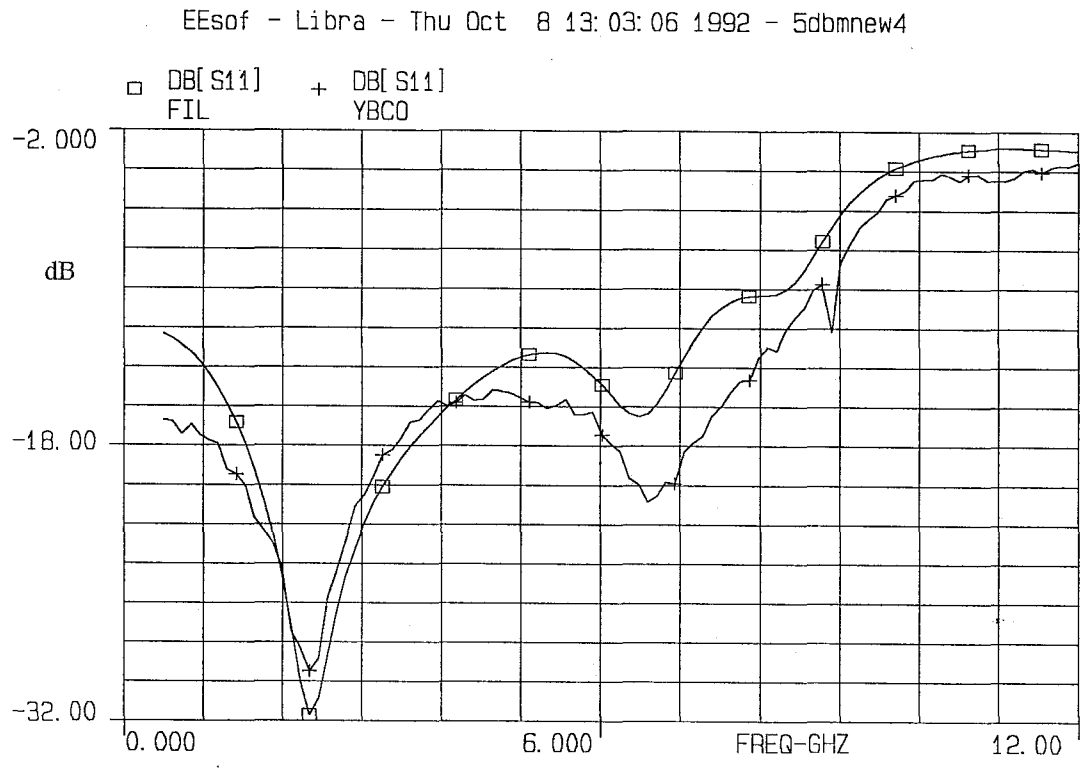

Figure 29 Magnitude of S11, model versus measured.

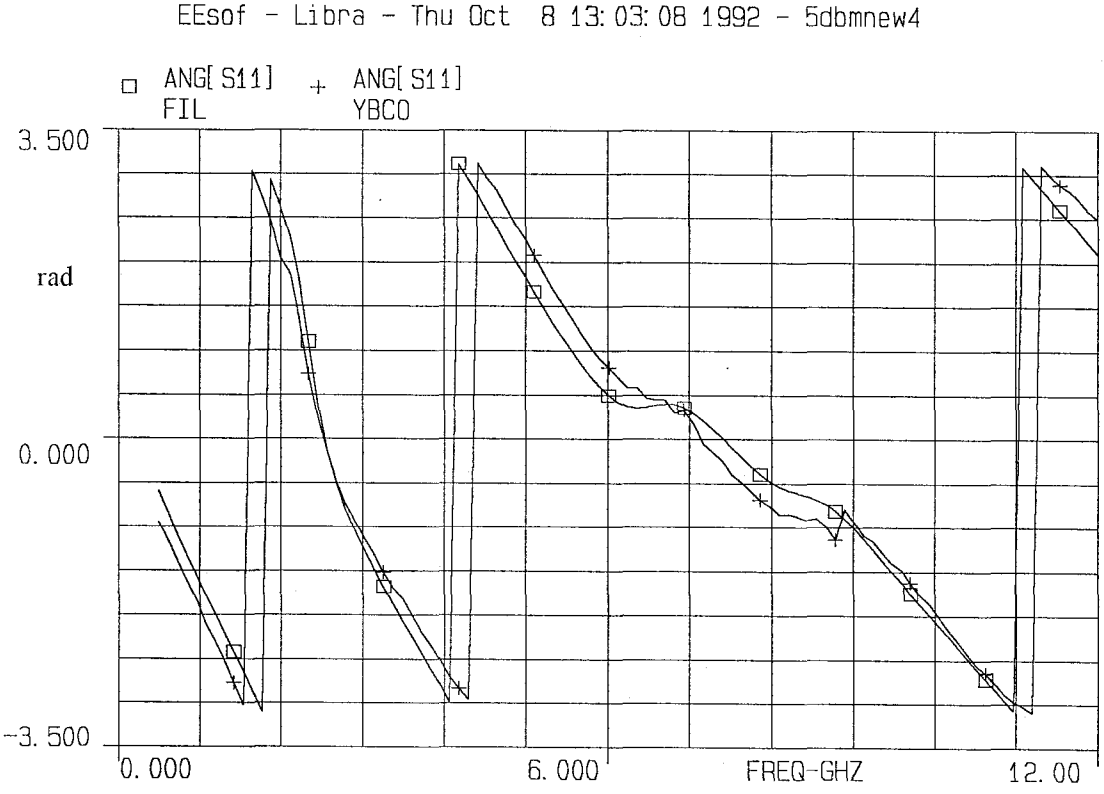

Figure 30 Phase of S11, model versus measured.

7.5.5 Conclusions

Although the above fit is encouraging and suggests that there may be a way to incorporate the line "narrowing" effect into the model while retaining its predictive value, the problem becomes non-linear and will only accept an iterative solution. More importantly, the measurements of the HTS CPW LPF are too intrinsic and involve too many unknown parameters that have to be optimized. With the increase of the number of these unknowns (as the model progresses form its initial simpler form to the current more complicated one), the hyper-surface describing the integrated squared error between measurements and model now has a multitude of local minima (rather than one global true minimum that can be found by a gradient algorithm). Even if the true minimum among these minima can be found (with respect to all the variables that are to be optimized), there is little confidence that this solution will, in fact, correspond to the true physical values of the unknowns. Hence, although the trends and results are encouraging, this formulation of the model should be used with caution.

7.6 References

[1] S. Ramo, J. R. Whinnery and T. Van Duzer, *Fields and Waves in Communication Electronics*, Wiley, New York, 1965.

[2] T. Van Duzer and C. W. Turner, *Principles of Superconductive Devices and Circuits*, Elsevier, New York, 1981.

Appendix A

First-Order HTS CPW LPF Touchstone Model (Low Power Response)

```
! MODEL OF THE YBCO FILTER FIT TO DATA USING LOSS AND LOSS TANGENT
! ALSO USING S2P FILE FOR 50 OHM TAPER K-CONNECTOR TO CPWG INTERFACE
! ALSO USING CONSTANT LOSS S-PAR FILE (ADJUST.S2P) TO CORRECT FOR
! CAL STANDARDS BEING AT ROOM TEMP (NOT DUNKED)
! USING LOW LOSS EQUATIONS FOR ALL ATTENUATIONS AS A FUNCTION OF LD AND
Sn
! BY DIMITRIOS ANTSOS (JULY 28, 1992)
! FILENAME REFERS TO (TRUE) POWER INTO FILTER
! FILTER USED IS LAST PACKAGED CPW FILTER LEFT



DIM
  LNG UM
  ANG RAD
VAR
  LD# 100E-9 7.77e-07 5E-6                !PENETRATION DEPTH FOR YBCO
  T = 77                                  !TEMPERATURE OF MEASUREMENT
  Tc = 83                                 !Critical Temperture of Sample
  Sn #1E4  1133285. 1E8                   !Normal Conductivity of Sample
  e0 = 8.854E-12                          !Permittivity of free space
  AGn = 5e-12                             !Dimension Variable ( Narrow
Line )
  Gn = 8.43479e4                          !Incremental Inductance Rule
Var (Narr
  AGw = 1e-10
  Gw = 1.7336e4
  AG5 = 2.5e-11
  G5 = 2.3501e4


  Z500 = 49.56
  ZN0  = 75.6614
  ZW0  = 22.64

  KI #12 14.26254 18

  K500 = 12.52
  KN0  = 12.468
  KW0  = 12.49

  LI # 2000 2446.013 2800

  L50 # 1800 2221.961 2800
  L1  = 720.8
  L2  = 997.0
  L3  = 1369.7
  L4  = 761.2
  L5H = 924.0


  ACI0 #1E-10  1.00e-08 1E-6          ! COPPER LOSS OF INPUT TAPER
(=5.02
  ADI00 # 3E-4 0.009000 9e-3        ! = 3.3E-4
```

```
  TAND # 0 0.000104 .01

EQN

  ADN0 = 3.086E-4*TAND
  AD500 = 3.093E-4*TAND
  ADW0 = 3.089E-4*TAND

  ADI0 = ADI00*TAND          ! DIELECTRIC LOSS OF INPUT CPW 50 OHM TAPER


  LI1 = -LI

  AI   = ACI0  * FREQ**2 + ADI0 * FREQ


! Computation of exact loss for narrow line
!       Constants

  U0 = 4*PI*1e-7                  !Magnetic Permeability of vacuum
  f = FREQ*1e9                    !Frequency in Hz
  Sr = Sn*(T/Tc)**4               !Real Part of conductivity of YBCO
  Si = (1-(T/Tc)**4)/(2*PI*f*U0*LD**2)  !Imaginary Part of conductivity
  P = ATAN(Si/Sr)-2*PI      !Angle of conductivity
  Th= PI/4-P/2                    !Auxiliary angle definition
  r = SQRT(SQR(Sr)+SQR(Si))       !Norm of conductivity
  c = 1/sqrt(e0*U0)               !Velocity of light

!       Narrow Line Parameters
  Bn= Gn*AGn*SQRT(2*PI*f*U0*r)    !Fudge Factors
  Cn= EXP(2*Bn*COS(Th))
  Dn= COS(2*Bn*SIN(Th))
  En= SIN(2*Bn*SIN(Th))
  Un= SQRT(SQR(Cn*Dn-1)+SQR(Cn*En))
  Wn= ATAN(Cn*En/(Cn*Dn-1))
  Fn= Bn/(AGn*r*Un)
  Mn= 2*Bn*SIN(Th)
  Nn= COS(PI/4+P/2-Wn)
  Rn= COS(Mn+PI/4+P/2-Wn)

  ReZn = Fn*(Nn+Cn*Rn)            !Real Part of Internal Impedance / Meter
  NIn= SIN(PI/4+P/2-Wn)
  RIn= SIN(Mn+PI/4+P/2-Wn)
  ImZn = Fn*(NIn+Cn*RIn)
  Zn = SQRT(SQR(ZN0)-(c*ZN0)/(2*PI*SQRT(KN0)*f)*ImZn)
  ACN = -(8.686e-6) * ReZn/(2*Zn)

  EFFN = ZN / ZN0

!       Wide Line Parameters
  Bw= Gw*AGw*SQRT(2*PI*f*U0*r)    !Fudge Factors
  Cw= EXP(2*Bw*COS(Th))
  Dw= COS(2*Bw*SIN(Th))
  Ew= SIN(2*Bw*SIN(Th))
  Uw= SQRT(SQR(Cw*Dw-1)+SQR(Cw*Ew))
```

```
   Ww= ATAN(Cw*Ew/(Cw*Dw-1))
   Fw= Bw/(AGw*r*Uw)
   Mw= 2*Bw*SIN(Th)
   Nw= COS(PI/4+P/2-Ww)
   Rw= COS(Mw+PI/4+P/2-Ww)

   ReZw = Fw*(Nw+Cw*Rw)          !Real Part of Internal Impedance / Meter
   NIw= SIN(PI/4+P/2-Ww)
   RIw= SIN(Mw+PI/4+P/2-Ww)
   ImZw = Fw*(NIw+Cw*RIw)
   Zw = SQRT(SQR(Zw0)-(c*Zw0)/(2*PI*SQRT(Kw0)*f)*ImZw)
   ACw = -(8.686e-6) * ReZw/(2*Zw)

   EFFw = Zw / Zw0

!      50 Ohm Line Parameters
   B5= G5*AG5*SQRT(2*PI*f*U0*r)    !Fudge Factors
   C5= EXP(2*B5*COS(Th))
   D5= COS(2*B5*SIN(Th))
   E5= SIN(2*B5*SIN(Th))
   U5= SQRT(SQR(C5*D5-1)+SQR(C5*E5))
   W5= ATAN(C5*E5/(C5*D5-1))
   F5= B5/(AG5*r*U5)
   M5= 2*B5*SIN(Th)
   N5= COS(PI/4+P/2-W5)
   R5= COS(M5+PI/4+P/2-W5)

   ReZ5 = F5*(N5+C5*R5)          !Real Part of Internal Impedance / Meter
   NI5= SIN(PI/4+P/2-W5)
   RI5= SIN(M5+PI/4+P/2-W5)
   ImZ5 = F5*(NI5+C5*RI5)
   Z50= SQRT(SQR(Z500)-(c*Z500)/(2*PI*SQRT(K500)*f)*ImZ5)
   AC50 = -(8.686e-6) * ReZ5/(2*Z50)

   EFF50 = Z50 / Z500

   K50  = K500 * EFF50 * EFF50
   KN   = KN0  * EFFN * EFFN
   KW   = KW0  * EFFW * EFFW


   A50  = AC50 + AD500 * FREQ
   AN   = ACN + ADN0 * FREQ
   AW   = ACW + ADW0 * FREQ

CKT
S2PA 1 2 0 costep1.s2p
DEF2P 1 2  BIG_STEP

S2PB 1 2 0 costep2.s2p
DEF2P 1 2 SML_STEP

S2PC 1 2 0 -5dbm.s2p
DEF2P 1 2 YBCO_RAW
```

```
S2PD 1 2 0 adjust.s2p
DEF2P 1 2 ADJ

S2PE 1 2 0 hts_50.s2p
DEF2P 1 2 FIFTY

ADJ 1 2
YBCO_RAW 2 3
DEF2P 1 3 YBCO

TLINP 1 2 Z=50 L^LI K^KI A^AI F=0
TLINP 2 3 Z=50 L^LI1 K^KI  A=0 F=0
FIFTY 3 4
TLINP_T1 4 5  Z^Z50 L^L50 K^K50 A^A50 F=0.0000000
SML_STEP    5 6
TLINP_T2 6 7  Z^ZW L^L1 K^KW A^AW F=0.0000000
BIG_STEP    7 8
TLINP_T3 8 9 Z^ZN L^L2 K^KN A^AN F=0
BIG_STEP 9 10
TLINP_T4 10 11 Z^ZW L^L3 K^KW A^AW F=0.0000000
BIG_STEP   11 12
TLINP_T5 12 13 Z^ZN L^L4 K^KN A^AN F=0.0000000
BIG_STEP  13 14
TLINP_T6 14 15 Z^ZW L^L5H K^KW A^AW F=0.0000000
DEF2P 1 15 HALF

HALF 1 2
HALF 3 2
DEF2P 1 3 FIL

!TLINP_T1 1 2  Z^Z50 L^L50 K^K50 A^A50 F=0.0000000
!TLINP_T2 2 3  Z^ZW L^L1 K^KW A^AW F=0.0000000
!TLINP_T3 3 4 Z^ZN L^L2 K^KN A^AN F=0
!TLINP_T4 4 5  Z^ZW L^L3 K^KW A^AW F=0.0000000
!TLINP_T5 5 6  Z^ZN L^L4 K^KN A^AN F=0.0000000
!TLINP_T6 6 7   Z^ZW L^L5H K^KW A^AW F=0.0000000

!DEF2P 1 7  HALF1


!HALF1 1 2
!HALF1 3 2
!DEF2P 1 3 NOSTEP

!RES 1 0 R^rez5
!DEF1P 1 TEST

FREQ
  SWEEP 0.5 12 .115
OUT
 FIL DB[S21] GR1
 YBCO DB[S21] GR1
!SILVER DB[S21] GR1
!NOSTEP DB[S21] GR1
```

```
 FIL DB[S11] GR3
 YBCO DB[S11] GR3
!SILVER DB[S11] GR3


 FIL ANG[S21] GR2
 YBCO ANG[S21] GR2
!SILVER ANG[S21] GR2

 FIL ANG[S11] GR4
 YBCO ANG[S11] GR4
!SILVER ANG[S11] GR4

  FIL S21 SC2
  YBCO S21 SC2
! TEST RE[Z11] GR5

! FIL DB[S21] GR6
! YBCO DB[S21] GR6
GRID
 RANGE 0 12 1

!RANGE 7 9 .2
! GR6 -2 0 .5
OPT
RANGE 1 11
YBCO MODEL FIL
```

Appendix B

High-Loss CPW LPF Touchstone Model (Low Power Response)

```
! MODEL OF THE YBCO FILTER FIT TO DATA USING LOSS AND LOSS TANGENT
! ALSO USING S2P FILE FOR 50 OHM TAPER K-CONNECTOR TO CPWG INTERFACE
! ALSO USING CONSTANT LOSS S-PAR FILE (ADJUST.S2P) TO CORRECT FOR
! CAL STANDARDS BEING AT ROOM TEMP (NOT DUNKED)
! USING LOW LOSS EQUATIONS FOR ALL ATTENUATIONS AS A FUNCTION OF LD AND
Sn
! BY DIMITRIOS ANTSOS (JULY 28, 1992)
! FILENAME REFERS TO (TRUE) POWER INTO FILTER
! FILTER USED IS LAST PACKAGED CPW FILTER LEFT



DIM
  LNG UM
  ANG RAD
VAR
  T = 77                                    !TEMPERATURE OF MEASUREMENT
  Tc =83                                            !Critical Temperture
of Sample
  LD# 100E-9 5.42e-07  5E-6                  !PENETRATION DEPTH FOR YBCO
  Sn #1E4  3418408. 1E8                     !Normal Conductivity of Sample
  e0 = 8.854E-12                            !Permittivity of free space
  AGn = 3e-12                               !Dimension Variable ( Narrow
Line )
  Gn = 1.255e5                              !Incremental Inductance Rule
Var (Narr
  AGw = 1e-10
  Gw = 1.7336e4
  AG5 = 2.5e-11
  G5 = 2.3501e4


  Z500 = 49.56
  ZNO  = 83.38
  ZWO  = 22.64

  KI #12 17.17221   18

  K500 = 12.52
  KNO  = 12.455
  KWO  = 12.49

  LI # 2000 2000.038 2800

  L50 # 1800 2443.082 2800          !# 4000  4335.155 4400
  L1  = 720.8
  L2  = 997.0
  L3  = 1369.7
  L4  = 761.2
  L5H = 924.0


  ACI0 #1E-10  1.00e-10 1E-6          ! COPPER LOSS OF INPUT TAPER
(=5.02
  ADI00 # 3E-4 0.000300 9e-3        ! = 3.3E-4
```

```
  TAND # 0 0.000248 .01

EQN

  ADN0 = 3.086E-4*TAND
  AD500 = 3.093E-4*TAND
  ADW0 = 3.089E-4*TAND

  ADI0 = ADI00*TAND          ! DIELECTRIC LOSS OF INPUT CPW 50 OHM TAPER


  LI1 = -LI

  AI   = ACI0  * FREQ**2 + ADI0 * FREQ


! Computation of exact loss for narrow line
!       Constants

  U0 = 4*PI*1e-7                  !Magnetic Permeability of vacuum
  f = FREQ*1e9                    !Frequency in Hz
  Sr = Sn*(T/Tc)**4               !Real Part of conductivity of YBCO
  Si = (1-(T/Tc)**4)/(2*PI*f*U0*LD**2)  !Imaginary Part of conductivity
  P =  ATAN(Si/Sr)-2*PI      !Angle of conductivity
  Th= PI/4-P/2                    !Auxiliary angle definition
  r = SQRT(SQR(Sr)+SQR(Si))       !Norm of conductivity
  c = 1/sqrt(e0*U0)               !Velocity of light

!       Narrow Line Parameters
  Vn= c/sqrt(KN0)                 !Phase velocity in line
  Bn= Gn*AGn*SQRT(2*PI*f*U0*r)    !Fudge Factors
  Cn= EXP(2*Bn*COS(Th))
  Dn= COS(2*Bn*SIN(Th))
  En= SIN(2*Bn*SIN(Th))
  Un= SQRT(SQR(Cn*Dn-1)+SQR(Cn*En))
  Wn= ATAN(Cn*En/(Cn*Dn-1))
  Fn= Bn/(AGn*r*Un)
  Mn= 2*Bn*SIN(Th)
  Nn= COS(PI/4+P/2-Wn)
  Rn= COS(Mn+PI/4+P/2-Wn)

  ReZn = -Fn*(Nn+Cn*Rn)           !Real Part of Internal Impedance /
Meter
  NIn= SIN(PI/4+P/2-Wn)
  RIn= SIN(Mn+PI/4+P/2-Wn)
  ImZn = -Fn*(NIn+Cn*RIn)
  LMn = ZN0/Vn+ImZn/(2*PI*f)
  CMN = 1/(ZN0*Vn)
  Zn = sqrt(LMn/CMn)
  RATn= ReZn/(2*PI*f*LMn)
  ANGn= 0.5*ATAN(RATn)

  ACN = (8.686e-6) *
(2*PI*f)*sqrt(LMn*CMn)*sqrt(sqrt(1+SQR(RATn)))*sin(ANGn)
```

```
  KN = LMn*CMn/(e0*u0)*sqrt(1+SQR(RATn))*SQR(cos(ANGn))

!       Wide Line Parameters
  Vw= c/sqrt(KW0)                  !Phase velocity in line
  Bw= Gw*AGw*SQRT(2*PI*f*U0*r)     !Fudge Factors
  Cw= EXP(2*Bw*COS(Th))
  Dw= COS(2*Bw*SIN(Th))
  Ew= SIN(2*Bw*SIN(Th))
  Uw= SQRT(SQR(Cw*Dw-1)+SQR(Cw*Ew))
  Ww= ATAN(Cw*Ew/(Cw*Dw-1))
  Fw= Bw/(AGw*r*Uw)
  Mw= 2*Bw*SIN(Th)
  Nw= COS(PI/4+P/2-Ww)
  Rw= COS(Mw+PI/4+P/2-Ww)

  ReZw =-Fw*(Nw+Cw*Rw)             !Real Part of Internal Impedance / Meter
  NIw= SIN(PI/4+P/2-Ww)
  RIw= SIN(Mw+PI/4+P/2-Ww)
  ImZw =-Fw*(NIw+Cw*RIw)
  LMw = ZW0/Vw+ImZw/(2*PI*f)
  CMw= 1/(ZW0*Vw)
  Zw = sqrt(LMw/CMw)
  RATw=  ReZw/(2*PI*f*LMw)
  ANGw= 0.5*ATAN(RATw)

  ACW = (8.686e-6) *
(2*PI*f)*sqrt(LMw*CMw)*sqrt(sqrt(1+SQR(RATw)))*sin(ANGw)

  KW = LMw*CMw/(e0*u0)*sqrt(1+SQR(RATw))*SQR(cos(ANGw))

!       50 Ohm Line Parameters
  V5= c/sqrt(K500)                 !Phase velocity in line
  B5= G5*AG5*SQRT(2*PI*f*U0*r)     !Fudge Factors
  C5= EXP(2*B5*COS(Th))
  D5= COS(2*B5*SIN(Th))
  E5= SIN(2*B5*SIN(Th))
  U5= SQRT(SQR(C5*D5-1)+SQR(C5*E5))
  W5= ATAN(C5*E5/(C5*D5-1))
  F5= B5/(AG5*r*U5)
  M5= 2*B5*SIN(Th)
  N5= COS(PI/4+P/2-W5)
  R5= COS(M5+PI/4+P/2-W5)

  ReZ5 =-F5*(N5+C5*R5)             !Real Part of Internal Impedance / Meter
  NI5= SIN(PI/4+P/2-W5)
  RI5= SIN(M5+PI/4+P/2-W5)
  ImZ5 =-F5*(NI5+C5*RI5)
  LM5 = Z500/V5+ImZ5/(2*PI*f)
  CM5 = 1/(Z500*V5)
  Z50 = sqrt(LM5/CM5)
  RAT5=  ReZ5/(2*PI*f*LM5)
  ANG5= 0.5*ATAN(RAT5)

  AC50 = (8.686e-6) *
```

```
(2*PI*f)*sqrt(LM5*CM5)*sqrt(sqrt(1+SQR(RAT5)))*sin(ANG5)

  K50 = LM5*CM5/(e0*u0)*sqrt(1+SQR(RAT5))*SQR(cos(ANG5))



  A50  = AC50 + AD500 * FREQ
  AN   = ACN + ADN0 * FREQ
  AW   = ACW + ADW0 * FREQ

CKT
S2PA 1 2 0 costep1.s2p
DEF2P 1 2  BIG_STEP

S2PB 1 2 0 costep2.s2p
DEF2P 1 2 SML_STEP

S2PC 1 2 0 -5dbm.s2p
DEF2P 1 2 YBCO_RAW

S2PD 1 2 0 adjust.s2p
DEF2P 1 2 ADJ

S2PE 1 2 0 hts_50.s2p
DEF2P 1 2 FIFTY

ADJ 1 2
YBCO_RAW 2 3
DEF2P 1 3 YBCO

TLINP 1 2 Z=50 L^LI K^KI A^AI F=0
TLINP 2 3 Z=50 L^LI1 K^KI  A=0 F=0
FIFTY 3 4
TLINP_T1 4 5  Z^Z50 L^L50 K^K50 A^A50 F=0.0000000
SML_STEP    5 6
TLINP_T2 6 7  Z^ZW L^L1 K^KW A^AW F=0.0000000
BIG_STEP    7 8
TLINP_T3 8 9 Z^ZN L^L2 K^KN A^AN F=0
BIG_STEP 9 10
TLINP_T4 10 11 Z^ZW L^L3 K^KW A^AW F=0.0000000
BIG_STEP   11 12
TLINP_T5 12 13 Z^ZN L^L4 K^KN A^AN F=0.0000000
BIG_STEP  13 14
TLINP_T6 14 15 Z^ZW L^L5H K^KW A^AW F=0.0000000
DEF2P 1 15 HALF

HALF 1 2
HALF 3 2
DEF2P 1 3 FIL

!TLINP_T1 1 2  Z^Z50 L^L50 K^K50 A^A50 F=0.0000000
!TLINP_T2 2 3  Z^ZW L^L1 K^KW A^AW F=0.0000000
!TLINP_T3 3 4 Z^ZN L^L2 K^KN A^AN F=0
!TLINP_T4 4 5  Z^ZW L^L3 K^KW A^AW F=0.0000000
!TLINP_T5 5 6  Z^ZN L^L4 K^KN A^AN F=0.0000000
```

```
!TLINP_T6 6 7   Z^ZW L^L5H K^KW A^AW F=0.0000000

!DEF2P 1 7  HALF1


!HALF1 1 2
!HALF1 3 2
!DEF2P 1 3 NOSTEP

 RES 1 0 R^AC50
 DEF1P 1 TEST

FREQ
  SWEEP  0.5 12 .115
!STEP 5
OUT
 FIL DB[S21] GR1
 YBCO DB[S21] GR1
!SILVER DB[S21] GR1
!NOSTEP DB[S21] GR1

 FIL DB[S11] GR3
 YBCO DB[S11] GR3
!SILVER DB[S11] GR3


 FIL ANG[S21] GR2
 YBCO ANG[S21] GR2
!SILVER ANG[S21] GR2

 FIL ANG[S11] GR4
 YBCO ANG[S11] GR4
!SILVER ANG[S11] GR4

  FIL S21 SC2
  YBCO S21 SC2
  TEST RE[Z11] GR5

  FIL DB[S21] GR6
  YBCO DB[S21] GR6
GRID
 RANGE 0 12 1

!RANGE 7 9 .2
! GR6 -2 0 .5
OPT
RANGE 1 11
YBCO MODEL FIL
```

Appendix C

High-Loss Touchstone Model (5 dBm Input Power)

```
! MODEL OF THE YBCO FILTER FIT TO DATA USING LOSS AND LOSS TANGENT
! ALSO USING S2P FILE FOR 50 OHM TAPER K-CONNECTOR TO CPWG INTERFACE
! ALSO USING CONSTANT LOSS S-PAR FILE (ADJUST.S2P) TO CORRECT FOR
! CAL STANDARDS BEING AT ROOM TEMP (NOT DUNKED)
! USING LOW LOSS EQUATIONS FOR ALL ATTENUATIONS AS A FUNCTION OF LD AND
Sn
! BY DIMITRIOS ANTSOS (JULY 28, 1992)
! FILENAME REFERS TO (TRUE) POWER INTO FILTER
! FILTER USED IS LAST PACKAGED CPW FILTER LEFT



DIM
  LNG UM
  ANG RAD
VAR
  T = 77                                    !TEMPERATURE OF MEASUREMENT
  Tc = 83                                   !Critical Temperture of Sample
  LD# 100E-9 6.72e-07  5E-6                  !PENETRATION DEPTH FOR YBCO
  Sn #1E4  9776496. 1E8                     !Normal Conductivity of Sample
  e0 = 8.854E-12                            !Permittivity of free space
  AGn = 3e-12                               !Dimension Variable ( Narrow
Line )
  Gn = 1.255e5                              !Incremental Inductance Rule
Var (Narr
  AGw = 1e-10
  Gw = 1.7336e4
  AG5 = 2.5e-11
  G5 = 2.3501e4


  Z500 = 49.56
  ZN0  = 83.38
  ZW0  = 22.64

  KI #10 10.74451   18

  K500 = 12.52
  KN0  = 12.455
  KW0  = 12.49

  LI # 2000 2314.353 2800

  L50 # 1800 2375.978 2800          !# 4000  4335.155 4400
  L1  = 720.8
  L2  = 997.0
  L3  = 1369.7
  L4  = 761.2
  L5H = 924.0


  ACI0 #1E-10  1.03e-10 1E-6          ! COPPER LOSS OF INPUT TAPER
(=5.02
  ADI00 # 3E-4 0.000542 9e-3        ! = 3.3E-4
```

```
   TAND # 0 0.010000 .01

EQN

   ADN0 = 3.086E-4*TAND
   AD500 = 3.093E-4*TAND
   ADW0 = 3.089E-4*TAND

   ADI0 = ADI00*TAND          ! DIELECTRIC LOSS OF INPUT CPW 50 OHM TAPER


   LI1 = -LI

   AI    = ACI0  * FREQ**2 + ADI0 * FREQ


! Computation of exact loss for narrow line
!       Constants

   U0 = 4*PI*1e-7                  !Magnetic Permeability of vacuum
   f = FREQ*1e9                    !Frequency in Hz
   Sr = Sn*(T/Tc)**4               !Real Part of conductivity of YBCO
   Si = (1-(T/Tc)**4)/(2*PI*f*U0*LD**2)  !Imaginary Part of conductivity
   P =  ATAN(Si/Sr)-2*PI      !Angle of conductivity
   Th= PI/4-P/2                    !Auxiliary angle definition
   r = SQRT(SQR(Sr)+SQR(Si))       !Norm of conductivity
   c = 1/sqrt(e0*U0)               !Velocity of light

!       Narrow Line Parameters
   Vn= c/sqrt(KN0)                 !Phase velocity in line
   Bn= Gn*AGn*SQRT(2*PI*f*U0*r)    !Fudge Factors
   Cn= EXP(2*Bn*COS(Th))
   Dn= COS(2*Bn*SIN(Th))
   En= SIN(2*Bn*SIN(Th))
   Un= SQRT(SQR(Cn*Dn-1)+SQR(Cn*En))
   Wn= ATAN(Cn*En/(Cn*Dn-1))
   Fn= Bn/(AGn*r*Un)
   Mn= 2*Bn*SIN(Th)
   Nn= COS(PI/4+P/2-Wn)
   Rn= COS(Mn+PI/4+P/2-Wn)

   ReZn = -Fn*(Nn+Cn*Rn)           !Real Part of Internal Impedance /
Meter
   NIn= SIN(PI/4+P/2-Wn)
   RIn= SIN(Mn+PI/4+P/2-Wn)
   ImZn = -Fn*(NIn+Cn*RIn)
   LMn = ZN0/Vn+ImZn/(2*PI*f)
   CMN = 1/(ZN0*Vn)
! Zn = sqrt(LMn/CMn)
   RATn= ReZn/(2*PI*f*LMn)
   ANGn= 0.5*ATAN(RATn)
   Zn= sqrt(LMn/CMn)*sqrt(sqrt(1+SQR(RATn)))
! Zn2= sqrt(LMn/CMn)*sqrt(sqrt(1+SQR(RATn)))*cos(ANGn)
```

```
  ACN = (8.686e-6) *
(2*PI*f)*sqrt(LMn*CMn)*sqrt(sqrt(1+SQR(RATn)))*sin(ANGn)

  KN = LMn*CMn/(e0*u0)*sqrt(1+SQR(RATn))*SQR(cos(ANGn))

!       Wide Line Parameters
  Vw= c/sqrt(KW0)                  !Phase velocity in line
  Bw= Gw*AGw*SQRT(2*PI*f*U0*r)     !Fudge Factors
  Cw= EXP(2*Bw*COS(Th))
  Dw= COS(2*Bw*SIN(Th))
  Ew= SIN(2*Bw*SIN(Th))
  Uw= SQRT(SQR(Cw*Dw-1)+SQR(Cw*Ew))
  Ww= ATAN(Cw*Ew/(Cw*Dw-1))
  Fw= Bw/(AGw*r*Uw)
  Mw= 2*Bw*SIN(Th)
  Nw= COS(PI/4+P/2-Ww)
  Rw= COS(Mw+PI/4+P/2-Ww)

  ReZw =-Fw*(Nw+Cw*Rw)             !Real Part of Internal Impedance / Meter
  NIw= SIN(PI/4+P/2-Ww)
  RIw= SIN(Mw+PI/4+P/2-Ww)
  ImZw =-Fw*(NIw+Cw*RIw)
  LMw = ZW0/Vw+ImZw/(2*PI*f)
  CMw= 1/(ZW0*Vw)
! Zw = sqrt(LMw/CMw)
  RATw=  ReZw/(2*PI*f*LMw)
  ANGw= 0.5*ATAN(RATw)
  Zw= sqrt(LMw/CMw)*sqrt(sqrt(1+SQR(RATw)))
! Zw2= sqrt(LMw/CMw)*sqrt(sqrt(1+SQR(RATw)))*cos(ANGw)

  ACW = (8.686e-6) *
(2*PI*f)*sqrt(LMw*CMw)*sqrt(sqrt(1+SQR(RATw)))*sin(ANGw)

  KW = LMw*CMw/(e0*u0)*sqrt(1+SQR(RATw))*SQR(cos(ANGw))

!       50 Ohm Line Parameters
  V5= c/sqrt(K500)                 !Phase velocity in line
  B5= G5*AG5*SQRT(2*PI*f*U0*r)     !Fudge Factors
  C5= EXP(2*B5*COS(Th))
  D5= COS(2*B5*SIN(Th))
  E5= SIN(2*B5*SIN(Th))
  U5= SQRT(SQR(C5*D5-1)+SQR(C5*E5))
  W5= ATAN(C5*E5/(C5*D5-1))
  F5= B5/(AG5*r*U5)
  M5= 2*B5*SIN(Th)
  N5= COS(PI/4+P/2-W5)
  R5= COS(M5+PI/4+P/2-W5)

  ReZ5 =-F5*(N5+C5*R5)             !Real Part of Internal Impedance / Meter
  NI5= SIN(PI/4+P/2-W5)
  RI5= SIN(M5+PI/4+P/2-W5)
  ImZ5 =-F5*(NI5+C5*RI5)
  LM5 = Z500/V5+ImZ5/(2*PI*f)
  CM5 = 1/(Z500*V5)
! Z50 = sqrt(LM5/CM5)
```

```
  RAT5=  ReZ5/(2*PI*f*LM5)
  ANG5= 0.5*ATAN(RAT5)
  Z50= sqrt(LM5/CM5)*sqrt(sqrt(1+SQR(RAT5)))
! Z52= sqrt(LM5/CM5)*sqrt(sqrt(1+SQR(RAT5)))*cos(ANG5)

  AC50 = (8.686e-6) *
(2*PI*f)*sqrt(LM5*CM5)*sqrt(sqrt(1+SQR(RAT5)))*sin(ANG5)

  K50 = LM5*CM5/(e0*u0)*sqrt(1+SQR(RAT5))*SQR(cos(ANG5))



  A50  = AC50 + AD500 * FREQ
  AN   = ACN + ADN0 * FREQ
  AW   = ACW + ADW0 * FREQ

CKT
S2PA 1 2 0 costep1.s2p
DEF2P 1 2  BIG_STEP

S2PB 1 2 0 costep2.s2p
DEF2P 1 2 SML_STEP

S2PC 1 2 0  5dbm.s2p
DEF2P 1 2 YBCO_RAW

S2PD 1 2 0 adjust.s2p
DEF2P 1 2 ADJ

S2PE 1 2 0 hts_50.s2p
DEF2P 1 2 FIFTY

ADJ 1 2
YBCO_RAW 2 3
DEF2P 1 3 YBCO

TLINP 1 2 Z=50 L^LI K^KI A^AI F=0
TLINP 2 3 Z=50 L^LI1 K^KI  A=0 F=0
FIFTY 3 4
TLINP_T1 4 5  Z^Z50 L^L50 K^K50 A^A50 F=0.0000000
SML_STEP    5 6
TLINP_T2 6 7  Z^ZW L^L1 K^KW A^AW F=0.0000000
BIG_STEP    7 8
TLINP_T3 8 9 Z^ZN L^L2 K^KN A^AN F=0
BIG_STEP 9 10
TLINP_T4 10 11 Z^ZW L^L3 K^KW A^AW F=0.0000000
BIG_STEP   11 12
TLINP_T5 12 13 Z^ZN L^L4 K^KN A^AN F=0.0000000
BIG_STEP  13 14
TLINP_T6 14 15 Z^ZW L^L5H K^KW A^AW F=0.0000000
DEF2P 1 15 HALF

HALF 1 2
HALF 3 2
DEF2P 1 3 FIL
```

```
 !TLINP_T1 1 2  Z^Z50 L^L50 K^K50 A^A50 F=0.0000000
 !TLINP_T2 2 3  Z^ZW L^L1 K^KW A^AW F=0.0000000
 !TLINP_T3 3 4 Z^ZN L^L2 K^KN A^AN F=0
 !TLINP_T4 4 5  Z^ZW L^L3 K^KW A^AW F=0.0000000
 !TLINP_T5 5 6  Z^ZN L^L4 K^KN A^AN F=0.0000000
 !TLINP_T6 6 7   Z^ZW L^L5H K^KW A^AW F=0.0000000

 !DEF2P 1 7  HALF1


 !HALF1 1 2
 !HALF1 3 2
 !DEF2P 1 3 NOSTEP

  RES 1 0 R^Zn
  DEF1P 1 TEST1

 !RES 1 0 R^Z51
 !DEF1P 1 TEST2

 !RES 1 0 R^Z52
 !DEF1P 1 TEST3

 FREQ
   SWEEP  0.5 12 .115
 !STEP 5
 OUT
  FIL DB[S21] GR1
  YBCO DB[S21] GR1
 !SILVER DB[S21] GR1
 !NOSTEP DB[S21] GR1

  FIL DB[S11] GR3
  YBCO DB[S11] GR3
 !SILVER DB[S11] GR3


  FIL ANG[S21] GR2
  YBCO ANG[S21] GR2
 !SILVER ANG[S21] GR2

  FIL ANG[S11] GR4
  YBCO ANG[S11] GR4
 !SILVER ANG[S11] GR4

   FIL S21 SC2
   YBCO S21 SC2
   TEST1 RE[Z11] GR5
 ! TEST2 RE[Z11] GR5
 ! TEST3 RE[Z11] GR5

   FIL DB[S21] GR6
   YBCO DB[S21] GR6
 GRID
```

```
 RANGE 0 12 1

!RANGE 7 9 .2
! GR6 -2 0 .5
OPT
RANGE 1 11
YBCO MODEL FIL
```

Appendix D

New Model with Improved Conductivity Equation

```
! MODEL OF THE YBCO FILTER FIT TO DATA USING LOSS AND LOSS TANGENT
! ALSO USING S2P FILE FOR 50 OHM TAPER K-CONNECTOR TO CPWG INTERFACE
! ALSO USING CONSTANT LOSS S-PAR FILE (ADJUST.S2P) TO CORRECT FOR
! CAL STANDARDS BEING AT ROOM TEMP (NOT DUNKED)
! USING LOW LOSS EQUATIONS FOR ALL ATTENUATIONS AS A FUNCTION OF LD AND
Sn
! BY DIMITRIOS ANTSOS (JULY 28, 1992)
! FILENAME REFERS TO (TRUE) POWER INTO FILTER
! FILTER USED IS LAST PACKAGED CPW FILTER LEFT



DIM
  LNG UM
  ANG RAD
VAR
! T = 77                                    !TEMPERATURE OF MEASUREMENT
! Tc = 83                                   !Critical Temperture of Sample
  LD1 # .5    0.588172  .75                       !PENETRATION DEPTH FOR
YBCO
  Sn #1E4  9607145. 5E8                     !Normal Conductivity of Sample
  XN # 0.73 0.885900 .93                          !Percentage of normal
electron
  XW # .050 0.072625 .251                          !Function of H and T
  X5 # 0.08 0.092468 .281
  tau#1e-18 1.27e-11 1e-10                 !Collision Relaxation time
  e0 = 8.854E-12                            !Permittivity of free space
  AGn = 3e-12                               !Dimension Variable ( Narrow
Line )
  Gn = 1.255e5                              !Incremental Inductance Rule
Var (Narr
  AGw = 1e-10
  Gw = 1.7336e4
  AG5 = 2.5e-11
  G5 = 2.3501e4


  Z500 = 49.56
  ZN0  = 83.38
  ZW0  = 22.64

  KI #5  14.44599   25

  K500 = 12.52
  KN0  = 12.455
  KW0  = 12.49

  LI # 1000 2391.998 3000

  L50 # 1800 2561.258 2900          !# 4000  4335.155 4400
  L1  = 720.8
  L2  = 997.0
  L3  = 1369.7
  L4  = 761.2
  L5H = 924.0
```

```
  ACI0  #1E-10  4.10e-09 1E-6          ! COPPER LOSS OF INPUT
  ADI00 # 3E-4 0.000707 9e-3         ! = 3.3E-4

  TAND  # 0 0.010000 .01

EQN
  LD = LD1*1e-6

  ADN0 = 3.086E-4*TAND
  AD500 = 3.093E-4*TAND
  ADW0 = 3.089E-4*TAND

  ADI0 = ADI00*TAND          ! DIELECTRIC LOSS OF INPUT CPW 50 OHM TAPER


  LI1 = -LI

  AI    = ACI0  * FREQ**2 + ADI0 * FREQ


! Computation of exact loss for narrow line
!       Constants

  U0 = 4*PI*1e-7                  !Magnetic Permeability of vacuum
  f = FREQ*1e9                    !Frequency in Hz
  SrN = Sn*XN                       !Real Part of conductivity of YBCO
  SiNa = (1-XN)/(2*PI*f*U0*LD**2)+XN*Sn*2*PI*f*tau
                                  !Imaginary Part of conductivity
  SrW = Sn*XW                       !Real Part of conductivity of YBCO
  SiW = (1-XW)/(2*PI*f*U0*LD**2)+XW*Sn*2*PI*f*tau
                                  !Imaginary Part of conductivity
  Sr5 = Sn*X5                       !Real Part of conductivity of YBCO
  Si5 = (1-X5)/(2*PI*f*U0*LD**2)+X5*Sn*2*PI*f*tau
                                  !Imaginary Part of conductivity
  PN =  ATAN(SiNa/SrN)-2*PI          !Angle of conductivity
  ThN= PI/4-PN/2                   !Auxiliary angle definition
  rNa= SQRT(SQR(SrN)+SQR(SiNa))      !Norm of conductivity
  PW =  ATAN(SiW/SrW)-2*PI          !Angle of conductivity
  ThW= PI/4-PW/2                   !Auxiliary angle definition
  rWi= SQRT(SQR(SrW)+SQR(SiW))      !Norm of conductivity
  P5 =  ATAN(Si5/Sr5)-2*PI          !Angle of conductivity
  Th5= PI/4-P5/2                   !Auxiliary angle definition
  r50= SQRT(SQR(Sr5)+SQR(Si5))      !Norm of conductivity
  c = 1/sqrt(e0*U0)               !Velocity of light

!       Narrow Line Parameters
  Vn= c/sqrt(KN0)                 !Phase velocity in line
  Bn= Gn*AGn*SQRT(2*PI*f*U0*rNa)   !Fudge Factors
  Cn= EXP(2*Bn*COS(ThN))
  Dn= COS(2*Bn*SIN(ThN))
  En= SIN(2*Bn*SIN(ThN))
  Un= SQRT(SQR(Cn*Dn-1)+SQR(Cn*En))
  Wn= ATAN(Cn*En/(Cn*Dn-1))
```

```
   Fn= Bn/(AGn*rNa*Un)
   Mn= 2*Bn*SIN(ThN)
   Nn= COS(PI/4+PN/2-Wn)
   Rn= COS(Mn+PI/4+PN/2-Wn)

   ReZn = -Fn*(Nn+Cn*Rn)          !Real Part of Internal Impedance /
Meter
   NIn= SIN(PI/4+PN/2-Wn)
   RIn= SIN(Mn+PI/4+PN/2-Wn)
   ImZn = -Fn*(NIn+Cn*RIn)
   LMn = ZN0/Vn+ImZn/(2*PI*f)
   CMN = 1/(ZN0*Vn)
   Zn = sqrt(LMn/CMn)
   RATn= ReZn/(2*PI*f*LMn)
   ANGn= 0.5*ATAN(RATn)

   ACN = (8.686e-6) *
(2*PI*f)*sqrt(LMn*CMn)*sqrt(sqrt(1+SQR(RATn)))*sin(ANGn)

   KN = LMn*CMn/(e0*u0)*sqrt(1+SQR(RATn))*SQR(cos(ANGn))

!       Wide Line Parameters
   Vw= c/sqrt(KW0)                !Phase velocity in line
   Bw= Gw*AGw*SQRT(2*PI*f*U0*rWi)    !Fudge Factors
   Cw= EXP(2*Bw*COS(ThW))
   Dw= COS(2*Bw*SIN(ThW))
   Ew= SIN(2*Bw*SIN(ThW))
   Uw= SQRT(SQR(Cw*Dw-1)+SQR(Cw*Ew))
   Ww= ATAN(Cw*Ew/(Cw*Dw-1))
   Fw= Bw/(AGw*rWi*Uw)
   Mw= 2*Bw*SIN(ThW)
   Nw= COS(PI/4+PW/2-Ww)
   Rw= COS(Mw+PI/4+PW/2-Ww)

   ReZw =-Fw*(Nw+Cw*Rw)           !Real Part of Internal Impedance / Meter
   NIw= SIN(PI/4+PW/2-Ww)
   RIw= SIN(Mw+PI/4+PW/2-Ww)
   ImZw =-Fw*(NIw+Cw*RIw)
   LMw = ZW0/Vw+ImZw/(2*PI*f)
   CMw= 1/(ZW0*Vw)
   Zw = sqrt(LMw/CMw)
   RATw=  ReZw/(2*PI*f*LMw)
   ANGw= 0.5*ATAN(RATw)

   ACW = (8.686e-6) *
(2*PI*f)*sqrt(LMw*CMw)*sqrt(sqrt(1+SQR(RATw)))*sin(ANGw)

   KW = LMw*CMw/(e0*u0)*sqrt(1+SQR(RATw))*SQR(cos(ANGw))

!       50 Ohm Line Parameters
   V5= c/sqrt(K500)               !Phase velocity in line
   B5= G5*AG5*SQRT(2*PI*f*U0*r50)    !Fudge Factors
   C5= EXP(2*B5*COS(Th5))
   D5= COS(2*B5*SIN(Th5))
   E5= SIN(2*B5*SIN(Th5))
```

```
  U5= SQRT(SQR(C5*D5-1)+SQR(C5*E5))
  W5= ATAN(C5*E5/(C5*D5-1))
  F5= B5/(AG5*r50*U5)
  M5= 2*B5*SIN(Th5)
  N5= COS(PI/4+P5/2-W5)
  R5= COS(M5+PI/4+P5/2-W5)

  ReZ5 =-F5*(N5+C5*R5)          !Real Part of Internal Impedance / Meter
  NI5= SIN(PI/4+P5/2-W5)
  RI5= SIN(M5+PI/4+P5/2-W5)
  ImZ5 =-F5*(NI5+C5*RI5)
  LM5 = Z500/V5+ImZ5/(2*PI*f)
  CM5 = 1/(Z500*V5)
  Z50 = sqrt(LM5/CM5)
  RAT5=  ReZ5/(2*PI*f*LM5)
  ANG5= 0.5*ATAN(RAT5)

  AC50 = (8.686e-6) *
(2*PI*f)*sqrt(LM5*CM5)*sqrt(sqrt(1+SQR(RAT5)))*sin(ANG5)

  K50 = LM5*CM5/(e0*u0)*sqrt(1+SQR(RAT5))*SQR(cos(ANG5))



  A50  = AC50 + AD500 * FREQ
  AN   = ACN + ADN0 * FREQ
  AW   = ACW + ADW0 * FREQ

CKT
S2PA 1 2 0 costep1.s2p
DEF2P 1 2  BIG_STEP

S2PB 1 2 0 costep2.s2p
DEF2P 1 2 SML_STEP

S2PC 1 2 0  5dbm.s2p
DEF2P 1 2 YBCO_RAW

S2PD 1 2 0 adjust.s2p
DEF2P 1 2 ADJ

S2PE 1 2 0 hts_50.s2p
DEF2P 1 2 FIFTY

ADJ 1 2
YBCO_RAW 2 3
DEF2P 1 3 YBCO

TLINP 1 2 Z=50 L^LI K^KI A^AI F=0
TLINP 2 3 Z=50 L^LI1 K^KI  A=0 F=0
FIFTY 3 4
TLINP_T1 4 5  Z^Z50 L^L50 K^K50 A^A50 F=0.0000000
SML_STEP    5 6
TLINP_T2 6 7  Z^ZW L^L1 K^KW A^AW F=0.0000000
BIG_STEP    7 8
```

```
TLINP_T3 8 9 Z^ZN L^L2 K^KN A^AN F=0
BIG_STEP 9 10
TLINP_T4 10 11 Z^ZW L^L3 K^KW A^AW F=0.0000000
BIG_STEP   11 12
TLINP_T5 12 13 Z^ZN L^L4 K^KN A^AN F=0.0000000
BIG_STEP  13 14
TLINP_T6 14 15 Z^ZW L^L5H K^KW A^AW F=0.0000000
DEF2P 1 15 HALF

HALF 1 2
HALF 3 2
DEF2P 1 3 FIL

!TLINP_T1 1 2  Z^Z50 L^L50 K^K50 A^A50 F=0.0000000
!TLINP_T2 2 3  Z^ZW L^L1 K^KW A^AW F=0.0000000
!TLINP_T3 3 4 Z^ZN L^L2 K^KN A^AN F=0
!TLINP_T4 4 5  Z^ZW L^L3 K^KW A^AW F=0.0000000
!TLINP_T5 5 6  Z^ZN L^L4 K^KN A^AN F=0.0000000
!TLINP_T6 6 7   Z^ZW L^L5H K^KW A^AW F=0.0000000

!DEF2P 1 7  HALF1


!HALF1 1 2
!HALF1 3 2
!DEF2P 1 3 NOSTEP

 RES 1 0 R^Zn
 DEF1P 1 TEST

FREQ
  SWEEP  0.5 12 .115
!STEP 2
OUT
 FIL DB[S21] GR1
 YBCO DB[S21] GR1
!SILVER DB[S21] GR1
!NOSTEP DB[S21] GR1

 FIL DB[S11] GR3
 YBCO DB[S11] GR3
!SILVER DB[S11] GR3


 FIL ANG[S21] GR2
 YBCO ANG[S21] GR2
!SILVER ANG[S21] GR2

 FIL ANG[S11] GR4
 YBCO ANG[S11] GR4
!SILVER ANG[S11] GR4

  FIL S21 SC2
  YBCO S21 SC2
  TEST RE[Z11] GR5
```

```
! FIL DB[S21] GR6
! YBCO DB[S21] GR6
GRID
 RANGE 0 12 1

!RANGE 7 9 .2
! GR6 -2 0 .5
OPT
RANGE  1  11
YBCO MODEL FIL
```

Appendix E

Touchstone Circuit File that Verifies the Conjecture of Section 7.5.4

```
! MODEL OF THE YBCO FILTER FIT TO DATA USING LOSS AND LOSS TANGENT
! ALSO USING S2P FILE FOR 50 OHM TAPER K-CONNECTOR TO CPWG INTERFACE
! ALSO USING CONSTANT LOSS S-PAR FILE (ADJUST.S2P) TO CORRECT FOR
! CAL STANDARDS BEING AT ROOM TEMP (NOT DUNKED)
! USING LOW LOSS EQUATIONS FOR ALL ATTENUATIONS AS A FUNCTION OF LD AND
Sn
! BY DIMITRIOS ANTSOS (JULY 28, 1992)
! FILENAME REFERS TO (TRUE) POWER INTO FILTER
! FILTER USED IS LAST PACKAGED CPW FILTER LEFT
! ALL Z's AND AG, G OPTIMIZED

DIM
  LNG UM
  ANG RAD
VAR
  LD1 # .5    0.749436  .75                    !PENETRATION DEPTH FOR
YBCO
  Sn #1E4  9.22e+07 5E8                  !Normal Conductivity of Sample
  XN # 0.73 0.929888 .93                        !Percentage of normal
electrons
  XW # .05 0.077046 .25                        !Function of H and T
  X5 # .08 0.105440 .28
  tau#1e-18 2.28e-13 1e-10              !Collision Relaxation time
  e0 = 8.854E-12                         !Permittivity of free space
  AGn #1e-14 1.03e-12 3e-9          != 3e-12   !Dimension
  Gn  #1e2 634085.0 1e8         != 1.255e5   ! Icremental Induc
  AGw #1e-12 1.00e-08 1e-8             != 1e-10
  Gw #1e1 77356.57 1e7              != 1.7336e4
  AG5 #2.5e-13 2.42e-08 2.5e-8         != 2.5e-11
  G5 #2.5e1  37.64339 2.3e7             ! 2.3501e4


  Z500 # 40  50.17075  190                    != 49.56
  ZN0  #75 114.7819     250                     ! = 83.38
  ZW0  #20 23.93472      150                   != 22.64

  KI #5  24.99001   25

  K500 = 12.52
  KN0  = 12.455
  KW0  = 12.49

  LI # 1500 2178.428 2900

  L50 # 1800 2664.809 2900          !# 4000  4335.155 4400
  L1  = 720.8
  L2  = 997.0
  L3  = 1369.7
  L4  = 761.2
  L5H = 924.0


  ACI0  #1E-10  1.47e-09 1E-6          ! COPPER LOSS OF INPUT
  ADI00 # 3E-4 0.005616 9e-3        ! = 3.3E-4
```

```
  TAND  # 0 0.006364 .01

EQN
  LD = LD1*1e-6

  ADN0 = 3.086E-4*TAND
  AD500 = 3.093E-4*TAND
  ADW0 = 3.089E-4*TAND

  ADI0 = ADI00*TAND          ! DIELECTRIC LOSS OF INPUT CPW 50 OHM TAPER


  LI1 = -LI

  AI    = ACI0  * FREQ**2 + ADI0 * FREQ


! Computation of exact loss for narrow line
!       Constants

  U0 = 4*PI*1e-7                  !Magnetic Permeability of vacuum
  f = FREQ*1e9                    !Frequency in Hz
  SrN = Sn*XN                       !Real Part of conductivity of YBCO
  SiNa = (1-XN)/(2*PI*f*U0*LD**2)+XN*Sn*2*PI*f*tau
                                  !Imaginary Part of conductivity
  SrW = Sn*XW                       !Real Part of conductivity of YBCO
  SiW = (1-XW)/(2*PI*f*U0*LD**2)+XW*Sn*2*PI*f*tau
                                  !Imaginary Part of conductivity
  Sr5 = Sn*X5                       !Real Part of conductivity of YBCO
  Si5 = (1-X5)/(2*PI*f*U0*LD**2)+X5*Sn*2*PI*f*tau
                                  !Imaginary Part of conductivity
  PN =  ATAN(SiNa/SrN)-2*PI           !Angle of conductivity
  ThN= PI/4-PN/2                    !Auxiliary angle definition
  rNa= SQRT(SQR(SrN)+SQR(SiNa))      !Norm of conductivity
  PW =  ATAN(SiW/SrW)-2*PI           !Angle of conductivity
  ThW= PI/4-PW/2                    !Auxiliary angle definition
  rWi= SQRT(SQR(SrW)+SQR(SiW))       !Norm of conductivity
  P5 =  ATAN(Si5/Sr5)-2*PI           !Angle of conductivity
  Th5= PI/4-P5/2                    !Auxiliary angle definition
  r50= SQRT(SQR(Sr5)+SQR(Si5))       !Norm of conductivity
  c = 1/sqrt(e0*U0)               !Velocity of light

!       Narrow Line Parameters
  Vn= c/sqrt(KN0)                 !Phase velocity in line
  Bn= Gn*AGn*SQRT(2*PI*f*U0*rNa)    !Fudge Factors
  Cn= EXP(2*Bn*COS(ThN))
  Dn= COS(2*Bn*SIN(ThN))
  En= SIN(2*Bn*SIN(ThN))
  Un= SQRT(SQR(Cn*Dn-1)+SQR(Cn*En))
  Wn= ATAN(Cn*En/(Cn*Dn-1))
  Fn= Bn/(AGn*rNa*Un)
  Mn= 2*Bn*SIN(ThN)
  Nn= COS(PI/4+PN/2-Wn)
  Rn= COS(Mn+PI/4+PN/2-Wn)
```

```
  ReZn = -Fn*(Nn+Cn*Rn)          !Real Part of Internal Impedance /
Meter
  NIn= SIN(PI/4+PN/2-Wn)
  RIn= SIN(Mn+PI/4+PN/2-Wn)
  ImZn = -Fn*(NIn+Cn*RIn)
  LMn = ZN0/Vn+ImZn/(2*PI*f)
  CMN = 1/(ZN0*Vn)
  Zn = sqrt(LMn/CMn)
  RATn= ReZn/(2*PI*f*LMn)
  ANGn= 0.5*ATAN(RATn)

  ACN = (8.686e-6) *
(2*PI*f)*sqrt(LMn*CMn)*sqrt(sqrt(1+SQR(RATn)))*sin(ANGn)

  KN = LMn*CMn/(e0*u0)*sqrt(1+SQR(RATn))*SQR(cos(ANGn))

!      Wide Line Parameters
  Vw= c/sqrt(KW0)                !Phase velocity in line
  Bw= Gw*AGw*SQRT(2*PI*f*U0*rWi)   !Fudge Factors
  Cw= EXP(2*Bw*COS(ThW))
  Dw= COS(2*Bw*SIN(ThW))
  Ew= SIN(2*Bw*SIN(ThW))
  Uw= SQRT(SQR(Cw*Dw-1)+SQR(Cw*Ew))
  Ww= ATAN(Cw*Ew/(Cw*Dw-1))
  Fw= Bw/(AGw*rWi*Uw)
  Mw= 2*Bw*SIN(ThW)
  Nw= COS(PI/4+PW/2-Ww)
  Rw= COS(Mw+PI/4+PW/2-Ww)

  ReZw =-Fw*(Nw+Cw*Rw)           !Real Part of Internal Impedance / Meter
  NIw= SIN(PI/4+PW/2-Ww)
  RIw= SIN(Mw+PI/4+PW/2-Ww)
  ImZw =-Fw*(NIw+Cw*RIw)
  LMw = ZW0/Vw+ImZw/(2*PI*f)
  CMw= 1/(ZW0*Vw)
  Zw = sqrt(LMw/CMw)
  RATw=  ReZw/(2*PI*f*LMw)
  ANGw= 0.5*ATAN(RATw)

  ACW = (8.686e-6) *
(2*PI*f)*sqrt(LMw*CMw)*sqrt(sqrt(1+SQR(RATw)))*sin(ANGw)

  KW = LMw*CMw/(e0*u0)*sqrt(1+SQR(RATw))*SQR(cos(ANGw))

!      50 Ohm Line Parameters
  V5= c/sqrt(K500)               !Phase velocity in line
  B5= G5*AG5*SQRT(2*PI*f*U0*r50)   !Fudge Factors
  C5= EXP(2*B5*COS(Th5))
  D5= COS(2*B5*SIN(Th5))
  E5= SIN(2*B5*SIN(Th5))
  U5= SQRT(SQR(C5*D5-1)+SQR(C5*E5))
  W5= ATAN(C5*E5/(C5*D5-1))
  F5= B5/(AG5*r50*U5)
  M5= 2*B5*SIN(Th5)
  N5= COS(PI/4+P5/2-W5)
```

```
  R5= COS(M5+PI/4+P5/2-W5)

  ReZ5 =-F5*(N5+C5*R5)          !Real Part of Internal Impedance / Meter
  NI5= SIN(PI/4+P5/2-W5)
  RI5= SIN(M5+PI/4+P5/2-W5)
  ImZ5 =-F5*(NI5+C5*RI5)
  LM5 = Z500/V5+ImZ5/(2*PI*f)
  CM5 = 1/(Z500*V5)
  Z50 = sqrt(LM5/CM5)
  RAT5=  ReZ5/(2*PI*f*LM5)
  ANG5= 0.5*ATAN(RAT5)

  AC50 = (8.686e-6) *
(2*PI*f)*sqrt(LM5*CM5)*sqrt(sqrt(1+SQR(RAT5)))*sin(ANG5)

  K50 = LM5*CM5/(e0*u0)*sqrt(1+SQR(RAT5))*SQR(cos(ANG5))



  A50  = AC50 + AD500 * FREQ
  AN   = ACN + ADN0 * FREQ
  AW   = ACW + ADW0 * FREQ

CKT
S2PA 1 2 0 costep1.s2p
DEF2P 1 2  BIG_STEP

S2PB 1 2 0 costep2.s2p
DEF2P 1 2 SML_STEP

S2PC 1 2 0  5dbm.s2p
DEF2P 1 2 YBCO_RAW

S2PD 1 2 0 adjust.s2p
DEF2P 1 2 ADJ

S2PE 1 2 0 hts_50.s2p
DEF2P 1 2 FIFTY

ADJ 1 2
YBCO_RAW 2 3
DEF2P 1 3 YBCO

TLINP 1 2 Z=50 L^LI K^KI A^AI F=0
TLINP 2 3 Z=50 L^LI1 K^KI  A=0 F=0
FIFTY 3 4
TLINP_T1 4 5  Z^Z50 L^L50 K^K50 A^A50 F=0.0000000
SML_STEP    5 6
TLINP_T2 6 7  Z^ZW L^L1 K^KW A^AW F=0.0000000
BIG_STEP    7 8
TLINP_T3 8 9 Z^ZN L^L2 K^KN A^AN F=0
BIG_STEP 9 10
TLINP_T4 10 11 Z^ZW L^L3 K^KW A^AW F=0.0000000
BIG_STEP   11 12
TLINP_T5 12 13 Z^ZN L^L4 K^KN A^AN F=0.0000000
```

```
BIG_STEP  13 14
TLINP_T6 14 15 Z^ZW L^L5H K^KW A^AW F=0.0000000
DEF2P 1 15 HALF

HALF 1 2
HALF 3 2
DEF2P 1 3 FIL

!TLINP_T1 1 2  Z^Z50 L^L50 K^K50 A^A50 F=0.0000000
!TLINP_T2 2 3  Z^ZW L^L1 K^KW A^AW F=0.0000000
!TLINP_T3 3 4 Z^ZN L^L2 K^KN A^AN F=0
!TLINP_T4 4 5  Z^ZW L^L3 K^KW A^AW F=0.0000000
!TLINP_T5 5 6  Z^ZN L^L4 K^KN A^AN F=0.0000000
!TLINP_T6 6 7   Z^ZW L^L5H K^KW A^AW F=0.0000000

!DEF2P 1 7  HALF1


!HALF1 1 2
!HALF1 3 2
!DEF2P 1 3 NOSTEP

 RES 1 0 R^Zn
 DEF1P 1 TEST

FREQ
  SWEEP  0.5 12 .115
!STEP 2
OUT
 FIL DB[S21] GR1
 YBCO DB[S21] GR1
!SILVER DB[S21] GR1
!NOSTEP DB[S21] GR1

 FIL DB[S11] GR3
 YBCO DB[S11] GR3
!SILVER DB[S11] GR3


 FIL ANG[S21] GR2
 YBCO ANG[S21] GR2
!SILVER ANG[S21] GR2

 FIL ANG[S11] GR4
 YBCO ANG[S11] GR4
!SILVER ANG[S11] GR4

  FIL S21 SC2
  YBCO S21 SC2
  TEST RE[Z11] GR5

! FIL DB[S21] GR6
! YBCO DB[S21] GR6
GRID
 RANGE 0 12 1
```

```
!RANGE 7 9 .2
! GR6 -2 0 .5
OPT
RANGE  1  11
YBCO MODEL FIL
```

CHAPTER 8

CLOSED RECTANGULAR HTS WAVEGUIDES

8.1 Introduction

This chapter is motivated by a question posed to me by Dr. Charles Elachi of JPL, during my oral candidacy examination. He inquired about the viability and usefulness of HTS waveguides. In the analysis that follows, closed rectangular HTS waveguides are assumed and the analysis concentrates on the Transverse Electric propagation mode of order (1,0) (TE10). This is because TE10, the lowest order mode (the one with the lowest cut-off frequency), is the most widely used one for transfer of power in real-life applications. A software program, presented below, using C language and incorporating many Fortran routines, has been created as a tool in accurately calculating the fundamental propagation parameters, fields and currents of arbitrary modes in waveguides of different sizes and material properties. The cross-section of a typical waveguide to be analyzed is shown in figure 1. It is beyond the scope of this chapter to address how a structure like the one shown in figure 1 could be fabricated, although fabrication should be possible. The cross-section shown in figure 1 is that of a regular closed rectangular metallic waveguide, the inside of which has been uniformly covered with a layer of HTS (possibly YBCO). The cross-hatched part in figure 1 is the metal and the single hatched part is the HTS layer. This layer is assumed

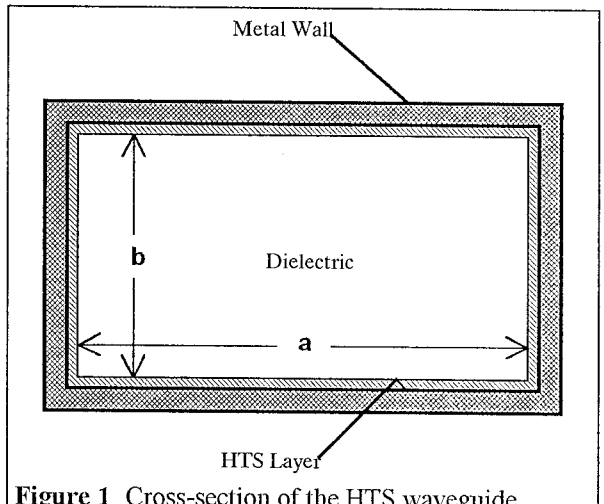

Figure 1 Cross-section of the HTS waveguide.

to be of thickness d, where $\frac{d}{\lambda} >> 1$ (actually $\frac{d}{\lambda} > 5$ should be sufficient for the desired boundary conditions to hold; see discussion at the end of section 3.3).

Some of the questions addressed in this chapter are, is there an advantage to using HTS waveguides over regular waveguides and if so when, what do the propagation characteristics of HTS waveguides look like and how high input-power can be applied before getting into trouble attributable to the nature of the HTS.

8.2 The Cross-Over Frequency

What I designate as the cross-over frequency, f_x, is defined as the frequency at which the surface resistance of a normal conductor is equal to that of an HTS. The normal conductor and the HTS can be at the same or at different temperatures. The cross-over frequency is independent of the geometry of the waveguide, and is rather a property of the material it is made of. It is a simple yet useful measure that can be used to determine whether it is advantageous or not, from a loss point of view, to use an HTS waveguide, since the losses in a waveguide, assuming a perfect dielectric filling, occur in the surface currents flowing in the walls, within a few skin-depths of the surface. As is demonstrated in equation (3.31), reproduced below for convenience, and in equation (1), the surface resistance of an HTS is proportional to the square of frequency whereas that of a normal metal is proportional to the square root of frequency [1].

$$Z_s = j\omega\mu_0\lambda_0\left(1 - j\frac{n_n}{2n_s}\omega\tau\right) = \frac{1}{2}\mu_0^{\,2}\omega^2\lambda_0^3\sigma_n\left(\frac{T}{T_c}\right)^4 + j\omega\mu_0\lambda_0 \equiv R_s + j\omega L_s \ , \qquad (3.31)$$

for an HTS and

$$Z_s = \sqrt{j\frac{2\pi f\mu_0}{\sigma}} = \sqrt{\frac{\pi f\mu_0}{\sigma}} + j\sqrt{\frac{\pi f\mu_0}{\sigma}} = R_s + jX_s \qquad (1)$$

for a normal conductor, where Z_S is the surface impedance, ω is the angular frequency of the excitation, μ_O is the magnetic permeability of vacuum, λ_O is the zero-temperature penetration depth of the electromagnetic fields in the HTS, n_n is the density of normal electrons in the HTS, n_s is the density of superconducting electrons in the HTS, τ is the electron collision relaxation time, σ_n is the normal conductivity of the HTS, T is the absolute temperature of the HTS, T_C is the critical temperature of the HTS, f is the frequency of the excitation and σ is the conductivity of the metal. Hence, in simplest terms, it is better to use a normal metal above the cross-over frequency and an HTS below the cross-over frequency. The equation for the cross-over frequency is easily derived by equating the real parts of equations (3.31) and (1) as

$$f_x = \frac{1}{\pi\mu_0\lambda_0^2}\left[4\sigma\sigma_n^2\left(\frac{T}{T_c}\right)^8\right]^{-\frac{1}{3}} . \qquad (2)$$

Table 1 shows a "worst", "average" and "best" case for the cross-over frequency with parameter values drawn from the discussions in chapters 3-7. In the worst case a "bad" HTS is compared to gold at 77 K. In the "best" case an "excellent" HTS is compared to an imaginary "hot", low conductivity metal. In the "average" case an HTS like the ones measured and described in chapters 3-7 is compared to gold at room temperature. In all of the cases the HTSs are assumed at the LN_2 temperature of 77 K.

Case...	λ_0 (nm)	σ (S/m)	σ_n (S/m)	T (K)	T_c (K)	f_x (GHz)
Best	140	10^7	$1.1*10^6$	77	90	5376
Average	430	$0.44*10^8$	$3*10^6$	77	87	163
Worst	800	$2*10^8$	$10*10^6$	77	85	12

Table 1 Three cases for the cross-over frequency

It is obvious from table 1 that the cross-over frequency is very sensitive to its parameters and spans a huge range (over 3 orders of magnitude) depending on their values. In the worst case, an X-band waveguide (WR90) is the highest frequency HTS waveguide that is less lossy than a corresponding metal one, whereas, in the best case an HTS waveguide is less lossy than the corresponding metal one in practically all frequencies.

However, the best and worst cases of table 1 are upper and lower limits that are rarely encountered in practice. Figures 2-4 are plots of the cross-over frequency versus zero-temperature penetration depth, critical temperature and normal conductivity, respectively, with the rest of the parameters kept at their average values (see table 1).

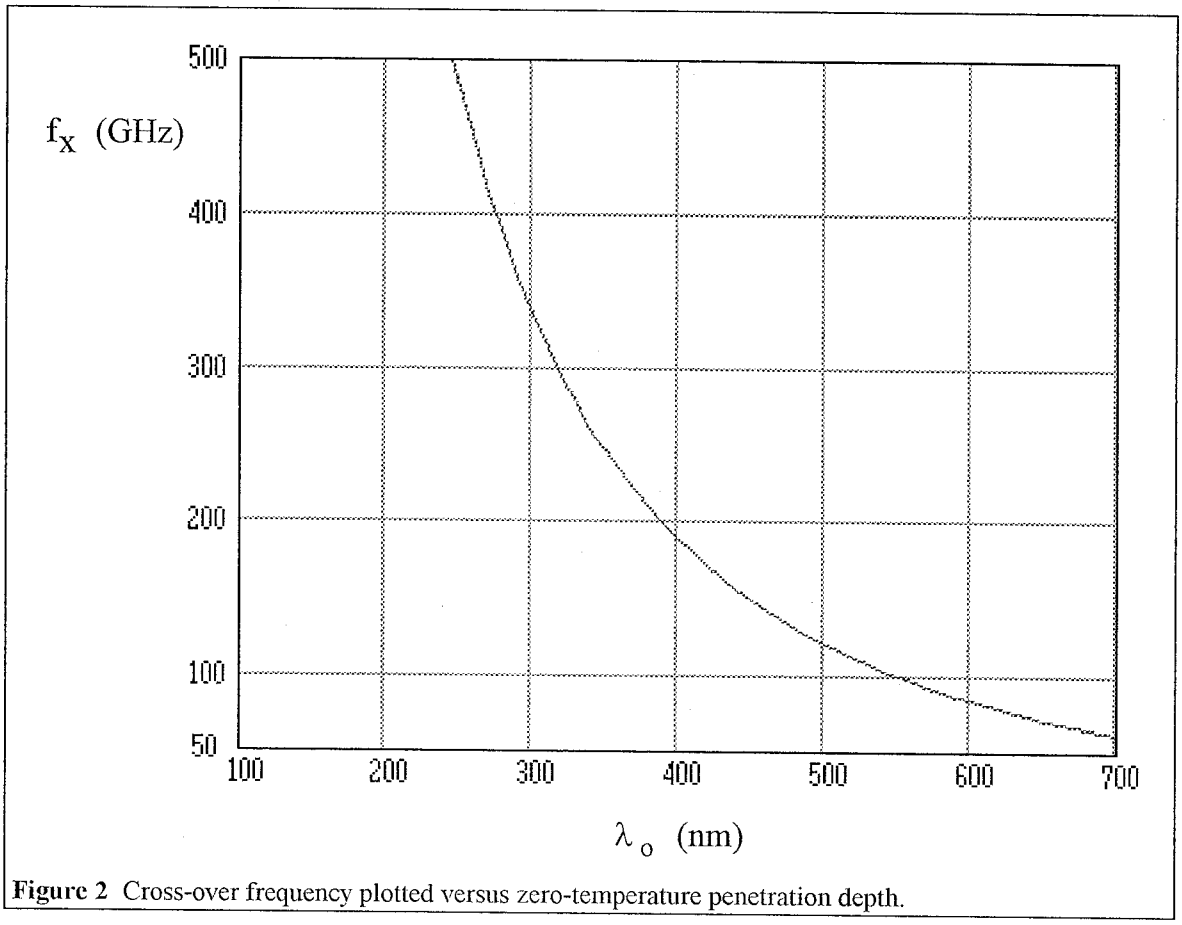

Figure 2 Cross-over frequency plotted versus zero-temperature penetration depth.

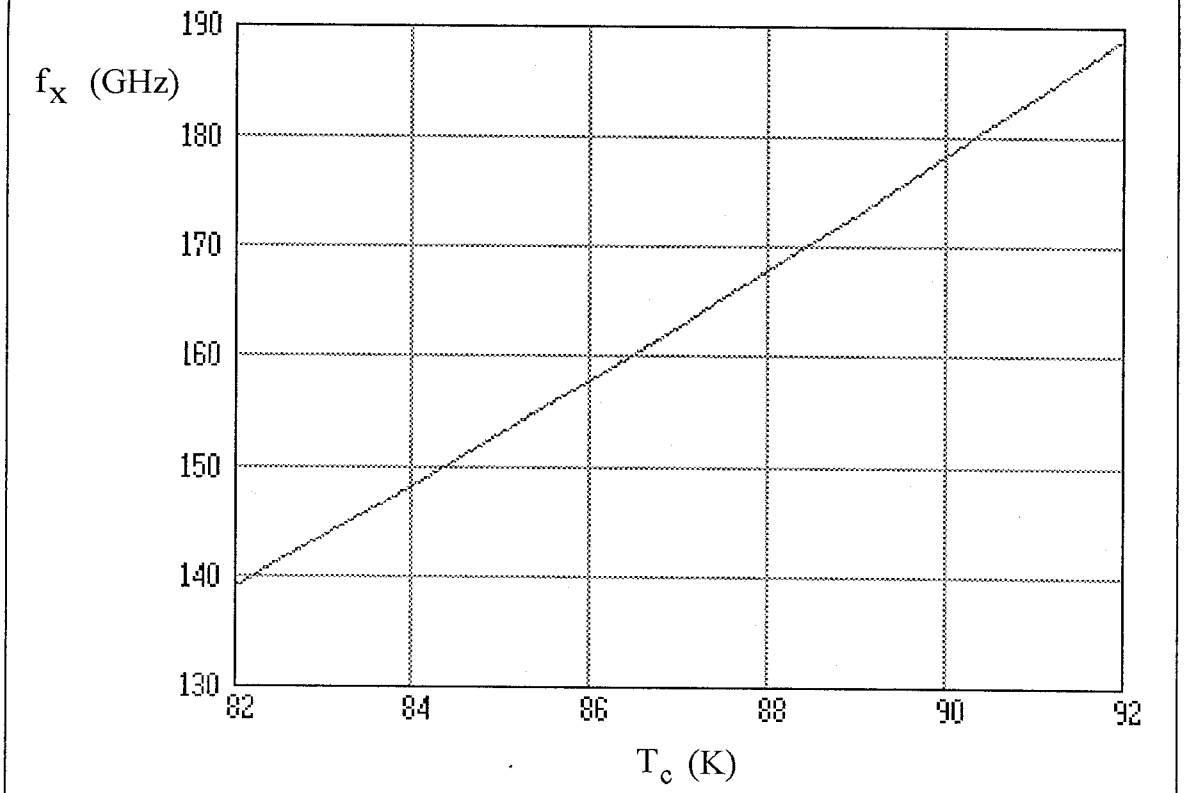

Figure 3 Cross-over frequency plotted versus critical temperature.

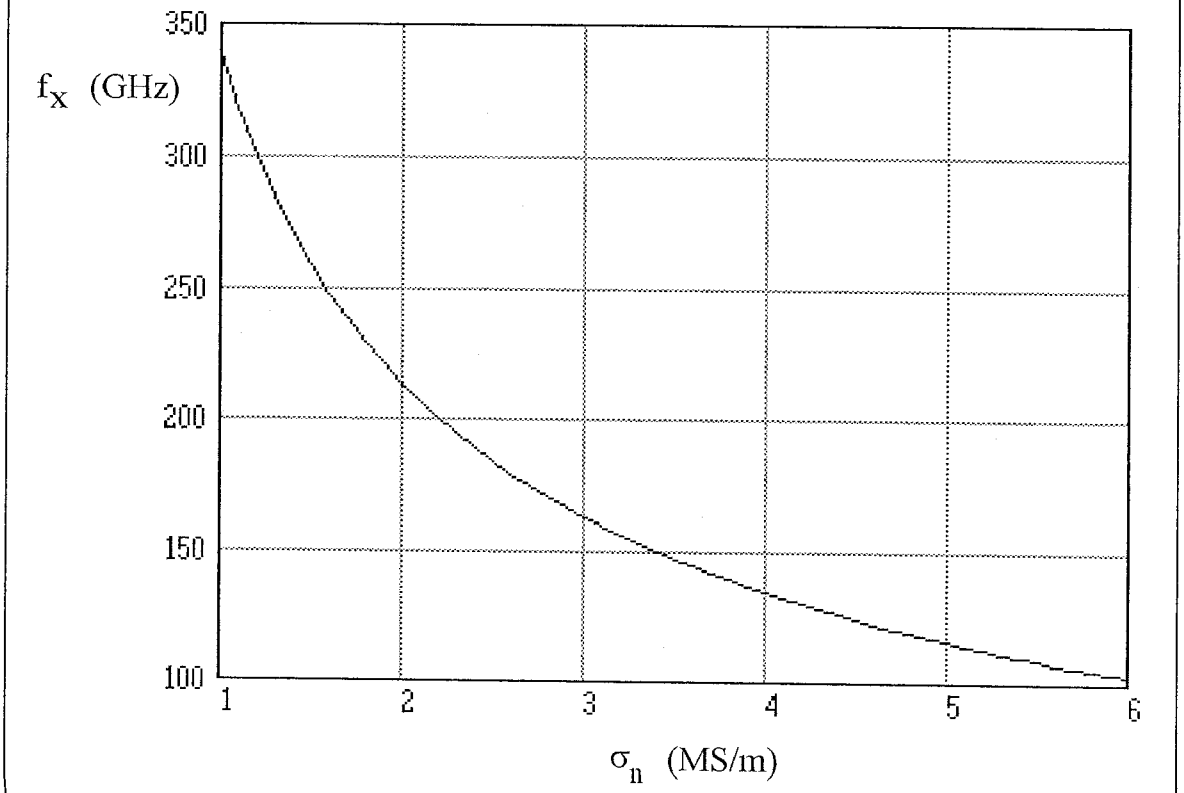

Figure 4 Cross-over frequency plotted versus normal conductivity.

Figures 2-4 were calculated and plotted using MathCAD. A print-out of the MathCAD file is included as appendix A of this chapter. Figures 2-4 bear out the fact that the average range of values of the cross-over frequency is not as extreme as table 1 indicates. In most cases the cross-over frequency will be found to lie between 100 and 300 GHz. Hence there is usually a number of waveguide types (up to WR10 and up to WR3 respectively) which will exhibit less loss if HTS walls are used.

8.3 A Contrast of the Exponential Attenuation of Normal and HTS Waveguides

In phasor notation, the electric and magnetic field solutions of the closed rectangular waveguide problem have a z-dependence and time dependence proportional to

$$e^{(j\omega t-\gamma z)} = e^{[j\omega t-(\alpha+j\beta)z]} = e^{-\alpha z}e^{j(\omega t-\beta z)} \tag{3}$$

where the positive z-axis is the longitudinal axis along which the energy propagates [1]. α, the exponential attenuation coefficient, is the reciprocal of the distance one has to move down the waveguide before the electric and magnetic fields are attenuated by a factor of e^{-1}. For the TE10 mode, the most commonly used mode of closed rectangular waveguides, the exponential attenuation coefficient is given by [1]

$$\alpha = \frac{R_s}{b\eta\sqrt{1-\left(\frac{f_c}{f}\right)^2}}\left[1+\frac{2b}{a}\left(\frac{f_c}{f}\right)^2\right] \tag{4}$$

where a and b are the width and height of the waveguide cross-section respectively ($a>b$ is needed; see figure 1), η is the impedance of the dielectric filling of the waveguide, R_S is the surface resistance of waveguide walls and f_C is the cutoff frequency of the TE10 mode. In the derivation of equation (4), a zero surface impedance (perfectly conducting walls) is first assumed, then the lossless fields are calculated and from these the exponential

attenuation coefficient is derived, given the surface resistance. In this sense, equation (4) is a first-order perturbation to the lossless field solution and is therefore expected to perform optimally for "small" surface impedances. Hence, at least for frequencies below the cross-over frequency, equation (4) should adequately model the behavior of an HTS waveguide with the surface resistance as given by equation (3.31), for reasonable parameter values.

Substituting the real part of (3.31) into (4) we obtain the expression for the exponential attenuation of an HTS waveguide as

$$\alpha = \frac{2\pi^2 \mu_0^2 \lambda_0^3 \sigma_n \left(\frac{T}{T_c}\right)^4}{b\eta} \cdot \frac{f^2 + \frac{2b}{a} f_c^2}{\sqrt{1-\left(\frac{f_c}{f}\right)^2}} \quad . \tag{5}$$

Equation (5) is plotted versus frequency in figure 5 for four different types of HTS waveguides (WR90, WR28, WR10 and WR5). Figure 5 also includes a plot of equation (4) for a gold waveguide, at room temperature, for comparison purposes. The vertical axis is normalized to one with respect to the exponential loss coefficient of a TEM wave propagating between two infinite parallel gold plates that are spaced a distance b apart at the cutoff frequency of each type of waveguide. The horizontal axis is normalized with respect to the cutoff frequency of each type of waveguide. Hence, with the above normalization conditions, the curve of the gold waveguide is the same for all of WR90, WR28, WR10 and WR5 types (since $b/a \approx 0.5$ for all of these types). The MathCAD file used to plot equations (4) and (5), as shown in figure 5, is included as appendix B of this chapter.

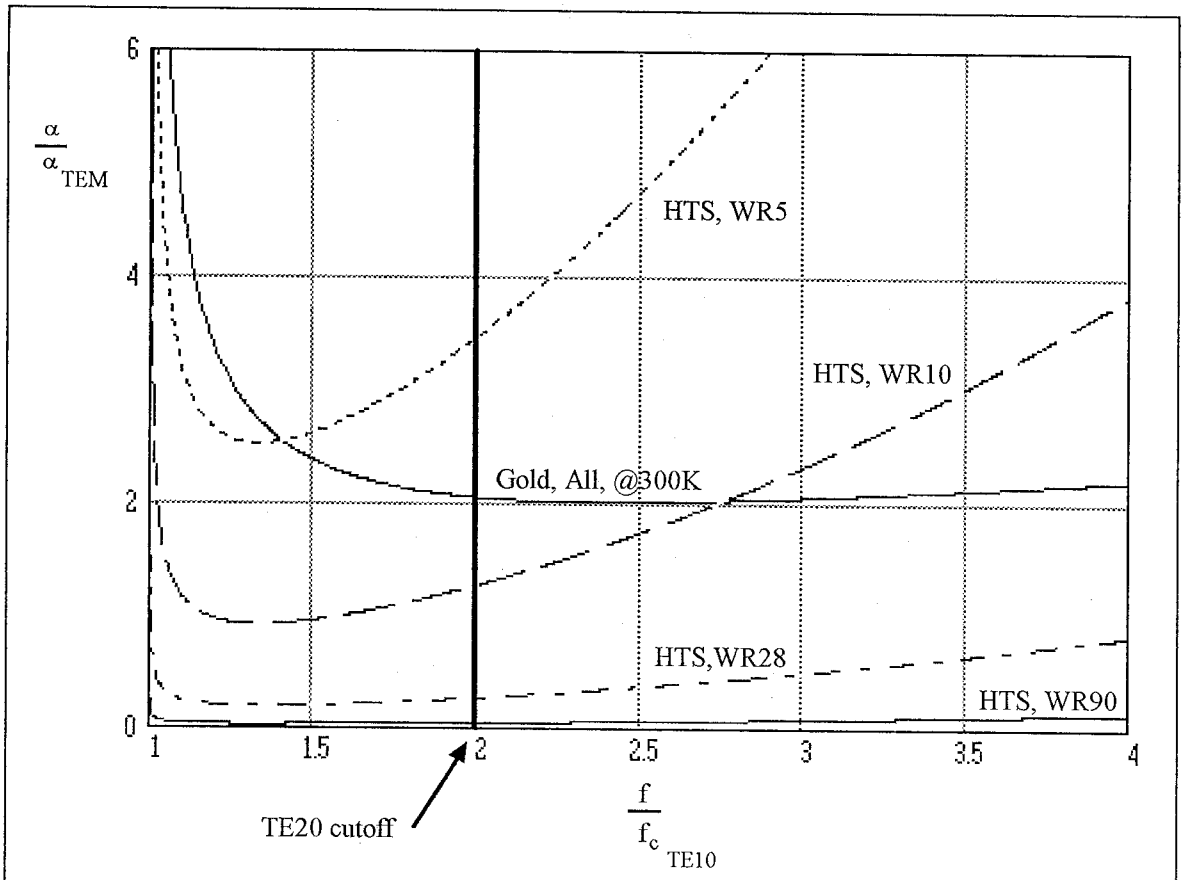

Figure 5 Normalized attenuation of different types of HTS and gold waveguide.

Table 2 lists the cutoff frequencies of the TE10 and TE20 modes of the types of waveguide considered above and in addition WR3 (considered later in the chapter). All of these waveguides for which $b/a \approx 0.5$ have $(f_c)_{TE20} = 2(f_c)_{TE10} \approx (f_c)_{TE01}$ (the exception is WR90 for which $\frac{b}{a} = \frac{4}{9}$, but this small deviation will be neglected). As expected, for the average set of parameters , it is advantageous, from the standpoint of loss, to use an HTS waveguide up to WR10 but not WR5 (see table 1). If we examine, as an example, the frequency at which the gold waveguide and the WR10 HTS waveguide loss curves cross, we read the corresponding normalized frequency as 2.75. Multiplying this by the

Type...	TE10 cutoff (GHz)	TE20 cutoff (GHz)
WR90	6.6	13.2
WR28	21.1	42.2
WR10	59.0	118.0
WR5	115.8	231.5
WR3	173.3	346.6

Table 2 Waveguide cutoff frequencies.

TE10 cutoff frequency of 59 GHz found in table 2 we obtain 162 GHz, which is the average case cross-over frequency, as expected (see table 1).

An advantage of HTS over metal waveguides is the location of the minimum loss frequency. In order to minimize distortion of the input signal as it travels in the waveguide, waveguides are almost always used in their single mode frequencies. Hence, the highest frequency that is recommended for use with a particular waveguide is just below the TE20 mode cutoff frequency. In figure 5 it can be seen that the minimum loss of metal waveguides is at a frequency higher than the TE20 cutoff frequency and hence cannot be used. In contrast, in HTS waveguides, the minimum loss lies below the TE20 cutoff frequency, an advantage not to be overlooked. A lower limit on the usable frequencies exists also, but is the same for HTS and metal waveguides, dictated by the TE10 cutoff frequency (it is not recommended to operate too close to the latter since the group velocity has a steep slope with respect to frequency and even a narrowband signal experiences high dispersion at these frequencies). The frequency of the minimum attenuation can be found by differentiating (5) with respect to frequency and setting the derivative equal to zero: It is given by

$$\frac{f_{\min}}{f_c} = \frac{1}{2}\sqrt{3+\sqrt{9+16\frac{b}{a}}} \quad . \tag{6}$$

In particular, for $b/a = 0.5$, we obtain $f_{\min} = \frac{1}{2}\sqrt{3+\sqrt{17}}\, f_c \approx 1.33 f_c < 2 f_c$, as claimed above. An equation for the minimum attenuation is obtained by substituting (6) into (5) as

$$\alpha_{\min} = \frac{\pi^2 \mu_0^2 \lambda_0^3 \sigma_n \left(\frac{T}{T_c}\right)^4}{2\sqrt{2}\,\eta b} f_c^2 \left(3+8\frac{b}{a}+\sqrt{9+16\frac{b}{a}}\right)\sqrt{\frac{3+4\frac{b}{a}+\sqrt{9+16\frac{b}{a}}}{1+2\frac{b}{a}}} \quad . \tag{7}$$

Equation (7) is plotted in figure 6 versus the width of the waveguide cross-section, a, assuming a constant ratio $b/a = 0.5$.

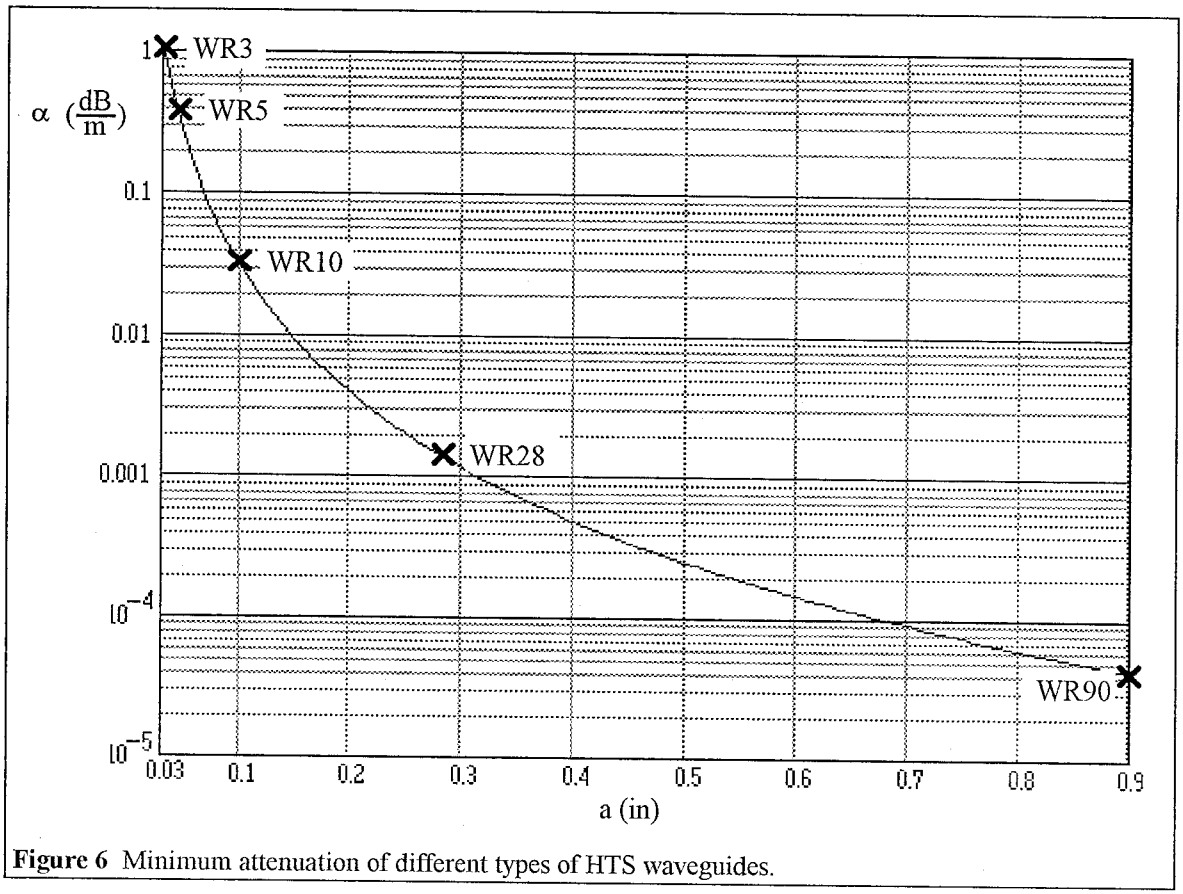

Figure 6 Minimum attenuation of different types of HTS waveguides.

8.4 A Finite-Difference Numerical Solution for the Modes of HTS Waveguides

8.4.1 The Problem

As mentioned in section 8.3, the exponential attenuation coefficient given by equations (4) and (5) is only a first-order perturbation approximation to the "true" value of the coefficient. In the derivation of equation (4), a zero surface impedance (perfectly conducting walls) is first assumed, then the lossless fields are calculated, and from these the exponential attenuation coefficient is derived, given the surface resistance [1]. In reality, of course, the walls have a finite surface impedance which affects the solution of the fields in the waveguide. Roughly speaking, one would expect the real part of the surface impedance, the surface resistance, to affect the exponential attenuation coefficient,

α, and the imaginary part of the surface impedance, the surface reactance, to affect the propagation constant, β, and the cutoff properties of the waveguide. However, this is not completely true, because the existence of a surface reactance, which affects the lossless solution of the fields, also indirectly affects the exponential attenuation coefficient, since, the fields and currents that dissipate energy at the walls are different in the presence of the surface reactance. Hence, α is expected to be a strong function of the surface resistance and a weak function of the surface reactance, whereas β is expected to be a strong function of the surface reactance and a weak function of the surface resistance. The question then becomes, how well does equation (5) represent the "true" exponential loss coefficient of an HTS waveguide?

To compound matters, in the case of HTSs, the complex surface impedance spans a wide range of arguments (angles) over the frequency range under consideration (1-300 GHz), whereas in the normal metal case, the argument of the complex surface impedance is

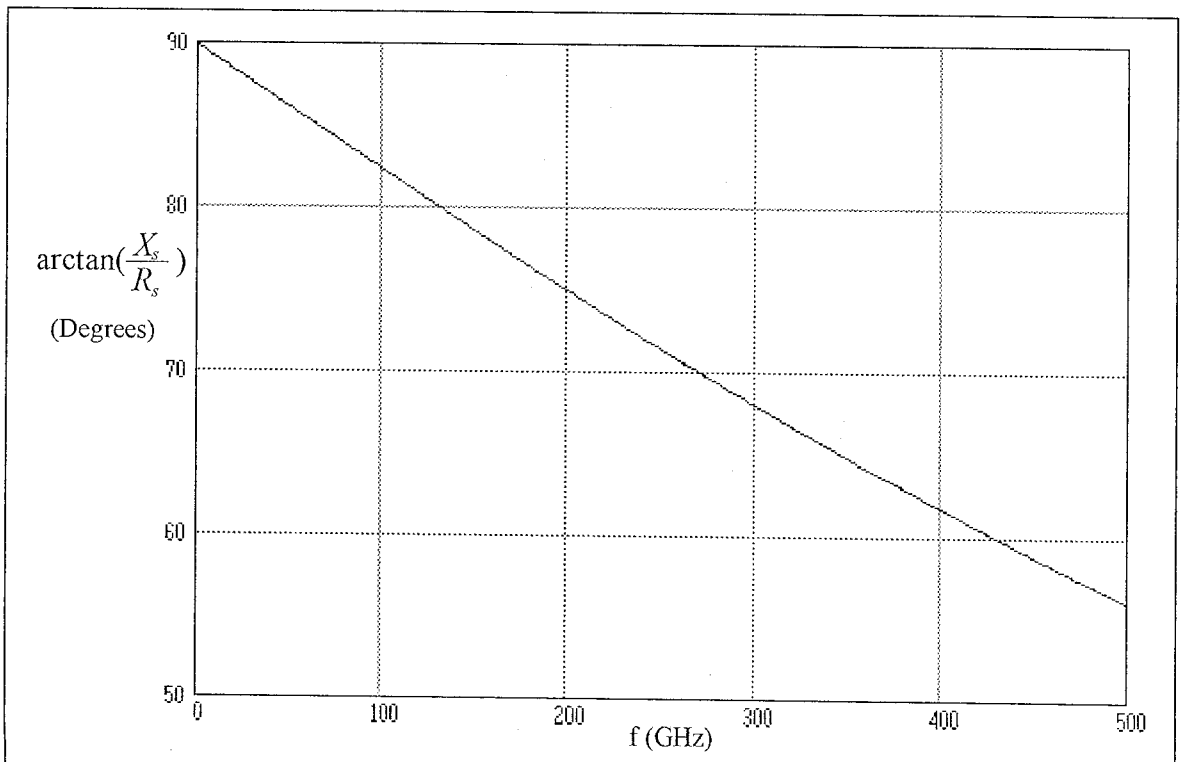

Figure 7 The argument (angle) of the surface impedance of an HTS.

constant and equal to $\frac{\pi}{4}$ or 45°[1]. Figure 7 is a plot of the argument of the surface impedance of an HTS versus frequency, using the average set of parameter values (table 1). Over the usable frequency range the angle of the surface impedance spans a range of 25 degrees for the average set of parameter values (figure 7) and a range of about 50 degrees from the worst-case to the best-case sets of parameter values. In this frequency range the surface impedance goes from being almost purely reactive to being almost equally resistive and reactive. Figure 8 is a log-log plot of the magnitude of the surface impedance of an HTS versus frequency, using the average set of parameters.

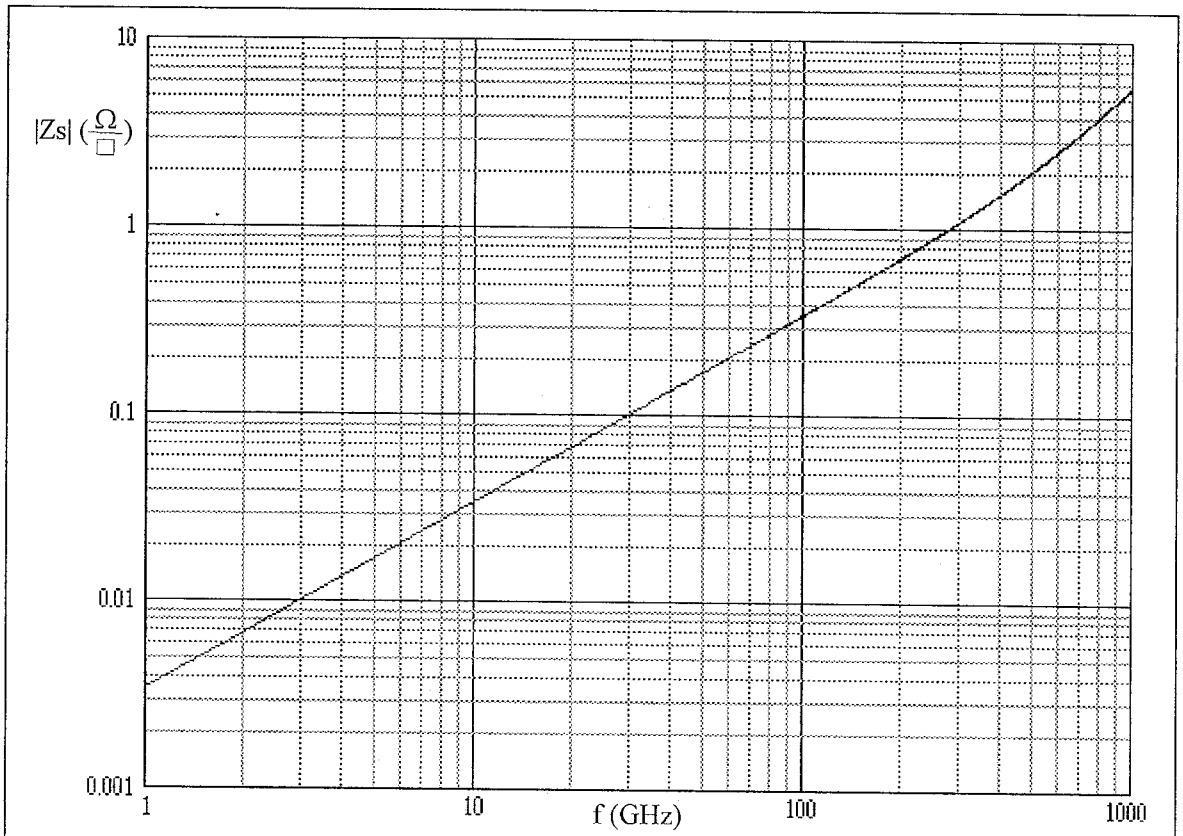

Figure 8 The magnitude of the surface impedance of an HTS.

Over the 1 to 300 GHz frequency domain, the magnitude of the surface impedance of the HTS spans a range of 2.5 decades, from 0.003 to 1 in magnitude. This large range is spanned because the surface resistance is proportional to the square of the frequency and the surface reactance is proportional to the frequency (as compared to both the surface

resistance and reactance being proportional to the square root of frequency in normal metals). Figures 7 and 8 bear out the fact that the equation for the boundary condition at the HTS walls is modified as $\mathbf{E}_{tangential} = |Z_s| e^{j\angle Z_s} \left(\hat{\mathbf{n}} \times \mathbf{H}_{tangential}\right)$ from the corresponding equation $\mathbf{E}_{tangential} = \mathbf{0}$ for the perfectly conducting walls, where Z_s spans a range from 0.003 to 1 in magnitude and 90 to 65 degrees in phase in the frequency domain from 1 to 300 GHz. With such a great range of boundary conditions there is the need for a way to validate and define the limits of usage of equation (5), and also accurately predict the magnetic fields and currents at the HTS walls. These are important since when they approach or exceed their critical values the behavior of the HTS changes drastically.

8.4.2 The Solution

The above problem is solved by a numerical solution of Maxwell's equations, with the appropriate boundary conditions for the HTS. Specifically, a finite-difference formulation of the Helmholtz wave equations, derived from Maxwell's equations, is employed. We start from the Helmholtz wave equations [1], [2]

$$\nabla_T^2 \mathbf{E} + \left(\gamma^2 + k^2\right)\mathbf{E} = \mathbf{0} \tag{8}$$

and

$$\nabla_T^2 \mathbf{H} + \left(\gamma^2 + k^2\right)\mathbf{H} = \mathbf{0} \ , \tag{9}$$

where $k^2 = \omega^2 \mu_0 \varepsilon$, ∇_T^2 is the transverse Laplacian operator, and sinusoidal phasor waves propagating in the positive z-direction, proportional to $e^{(j\omega t - \gamma z)}$, have been assumed. Actually, only the z-components of (8) and (9) need to be solved for. The other four field components (E_x, E_y, H_x and H_y) may be obtained from E_z and H_z using the four auxiliary equations listed below [1]:

$$E_x = -\frac{1}{\gamma^2 + k^2}\left(\gamma \frac{\partial E_z}{\partial x} + j\omega\mu_0 \frac{\partial H_z}{\partial y}\right) \tag{10}$$

$$E_y = \frac{1}{\gamma^2 + k^2}\left(-\gamma\frac{\partial E_z}{\partial y} + j\omega\mu_0\frac{\partial H_z}{\partial x}\right) \tag{11}$$

$$H_x = -\frac{1}{\gamma^2 + k^2}\left(j\omega\varepsilon\frac{\partial E_z}{\partial y} - \gamma\frac{\partial H_z}{\partial x}\right) \tag{12}$$

$$H_y = -\frac{1}{\gamma^2 + k^2}\left(j\omega\varepsilon\frac{\partial E_z}{\partial x} + \gamma\frac{\partial H_z}{\partial y}\right) . \tag{13}$$

The waveguide is first sub-sectioned in a uniform rectangular grid, as shown in figure 9.

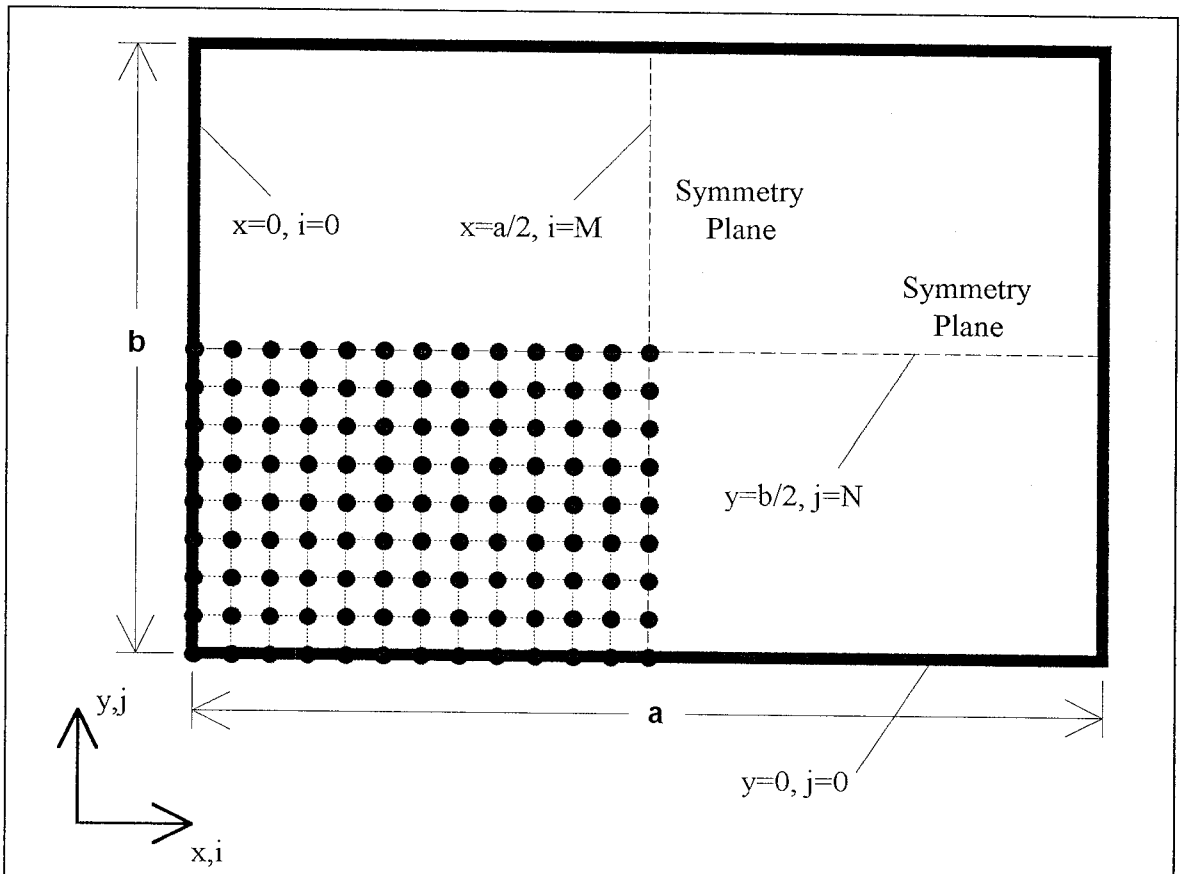

Figure 9 The cross-section of the HTS waveguide sub-sectioned by a uniform rectangular grid.

Because of the symmetry planes, shown in figure 9, only one quarter of the waveguide cross-section needs to be sub-sectioned. The uniform rectangular grid comprises M+1 points in the x-direction ($i = 0,1\ldots M$) and N+1 points in the y-direction ($j = 0,1\ldots N$).

Hence, the grid spacing is

$$\Delta x = \frac{a}{2M} \tag{14}$$

in the x-direction and

$$\Delta y = \frac{b}{2N} \tag{15}$$

in the y-direction.

The z-components of equations (8) and (9) are discretized, by approximating derivatives with ratios of finite (but small) differences. The discretized equations are [3]

$$E_z(i+1,j)+E_z(i-1,j)+R^2E_z(i,j+1)+R^2E_z(i,j-1)+\left[\left(\gamma^2+k^2\right)\Delta x^2-2\left(1+R^2\right)\right]E_z(i,j)=0 \tag{16}$$

and

$$H_z(i+1,j)+H_z(i-1,j)+R^2H_z(i,j+1)+R^2H_z(i,j-1)+\left[\left(\gamma^2+k^2\right)\Delta x^2-2\left(1+R^2\right)\right]H_z(i,j)=0 \tag{17}$$

where $(i,j)\in\{1,2\ldots M-1\}\times\{1,2\ldots N-1\}$, $R=\dfrac{\Delta x}{\Delta y}$ and a center-differences discretization is employed to maintain second-order accuracy. It will be noted that equations (16) and (17) can only be used at the "interior" points, away from the walls, and they constitute a total of 2(M-1)(N-1) equations. The total number of unknowns (E_z and H_z at every grid point) is 2(M+1)(N+1). Hence, a further 4(M+N) equations are required to give the problem a unique solution. There are 2(M+N) grid points on the walls. Hence 2 equations are needed from each grid point. The equations used are shown below for each boundary.

a. BOTTOM WALL ($j=0, i=1,2\ldots M-1$)

This is an HTS wall. Equation (3.31) is used for the surface impedance. $E_z(i,j) = -Z_s H_x(i,j)$ combined with a discretized version of equation (12) give

$$
\begin{aligned}
&2\Delta x\left(k^2+\alpha^2-\beta^2+j2\alpha\beta\right)E_z(i,j)+\\
&+\left(j2RR_s\omega\varepsilon-2RX_s\omega\varepsilon\right)\left[E_z(i,j+1)-E_z(i,j)\right]+\\
&-\left[\alpha R_s-\beta X_s+j\left(\beta R_s+\alpha X_s\right)\right]\left[H_z(i+1,j)-H_z(i-1,j)\right]=0 \quad .
\end{aligned}
\tag{18}
$$

$E_x(i,j) = Z_s H_z(i,j)$ combined with a discretized version of equation (10) give

$$
\begin{aligned}
&2\Delta x\left\{R_s\left(k^2+\alpha^2-\beta^2\right)-2\alpha\beta X_s+j\left[X_s\left(k^2+\alpha^2-\beta^2\right)+2\alpha\beta R_s\right]\right\}H_z(i,j)+\\
&+j2\omega\mu_0 R\left[H_z(i,j+1)-H_z(i,j)\right]+\\
&+\left(\alpha+j\beta\right)\left[E_z(i+1,j)-E_z(i-1,j)\right]=0 .
\end{aligned}
\tag{19}
$$

b. LEFT WALL ($i = 0,\ j = 1,2\ldots N-1$)

This is an HTS wall. $E_z(i,j) = Z_s H_y(i,j)$ combined with a discretized version of equation (13) give

$$
\begin{aligned}
&2\Delta x\left(k^2+\alpha^2-\beta^2+j2\alpha\beta\right)E_z(i,j)+\\
&+\left(j2R_s\omega\varepsilon-2X_s\omega\varepsilon\right)\left[E_z(i+1,j)-E_z(i,j)\right]+\\
&+\left[\alpha RR_s-\beta RX_s+j\left(\beta RR_s+\alpha RX_s\right)\right]\left[H_z(i,j+1)-H_z(i,j-1)\right]=0 \quad .
\end{aligned}
\tag{20}
$$

$E_y(i,j) = -Z_s H_z(i,j)$ combined with a discretized version of equation (11) give

$$
\begin{aligned}
&2\Delta x\left\{R_s\left(k^2+\alpha^2-\beta^2\right)-2\alpha\beta X_s+j\left[X_s\left(k^2+\alpha^2-\beta^2\right)+2\alpha\beta R_s\right]\right\}H_z(i,j)+\\
&+j2\omega\mu_0\left[H_z(i+1,j)-H_z(i,j)\right]+\\
&-\left(R\alpha+jR\beta\right)\left[E_z(i,j+1)-E_z(i,j-1)\right]=0 .
\end{aligned}
\tag{21}
$$

c. TOP SYMMETRY PLANE ($j = N, i = 1,2\ldots M-1$)

This is a perfect electric wall, if a TEmn or TMmn mode is sought, where n is even, and a perfect magnetic wall otherwise.

i. Perfect Electric Symmetry Plane

$$E_z(i,j) = 0 \tag{22}$$

and $E_x(i,j) = 0$ combined with a discretized version of equation (10) give

$$j2R\omega\mu_0\left[H_z(i,j) - H_z(i,j-1)\right] + (\alpha + j\beta)\left[E_z(i+1,j) - E_z(i-1,j)\right] = 0 \ . \tag{23}$$

ii. Perfect Magnetic Symmetry Plane

$$H_z(i,j) = 0 \tag{24}$$

and $H_x(i,j) = 0$ combined with a discretized version of equation (12) give

$$j2R\omega\varepsilon\left[E_z(i,j) - E_z(i,j-1)\right] - (\alpha + j\beta)\left[H_z(i+1,j) - H_z(i-1,j)\right] = 0 \ . \tag{25}$$

d. RIGHT SYMMETRY PLANE ($i = M, j = 1,2\ldots N-1$)

This is a perfect electric wall, if a TEmn or TMmn mode is sought, where m is even, and a perfect magnetic wall otherwise.

i. Perfect Electric Symmetry Plane

$$E_z(i,j) = 0 \tag{26}$$

and $E_y(i,j)=0$ combined with a discretized version of equation (11) give

$$j2\omega\mu_0\left[H_z(i,j)-H_z(i-1,j)\right]-\left(R\alpha+jR\beta\right)\left[E_z(i,j+1)-E_z(i,j-1)\right]=0 \quad . \tag{27}$$

ii. Perfect Magnetic Symmetry Plane

$$H_z(i,j)=0 \tag{28}$$

and $H_y(i,j)=0$ combined with a discretized version of equation (13) give

$$j2\omega\varepsilon\left[E_z(i,j)-E_z(i-1,j)\right]+\left(R\alpha+jR\beta\right)\left[H_z(i,j+1)-H_z(i,j-1)\right]=0 \quad . \tag{29}$$

e. CORNERS

i. Bottom Left Corner($i=0,\ j=0$)

This is an HTS corner on both sides. Equations (18) and (19) are modified as follows, so as not to contain terms like $H_z(i-1,j)$, which do not make sense.

$$\begin{aligned}&\Delta x\left(k^2+\alpha^2-\beta^2+j2\alpha\beta\right)E_z(i,j)+\\&+\left(jRR_s\omega\varepsilon-RX_s\omega\varepsilon\right)\left[E_z(i,j+1)-E_z(i,j)\right]+\\&-\left[\alpha R_s-\beta X_s+j\left(\beta R_s+\alpha X_s\right)\right]\left[H_z(i+1,j)-H_z(i,j)\right]=0\end{aligned} \tag{30}$$

and

$$\begin{aligned}&\Delta x\left\{R_s\left(k^2+\alpha^2-\beta^2\right)-2\alpha\beta X_s+j\left[X_s\left(k^2+\alpha^2-\beta^2\right)+2\alpha\beta R_s\right]\right\}H_z(i,j)+\\&+j\omega\mu_0R\left[H_z(i,j+1)-H_z(i,j)\right]+\\&+\left(\alpha+j\beta\right)\left[E_z(i+1,j)-E_z(i,j)\right]=0\,.\end{aligned} \tag{31}$$

ii. Bottom Right Corner ($i = M, j = 0$)

This corner is HTS on one side and perfect electric or magnetic on the other side. However, by contrasting theoretical and computer results in a low-loss case, it is determined that the best accuracy solutions are obtained when both boundary conditions are drawn from the perfect boundary side.

1. Perfect Electric Symmetry Plane

$$E_z(i,j) = 0 \tag{32}$$

and $E_y(i,j) = 0$ combined with a discretized version of equation (11) give

$$j\omega\mu_0\left[H_z(i,j) - H_z(i-1,j)\right] - (R\alpha + jR\beta)\left[E_z(i,j+1) - E_z(i,j)\right] = 0 \ . \tag{33}$$

2. Perfect Magnetic Symmetry Plane

$$H_z(i,j) = 0 \tag{34}$$

and $H_y(i,j) = 0$ combined with a discretized version of equation (13) give

$$j\omega\varepsilon\left[E_z(i,j) - E_z(i-1,j)\right] + (R\alpha + jR\beta)\left[H_z(i,j+1) - H_z(i,j)\right] = 0 \ . \tag{35}$$

iii. Top Left Corner ($i = 0, j = N$)

The boundary conditions from the perfect boundary are used, as in case c.ii above.

1. Perfect Electric Symmetry Plane

$$E_z(i,j) = 0 \tag{36}$$

and $E_x(i,j) = 0$ combined with a discretized version of equation (10) give

$$jR\omega\mu_0\left[H_z(i,j) - H_z(i,j-1)\right] + (\alpha + j\beta)\left[E_z(i+1,j) - E_z(i,j)\right] = 0 \ . \tag{37}$$

2. Perfect Magnetic Symmetry Plane

$$H_z(i,j) = 0 \tag{38}$$

and $H_x(i,j) = 0$ combined with a discretized version of equation (12) give

$$jR\omega\varepsilon\left[E_z(i,j) - E_z(i,j-1)\right] - (\alpha + j\beta)\left[H_z(i+1,j) - H_z(i,j)\right] = 0 \ . \tag{39}$$

iv. Top Right Corner ($i = M, j = N$)

The applicable boundary conditions are as follows.

1. Top Perfect Electric Symmetry Plane

$$E_z(i,j) = 0 \tag{40}$$

and $E_x(i,j) = 0$ combined with a discretized version of equation (10) give

$$jR\omega\mu_0\left[H_z(i,j) - H_z(i,j-1)\right] + (\alpha + j\beta)\left[E_z(i,j) - E_z(i-1,j)\right] = 0 \ . \tag{41}$$

2. Top Perfect Magnetic Symmetry Plane

$$H_z(i,j) = 0 \tag{42}$$

and $H_x(i,j) = 0$ combined with a discretized version of equation (12) give

$$jR\omega\varepsilon\left[E_z(i,j)-E_z(i,j-1)\right]-(\alpha+j\beta)\left[H_z(i,j)-H_z(i-1,j)\right]=0 \quad . \tag{43}$$

3. Right Perfect Electric Symmetry Plane

$$E_z(i,j)=0 \tag{44}$$

and $E_y(i,j)=0$ combined with a discretized version of equation (11) give

$$j\omega\mu_0\left[H_z(i,j)-H_z(i-1,j)\right]-(R\alpha+jR\beta)\left[E_z(i,j)-E_z(i,j-1)\right]=0 \quad . \tag{45}$$

4. Right Perfect Magnetic Symmetry Plane

$$H_z(i,j)=0 \tag{46}$$

and $H_y(i,j)=0$ combined with a discretized version of equation (13) give

$$j\omega\varepsilon\left[E_z(i,j)-E_z(i-1,j)\right]+(R\alpha+jR\beta)\left[H_z(i,j)-H_z(i,j-1)\right]=0 \quad . \tag{47}$$

If the corner is electric-electric, (40) and (41) are used. If the corner is magnetic-magnetic, (42) and (43) are used. If the corner is electric-magnetic (40) and (42) are used.

The $2(M\text{-}1)(N\text{-}1)$ interior equations and the $4(M+N)$ boundary equations, two from each boundary grid point, constitute a total of $2(M+1)(N+1)$ homogeneous equations with $2(M+1)(N+1)$ unknowns (E_z and H_z at every grid point). They may be written in matrix notation as

$$\mathbf{A}(\gamma)\mathbf{X}=\mathbf{0} \quad , \tag{48}$$

where $\mathbf{X}$ is the vector of the unknowns,

$$\mathbf{X}=\left.\begin{bmatrix} E_z(0,0) \\ H_z(0,0) \\ E_z(1,0) \\ H_z(1,0) \\ \vdots \\ E_z(M,0) \\ H_z(M,0) \\ E_z(0,1) \\ H_z(0,1) \\ \vdots \\ E_z(M,1) \\ H_z(M,1) \\ \vdots \\ E_z(M,N) \\ H_z(M,N) \end{bmatrix}\right\} 2(M+1)(N+1) \text{ rows}, \tag{49}$$

A is a $2(M+1)(N+1)\times 2(M+1)(N+1)$ matrix of coefficients and the right-hand side of (48) is the $2(M+1)(N+1)$ element zero column-vector. **A** is very sparse (there are at most 5 non-zero elements in any row) and a function of γ, with the frequency f as a parameter. Equation (48) has a non-trivial solution if and only if it is singular, i.e., if and only if $\det[\mathbf{A}(\gamma)]=0$. This condition resembles an eigenvalue problem. Unfortunately, because **A** is a function of both γ and γ^2, it is a non-linear eigenvalue problem that cannot be reduced to a linear one. This increases the computational complexity of finding the γ that make the determinant of the matrix zero, by one to two orders of magnitude. These γ correspond to the modes that are launched in the waveguide (both propagating and evanescent). They are found by locating the roots of the characteristic polynomial. In the general case, the characteristic polynomial $P(\gamma)=\det[\mathbf{A}(\gamma)]$ is a complex-valued polynomial of a complex variable, with complex coefficients. To demonstrate the principle and study an example of a polynomial, **A** is entered into *Mathematica* (TM) by Wolfram Inc. for the next to smallest possible grid: four interior points and twelve

boundary points, or M=N=3. Mathematica is used here because of its symbolic manipulation capability. Appendix C contains the matrix and its factored determinant as returned by Mathematica. In this example symmetry planes are not used (i.e., the whole waveguide cross-section is sub-sectioned) and perfectly conducting walls are assumed. The characteristic polynomial for this case is

$$P(\gamma)=\frac{\mu_0^{12}\omega^{12}}{\Delta x^4\Delta y^8}\left(\gamma^2+\omega^2\mu_0\varepsilon\right)\left(\gamma^2+\omega^2\mu_0\varepsilon-\frac{2}{\Delta x^2}\right)\left(\gamma^2+\omega^2\mu_0\varepsilon-\frac{3}{\Delta x^2}-\frac{3}{\Delta y^2}\right)$$
$$\cdot\left(\gamma^2+\omega^2\mu_0\varepsilon-\frac{1}{\Delta x^2}-\frac{3}{\Delta y^2}\right)\left(\gamma^2+\omega^2\mu_0-\frac{2}{\Delta y^2}\right)\left(\gamma^2+\omega^2\mu_0\varepsilon-\frac{2}{\Delta x^2}-\frac{2}{\Delta y^2}\right) \tag{50}$$
$$\cdot\left(\gamma^2+\omega^2\mu_0\varepsilon-\frac{3}{\Delta x^2}-\frac{1}{\Delta y^2}\right)\left(\gamma^2+\omega^2\mu_0\varepsilon-\frac{1}{\Delta x^2}-\frac{1}{\Delta y^2}\right).$$

The first factor in the right-hand side of equation (50) represents the TEM solution. Unfortunately this pops up because the characteristic polynomial does not "recognize" that the TEM solution has the **X** vector identically equal to zero. The second factor is the factor of interest. Remembering that in this case $\Delta x=\frac{a}{3}$, the zero of this factor may be expressed as

$$\gamma=j\beta=j\sqrt{\omega^2\mu_0\varepsilon-\frac{2}{\left(\frac{a}{3}\right)^2}}=j\omega\sqrt{\mu_0\varepsilon}\sqrt{1-\frac{\frac{18}{a^2\mu_0\varepsilon}}{\omega^2}}= \tag{51}$$
$$=j\omega\sqrt{\mu_0\varepsilon}\sqrt{1-\left(\frac{\frac{3\sqrt{2}}{a\sqrt{\mu_0\varepsilon}}}{\omega}\right)^2}.$$

Combining this with the equation for the propagation constant of a waveguide [1]

$$\beta = \omega\sqrt{\mu_0\varepsilon}\sqrt{1-\left(\frac{\omega_c}{\omega}\right)^2} \tag{52}$$

we find that the effective cutoff frequency of the TE10 mode, as predicted by the characteristic polynomial, is

$$\omega_c = \frac{3\sqrt{2}}{\sqrt{\mu_0\varepsilon}a} = \frac{3\sqrt{2}}{\pi}\frac{\pi}{\sqrt{\mu_0\varepsilon}a} \approx 1.35(\omega_c)_{\text{true}} \ , \tag{53}$$

only 35 % off from its true value for such a coarse grid. Also we notice that the characteristic polynomial root has the correct dimensions (of angular frequency).

Here we briefly digress to explain why equation (52), for the propagation constant, still applies, despite the presence of the surface reactance, X_s, which might affect the propagation constant. The proof extends the first-order perturbational solution for the attenuation coefficient, which assumes the lossless modes in the waveguide and from these calculates the extra loss, due to the surface resistance. The extension uses a complex surface impedance in place of the surface resistance and interprets the imaginary part of the attenuation coefficient as a perturbation on the propagation constant. First, however, we have to motivate this approach from physical laws. We start with Poynting's equation; equation (3.22). The last term, $\mathbf{e}\cdot\mathbf{j}$, represents the instantaneous power per unit volume converted to heat. If instead we switch to phasors and use a surface current density instead of a volume current density, we obtain the expression $\frac{1}{2}\mathbf{E}\cdot\mathbf{J}_s^*$, the real part of which represents the instantaneous power per unit surface area lost to heat on the walls. The imaginary part of this expression represents a power density that "sloshes" back and forth between different forms of energy, but is not dissipated because the current is 90 degrees out of phase with the electric field. If we allow this component to enter our calculation of the exponential attenuation, we obtain an imaginary component of the latter which may be interpreted as a correction to the propagation constant, as a result of the

presence of the surface reactance. The formula for calculating α, the exponential attenuation, is [1]:

$$\alpha = \frac{Power\ Lost \Big/ Unit\ Length}{2 \cdot Power\ Transmitted} \quad . \tag{54}$$

The now complex numerator of equation (54) is given by

$$W_{Loss} + jW_{Reactive} = \int_0^a \frac{1}{2}\mathbf{E}\cdot\mathbf{J}_s^* dx \quad , \tag{55}$$

using the bottom wall as an example. We continue the derivation as follows:

$$\begin{aligned} W_{Loss} + jW_{Reactive} &= \frac{1}{2}\int_0^a \mathbf{E}\cdot\mathbf{J}_s^* dx = \frac{1}{2}\int_0^a \left(E_x J_{sx}^* + E_z J_{sz}^*\right)dx = \\ &= \frac{1}{2}\int_0^a \left[\left(Z_s H_z\right)J_{sx}^* + \left(-Z_s H_x\right)J_{sz}^*\right]dx = \frac{1}{2}Z_s\int_0^a \left(H_z J_{sx}^* - H_x J_{sz}^*\right)dx = \\ &= \frac{1}{2}Z_s\int_0^a \left[J_{sx}J_{sx}^* - \left(-J_{sz}\right)J_{sz}^*\right]dx = \frac{1}{2}Z_s\int_0^a \left(\left|J_{sx}\right|^2 + \left|J_{sz}\right|^2\right)dx \end{aligned} \tag{56}$$

The last part of (56) is almost identical to the standard equation used to derive the power loss per unit length in a waveguide [1], only R_S is substituted by Z_S. What this means is that we do not have to perform the long series of calculations that equation (54) calls for, but instead we can use equation (4) with X_S in place of R_S. Hence

$$\Delta\beta = \frac{X_s}{b\eta\sqrt{1-\left(\frac{f_c}{f}\right)^2}}\left[1+\frac{2b}{a}\left(\frac{f_c}{f}\right)^2\right] \quad . \tag{57}$$

Combining equations (57) and (3.31) we obtain the final expression for the expected perturbation in the propagation constant due to the existence of surface reactance:

$$\Delta\beta = \frac{2\pi f\mu_0\lambda_0}{b\eta\sqrt{1-\left(\frac{f_c}{f}\right)^2}}\left[1+\frac{2b}{a}\left(\frac{f_c}{f}\right)^2\right] \quad . \tag{58}$$

Table 3 shows the fractional perturbation, $\Delta\beta/\beta$, calculated using equations (58) and (52) for WR90, WR28, WR10, WR5 and WR3 waveguides, of average HTS parameters, at a frequency that is at the upper limit of the recommended operating range for the TE10 mode, according to the Handbook for Normal Waveguides. Table 3 indicates that for all intents and purposes equation (52) is accurate enough to use, and also agrees with the output of the finite-difference program reported below (see figures 31, 33, 35, 37 and 39).

Type...	f (GHz)	$\Delta\beta/\beta$
WR90	12.4	$7.33\cdot10^{-5}$
WR28	40.0	$2.14\cdot10^{-4}$
WR10	110.0	$6.12\cdot10^{-4}$
WR5	220.0	$1.17\cdot10^{-3}$
WR3	325.0	$4.28\cdot10^{-3}$

Table 3 Fractional Perturbation of the Propagation Constant.

After legitimizing the use of equation (52), we return to the characteristic polynomial, $P(\gamma) = \det[\mathbf{A}(\gamma)]$. In general, the roots of the characteristic polynomial can be located by locating a local minimum of $|P(\gamma)|$. An initial guess is required, which, in this case, can be provided by equation (5) for α and equation (52) for β, given the right cutoff frequency of the mode sought. Once the value γ_o has been found, that makes the matrix $\mathbf{A}(\gamma)$ singular, for a given frequency, the matrix is then evaluated at γ_o and the resulting matrix, say $\mathbf{A}_0$ is singular. Therefore the rank of $\mathbf{A}_0$ is less than full. The unknown vector $\mathbf{X}$ is then a member of the nullspace of $\mathbf{A}_0$. If the nullity of $\mathbf{A}_0$ is 1, $\mathbf{X}$ is unique modulo a scale factor. If, however, the nullity of $\mathbf{A}_0$ is n>1, then there are n orthonormal vectors $\mathbf{X}$ that satisfy $\mathbf{A}_0\mathbf{X}=\mathbf{0}$. This corresponds to the case in which there is no loss (α=0) and higher order TE and a TM solutions exist for the same γ_o. Hence, n is 1, when loss is included or the TE10 mode is considered, and 2 when loss is neglected and modes higher than TE10 are considered. Therefore, in the "interesting" cases n is always 1 and a unique solution $\mathbf{X}_0$ (modulo a scale factor) exists. The null vector $\mathbf{X}_0$ can be found by performing a singular value decomposition (SVD) on the matrix $\mathbf{A}_0$. This is to express $\mathbf{A}_0$ in the form

$$\mathbf{A}_0 = \mathbf{U}\Sigma\mathbf{V}^H \quad , \tag{59}$$

where H is the hermitian conjugate operator, Σ is a square diagonal matrix with the singular values in the main diagonal, and **U** and **V** are square unitary matrices. The diagonal entries of Σ, σ_i, are always non-negative and can be made to decrease in value with respect to i. The nullity of $\mathbf{A}_0$ is equal to the number of σ_i that are equal to zero (or, in practice, very small compared to σ_1). The columns of **V** whose same-numbered elements σ_i are zero are an orthonormal basis for the nullspace. In practice this means that, in all interesting cases, the last column of **V** is the unknown null vector $\mathbf{X}_0$. Using the SVD method has the advantage that if, for some reason, the γ_o located by the minimization process does not truly render the matrix **A** singular, then the last singular value is not small compared to the other singular values, and the error is thus uncovered. Conversely, when $\mathbf{A}_0$ is singular with nullity one it is $\frac{\sigma_{2(M+1)(N+1)}}{\sigma_{2(M+1)(N+1)-1}} << 1$ and the resulting $\mathbf{X}_0$ is known to be a good solution.

8.4.3 The Program

A program is written in C language, utilizing many Fortran library routines, and compiled on the JPL CRAY Y-MP2E computer system, voyager, and the Goddard Space Flight Center CRAY C98 computer system, *charney*. The former uses the Unicos 7.0 operating system and the latter Unicos 7.C.3. A listing of the program C-code is included as appendix D of this chapter.

The name of the program is *wg_plot.c* and it implements the steps described in section 8.4.2 above to calculate the propagation and attenuation constants, electric and magnetic fields, total power and maximum tangential fields on the walls of a closed rectangular HTS waveguide. SI units are used consistently throughout the program for all variables. In the

description of the code that follows, it may be helpful to the reader to follow along in appendix D.

The first variables defined in the code are *M*, *N* and *ROWLENGTH*. *M* and *N* correspond to the homonymous variables defined above. *ROWLENGTH* is equal to $2(M+1)(N+1)$, the number of rows and columns of the matrix **A**.

The first function called by the function *main*, which is the function the program launches into and calls all other functions from, is *vector*. This function, which is adopted from the *Numerical Recipes in C* software package [4], reserves a memory chunk of a given size for use by the program and returns a pointer to it. In this case $2 \cdot ROWLENGTH^{2}$ words (units of memory equal to 8 bytes long that are used by the Cray for one single precision number) are reserved for the matrix **A** and a pointer called *matrix* is assigned to that memory location. Henceforth in the program *matrix* refers to what has hitherto been called **A**.

The next set of commands asks the user to input the parameters of the waveguide to be analyzed. These parameters are assigned to an array of eight real numbers called *params*, with *params*[0] the width of the waveguide cross-section, *params*[1] the height of the waveguide cross-section, *params*[2] the relative dielectric constant of the waveguide interior, *params*[3] is frequency to be analyzed, *params*[4] the effective zero temperature penetration depth of the HTS walls, *params*[5] the normal conductivity of the HTS walls. *params*[6] the temperature of the HTS walls and *params*[7] the critical temperature of the HTS walls. The programs asks for each of these parameters to be input from the standard input sequentially. Then the program asks for the *m* and the *n* of the mode you are seeking (assuming TE*mn* or TM*mn* is being sought, depending on the symmetries used in the function *matr*; see below).

Then *params*, *m* and *n* are passed to the next function called by *main*, which is called *guess_gamma*. As its name implies, the purpose of this function is to provide a starting point for locating the zero of the characteristic polynomial. It calculates the theoretical attenuation and propagation constant, using equations (5) for the attenuation of TE*m*0 modes and the corresponding one for other modes (see [1]) and equation (52) for the propagation constant. It returns these values, via a pointer, to a real array of two numbers called *gamma*, with *gamma*[1] the guess for α and *gamma*[2] the guess for β.

The next function called is *determinant*. This function takes *gamma*, *params* and *matrix* as its input and returns the magnitude of the determinant of *matrix* divided by the magnitude of the factor $\left(\gamma^2+\omega^2\mu_0\varepsilon\right)^{M+N+1}$. This is done to remove the corresponding TEM factor from the characteristic polynomial, because it acts as a strong "attractor" of the root-finding process. Frequently the minimization inadvertently ends at the TEM solution, when this factor is not divided out. The function itself calls two Fortran library routines: *CGEFA* and *CGED*. These are modifications of the corresponding well known *LINPACK* routines [5], which are included in the JPL custom Fortran mathematical library called *MATH77* [6]. *CGEFA* performs the LU decomposition [7] of a general complex matrix (in this case *matrix*). Then *CGED* takes the result and computes the determinant of the original matrix by multiplying the diagonal elements of the upper triangular matrix [7]. The function *determinant* also calls *matr*. The function *matr* initializes *matrix* to the correct values for all its elements. The function *matr* calls two other functions: *putreal* and *putimag*. These two functions merely assign a value, real or imaginary respectively, to a certain element of *matrix*. The value to be assigned and the row and column coordinates of the element are passed to *putreal* and *putimag* as arguments. The function *matr* also calls *Ez* and *Hz*, as arguments to *putreal* and *putimag*. These functions translate grid coordinates to matrix row coordinates. For example, for *M*=2, *N*=2 (3 by 3 grid, 18 by 18 matrix) $E_z(1,1)$ is in the 9^{th} column of the matrix (see equation (49)). The functions

putreal and *putimag* place all the appropriate coefficients, seen in equations (16)-(45), of every equation in the proper memory locations reserved as *matrix*. The function *matr* also calls another function called *initmatrix* which zeros out every element of *matrix*.

The function *determinant* is called thrice by *main*, via a for-loop, and initializes the 3-element real array *y* to the determinant values of three points in the complex gamma plane, one at the value returned by *guess_gamma* and the other two *lalpha* and *lbeta* away. The minimization routine (called next) works optimally (minimum number of iterations) when *lalpha* and *lbeta* are chosen such that the three initial points in the complex-gamma plane are approximately equidistant from the true minimum. The optimum *lalpha* and *lbeta* depend on the grid size (*M* and *N*), but a good rule of thumb is found to be $lalpha = 0.03\alpha$ and $lbeta = 0.02\beta$.

The function *amoeba* is called by *main* next. The function *amoeba* (and its sister function *amotry*, which it calls) has been adopted from the *Numerical Recipes in C* software package [4] and modified. *amoeba* implements Nelder and Mead's downhill simplex minimization method in multi-dimensions (two dimensions in our case) [8]. This method is found to be faster than successive one-dimensional minimizations in normal directions. The function takes as its arguments the three complex gamma-plane points guessed, as described above, and their respective determinants (pre-calculated in *y*), and iterates until it locates a minimum to within a given fractional tolerance of the determinant value. It is modified so that it also stops iterating when the minimum has been located to within a fractional tolerance of the determinant's arguments (i.e., *gamma*). Hence the calculation of *gamma* does not go beyond the specified number of significant figures and CPU time is not wasted. The magnitude of the characteristic polynomial equals zero only at the zeros of the polynomial. Hence, *amoeba* searches and locates the closest to the initial guess zero of the characteristic polynomial. As *amoeba* iterates searching for the minimum, the values of *gamma* it guesses are printed to the standard output for traceability purposes.

When *amoeba* exits, this zero is stored in the first row of a two-dimensional real array named p. Hence, $p[1][1]$ is the attenuation and $p[1][2]$ is the propagation constant.

After these variables are printed to the standard output for the information of the user, the solution vector $\mathbf{X_0}$ is calculated, via the SVD process described in section 8.4.2. This is done by the next function called by *main*, called *svd*. The function *svd* takes the array p (which now contains the value of γ that makes *matrix* singular), *matrix* and *params* as its arguments. First it calls *matr* to re-initialize *matrix* for the singular value of *gamma* (i.e., *matrix* is now what has been called $\mathbf{A_0}$ above). Then it uses three Fortran routines adopted from the Fortran mathematical routine package *LAPACK* [9]. The names of the three routines are *CGEBRD*, *CUNGBR*, and *CBDSQR*. *CGEBRD* reduces a general complex m-by-n matrix $\mathbf{A}$ to upper or lower bi-diagonal form $\mathbf{B}$ by a unitary transformation $\mathbf{Q}_1{}^H\mathbf{A}\mathbf{P}_1 = \mathbf{B}$. *CUNGBR* generates one of the unitary matrices $\mathbf{Q}_1$ or $\mathbf{P}_1^H$ determined by *CGEBRD* when reducing a complex matrix to bidiagonal form. *CBDSQR* computes the SVD of a real n-by-n bidiagonal matrix $\mathbf{B}$: $\mathbf{B} = \mathbf{Q}_2\mathbf{S}\mathbf{P}_2{}^T$, where $\mathbf{S}$ is a diagonal matrix with non-negative diagonal elements (the singular values of $\mathbf{B}$) and $\mathbf{Q}_2$ and $\mathbf{P}_2$ are orthogonal matrices. Combining *CGEBRD* and *CBDSQR* we obtain

$$\mathbf{A} = \mathbf{Q}_1\mathbf{Q}_2\mathbf{S}\mathbf{P}_2^T\mathbf{P}_1^H = \underbrace{(\mathbf{Q}_1\mathbf{Q}_2)}_{\mathbf{U}}\mathbf{S}\underbrace{(\mathbf{P}_1\mathbf{P}_2)^H}_{\mathbf{V}}, \tag{60}$$

which is equivalent to equation (59). The diagonal elements of $\mathbf{S}$, the singular values, are returned to *main* in a variable called *diag*. The last 10 are printed to the standard output to assure the user of a converged solution (see last paragraph of section 8.4.2). $\mathbf{V}$ (the last column of which is $\mathbf{X_0}$, the solution) is calculated by feeding $\mathbf{P}_1^H$, calculated by *CUNGBR*, into *CGEBRD*. The resulting matrix $\mathbf{V}$ is stored in the same memory location as *matrix* (which has by now been overwritten as it is no longer needed) to conserve memory. *main* then stores $\mathbf{X_0}$, the last column of $\mathbf{V}$, into a new complex vector called *res*.

The function *main* then calls *free_vector*, another function from *Numerical Recipes in C* which reverses the function performed in the beginning by *vector* and frees the memory locations reserved for storing *matrix*.

Next, *EH_Power_calc* is called by *main*. This function calculates all the complex phasor electric and magnetic field components $(E_x(x,y), E_y(x,y), E_z(x,y), H_x(x,y), H_y(x,y), H_z(x,y))$ and all the real electric and magnetic field components $(e_x(x,y,z,t), e_y(x,y,z,t), e_z(x,y,z,t), h_x(x,y,z,t), h_y(x,y,z,t), h_z(x,y,z,t))$, given *res*, *z*, and *t*. It also calculates the power flowing down the waveguide at the z=0 plane and the maximum tangential field at the bottom and left walls. The latter is important for HTS waveguides, because if the tangential fields and surface currents in the walls exceed their respective critical values, the HTS ceases to be superconducting and becomes an insulator and power propagation becomes impossible. *EH_Power_calc* calculates the transverse field phasor quantities from *res* (i.e., the longitudinal field components) using appropriately discretized versions of equations (10)-(13). Then it uses

$$\begin{matrix} e_{x,y,z}(x,y,z,t) \\ h_{x,y,z}(x,y,z,t) \end{matrix} = \mathrm{Re}\left[\begin{matrix} E_{x,y,z}(x,y) \\ H_{x,y,z}(x,y) \end{matrix} \cdot e^{(j\omega t - \gamma z)} \right] \tag{61}$$

to calculate the real field quantities in the lower left quadrant of the waveguide cross-section ($(i,j) = \{0,1,\ldots,M\} \times \{0,1,\ldots,N\}$, see figure 9). Then, depending on the types of symmetry used in calculating the original matrix, the following equations are used to calculate the fields in the whole waveguide cross-section.

i. Top Magnetic Symmetry Plane, Right Magnetic Symmetry Plane

$e_x[i][2N-j] = e_x[i][j]$ $e_y[i][2N-j] = -e_y[i][j]$ $e_z[i][2N-j] = e_z[i][j]$ $h_x[i][2N-j] = -h_x[i][j]$ $h_y[i][2N-j] = h_y[i][j]$ $h_z[i][2N-j] = -h_z[i][j]$	$e_x[2M-i][2N-j] = -e_x[i][j]$ $e_y[2M-i][2N-j] = -e_y[i][j]$ $e_z[2M-i][2N-j] = e_z[i][j]$ $h_x[2M-i][2N-j] = -h_x[i][j]$ $h_y[2M-i][2N-j] = -h_y[i][j]$ $h_z[2M-i][2N-j] = h_z[i][j]$
FIELDS KNOWN	$e_x[2M-i][j] = -e_x[i][j]$ $e_y[2M-i][j] = e_y[i][j]$ $e_z[2M-i][j] = e_z[i][j]$ $h_x[2M-i][j] = h_x[i][j]$ $h_y[2M-i][j] = -h_y[i][j]$ $h_z[2M-i][j] = -h_z[i][j]$

ii. Top Magnetic Symmetry Plane, Right Electric Symmetry Plane

$e_x[i][2N-j] = e_x[i][j]$ $e_y[i][2N-j] = -e_y[i][j]$ $e_z[i][2N-j] = e_z[i][j]$ $h_x[i][2N-j] = -h_x[i][j]$ $h_y[i][2N-j] = h_y[i][j]$ $h_z[i][2N-j] = -h_z[i][j]$	$e_x[2M-i][2N-j] = e_x[i][j]$ $e_y[2M-i][2N-j] = e_y[i][j]$ $e_z[2M-i][2N-j] = -e_z[i][j]$ $h_x[2M-i][2N-j] = h_x[i][j]$ $h_y[2M-i][2N-j] = h_y[i][j]$ $h_z[2M-i][2N-j] = -h_z[i][j]$
FIELDS KNOWN	$e_x[2M-i][j] = e_x[i][j]$ $e_y[2M-i][j] = -e_y[i][j]$ $e_z[2M-i][j] = -e_z[i][j]$ $h_x[2M-i][j] = -h_x[i][j]$ $h_y[2M-i][j] = h_y[i][j]$ $h_z[2M-i][j] = h_z[i][j]$

iii. Top Electric Symmetry Plane, Right Magnetic Symmetry Plane

$e_x[i][2N-j] = -e_x[i][j]$ $e_y[i][2N-j] = e_y[i][j]$ $e_z[i][2N-j] = -e_z[i][j]$ $h_x[i][2N-j] = h_x[i][j]$ $h_y[i][2N-j] = -h_y[i][j]$ $h_z[i][2N-j] = h_z[i][j]$	$e_x[2M-i][2N-j] = e_x[i][j]$ $e_y[2M-i][2N-j] = e_y[i][j]$ $e_z[2M-i][2N-j] = -e_z[i][j]$ $h_x[2M-i][2N-j] = h_x[i][j]$ $h_y[2M-i][2N-j] = h_y[i][j]$ $h_z[2M-i][2N-j] = -h_z[i][j]$
FIELDS KNOWN	$e_x[2M-i][j] = -e_x[i][j]$ $e_y[2M-i][j] = e_y[i][j]$ $e_z[2M-i][j] = e_z[i][j]$ $h_x[2M-i][j] = h_x[i][j]$ $h_y[2M-i][j] = -h_y[i][j]$ $h_z[2M-i][j] = -h_z[i][j]$

iv. Top Electric Symmetry Plane, Right Electric Symmetry Plane

$e_x[i][2N-j] = -e_x[i][j]$ $e_y[i][2N-j] = e_y[i][j]$ $e_z[i][2N-j] = -e_z[i][j]$ $h_x[i][2N-j] = h_x[i][j]$ $h_y[i][2N-j] = -h_y[i][j]$ $h_z[i][2N-j] = h_z[i][j]$	$e_x[2M-i][2N-j] = -e_x[i][j]$ $e_y[2M-i][2N-j] = -e_y[i][j]$ $e_z[2M-i][2N-j] = e_z[i][j]$ $h_x[2M-i][2N-j] = -h_x[i][j]$ $h_y[2M-i][2N-j] = -h_y[i][j]$ $h_z[2M-i][2N-j] = h_z[i][j]$
FIELDS KNOWN	$e_x[2M-i][j] = e_x[i][j]$ $e_y[2M-i][j] = -e_y[i][j]$ $e_z[2M-i][j] = -e_z[i][j]$ $h_x[2M-i][j] = -h_x[i][j]$ $h_y[2M-i][j] = h_y[i][j]$ $h_z[2M-i][j] = h_z[i][j]$

The total power at z=0 is calculated using [1]

$$P = \frac{1}{2}\int_0^a \int_0^b \mathrm{Re}\left(\mathbf{E}\times\mathbf{H}^*\right)\cdot\hat{\mathbf{n}}\,dxdy \quad , \tag{62}$$

where $\hat{\mathbf{n}}$ is a unit vector normal to the surface of integration. In our case $\hat{\mathbf{n}} = \hat{\mathbf{z}}$, and therefore (62) becomes

$$P = \frac{1}{2}\int_0^a \int_0^b \mathrm{Re}\left(E_x H_y^* - E_y H_x^*\right)dxdy \quad . \tag{63}$$

When discretized equation (63) becomes

$$\begin{aligned} P = \frac{1}{2}\mathrm{Re}\Bigg\{ & 4\sum_{i=0}^{M-1}\sum_{j=0}^{N-1}\left[E_x(i,j)H_y^*(i,j) - E_y(i,j)H_x^*(i,j)\right] + \\ & + 2\sum_{i=0}^{M-1}\left[E_x(i,N)H_y^*(i,N) - E_y(i,N)H_x^*(i,N)\right] + \\ & + 2\sum_{j=0}^{N-1}\left[E_x(M,j)H_y^*(M,j) - E_y(M,j)H_x^*(M,j)\right] + \\ & + E_x(M,N)H_y^*(M,N) - E_y(M,N)H_x^*(M,N)\Bigg\}\Delta x\Delta y \end{aligned} \tag{64}$$

which is used for the power calculation.

The maximum tangential magnetic fields at the bottom and left walls (and therefore, by symmetry, also to the top and right wall) are calculated next. It can be shown, by differentiating and setting the derivative equal to zero, that the maximum real field value, with respect to phase, for two vectorially added phasors normal to each other is (using $\mathbf{H}_x$ and $\mathbf{H}_z$ at the bottom wall as an example)

$$h_{\max} = \sqrt{\frac{1}{2}\left[H_{xr}^2 + H_{xi}^2 + H_{zr}^2 + H_{zi}^2 + \sqrt{\left(H_{xr}^2 - H_{xi}^2 + H_{zr}^2 - H_{zi}^2\right)^2 + 4\left(H_{xr}H_{xi} + H_{zr}H_{zi}\right)^2}\right]} \tag{65}$$

where $H_{xr} = \mathrm{Re}(\mathbf{H}_x)$, $H_{xi} = \mathrm{Im}(\mathbf{H}_x)$, $H_{zr} = \mathrm{Re}(\mathbf{H}_z)$ and $H_{zi} = \mathrm{Im}(\mathbf{H}_z)$. The function *EH_Power_calc* returns the calculated power and maximum tangential magnetic fields to *main*, which prints these values to the standard output.

Next *main* calls *openplot*. This function calls four Fortran library routines (*OPNGKS*, *GQCNTN*, *GSELNT* and *WTSTR*) that initialize the *NCAR Graphics* software package on the CRAY [10]. This Graphics package uses a number of Fortran routines that create graphs and write the output in Computer Graphics Metafiles (CGM) which can then be viewed on an X11 host via the Internet, or plotted in Hewlett-Packard Graphics Language (HPGL) file format.

The function *main* then calls *plotmatr* which takes and plots a vector velocity field, given two matrices of vector components. Th function *plotmatr* uses the *NCAR Graphics* routine *EZVEC*. *plotmatr* is called twice, to plot the cross-sectional view of the electric and magnetic fields in the z=0 plane, respectively. The plot goes to an output CGM called *gmeta*, by default.

Then *calc_long* is called. The function *calc_long* calls *EH_Power_calc NOFDZ* times (*NOFDZ* is defined before *main* and presently equals 65) and calculates all the real field quantities on *NOOFDZ* uniformly spaced cross-sectional planes. The spacing between the planes is necessarily equal to Δx, because the plotting routine *EZVEC* assumes the plotted grid points to be equi-spaced in both directions. The field components along three different planes are stored in new variables for plotting purposes. The planes chosen are the $j = N$ $(y = \frac{b}{2})$ plane for both **e** and **h**, the $i = M$ $(x = \frac{a}{2})$ plane for **e** and the $i = 2M$ $(x = a)$ plane for **h**.

Next *plotmatr* is called four times successively to plot the four field snapshots described above in *gmeta*. Finally, *closeplot*, whose purpose is to close *gmeta*, is called. The function *closeplot* simply calls the *NCAR Graphics* Fortran library routine *CLSGKS* and returns. Then the program returns and execution terminates. On exit, three views of the electric and magnetic fields are saved in *gmeta*: a cross-sectional view, a surface view and a longitudinal view.

8.4.4 Running the Program

The program is compiled on the JPL CRAY Y-MP2E computer *voyager* and on the Goddard Space Flight Center CRAY C98 computer *charney*. On August 30, 1992 charney was upgraded from an 8 processor CRAY Y-MP2E to a 6 processor CRAY C98. The difference in CPU time from voyager is dramatic. The program runs 4 to 5 times faster on voyager than on charney. Also the maximum memory available in the queues of voyager is 16 MW (MegaWords) whereas on charney it is 60 MW. Because of these advantages the program is mainly run on charney and these statistics will be reported here. The SVD and plotting parts of the program are only required for plotting the fields out and are CPU intensive, time-costly and memory-hungry. If one only wants to know accurate propagation characteristics of an HTS waveguide for a range of frequencies, it is better to implement another program without these features (i.e., with the code terminating right after *amoeba* and iterating for a range of frequencies). This stripped-down version of the program is called *wg_sweep.c*. The purpose of *wg_sweep* is to accurately calculate Υ for a range of frequencies in the minimum possible time, whereas that of *wg_plot* is to calculate and plot the fields for a single frequency and mode. In *wg_sweep* a grid as dense as possible is required (i.e., maximum M and N given memory and time constraints). In *wg_plot*, too dense a grid would not only make execution very slow, but also would make the final plots of the fields crowded and almost unreadable. Following are some of the statistics of the program. An example of the output of *wg_sweep* is included as appendix E of this chapter.

8.4.4.1 CPU Time and Memory Usage

The main memory storage requirement is due to the need of storing *matrix*. Its size is $2 \cdot ROWLENGTH^{\,2}$ Words, or $8(M+1)^2(N+1)^2$ Words. It has been empirically found

that the program is most accurate when $\Delta x = \Delta y$. Hence, for the usual waveguides ($b/a = 0.5$), $M = 2N$ is a good rule of thumb to observe. Given an upper memory limit of 60 MW (or 62914560 Words) the maximum M usable is 72, noting that some extra memory has to be reserved for the rest of the variables. As only one quarter of the waveguide is sub-sectioned, the effective grid size, in this case, is 144-by-72. With this grid size charney can analyze one frequency in about 3.5 CPU hours. The maximum CPU time limit on any job is 4 hours. Therefore the memory ceiling and the time ceiling are well matched. However the 144-by-72 grid is found to be unnecessarily fine and the values for M and N used in *wg_sweep* are M=58, N=29, which are equivalent to a 116-by-58 effective grid size. With this grid size *wg_sweep* needs 25 MW of memory and charney can analyze about 9 frequencies in 4 CPU hours. It has been found that the CPU time required to run a given job roughly obeys the law $CPU\ Time \propto ROWLENGTH^{2.2}$.

The standard M and N values used in *wg_plot* are M=30, N=15. These have been found to provide fairly accurate results with good arrow density in the output field plots. With this grid size *wg_plot* needs 3 MW of memory and charney executes it in 5 CPU minutes.

8.4.5 The Results

Figure 10 defines the cut-planes, across the body of the waveguide, on which the fields are plotted in the following figures.

Figures 11-15 show examples of the output of *wg_plot* for the TE10 mode of a WR90 HTS

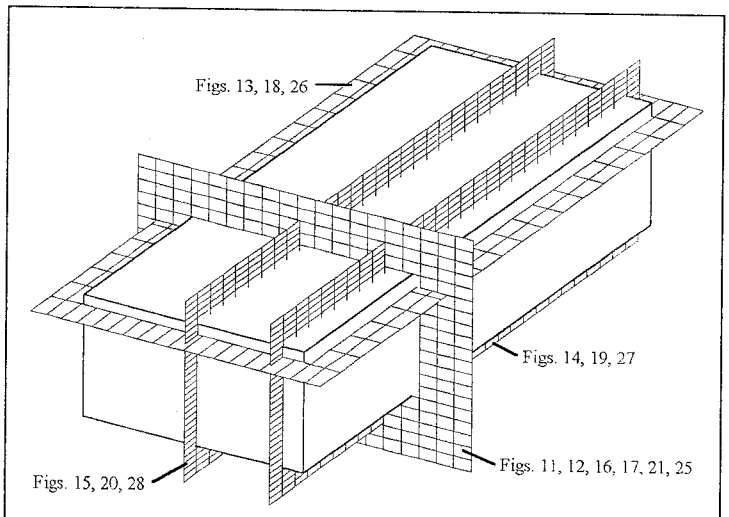

Figure 10 Definitions of the cut-planes of the field plots.

waveguide, of average HTS parameters, at 12 GHz. In this lowest frequency example, there is no visible difference between the calculated fields and the ideal fields of a perfect-conductor WR90 waveguide.

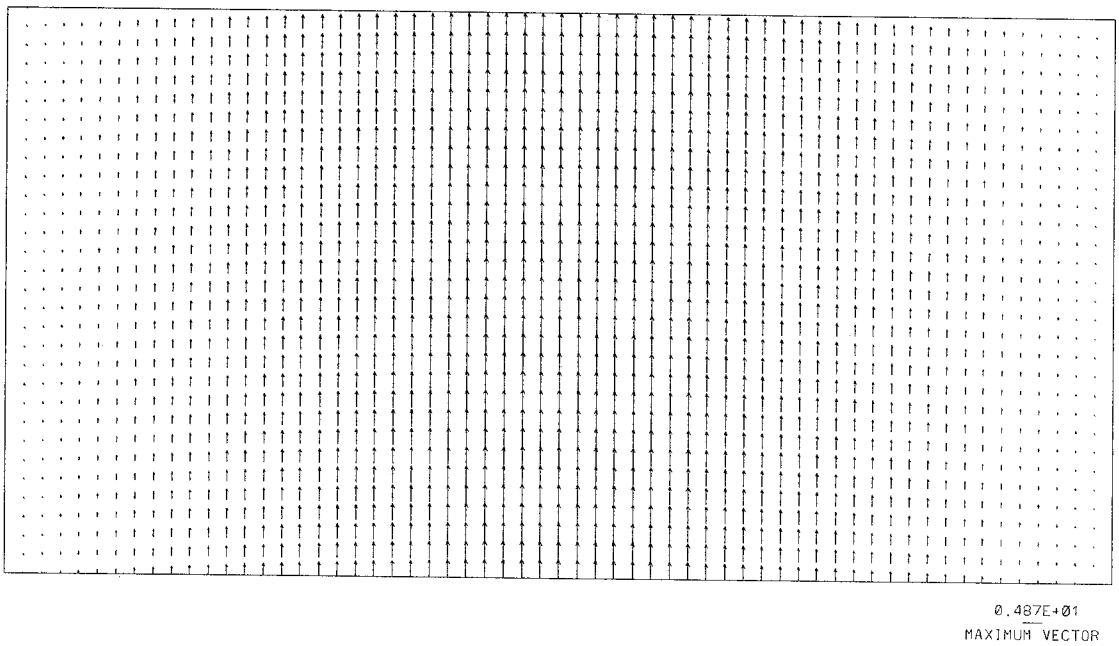

Figure 11 Cross-sectional view of the electric field of the TE10 mode in a WR90 HTS waveguide of average HTS parameters at 12 GHz.

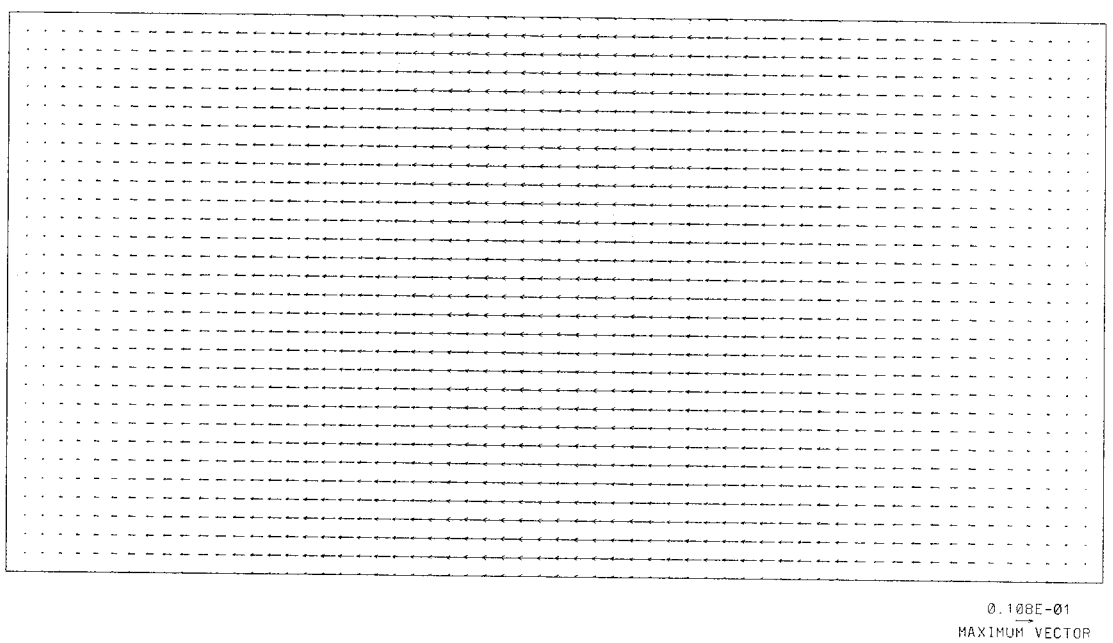

Figure 12 Cross-sectional view of the magnetic field of the TE10 mode in a WR90 HTS waveguide of average HTS parameters at 12 GHz.

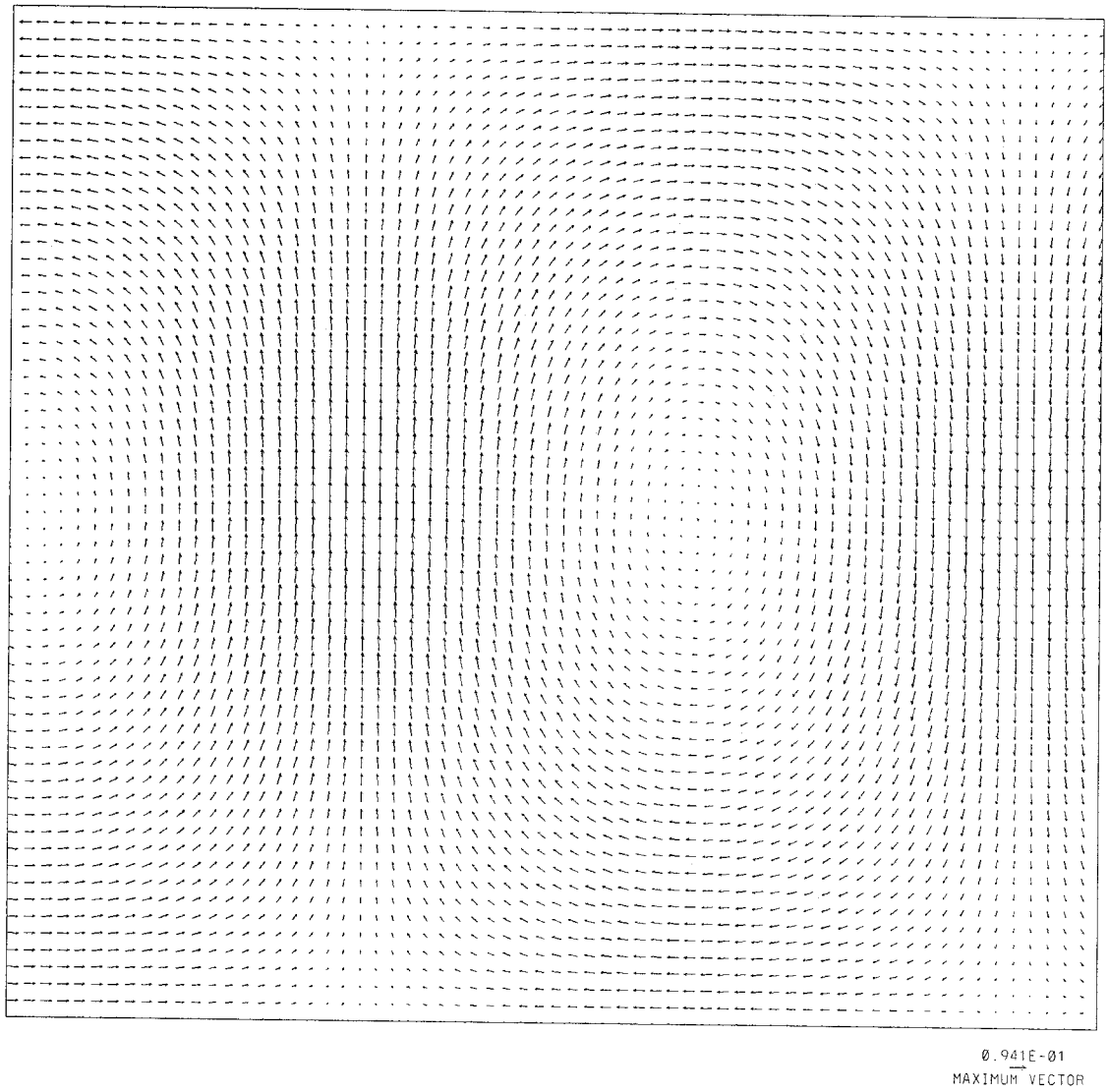

Figure 13 Surface view of the magnetic field of the TE10 mode in a WR90 HTS waveguide of average HTS parameters at 12 GHz.

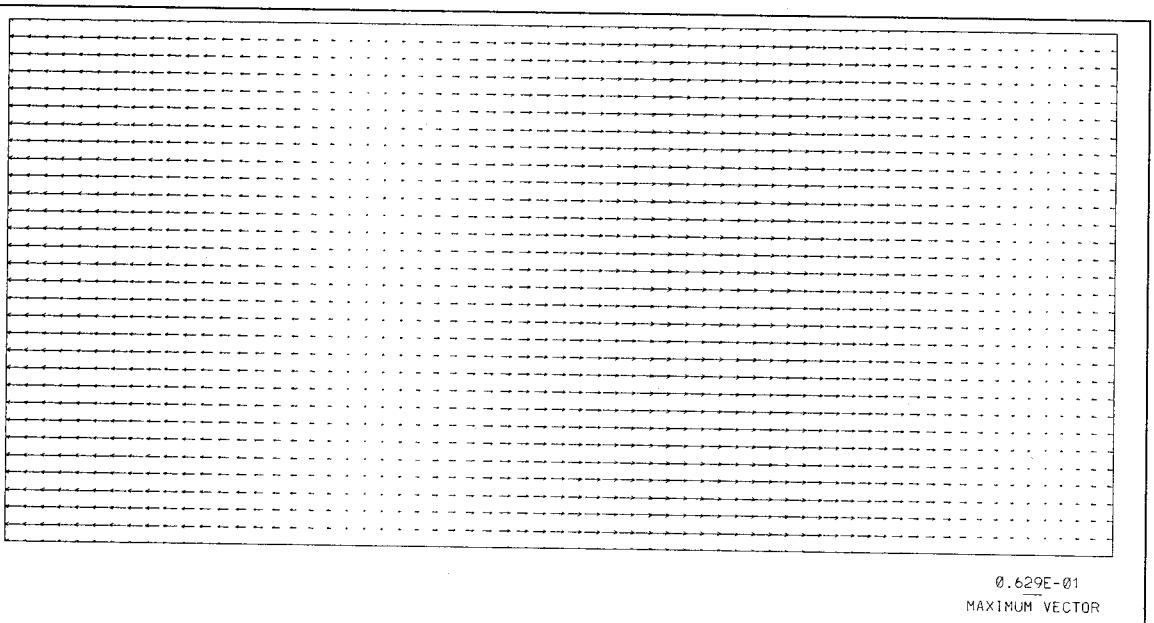

Figure 14 Longitudinal view of the magnetic field of the TE10 mode in a WR90 HTS waveguide of average HTS parameters at 12 GHz.

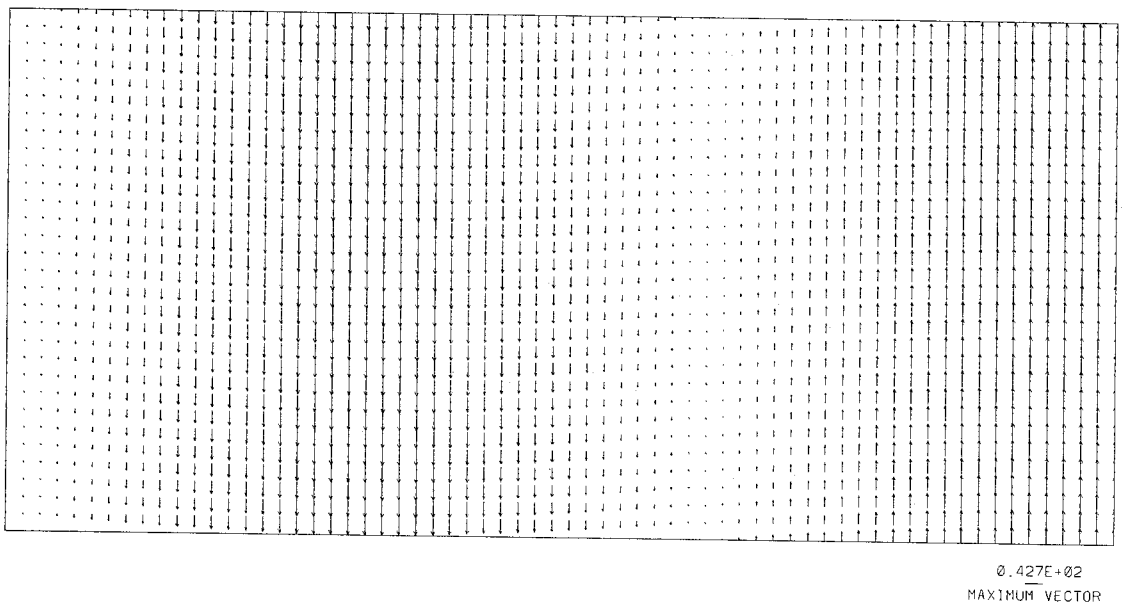

Figure 15 Longitudinal view of the electric field of the TE10 mode in a WR90 HTS waveguide of average HTS parameters at 12 GHz.

Figures 16-20 show examples of the output of *wg_plot* for the TM32 mode of a WR90 HTS waveguide with the average set of parameters at 12 GHz. The TM32 mode is more "interesting" and has more salient features than the TE10 more, and is, therefore, a better example to help illustrate the validity of the results of *wg_plot*.

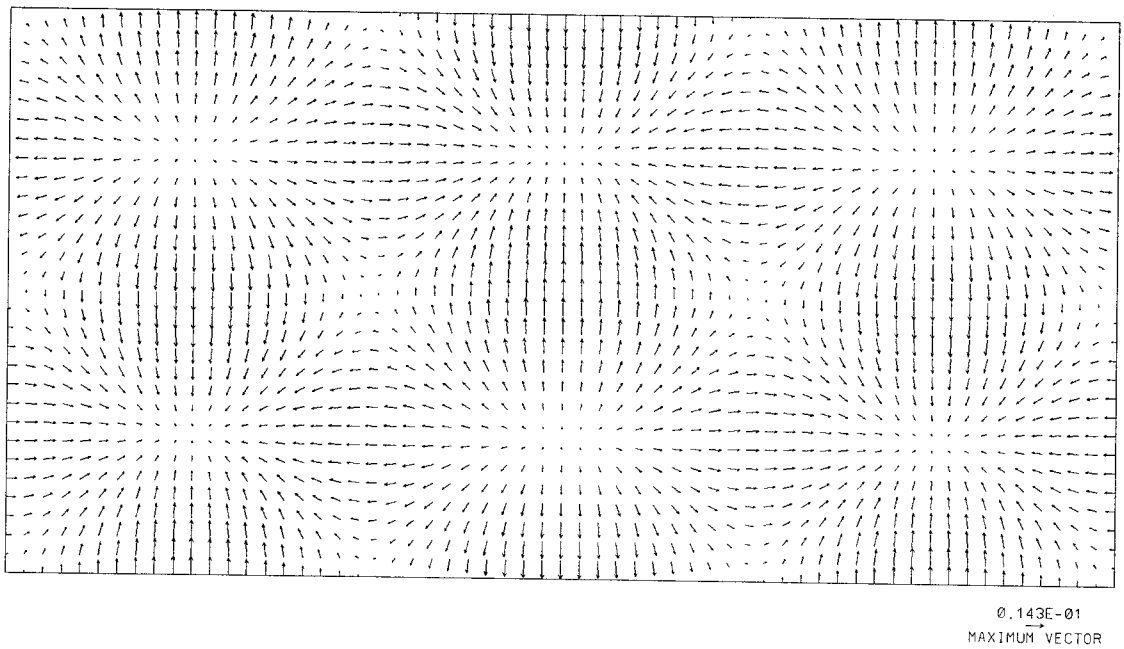

Figure 16 Cross-sectional view of the electric field of the TM32 mode in a WR90 HTS waveguide of average HTS parameters at 40 GHz.

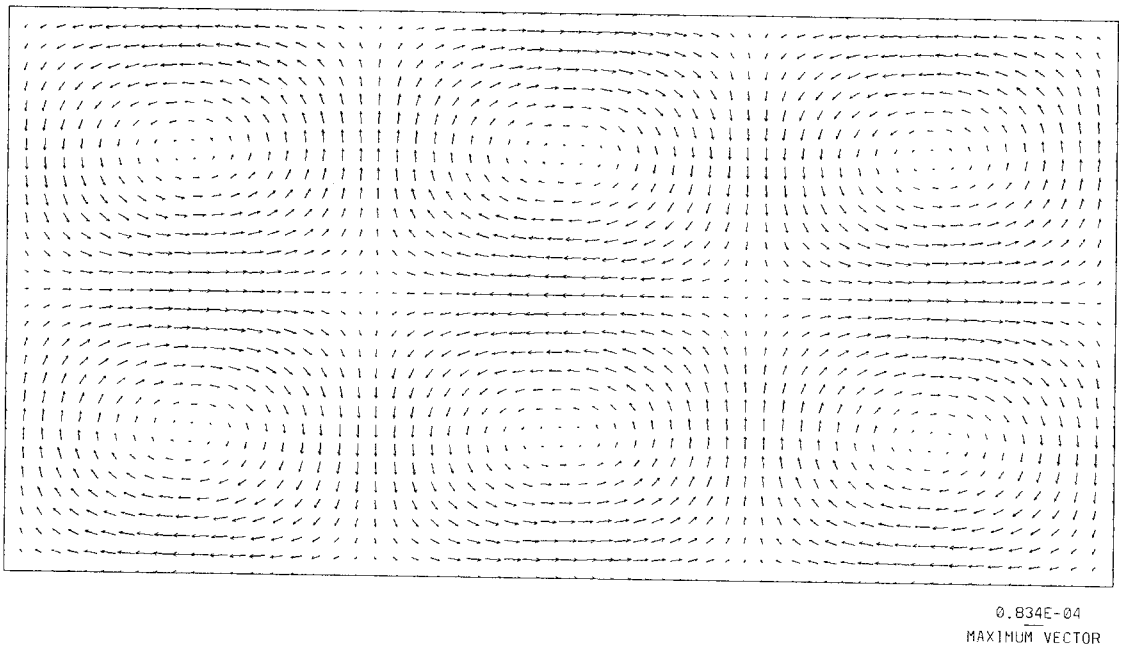

Figure 17 Cross-sectional view of the magnetic field of the TM32 mode in a WR90 HTS waveguide of average HTS parameters at 40 GHz.

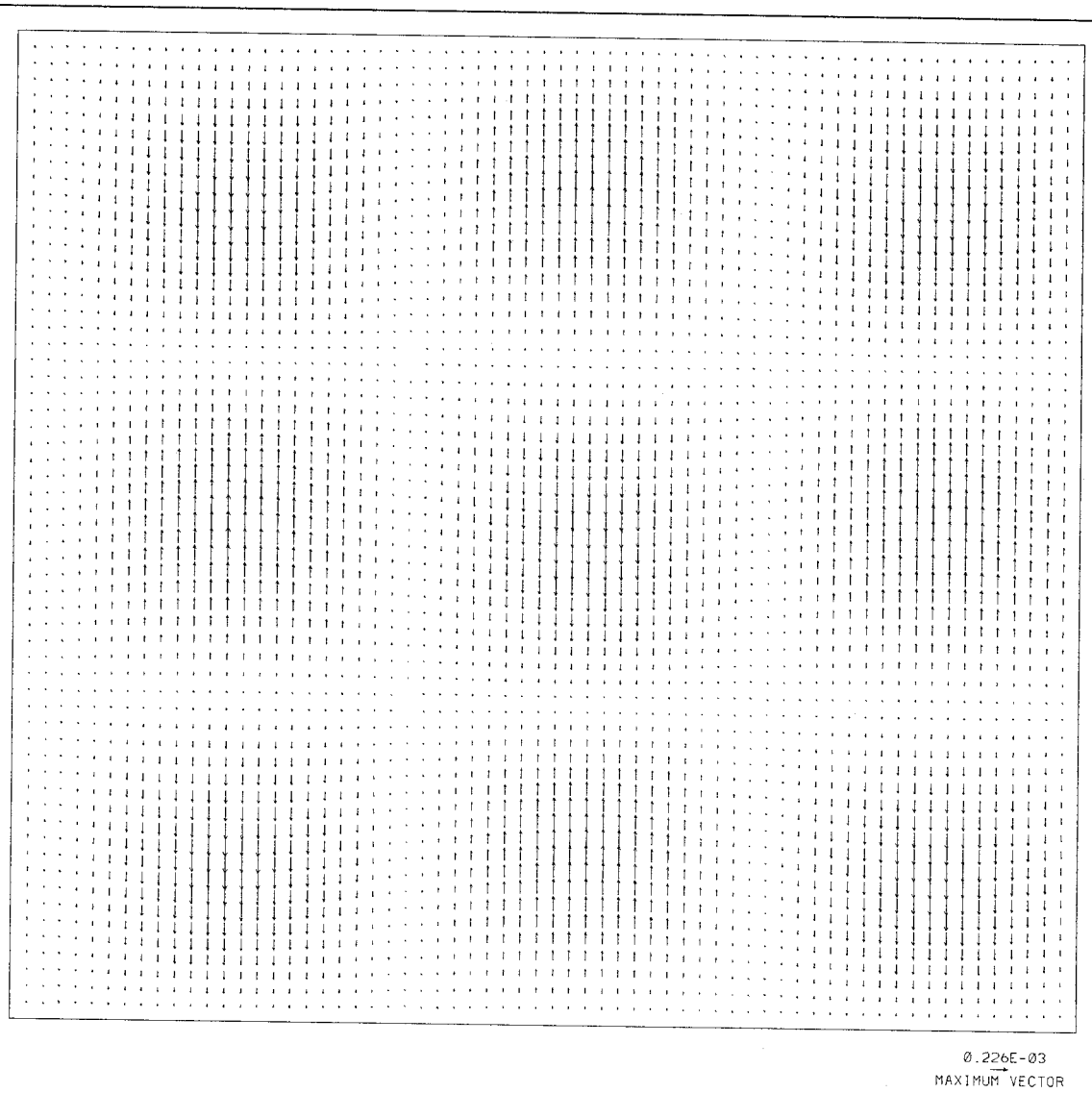

Figure 18 Surface view of the magnetic field of the TM32 mode in a WR90 HTS waveguide of average HTS parameters at 40 GHz.

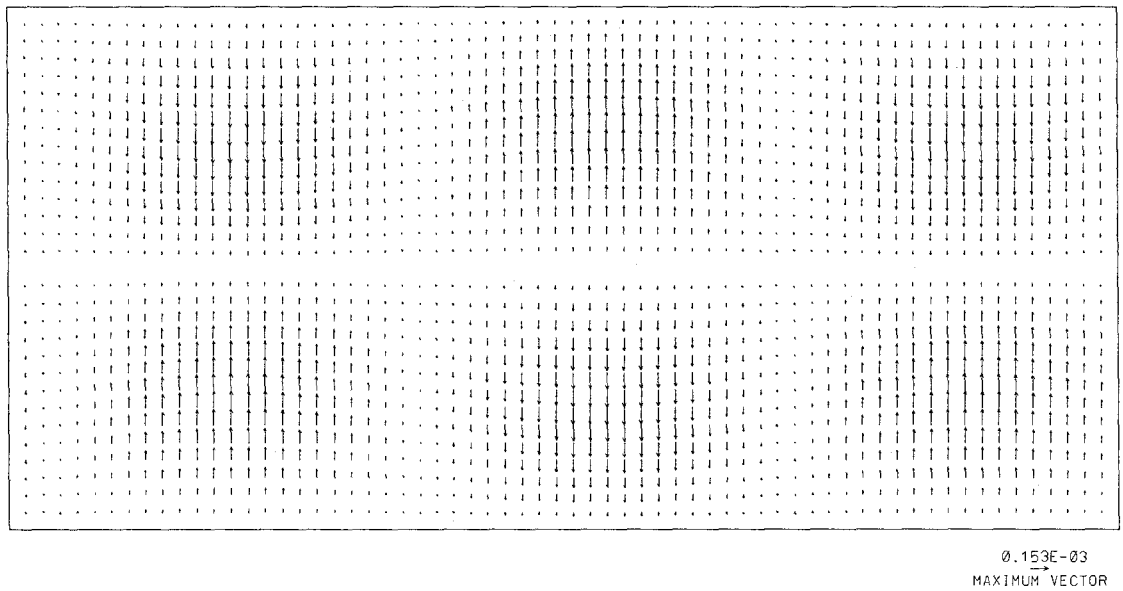

Figure 19 Longitudinal view of the magnetic field of the TM32 mode in a WR90 HTS waveguide of average HTS parameters at 40 GHz.

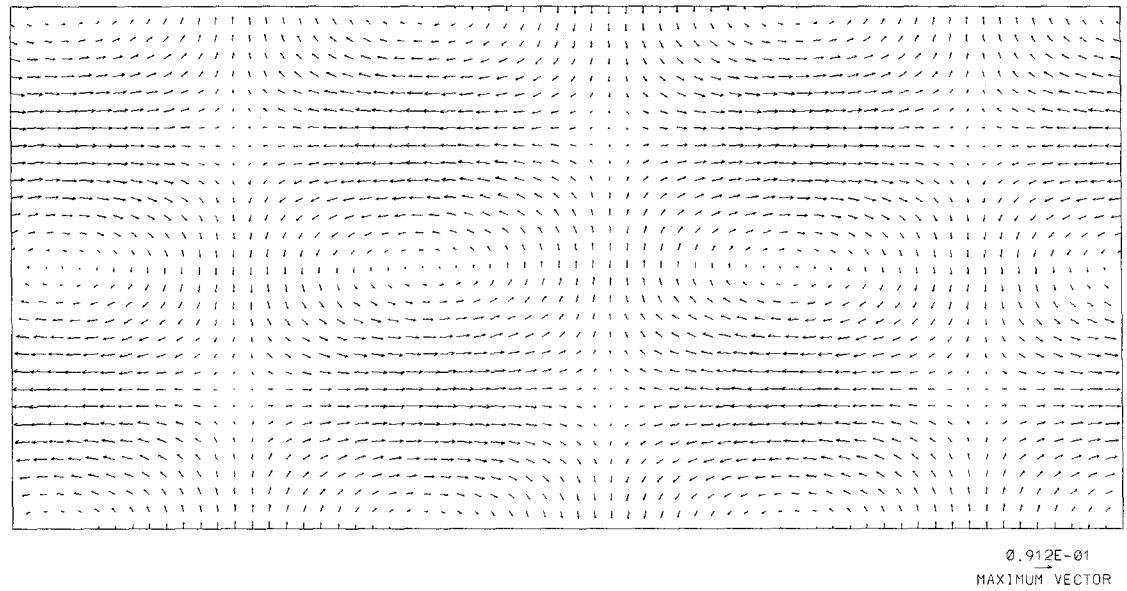

Figure 20 Longitudinal view of the electric field of the TM32 mode in a WR90 HTS waveguide of average HTS parameters at 40 GHz.

In both the examples above the average HTS parameters are used and therefore the surface resistance of the walls is small (less than 0.2, see figure 8). Hence, as expected, the fields in figures 11-20 look like the fields in a waveguide with perfectly conducting walls. To consider an example where there is a visible difference between the fields of a

waveguide with perfectly conducting walls and a waveguide with HTS walls, the HTS parameters must be chosen so that the magnitude of the surface impedance is large. Hence the best example is at a high frequency and with the worst case HTS parameters (see table 1). Figure 21 is an arrow plot of the cross-sectional view of the electric field of the TE10 mode in a WR3 HTS waveguide of the worst case HTS parameters at 380 GHz.

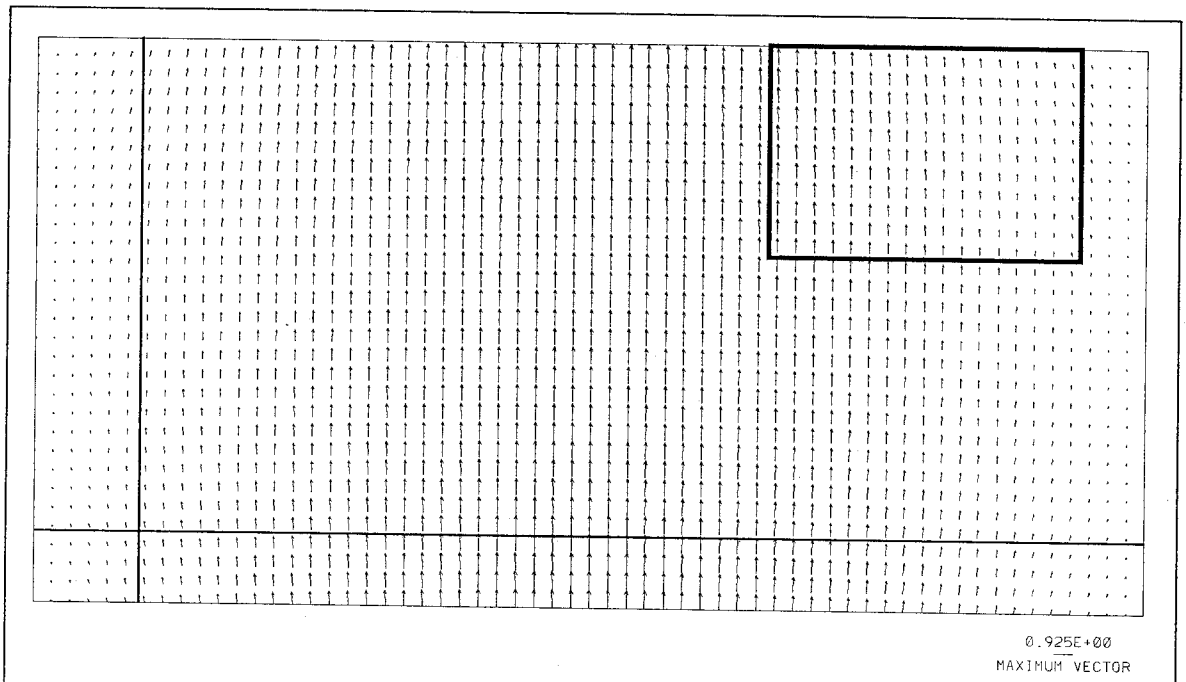

Figure 21 Cross-sectional view of the electric field of the TE10 mode in a WR3 HTS waveguide of worst-case HTS parameters at 380 GHz.

Figure 22 is a blow-up of the region of figure 21 below and to the right of the center of the top wall, as shown in figure 21. Figures 23 and 24 are plots of the angle of deviation of the electric field vectors from their (ideal) vertical orientation, along the vertical line and horizontal lines shown in figure 21, respectively.

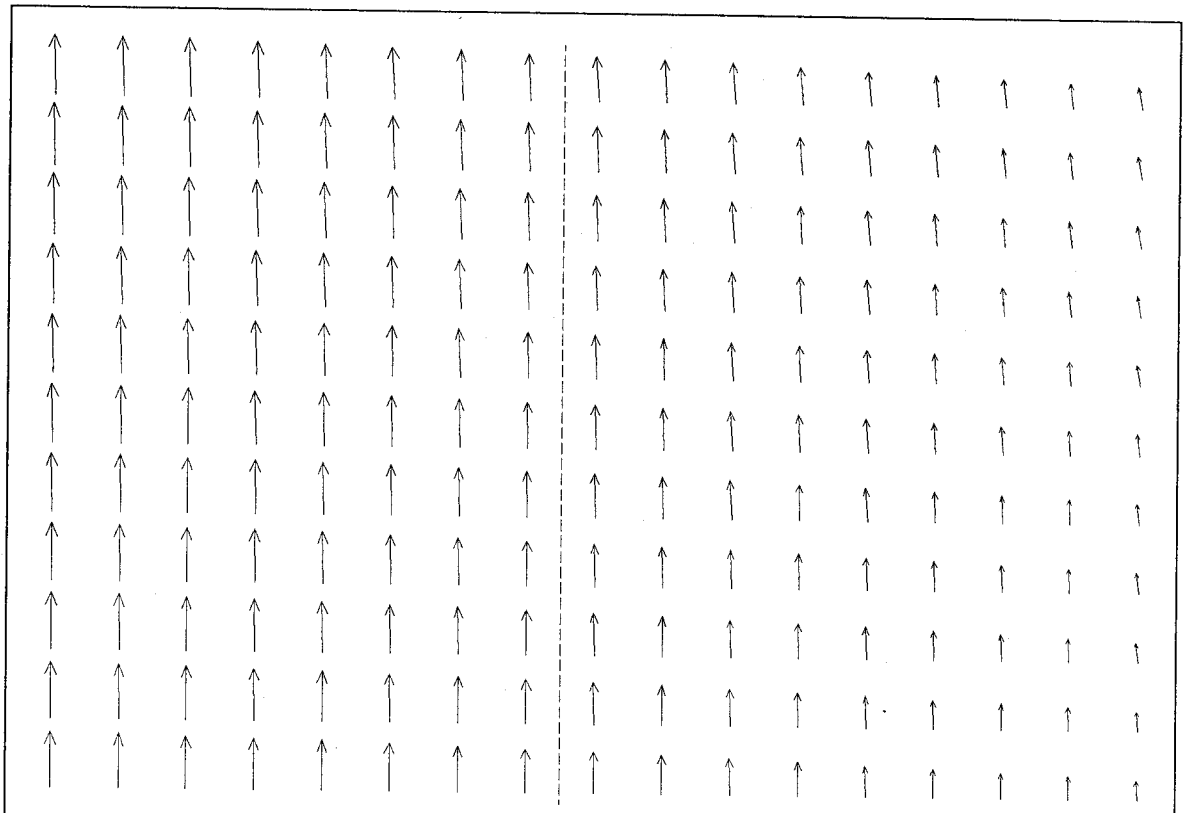

Figure 22 Blow-up of the region of figure 19 below and to the right of the middle of the top wall. The vertical line in the middle is drawn for eye-reference.

Clearly, the electric field is not purely y-directed as in the case of a waveguide with perfectly conducting walls. Here, the electric field visibly bows in away from the perpendicular bisector of the top and bottom walls. The x-component of the electric field is required to produce the surface current that supports the necessary magnetic field at the wall. Figure 25 shows a cross-sectional view of the magnetic field for the same waveguide.

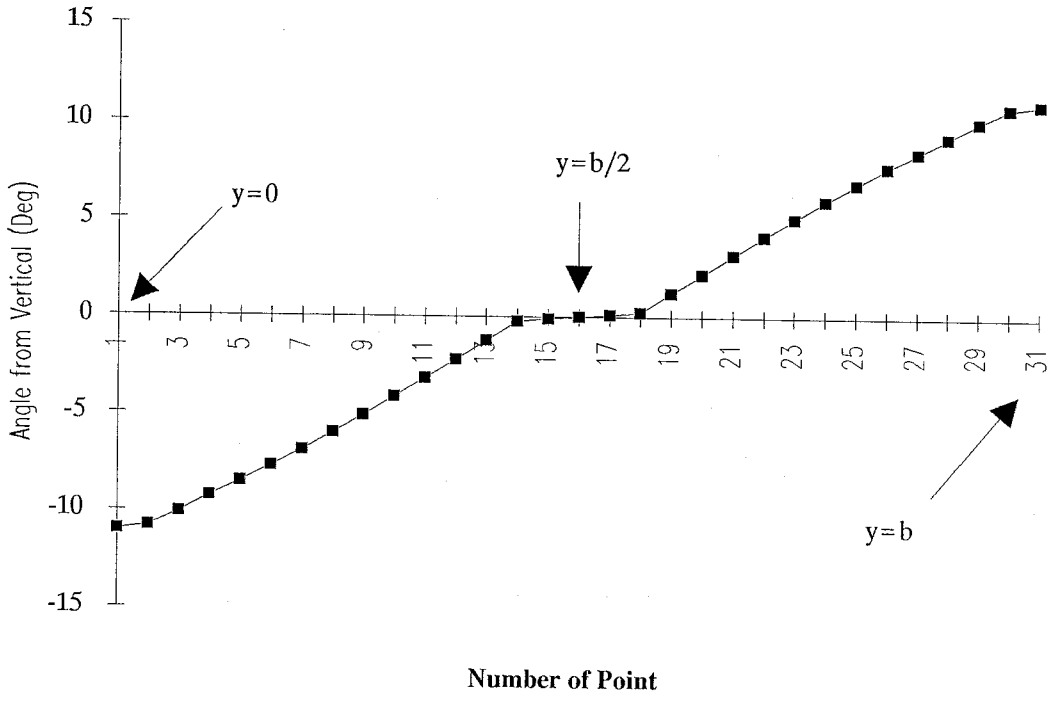

Figure 23 Deviation angle of the electric field vectors from the vertical, along a line parallel to the y-axis.

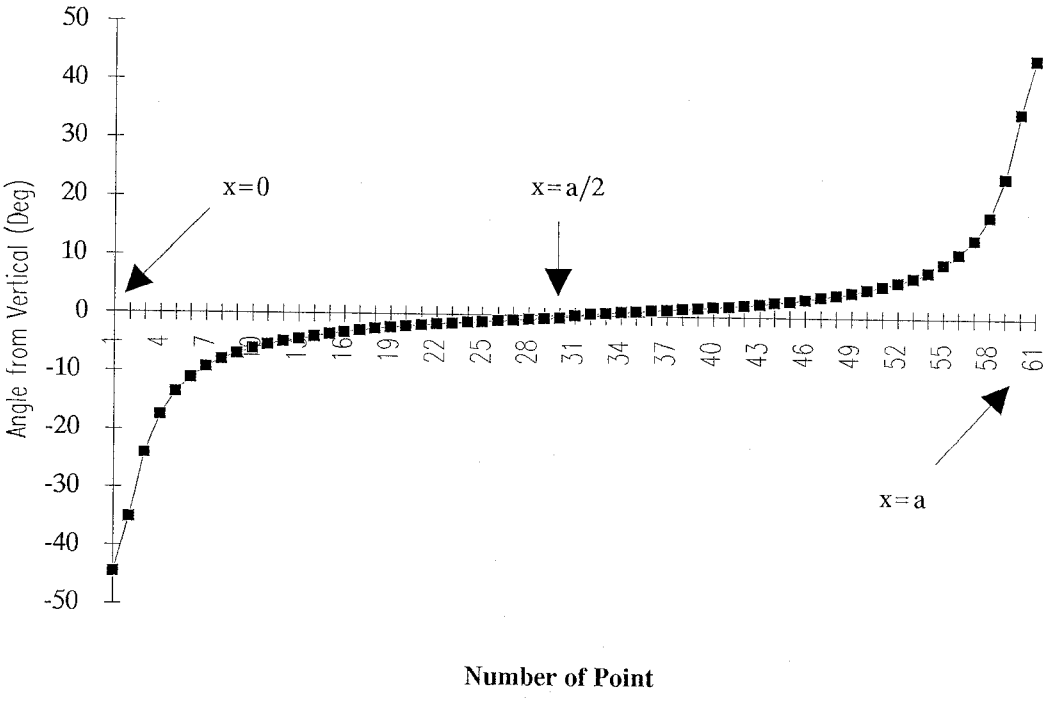

Figure 24 Deviation angle of the electric field vectors from the vertical, along a line parallel to the x-axis.

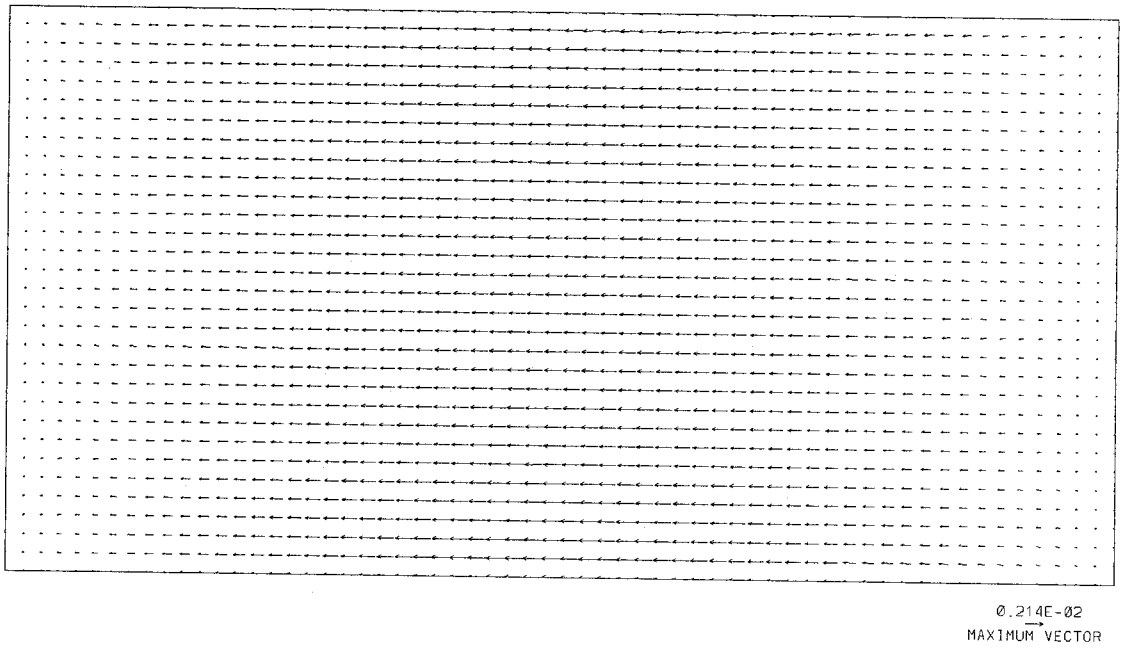

Figure 25 Cross-sectional view of the magnetic field of the TE10 mode in a WR3 HTS waveguide of worst-case HTS parameters at 380 GHz.

Although there are slight differences between figures 11 and 22, there is no noticeable systematic difference as in the case of figures 10 and 20. The magnetic field is not affected as strongly by the existence of the high surface impedance.

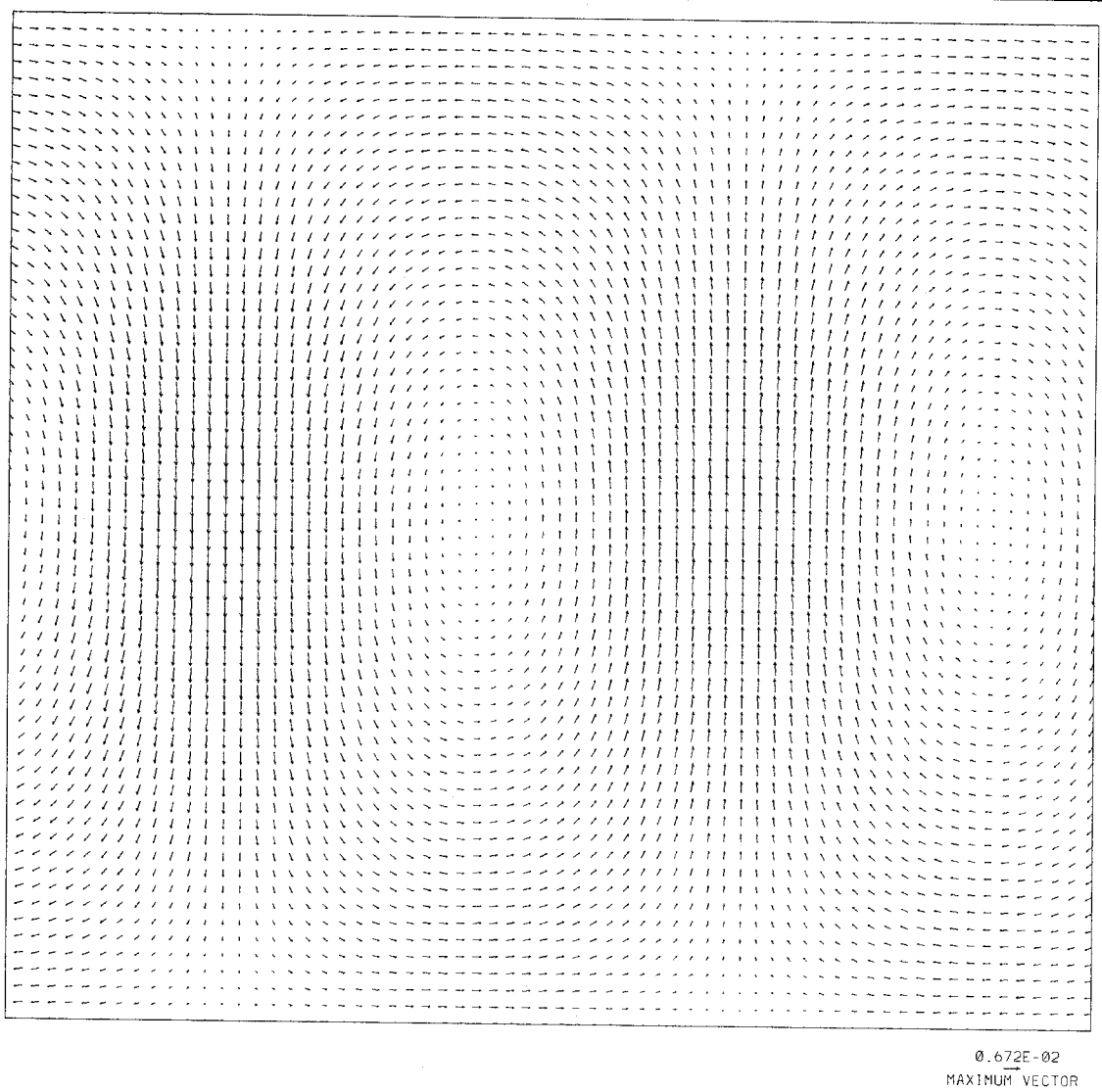

Figure 26 Surface view of the magnetic field of the TE10 mode in a WR3 HTS waveguide of worst-case HTS parameters at 380 GHz.

Figure 26 and figure 13 are very similar, and there are no salient differences between them. This confirms that the magnetic field solution is not very affected by the high surface impedance of this example. Figure 27 shows the longitudinal view of the magnetic field, which supports the same conclusion (compare with figure 14).

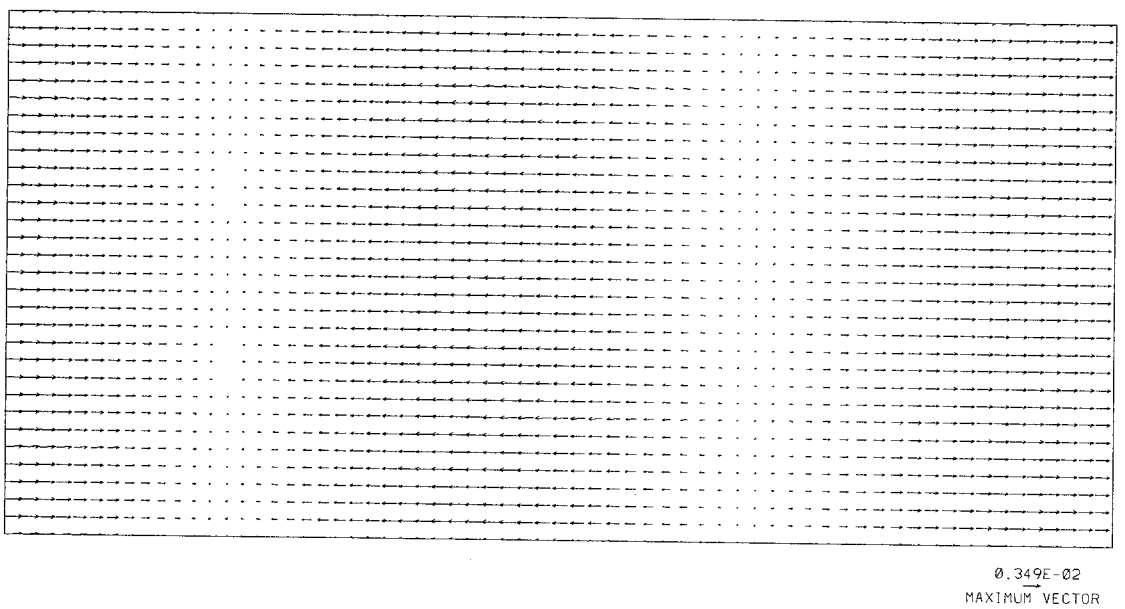

Figure 27 Longitudinal view of the magnetic field of the TE10 mode in a WR3 HTS waveguide of worst-case HTS parameters at 380 GHz.

Figure 28 shows a longitudinal view of the electric field in the waveguide.

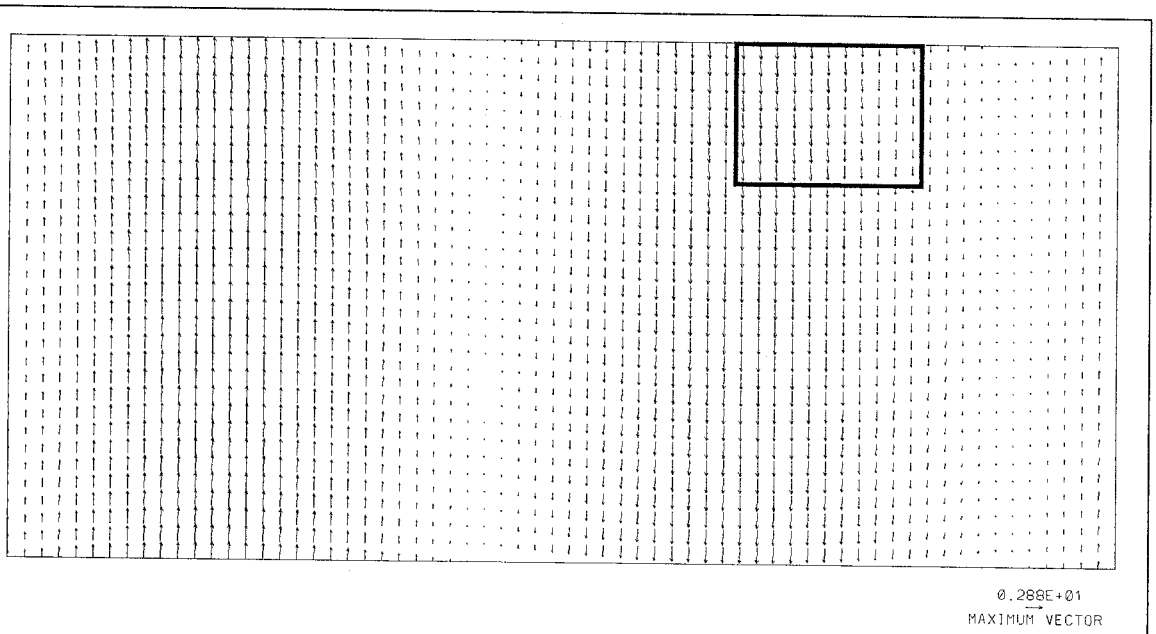

Figure 28 Longitudinal view of the electric field of the TE10 mode in a WR3 HTS waveguide of worst-case HTS parameters at 380 GHz.

Here again we see the electric field solution depart from the pure TE character, and a longitudinal component appears. Figure 29 is a blow-up of a region of figure 28, right under the top wall, showing this effect, as shown in figure 28.

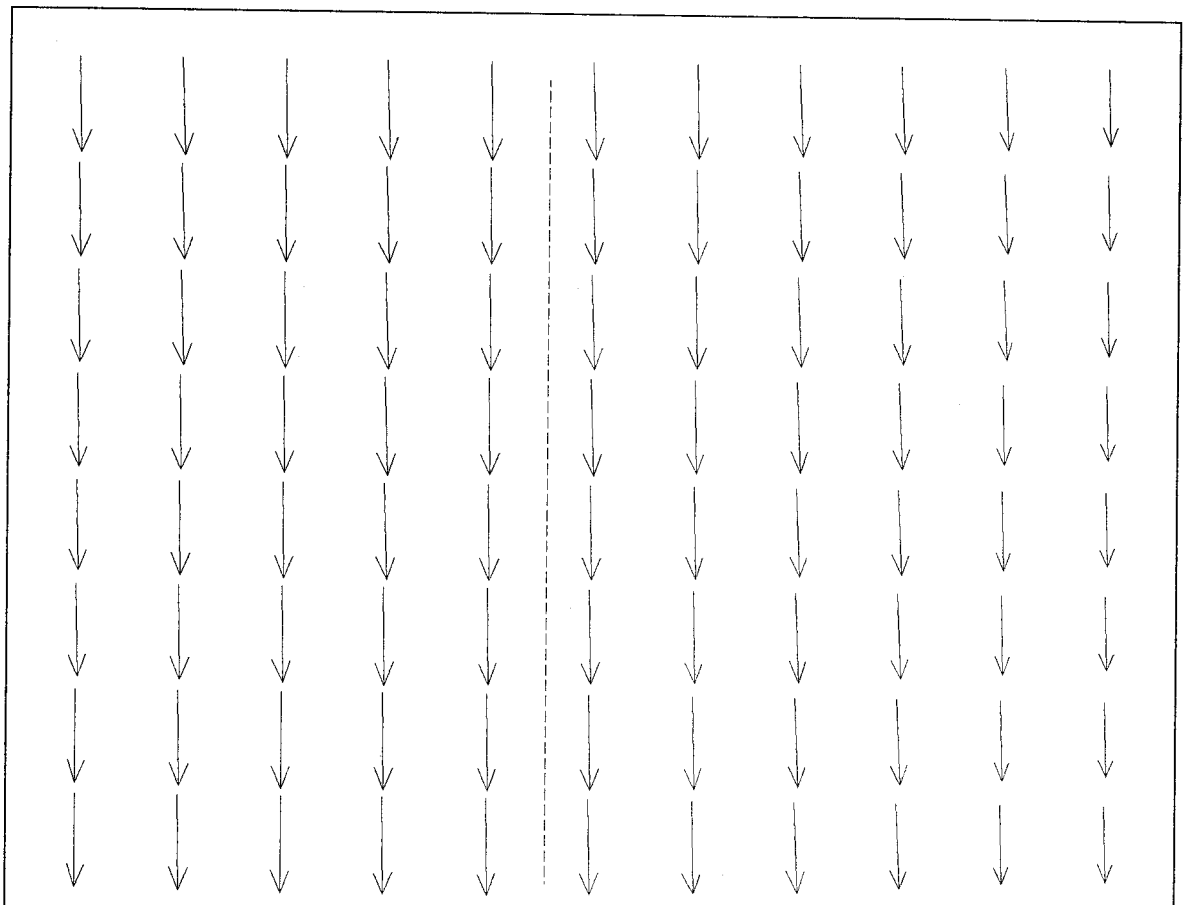

Figure 29 Blow-up of the region of figure 25 below and to the right of the middle of the top wall. The vertical line in the middle is drawn for eye-reference.

The following 10 figures are plots of attenuation and propagation constant versus frequency comparing the theoretical values (equations (5) and (52)) to the output of *wg_sweep*.

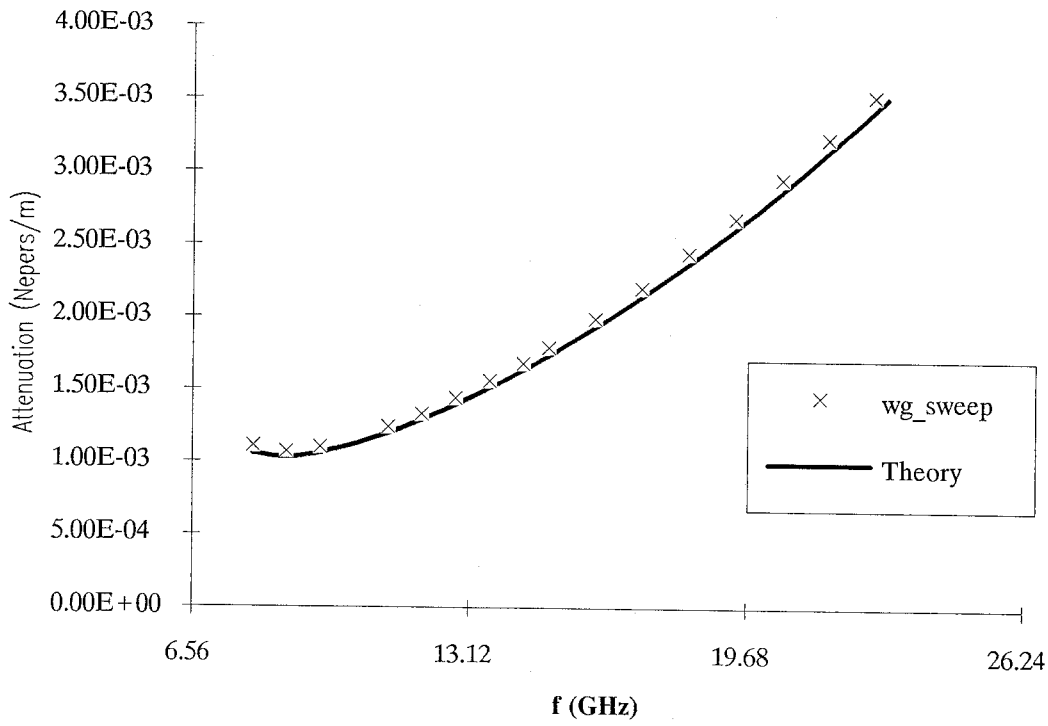

Figure 30 Attenuation versus frequency in a WR90 HTS waveguide.

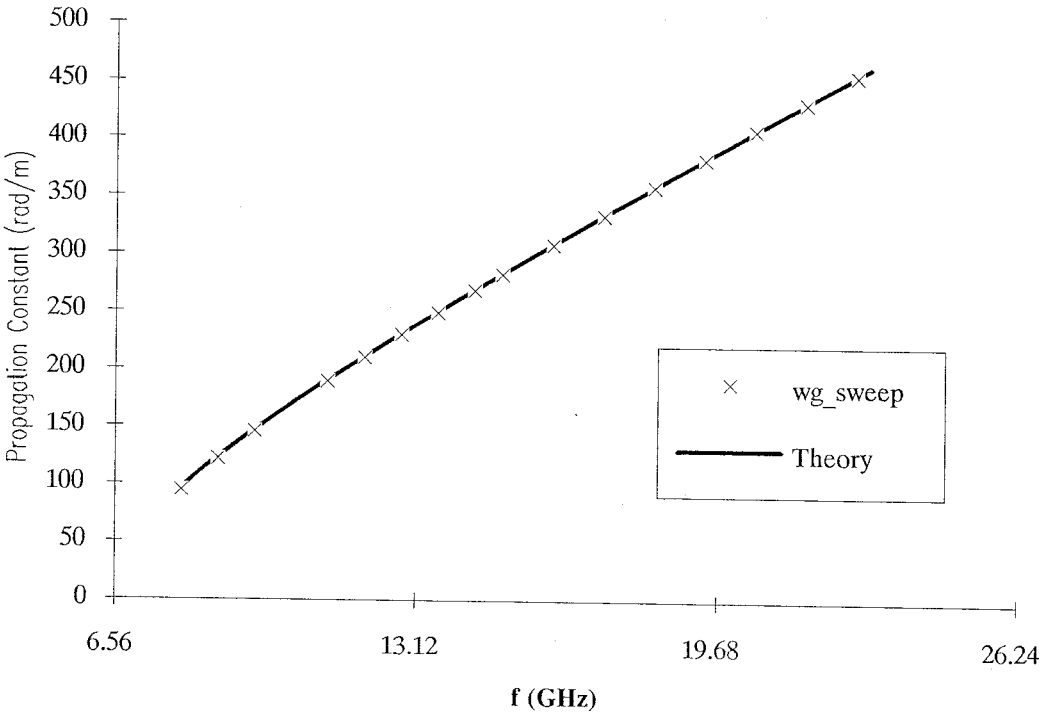

Figure 31 Propagation constant versus frequency in a WR90 HTS waveguide.

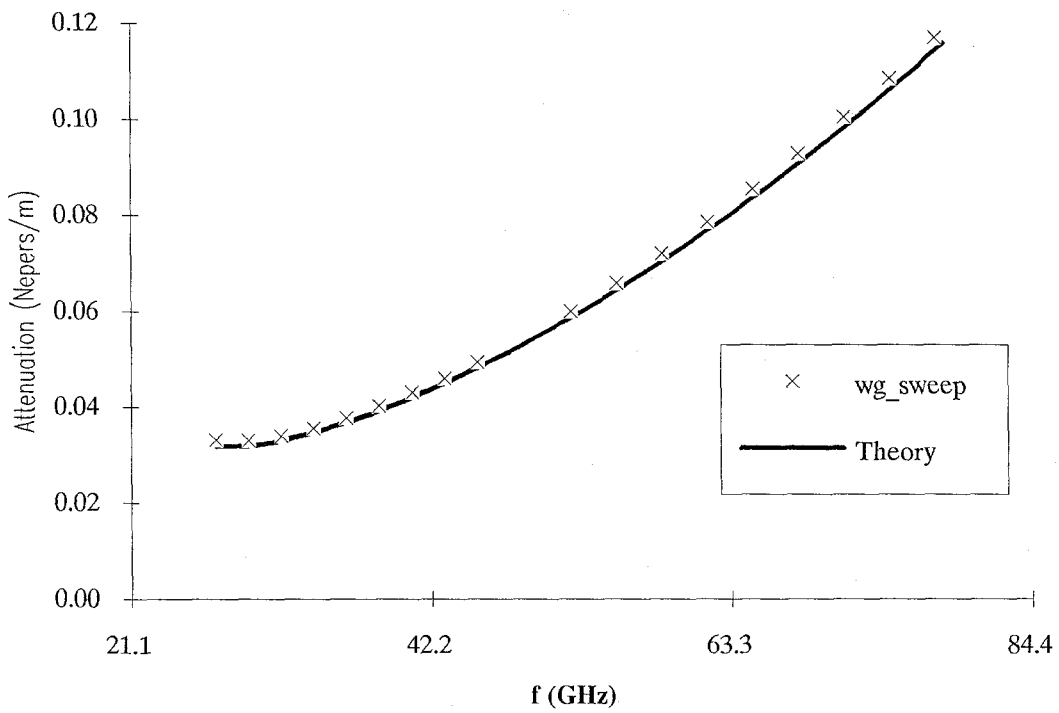

Figure 32 Attenuation versus frequency in a WR28 HTS waveguide.

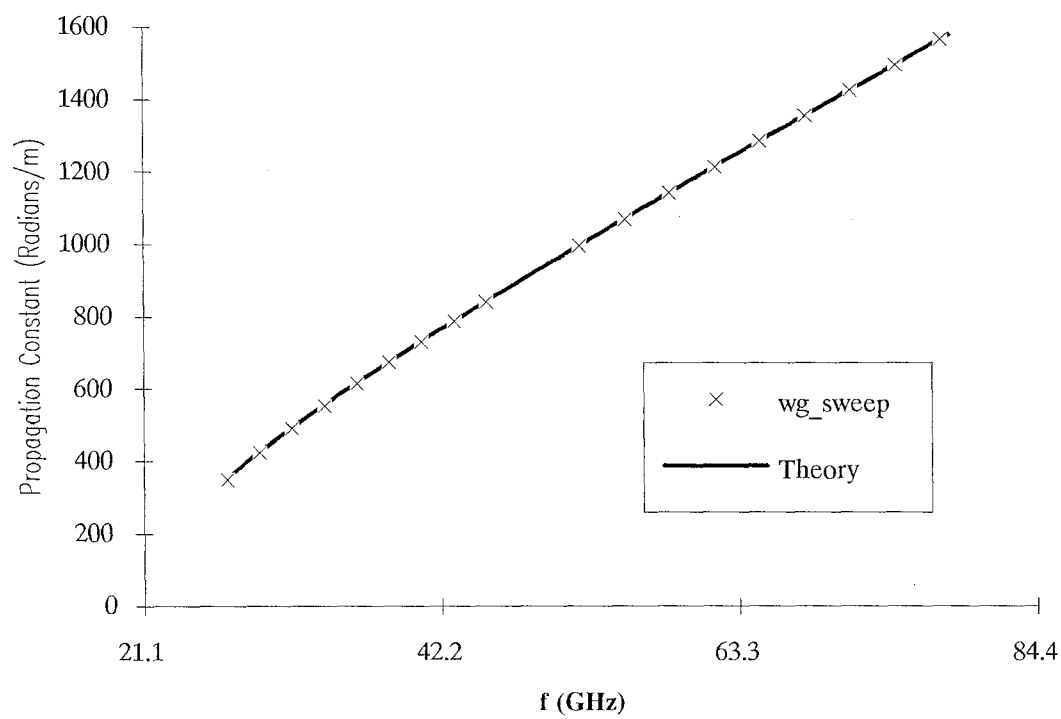

Figure 33 Propagation constant versus frequency in a WR28 HTS waveguide.

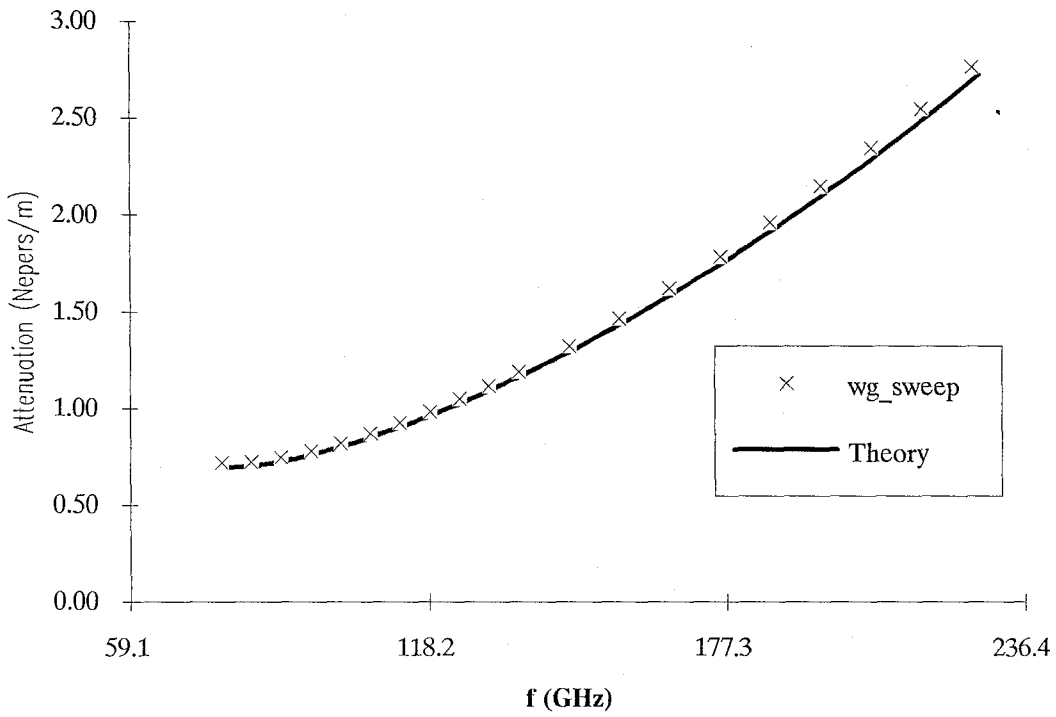

Figure 34 Attenuation versus frequency in a WR10 HTS waveguide.

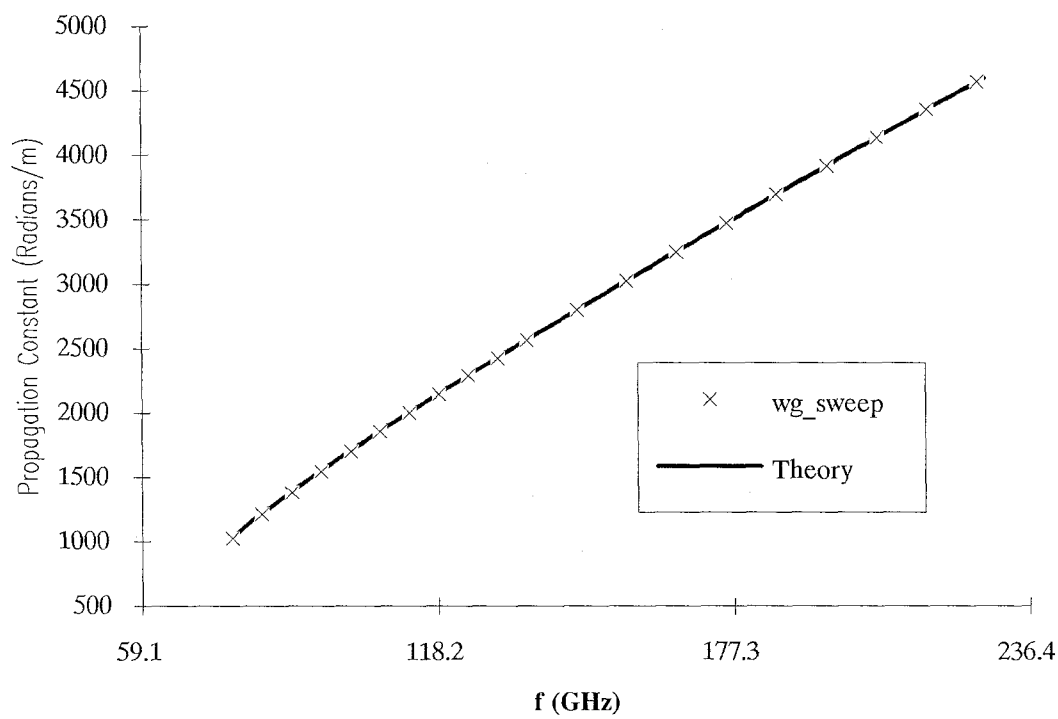

Figure 35 Propagation constant versus frequency in a WR10 HTS waveguide.

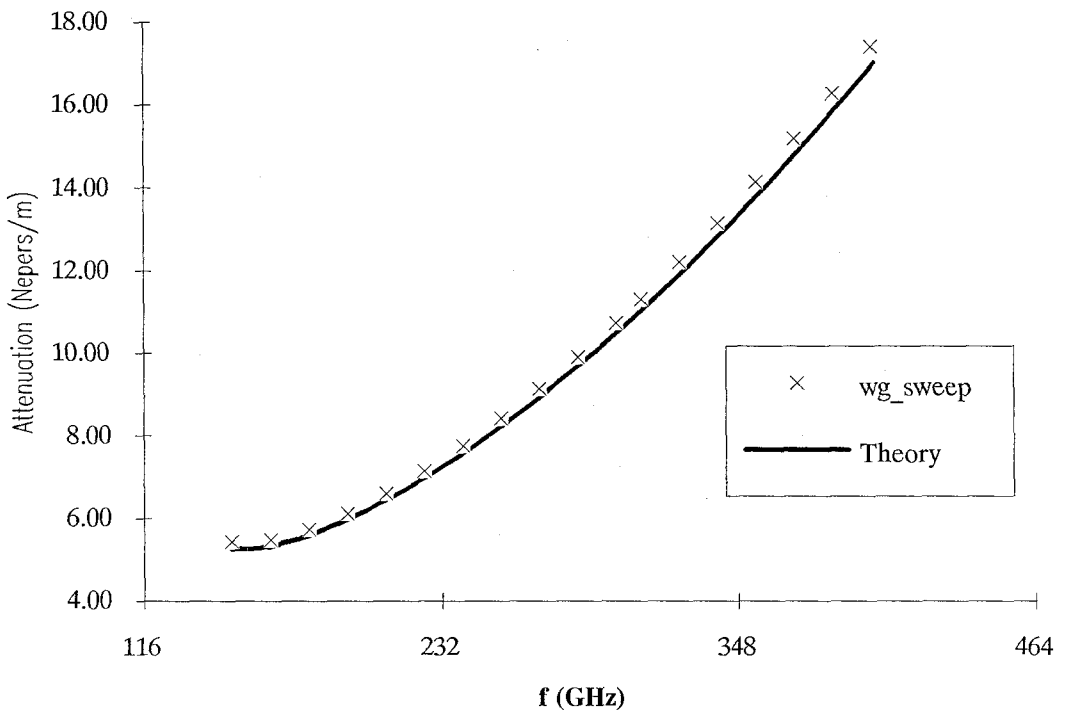

Figure 36 Attenuation versus frequency in a WR5 HTS waveguide.

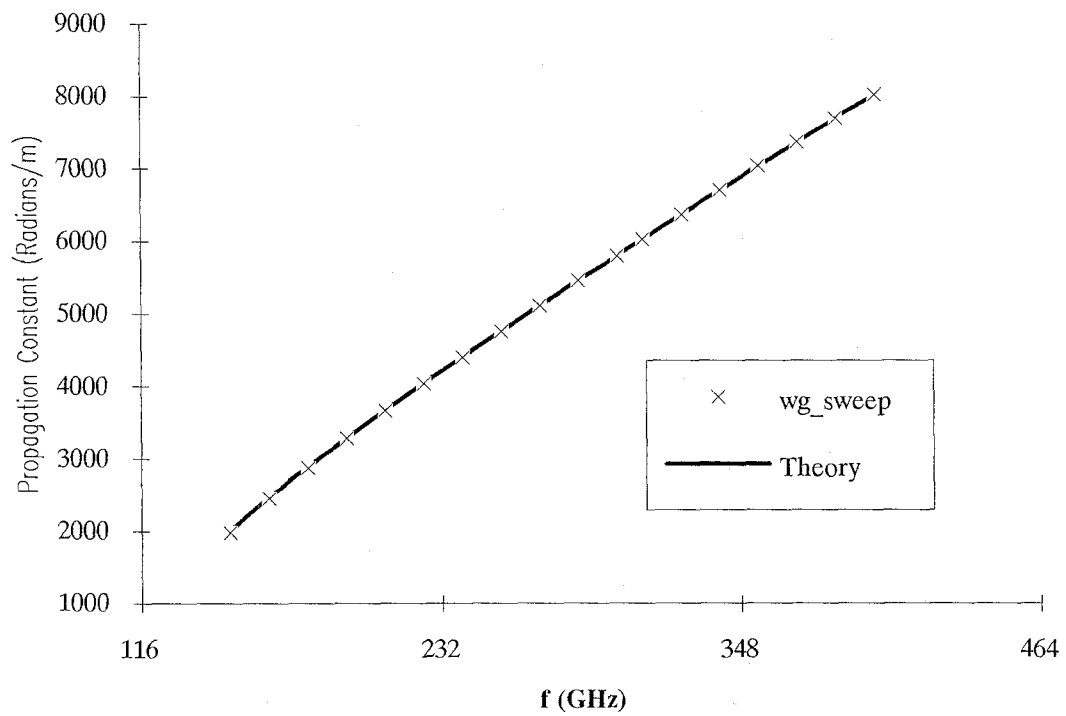

Figure 37 Propagation constant versus frequency in a WR5 HTS waveguide.

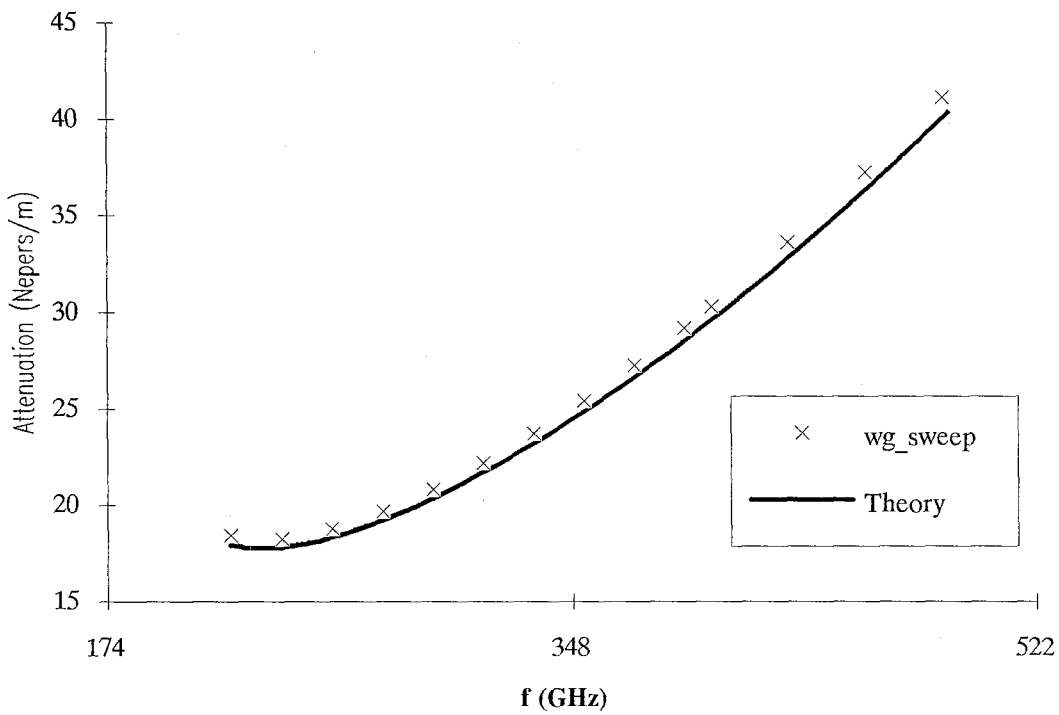

Figure 38 Attenuation versus frequency in a WR3 HTS waveguide.

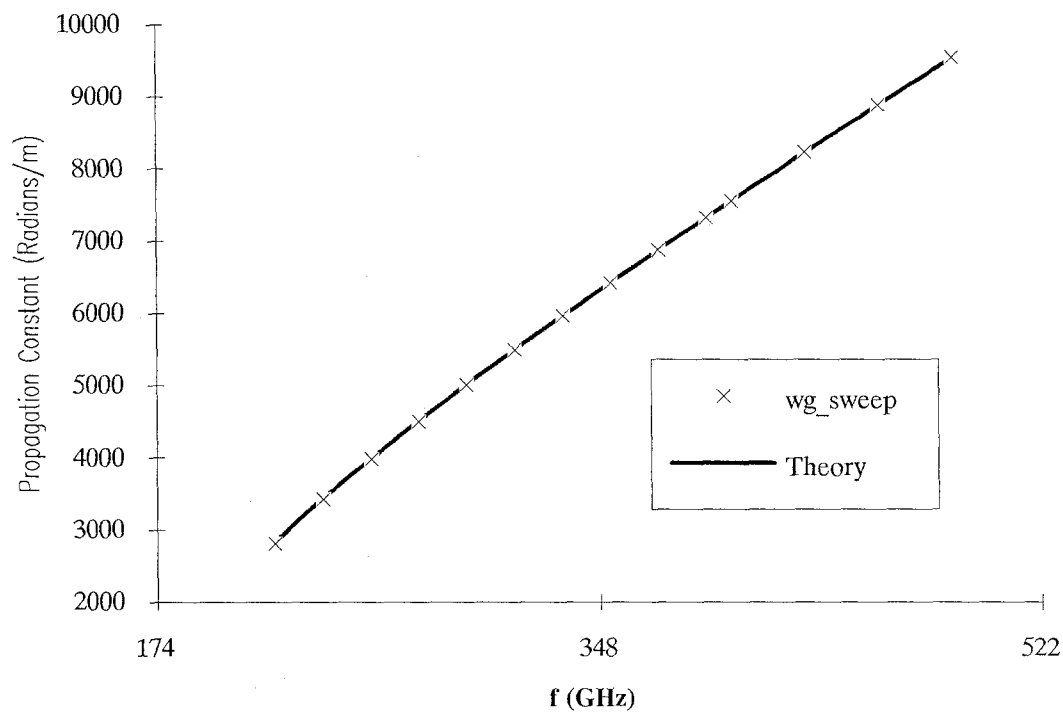

Figure 39 Propagation constant versus frequency in a WR3 HTS waveguide.

8.4.6 Conclusions

A program has been presented that accurately predicts the electric and magnetic fields in an HTS waveguide, as well as the attenuation and propagation for arbitrary choice of HTS parameters and mode. Figures 30-39 show a very good agreement between the simple perturbation theory based on ideal fields and the program.

Figures 21, 33, 35, 37 and 39 show comparisons of the calculated and predicted propagation constants. The agreement is to within 0.1 % error in the worst case, consistent with a simple perturbational refinement of the propagation constant, as expressed by equation (58). The propagation constant proves virtually unaffected by the increase of the surface reactance of the walls with frequency. The latter is true both for a single waveguide across the plotted frequency range and in comparison of different waveguides. The conclusion is, therefore, that equation (52) is very accurate and may be used with a wide range of HTS parameters, resulting in surface impedances of magnitude as high as 2 Ohms per square.

Figures 30, 32, 34, 36 and 38 show comparisons of the predicted exponential attenuation constants. There is good agreement between equation (5) and the predictions of the program. The typical error between the two is 2.5 %, for the 118-by-60 grid. This error, however, is due to the discretization of the equations (quantization error) and clearly does not represent a "real" difference since increasing the grid to its maximum (from a memory limit standpoint) size of 132-by-72 reduces the error to 1.9 %. By observing the tendency of the error with respect to grid size, it becomes a plausible conjecture that the error does not in fact asymptote to zero with respect to grid size.

Also, in the case of the two highest frequency waveguides considered (WR5 and WR3) the error increases from about 2.2 % at the frequency of minimum attenuation to 2.9 % at

the highest frequency considered (about three times the cutoff frequency), although in the two lowest frequency waveguides considered (WR90 and WR28) the error is almost constant with respect to frequency (2nd decimal point variations in percentage). This trend is believed to be a "true" event and verifies the conjecture posed in section 8.4.1. That is, at the high end of the frequency spectrum considered the real loss does start to increase a little faster than the equation (5) predicts. Nevertheless, the above results show that equations (5) and (52) are "accurate enough" even for the worst-case HTS waveguides and their use is recommended. Also these results validate the analysis presented in section 8.3.

8.5 Power Handling Capability

HTSs have a maximum current carrying capability, beyond which they turn into their normal crystalline and therefore insulating state. This maximum current density, J_c, is called the critical current density and is an intrinsic property of the HTS. Hence, there is a limit on the input power that any HTS waveguide can carry. This section investigates what this limit is for the HTS waveguides of average HTS parameters used above as examples.

We start with equations (3.28) and (3.29). The surface current per unit width flowing under the walls is equal to the magnetic field tangential to the walls. Hence, we have

$$H_{\max} = \frac{J_c}{|\zeta|} \quad , \tag{66}$$

where ζ is defined in equation (3.25). Substituting equation (3.29) into (66) and remembering that $P \propto H^2$, we obtain

$$P_{\max} = \frac{P_1}{H_1^2} \frac{J_c^2}{\left[\lambda^{-2} + \pi^2 f^2 \mu_0^2 \sigma_n^2 \left(\frac{T}{T_c} \right)^8 \right]} . \qquad (67)$$

A typical value of the critical current density of YBCO is ([11], [12]) $10^7 \frac{A}{cm^2} = 10^{11} \frac{A}{m^2}$. Using this value for the critical current density and equation (67), table 4 is obtained for HTS waveguides of average HTS parameters at their respective frequencies of minimum attenuation.

Type of Waveguide	Maximum Input Power (dBm)
WR90	21.2
WR28	1.56
WR10	-16.2
WR5	-27.9
WR3	-35.0

Table 4 Maximum Powers of HTS Waveguides.

8.6 References

[1] S. Ramo, J. R. Whinnery and T. Van Duzer, *Fields and Waves in Communication Electronics*, Wiley, New York, 1965.

[2] Douglas G. Corr and J. Brian Davies, "Computer Analysis of the Fundamental and Higher Order Modes in Single and Coupled Microstrip," IEEE Transactions on Microwave Theory and Techniques, Vol. MTT-20, No. 10, pp. 669-678, October 1972.

[3] J. S. Hornsby and A. Gopinath, "Numerical Analysis of a Dielectric-Loaded Waveguide with a Microstrip Line -- Finite Difference Methods," IEEE Transactions on Microwave Theory and Techniques, Vol. MTT-17, No. 9, pp. 684-690, September 1969.

[4] William H. Press et al., *Numerical Recipes in C*, Cambridge University Press, Cambridge, 1988.

[5] J. J. Dongara, et al., *LINPACK User's Guide*, Society for Industrial and Applied Mathematics, Philadelphia, 1979.

[6] *MATH77 Release 4.0*, JPL Document JPL-D-1341, Rev. C, May 1992.

[7] Gene H. Golub and Charles F. Van Loan, *Matrix Computations*, The Johns Hopkins University Press, Baltimore, 1983.

[8] J. A. Nelder and R. Mead, *Computer Journal*, Vol. 7, p. 308, 1965.

[9] E. Anderson et al., *LAPACK User's Guide*, Society for Industrial and Applied Mathematics, Philadelphia, 1992.

[10] Fred Clare and Dave Kennison, *NCAR Graphics Guide to Utitlities, Version 3.0*, National Center for Atmospheric Research, Scientific Computing Division, Boulder, Colorado, 1989.

[11] W. Chew et al., "Design and Performance of a High-T_c Superconductor Coplanar Waveguide Filter," IEEE Transactions on Microwave Theory and Techniques, Vol. 39, No. 9, pp. 1455-1461, September 1991.

[12] D. E. Oates, A. C. Anderson and P. M. Mankiewich, "Measurement of the Surface Resistance of $YBa_2Cu_3O_{7-x}$ Thin Films Using Stripline Resonators," Journal of Superconductivity, Vol. 3, No. 3, 1990.

Appendix A

MathCAD File Used to Calculate and Plot the Cross-Over Frequency

Cross-over Frequency

$\mu_o := 4 \cdot \pi \cdot 10^{-7}$

$$f_x\left[\lambda, \sigma, \sigma_v, T, T_c\right] := \frac{1}{\left[\pi \cdot \mu_o \cdot \lambda^2\right]} \cdot \left[4 \cdot \sigma \cdot {\sigma_v}^2 \cdot \left[\frac{T}{T_c}\right]^8\right]^{\left[\frac{1}{3}\right]}$$

Worst Case:

$f_x\left[800 \cdot 10^{-9}, 2 \cdot 10^8, 10 \cdot 10^6, 77, 85\right] = 11.95610^9$

Best Case:

$f_x\left[140 \cdot 10^{-9}, 10^7, 1.1 \cdot 10^6, 77, 90\right] = 5375.768 \cdot 10^9$

Average Case:

$f_x\left[430 \cdot 10^{-9}, 0.44 \cdot 10^8, 3 \cdot 10^6, 77, 87\right] = 162.753 \cdot 10^9$

$\lambda := 140 \cdot 10^{-9}, 150 \cdot 10^{-9} .. 700 \cdot 10^{-9}$

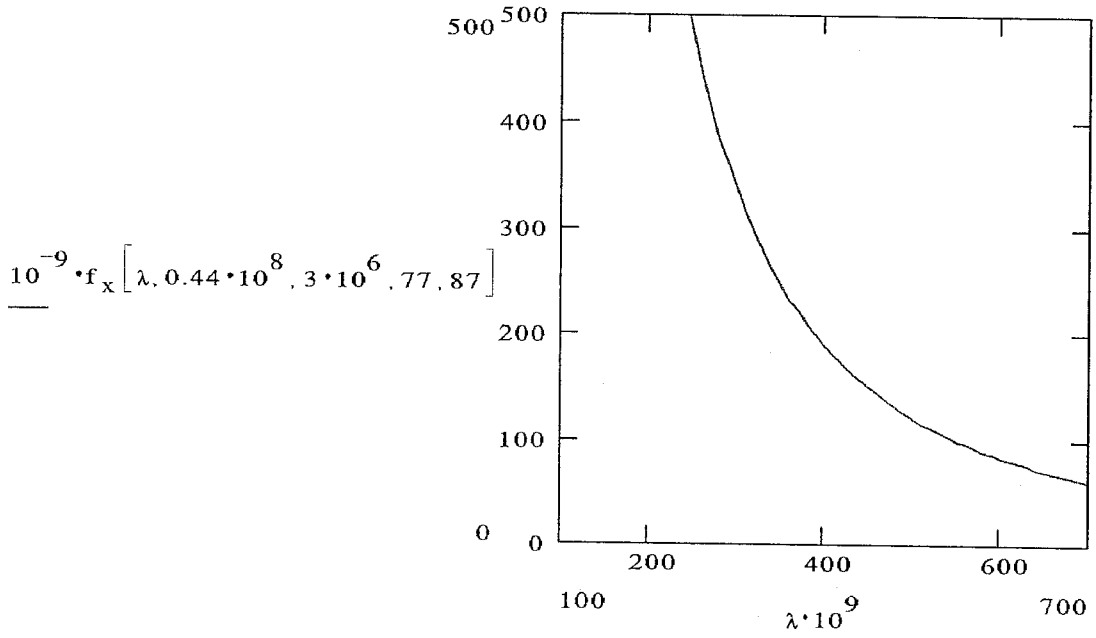

$T_c := 82, 82.5 .. 92$

$$\underline{f_x}\left[430 \cdot 10^{-9}, 0.44 \cdot 10^{8}, 3 \cdot 10^{6}, 77, T_c\right] \cdot 10^{-9}$$

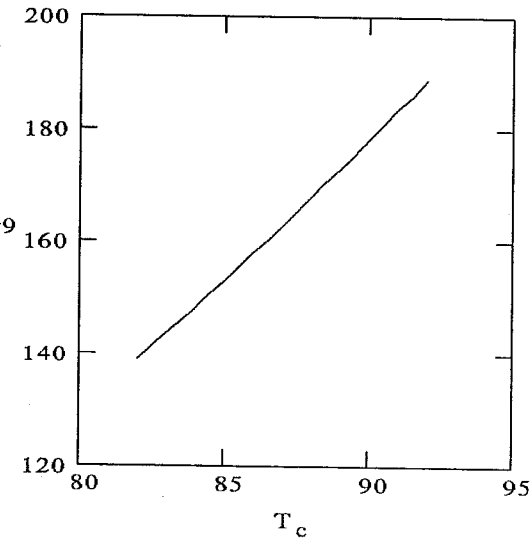

$\sigma_v := 1 \cdot 10^{6}, 1.1 \cdot 10^{6} .. 6 \cdot 10^{6}$

$$\underline{f_x}\left[430 \cdot 10^{-9}, 0.44 \cdot 10^{8}, \sigma_v, 77, 87\right] \cdot 10^{-9}$$

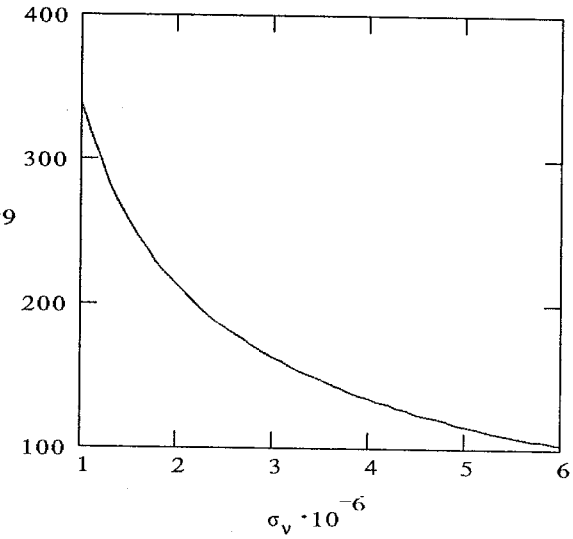

Appendix B

MathCAD File Used to Calculate and Plot the Exponential Attenuation versus Frequency

Attenuation due conductor and HTS losses
in closed rectangular waveguides
8-6-93

CONSTANTS:

$\mu := 4 \cdot \pi \cdot 10^{-7}$ $\quad \varepsilon := 8.854 \cdot 10^{-12}$ $\quad \lambda := 430 \cdot 10^{-9}$

$\sigma := 0.44 \cdot 10^{8}$ $\quad \sigma_v := 3 \cdot 10^{6}$

$c := \frac{1}{\sqrt{[\mu \cdot \varepsilon]}}$ $\quad \eta := \sqrt{\left[\frac{\mu}{\varepsilon}\right]}$ $\quad T := 77$

$T_c := 87$

$f_c(a) := \frac{c}{[2 \cdot a \cdot 2.54 \cdot 10^{-2}]}$

$f_{c.TE11}(a,b) := \frac{c}{2} \cdot \sqrt{\left[\left[2.54 \cdot 10^{-2} \cdot a\right]^{-2} + \left[2.54 \cdot 10^{-2} \cdot b\right]^{-2}\right]}$

TE10:

$R_{sc}(f) := \sqrt{\left[\pi \cdot \frac{\mu}{\sigma} \cdot f\right]}$

$alpha_c(a,b,x) := \frac{R_{sc}[x \cdot f_c(a)]}{\left[R_{sc}[f_c(a)] \cdot \sqrt{\left[1 - \left[\frac{1}{x}\right]^2\right]}\right]} \cdot \left[1 + \frac{(2 \cdot b)}{a} \cdot \left[\frac{1}{x}\right]^2\right]$

HTS

$R_{ss}(f) := 2 \cdot \mu^2 \cdot \pi^2 \cdot f^2 \cdot \lambda^3 \cdot \sigma_v \cdot \left[\frac{T}{T_c}\right]^4$

$alpha_s(a,b,x) := \frac{R_{ss}[x \cdot f_c(a)]}{\left[R_{sc}[f_c(a)] \cdot \sqrt{\left[1 - \left[\frac{1}{x}\right]^2\right]}\right]} \cdot \left[1 + \frac{(2 \cdot b)}{a} \cdot \left[\frac{1}{x}\right]^2\right]$

$x := 1.001, 1.01 .. 4$

$\text{alpha}_c[0.1, 0.05, x]$ —

$\text{alpha}_s[0.051, 0.0255, x]$ - -

$\text{alpha}_s[0.1, 0.05, x]$ —

$\text{alpha}_s[0.28, 0.14, x]$ —

$\text{alpha}_s[0.9, 0.4, x]$ —

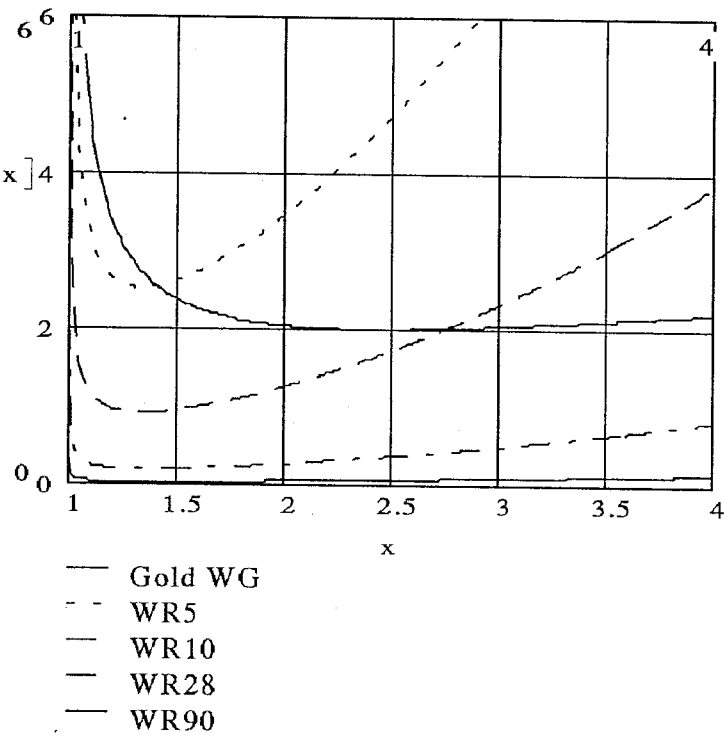

$$f_x := \frac{1}{\left[\pi \cdot \mu \cdot \lambda^2\right]} \cdot \left[\frac{\left[\frac{T_c}{T}\right]^8}{\left[4 \cdot \sigma_v{}^2 \cdot \sigma\right]}\right]^{\left[\frac{1}{3}\right]}$$

$$\frac{f_x}{f_c(0.051)} = 1.406$$

Appendix C

Mathematica Results on Characteristic Equation of 32-by-32 Lossless **A**-Matrix

```
In[5]:= !cc eh33_stdout.c

In[5]:= In[1]

Out[5]= {{0, 0, uy^2, 0, 0, 0, 0, 0, ux^2, 0, g^2 - 2 ux^2 - 2 uy^2 + eps mu w^2,
>     0, ux^2, 0, 0, 0, 0, 0, uy^2, 0, 0, 0, 0, 0, 0, 0, 0, 0, 0, 0, 0},
>    {0, 0, 0, uy^2, 0, 0, 0, 0, 0, ux^2, 0, g^2 - 2 ux^2 - 2 uy^2 + eps mu w^2, 0,
>     ux^2, 0, 0, 0, 0, 0, uy^2, 0, 0, 0, 0, 0, 0, 0, 0, 0, 0, 0, 0},
>    {0, 0, 0, 0, uy^2, 0, 0, 0, 0, 0, ux^2, 0, g^2 - 2 ux^2 - 2 uy^2 + eps mu w^2,
>     0, ux^2, 0, 0, 0, 0, 0, uy^2, 0, 0, 0, 0, 0, 0, 0, 0, 0, 0, 0},
>    {0, 0, 0, 0, 0, uy^2, 0, 0, 0, 0, 0, ux^2, 0,
>     g^2 - 2 ux^2 - 2 uy^2 + eps mu w^2, 0, ux^2, 0, 0, 0, 0, 0, uy^2, 0, 0, 0, 0,
>     0, 0, 0, 0, 0, 0}, {0, 0, 0, 0, 0, 0, 0, 0, 0, 0, uy^2, 0, 0, 0, 0, 0,
>     ux^2, 0, g^2 - 2 ux^2 - 2 uy^2 + eps mu w^2, 0, ux^2, 0, 0, 0, 0, 0, uy^2, 0,
>     0, 0, 0, 0}, {0, 0, 0, 0, 0, 0, 0, 0, 0, 0, 0, uy^2, 0, 0, 0, 0, 0, ux^2,
>     0, g^2 - 2 ux^2 - 2 uy^2 + eps mu w^2, 0, ux^2, 0, 0, 0, 0, 0, uy^2, 0, 0, 0,
>     0}, {0, 0, 0, 0, 0, 0, 0, 0, 0, 0, 0, 0, uy^2, 0, 0, 0, 0, 0, ux^2, 0,
>     g^2 - 2 ux^2 - 2 uy^2 + eps mu w^2, 0, ux^2, 0, 0, 0, 0, 0, uy^2, 0, 0, 0},
>    {0, 0, 0, 0, 0, 0, 0, 0, 0, 0, 0, 0, 0, uy^2, 0, 0, 0, 0, 0, ux^2, 0,
>     g^2 - 2 ux^2 - 2 uy^2 + eps mu w^2, 0, ux^2, 0, 0, 0, 0, 0, uy^2, 0, 0},
>    {0, 0, 1, 0, 0, 0, 0, 0, 0, 0, 0, 0, 0, 0, 0, 0, 0, 0, 0, 0, 0, 0, 0, 0, 0,
>     0, 0, 0, 0, 0, 0, 0, 0}, {-(g ux)/2, 0, 0, -I mu uy w, g ux/2, 0, 0, 0, 0,
>     0, 0, I mu uy w, 0, 0, 0, 0, 0, 0, 0, 0, 0, 0, 0, 0, 0, 0, 0, 0, 0, 0, 0,
>     0, 0}, {0, 0, 0, 0, 1, 0, 0, 0, 0, 0, 0, 0, 0, 0, 0, 0, 0, 0, 0, 0, 0, 0,
>     0, 0, 0, 0, 0, 0, 0, 0, 0, 0, 0},
>    {0, 0, -(g ux)/2, 0, 0, -I mu uy w, g ux/2, 0, 0, 0, 0, 0, 0, I mu uy w, 0,
```

```
>     0, 0, 0, 0, 0, 0, 0, 0, 0, 0, 0, 0, 0, 0, 0, 0, 0},
>    {0, 0, 0, 0, 0, 0, 0, 0, 0, 0, 0, 0, 0, 0, 0, 0, 0, 0, 0, 0, 0, 0, 0, 0,
>     0, 0, 1, 0, 0, 0, 0, 0}, {0, 0, 0, 0, 0, 0, 0, 0, 0, 0, 0, 0, 0, 0, 0,
>     0, 0, 0, 0, -I mu uy w, 0, 0, 0, 0, -(g ux)/2, 0, 0, I mu uy w, g ux/2, 0,
>     0, 0}, {0, 0, 0, 0, 0, 0, 0, 0, 0, 0, 0, 0, 0, 0, 0, 0, 0, 0, 0, 0, 0, 0,
>     0, 0, 0, 0, 0, 0, 0, 1, 0, 0, 0},
>    {0, 0, 0, 0, 0, 0, 0, 0, 0, 0, 0, 0, 0, 0, 0, 0, 0, 0, 0, 0, 0, 0, 0, 0,
>     -I mu uy w, 0, 0, 0, 0, -(g ux)/2, 0, 0, I mu uy w, g ux/2, 0},
>    {0, 0, 0, 0, 0, 0, 0, 0, 1, 0, 0, 0, 0, 0, 0, 0, 0, 0, 0, 0, 0, 0, 0, 0, 0,
>     0, 0, 0, 0, 0, 0, 0, 0}, {-(g uy)/2, 0, 0, 0, 0, 0, 0, 0, 0, I mu ux w,
>     0, -I mu ux w, 0, 0, 0, 0, g uy/2, 0, 0, 0, 0, 0, 0, 0, 0, 0, 0, 0, 0, 0,
>     0, 0}, {0, 0, 0, 0, 0, 0, 0, 0, 0, 0, 0, 0, 0, 0, 0, 1, 0, 0, 0, 0,
>     0, 0, 0, 0, 0, 0, 0, 0, 0, 0, 0},
>    {0, 0, 0, 0, 0, 0, 0, 0, -(g uy)/2, 0, 0, 0, 0, 0, 0, 0, 0, I mu ux w, 0,
>     -I mu ux w, 0, 0, 0, 0, g uy/2, 0, 0, 0, 0, 0, 0, 0},
>    {0, 0, 0, 0, 0, 0, 0, 0, 0, 0, 0, 0, 0, 0, 1, 0, 0, 0, 0, 0, 0, 0, 0, 0,
>     0, 0, 0, 0, 0, 0, 0, 0}, {0, 0, 0, 0, 0, 0, -(g uy)/2, 0, 0, 0, 0, 0, 0,
>     I mu ux w, 0, -I mu ux w, 0, 0, 0, 0, 0, 0, g uy/2, 0, 0, 0, 0, 0, 0, 0,
>     0, 0}, {0, 0, 0, 0, 0, 0, 0, 0, 0, 0, 0, 0, 0, 0, 0, 0, 0, 0, 0, 0, 0, 0,
>     0, 1, 0, 0, 0, 0, 0, 0, 0, 0, 0},
>    {0, 0, 0, 0, 0, 0, 0, 0, 0, 0, 0, 0, 0, 0, -(g uy)/2, 0, 0, 0, 0, 0, 0,
>     I mu ux w, 0, -I mu ux w, 0, 0, 0, 0, 0, 0, g uy/2, 0},
>    {1, 0, 0, 0, 0, 0, 0, 0, 0, 0, 0, 0, 0, 0, 0, 0, 0, 0, 0, 0, 0, 0, 0, 0,
```

```
>      0, 0, 0, 0, 0, 0, 0, 0}, {-(g ux), -I mu uy w, g ux, 0, 0, 0, 0, 0, 0,
>      I mu uy w, 0, 0, 0, 0, 0, 0, 0, 0, 0, 0, 0, 0, 0, 0, 0, 0, 0, 0, 0, 0,
>      0, 0}, {0, 0, 0, 0, 0, 0, 1, 0, 0, 0, 0, 0, 0, 0, 0, 0, 0, 0, 0, 0, 0,
>      0, 0, 0, 0, 0, 0, 0, 0, 0, 0, 0},
>     {0, 0, 0, 0, -(g ux), 0, g ux, -I mu uy w, 0, 0, 0, 0, 0, 0, 0,
>      I mu uy w, 0, 0, 0, 0, 0, 0, 0, 0, 0, 0, 0, 0, 0, 0, 0, 0, 0},
>     {0, 0, 0, 0, 0, 0, 0, 0, 0, 0, 0, 0, 0, 0, 0, 0, 0, 0, 0, 0, 0, 0, 0, 0,
>      1, 0, 0, 0, 0, 0, 0, 0}, {0, 0, 0, 0, 0, 0, 0, 0, 0, 0, 0, 0, 0, 0, 0,
>      0, 0, -I mu uy w, 0, 0, 0, 0, 0, 0, -(g ux), I mu uy w, g ux, 0, 0, 0,
>      0, 0}, {0, 0, 0, 0, 0, 0, 0, 0, 0, 0, 0, 0, 0, 0, 0, 0, 0, 0, 0, 0, 0,
>      0, 0, 0, 0, 0, 0, 0, 0, 0, 1, 0},
>     {0, 0, 0, 0, 0, 0, 0, 0, 0, 0, 0, 0, 0, 0, 0, 0, 0, 0, 0, 0, 0, 0, 0, 0,
>      -I mu uy w, 0, 0, 0, 0, -(g ux), 0, g ux, I mu uy w}}

In[6]:= In[2]

Out[6]= {32, 32}

In[7]:= d=Det[A]
Factor[d]

                16   12   4   8  12          14   12   6   8  12
Out[7]= g    mu   ux  uy  w   - 12 g    mu   ux  uy  w   +

          12   12   8   8  12          10   12   10   8  12
>    58 g    mu   ux  uy  w   - 144 g    mu   ux   uy  w   +

           8   12   12   8  12          6   12   14   8  12
>    193 g  mu   ux   uy  w   - 132 g  mu   ux   uy  w   +

          4   12   16   8  12          14   12   4   10  12
>    36 g  mu   ux   uy  w   - 12 g    mu   ux  uy   w   +

          12   12   6   10  12          10   12   8   10  12
>    124 g    mu   ux  uy   w   - 504 g    mu   ux  uy   w   +

           8   12   10   10  12           6   12   12   10  12
>    1016 g  mu   ux   uy   w   - 1044 g  mu   ux   uy   w   +

          4   12   14   10  12          2   12   16   10  12
>    492 g  mu   ux   uy   w   - 72 g  mu   ux   uy   w   +

          12   12   4   12  12          10   12   6   12  12
>    58 g    mu   ux  uy   w   - 504 g    mu   ux  uy   w   +

           8   12   8   12  12           6   12   10   12  12
>    1662 g  mu   ux  uy   w   - 2568 g  mu   ux   uy   w   +

          4   12   12   12  12          2   12   14   12  12
>    1820 g  mu   ux   uy   w   - 456 g  mu   ux   uy   w   -

          10   12   4   14  12          8   12   6   14  12
>    144 g    mu   ux  uy   w   + 1016 g  mu   ux  uy   w   -

           6   12   8   14  12          4   12   10   14  12
```

```
>    2568 g  mu  ux  uy  w  + 2728 g  mu  ux  uy  w  -

>    1008 g 2 mu 12 ux 12 uy 14 w 12 + 193 g 8 mu 12 ux 4 uy 16 w 12 -

>    1044 g 6 mu 12 ux 6 uy 16 w 12 + 1820 g 4 mu 12 ux 8 uy 16 w 12 -

>    1008 g 2 mu 12 ux 10 uy 16 w 12 - 132 g 6 mu 12 ux 4 uy 18 w 12 +

>    492 g 4 mu 12 ux 6 uy 18 w 12 - 456 g 2 mu 12 ux 8 uy 18 w 12 +

>    36 g 4 mu 12 ux 4 uy 20 w 12 - 72 g 2 mu 12 ux 6 uy 20 w 12 +

>    8 eps g 14 mu 13 ux 4 uy 8 w 14 - 84 eps g 12 mu 13 ux 6 uy 8 w 14 +

>    348 eps g 10 mu 13 ux 8 uy 8 w 14 - 720 eps g 8 mu 13 ux 10 uy 8 w 14 +

>    772 eps g 6 mu 13 ux 12 uy 8 w 14 - 396 eps g 4 mu 13 ux 14 uy 8 w 14 +

>    72 eps g 2 mu 13 ux 16 uy 8 w 14 - 84 eps g 12 mu 13 ux 4 uy 10 w 14 +

>    744 eps g 10 mu 13 ux 6 uy 10 w 14 - 2520 eps g 8 mu 13 ux 8 uy 10 w 14 +

>    4064 eps g 6 mu 13 ux 10 uy 10 w 14 - 3132 eps g 4 mu 13 ux 12 uy 10 w 14 +

>    984 eps g 2 mu 13 ux 14 uy 10 w 14 - 72 eps mu 13 ux 16 uy 10 w 14 +

>    348 eps g 10 mu 13 ux 4 uy 12 w 14 - 2520 eps g 8 mu 13 ux 6 uy 12 w 14 +

>    6648 eps g 6 mu 13 ux 8 uy 12 w 14 - 7704 eps g 4 mu 13 ux 10 uy 12 w 14 +

>    3640 eps g 2 mu 13 ux 12 uy 12 w 14 - 456 eps mu 13 ux 14 uy 12 w 14 -

>    720 eps g 8 mu 13 ux 4 uy 14 w 14 + 4064 eps g 6 mu 13 ux 6 uy 14 w 14 -

>    7704 eps g 4 mu 13 ux 8 uy 14 w 14 + 5456 eps g 2 mu 13 ux 10 uy 14 w 14 -

>    1008 eps 13 mu 12 ux 14 uy 14 w + 772 eps g 6 mu 13 ux 4 uy 16 w 14 -

>    3132 eps g 4 mu 13 ux 6 uy 16 w 14 + 3640 eps g 2 mu 13 ux 8 uy 16 w 14 -

>    1008 eps 13 mu 10 ux 16 uy 14 w - 396 eps g 4 mu 13 ux 4 uy 18 w 14 +

>    984 eps g 2 mu 13 ux 6 uy 18 w 14 - 456 eps 13 mu 8 ux 18 uy 14 w +

>    72 eps g 2 mu 13 ux 4 uy 20 w 14 - 72 eps 13 mu 6 ux 20 uy 14 w +
```

> $28\ eps^{2}\ g^{12}\ mu^{14}\ ux^{4}\ uy^{8}\ w^{16} - 252\ eps^{2}\ g^{10}\ mu^{14}\ ux^{6}\ uy^{8}\ w^{16} +$

> $870\ eps^{2}\ g^{8}\ mu^{14}\ ux^{8}\ uy^{8}\ w^{16} - 1440\ eps^{2}\ g^{6}\ mu^{14}\ ux^{10}\ uy^{8}\ w^{16} +$

> $1158\ eps^{2}\ g^{4}\ mu^{14}\ ux^{12}\ uy^{8}\ w^{16} - 396\ eps^{2}\ g^{2}\ mu^{14}\ ux^{14}\ uy^{8}\ w^{16} +$

> $36\ eps^{2}\ mu^{14}\ ux^{16}\ uy^{8}\ w^{16} - 252\ eps^{2}\ g^{10}\ mu^{14}\ ux^{4}\ uy^{10}\ w^{16} +$

> $1860\ eps^{2}\ g^{8}\ mu^{14}\ ux^{6}\ uy^{10}\ w^{16} - 5040\ eps^{2}\ g^{6}\ mu^{14}\ ux^{8}\ uy^{10}\ w^{16} +$

> $6096\ eps^{2}\ g^{4}\ mu^{14}\ ux^{10}\ uy^{10}\ w^{16} - 3132\ eps^{2}\ g^{2}\ mu^{14}\ ux^{12}\ uy^{10}\ w^{16} +$

> $492\ eps^{2}\ mu^{14}\ ux^{14}\ uy^{10}\ w^{16} + 870\ eps^{2}\ g^{8}\ mu^{14}\ ux^{4}\ uy^{12}\ w^{16} -$

> $5040\ eps^{2}\ g^{6}\ mu^{14}\ ux^{6}\ uy^{12}\ w^{16} + 9972\ eps^{2}\ g^{4}\ mu^{14}\ ux^{8}\ uy^{12}\ w^{16} -$

> $7704\ eps^{2}\ g^{2}\ mu^{14}\ ux^{10}\ uy^{12}\ w^{16} + 1820\ eps^{2}\ mu^{14}\ ux^{12}\ uy^{12}\ w^{16} -$

> $1440\ eps^{2}\ g^{6}\ mu^{14}\ ux^{4}\ uy^{14}\ w^{16} + 6096\ eps^{2}\ g^{4}\ mu^{14}\ ux^{6}\ uy^{14}\ w^{16} -$

> $7704\ eps^{2}\ g^{2}\ mu^{14}\ ux^{8}\ uy^{14}\ w^{16} + 2728\ eps^{2}\ mu^{14}\ ux^{10}\ uy^{14}\ w^{16} +$

> $1158\ eps^{2}\ g^{4}\ mu^{14}\ ux^{4}\ uy^{16}\ w^{16} - 3132\ eps^{2}\ g^{2}\ mu^{14}\ ux^{6}\ uy^{16}\ w^{16} +$

> $1820\ eps^{2}\ mu^{14}\ ux^{8}\ uy^{16}\ w^{16} - 396\ eps^{2}\ g^{2}\ mu^{14}\ ux^{4}\ uy^{18}\ w^{16} +$

> $492\ eps^{2}\ mu^{14}\ ux^{6}\ uy^{18}\ w^{16} + 36\ eps^{2}\ mu^{14}\ ux^{4}\ uy^{20}\ w^{16} +$

> $56\ eps^{3}\ g^{10}\ mu^{15}\ ux^{4}\ uy^{8}\ w^{18} - 420\ eps^{3}\ g^{8}\ mu^{15}\ ux^{6}\ uy^{8}\ w^{18} +$

> $1160\ eps^{3}\ g^{6}\ mu^{15}\ ux^{8}\ uy^{8}\ w^{18} - 1440\ eps^{3}\ g^{4}\ mu^{15}\ ux^{10}\ uy^{8}\ w^{18} +$

> $772\ eps^{3}\ g^{2}\ mu^{15}\ ux^{12}\ uy^{8}\ w^{18} - 132\ eps^{3}\ mu^{15}\ ux^{14}\ uy^{8}\ w^{18} -$

> $420\ eps^{3}\ g^{8}\ mu^{15}\ ux^{4}\ uy^{10}\ w^{18} + 2480\ eps^{3}\ g^{6}\ mu^{15}\ ux^{6}\ uy^{10}\ w^{18} -$

> $5040\ eps^{3}\ g^{4}\ mu^{15}\ ux^{8}\ uy^{10}\ w^{18} + 4064\ eps^{3}\ g^{2}\ mu^{15}\ ux^{10}\ uy^{10}\ w^{18} -$

> $1044\ eps^{3}\ mu^{15}\ ux^{12}\ uy^{10}\ w^{18} + 1160\ eps^{3}\ g^{6}\ mu^{15}\ ux^{4}\ uy^{12}\ w^{18} -$

> $5040\ eps^{3}\ g^{4}\ mu^{15}\ ux^{6}\ uy^{12}\ w^{18} + 6648\ eps^{3}\ g^{2}\ mu^{15}\ ux^{8}\ uy^{12}\ w^{18} -$

> $2568\ eps^{3}\ mu^{15}\ ux^{10}\ uy^{12}\ w^{18} - 1440\ eps^{3}\ g^{4}\ mu^{15}\ ux^{4}\ uy^{14}\ w^{18} +$

```
                3  2   15   6   14  18              3   15   8   14  18
>     4064 eps  g  mu   ux  uy   w   - 2568 eps  mu   ux  uy   w   +

               3  2   15   4   16  18              3   15   6   16  18
>     772 eps  g  mu   ux  uy   w   - 1044 eps  mu   ux  uy   w   -

              3   15   4   18  18             4  8   16   4   8  20
>     132 eps  mu   ux  uy   w   + 70 eps  g  mu   ux  uy  w   -

              4  6   16   6   8  20             4  4   16   8   8  20
>     420 eps  g  mu   ux  uy  w   + 870 eps  g  mu   ux  uy  w   -

              4  2   16   10   8  20             4   16   12   8  20
>     720 eps  g  mu   ux   uy  w   + 193 eps  mu   ux   uy  w   -

              4  6   16   4   10  20             4  4   16   6   10  20
>     420 eps  g  mu   ux  uy   w   + 1860 eps  g  mu   ux  uy   w   -

               4  2   16   8   10  20             4   16   10   10  20
>     2520 eps  g  mu   ux  uy   w   + 1016 eps  mu   ux   uy   w   +

              4  4   16   4   12  20             4  2   16   6   12  20
>     870 eps  g  mu   ux  uy   w   - 2520 eps  g  mu   ux  uy   w   +

               4   16   8   12  20             4  2   16   4   14  20
>     1662 eps  mu   ux  uy   w   - 720 eps  g  mu   ux  uy   w   +

               4   16   6   14  20             4   16   4   16  20
>     1016 eps  mu   ux  uy   w   + 193 eps  mu   ux  uy   w   +

             5  6   17   4   8  22             5  4   17   6   8  22
>     56 eps  g  mu   ux  uy  w   - 252 eps  g  mu   ux  uy  w   +

             5  2   17   8   8  22             5   17   10   8  22
>     348 eps  g  mu   ux  uy  w   - 144 eps  mu   ux   uy  w   -

             5  4   17   4   10  22             5  2   17   6   10  22
>     252 eps  g  mu   ux  uy   w   + 744 eps  g  mu   ux  uy   w   -

             5   17   8   10  22             5  2   17   4   12  22
>     504 eps  mu   ux  uy   w   + 348 eps  g  mu   ux  uy   w   -

             5   17   6   12  22             5   17   4   14  22
>     504 eps  mu   ux  uy   w   - 144 eps  mu   ux  uy   w   +

             6  4   18   4   8  24             6  2   18   6   8  24
>     28 eps  g  mu   ux  uy  w   - 84 eps  g  mu   ux  uy  w   +

             6   18   8   8  24             6  2   18   4   10  24
>     58 eps  mu   ux  uy  w   - 84 eps  g  mu   ux  uy   w   +

             6   18   6   10  24             6   18   4   12  24
>     124 eps  mu   ux  uy   w   + 58 eps  mu   ux  uy   w   +

            7  2   19   4   8  26             7   19   6   8  26
>     8 eps  g  mu   ux  uy  w   - 12 eps  mu   ux  uy  w   -

             7   19   4   10  26      8   20   4   8  28
>     12 eps  mu   ux  uy   w   + eps  mu   ux  uy  w

In[8]:= N[Pi]

           12   4   8  12   2           2    2       2           2
Out[8]= mu   ux  uy  w   (g  + eps mu w ) (g  - 2 ux  + eps mu w )

       2       2       2           2    2     2       2           2
>     (g  - 3 ux  - 3 uy  + eps mu w ) (g  - ux  - 3 uy  + eps mu w )
```

```
>     (g^2 - 2 uy^2 + eps mu w^2) (g^2 - 2 ux^2 - 2 uy^2 + eps mu w^2)

>     (g^2 - 3 ux^2 - uy^2 + eps mu w^2) (g^2 - ux^2 - uy^2 + eps mu w^2)
```

Appendix D

C-code Listing of the *wg_plot.c* Program

```
#include <stdlib.h>
#include <stdio.h>
#include <math.h>
#include <malloc.h>
#include <complex.h>
#include "nrutil.h"

#define M  30
#define N  15
#define NOOFDZ 65
#define ROWLENGTH (2*(M+1)*(N+1))
#define NMAX 5000
#define GET_PSUM \
                                        for (j=1;j<=ndim;j++) {\
                                        for (sum=0.0,i=1;i<=mpts;i++) sum += p[i][j];\
                                        psum[j]=sum;}
#define SWAP(a,b) {swap=(a);(a)=(b);(b)=swap;}
#define J CMPLXF(0.0,1.0)


void main()
{
float *svd(), *vector(), el3(), determinant(),*guess_gamma(),*EH_Power_calc();
void amoeba(),openplot(),plotmatr(),closeplot(),calc_long();
void free_vector();
float  params[8], *gamma, p[4][3],y[4],*matrix,res[ROWLENGTH][2],*diag;
float ex[2*N+1][2*M+1], ey[2*N+1][2*M+1], ez[2*N+1][2*M+1], hx[2*N+1][2*M+1],
hy[2*N+1][2*M+1], hz[2*N+1][2*M+1], hz_long[2*M+1][NOOFDZ+1],
hx_long[2*M+1][NOOFDZ+1], ez_long[2*M+1][NOOFDZ+1], ex_long[2*M+1][NOOFDZ+1],
hz_long2[2*N+1][NOOFDZ+1], hy_long[2*N+1][NOOFDZ+1], ez_long2[2*N+1][NOOFDZ+1],
ey_long[2*N+1][NOOFDZ+1];
float lalpha, lbeta, *Power_Hmax;
int i, iter, m,n;
matrix=vector(0,2*ROWLENGTH*ROWLENGTH-1);
/*
params[0]=0.02286;      Width of Box
params[1]=0.01016;      Height of Box
params[2]=1.0;          Relative Dielectric Constant of Interior
params[3]=10e9;         Frequency
params[4]=450e-9;       Zero Temperature Penetration Depth
params[5]=3e6;          Normal Conductivity in S/m
params[6]=77;           Temperature of WG
params[7]=90;           Critical Temperature of HTS
*/
printf("\nEnter width of waveguide cross-section : ");
scanf("%f",&params[0]);
printf("Enter height of waveguide cross-section : ");
scanf("%f",&params[1]);
printf("Enter relative dielectric constant of waveguide interior : ");
scanf("%f",&params[2]);
printf("Enter effective zero-temperature penetration depth of HTS walls : ");
scanf("%f",&params[4]);
printf("Enter normal conductivity of HTS walls : ");
scanf("%f",&params[5]);
```

```
printf("Enter temperature of HTS walls : ");
scanf("%f",&params[6]);
printf("Enter critical temperature of HTS walls : ");
scanf("%f",&params[7]);
printf("Enter 'm' of the mode you are interested in : ");
scanf("%d",&m);
printf("Enter 'n' of the mode you are interested in : ");
scanf("%d",&n);
printf("Enter frequency : ");
scanf("%f",&params[3]);
gamma=guess_gamma(m,n,params);
lalpha=0.03*gamma[1];
lbeta=0.02*gamma[2];
p[1][1]=gamma[1];
p[1][2]=gamma[2];
p[2][1]=p[1][1]+lalpha;
p[2][2]=p[1][2]-lbeta;
p[3][1]=p[1][1]-lalpha;
p[3][2]=p[1][2]-lbeta;
for (i=1;i<=3;i++)
      y[i]=determinant(&p[i][0],matrix,params);
amoeba(p,y,2,1e-6,1e-5,determinant,&iter,matrix,params);
printf("\n%d Iterations.\n",iter);
printf("\nAt frequency %e Hz, (alpha,beta)=(%.5e,%.5e)\n",params[3],p[1][1],p[1][2]);
fflush(NULL);
printf("\nCalculating solution vector...\n");
diag=svd(&p[1][0],matrix,params);
printf("Maximum Singular Value: %f\n",diag[0]);
printf("Last 5 Singular Values: \n");
for (i=ROWLENGTH-5;i<=ROWLENGTH-1;i++)
      printf("%d   %.3e\n",i+1,diag[i]);
for (i=0;i<=ROWLENGTH-1;i++)
          {
          res[i][0]=el3(matrix,i,ROWLENGTH-1,0,ROWLENGTH,ROWLENGTH,2);
          res[i][1]=-1.0*el3(matrix,i,ROWLENGTH-1,1,ROWLENGTH,ROWLENGTH,2);
          }
free_vector(matrix,0,2*ROWLENGTH*ROWLENGTH-1);
Power_Hmax=EH_Power_calc(CMPLXF(p[1][1],p[1][2]),res,params,0.0,0.0,ex,ey,ez,hx,hy,hz);
printf("\nPower at z=0 : %e W\nBottom Wall Maximum Tangential Magnetic Field: %e A/m\nLeft Wall
Maximum Tangential Magnetic Field: %e A/m\n",Power_Hmax[2],Power_Hmax[0],Power_Hmax[1]);
fflush(NULL);
openplot();
plotmatr(ex,ey,2*M+1,2*N+1);
plotmatr(hx,hy,2*M+1,2*N+1);
calc_long(hx_long,hz_long,ex_long,ez_long,hy_long,hz_long2,ey_long,ez_long2,ex,ey,ez,hx,hy,hz,para
ms,CMPLXF(p[1][1],p[1][2]),res);
plotmatr(hz_long,hx_long,NOOFDZ+1,2*M+1);
plotmatr(ez_long,ex_long,NOOFDZ+1,2*M+1);
plotmatr(hz_long2,hy_long,NOOFDZ+1,2*N+1);
plotmatr(ez_long2,ey_long,NOOFDZ+1,2*N+1);
closeplot();
return;
}
```

```
float *guess_gamma(m,n,params)
float *params;
int m,n;
{
float fc,Rs,mu,eps,w;
static float gamma[3];
mu=4*M_PI*1e-7;
eps=params[2]*8.854e-12;
w=2*M_PI*params[3];

Rs=0.5*SQR(mu)*SQR(w)*pow(params[4],3.0)*params[5]*pow((params[6]/params[7]),4.0);

fc=1/(2*sqrt(mu*eps))*sqrt(SQR(m/params[0])+SQR(n/params[1]));

if (params[3]>fc)
        {
    if (n==0)
        {
        gamma[1]=Rs/(sqrt(mu/eps)*params[1]*sqrt(1-
SQR(fc/params[3])))*(1+2*params[1]/params[0]*SQR(fc/params[3]));
        }
    else
        {
        gamma[1]=2*Rs/(sqrt(mu/eps)*params[1]*sqrt(1-
SQR(fc/params[3])))*((1+params[1]/params[0])*SQR(fc/params[3])+(1-
SQR(fc/params[3]))*((params[1]/params[0]*(params[1]/params[0]*SQR(m)+SQR(n)))/(SQR(params[1]*
m/params[0])+SQR(n))));
        }
        gamma[2]=2*M_PI*params[3]*sqrt(mu*eps)*sqrt(1-SQR(fc/params[3]));
        }
else
        {
        gamma[1]=2*M_PI*fc*sqrt(mu*eps)*sqrt(1-SQR(params[3]/fc));
        gamma[2]=0.0;
        }
printf("\nFc: %e Hz\nTheoretical TE%d%d alpha : %e Nepers/m\nLossless beta: %e
rad/m\n\n",fc,m,n,gamma[1],gamma[2]);
return(gamma);
}


float el3(matrix,l,m,n,o,p,q)
float *matrix;
int l,m,n,o,p,q;
{
return(matrix[l*p*q+m*q+n]);
}


void matr(gamma,matrix,params)
float *gamma, *matrix, *params;
{
void initmatrix(), putreal(), putimag();
```

```
int Ez(), Hz();
int i,j,rowindex;
float alpha,beta,Dx,Dy;
float a,b,eps,mu,w,R,Rs,Xs,ksq;

a=params[0];
b=params[1];
eps=params[2]*8.854e-12;
w=2*M_PI*params[3];
mu=4*M_PI*1e-7;
Rs=0.5*SQR(mu)*SQR(w)*pow(params[4],3.0)*params[5]*pow((params[6]/params[7]),4.0);
Xs=mu*w*params[4];
Dx=a/(2*M);
Dy=b/(2*N);

R=Dx/Dy;
alpha=gamma[1];
beta=gamma[2];
printf("\n(%.4e,%.4e)",alpha,beta);
fflush(NULL);
ksq=w*w*mu*eps+alpha*alpha-beta*beta;

rowindex=0;

initmatrix(matrix);

/* Inside Points.  Helmholtz Equation.  */

for (j=1;j<=N-1;j++)
        for (i=1;i<=M-1;i++)
                {
                putreal(rowindex,Ez(i+1,j),1.0,matrix);
                putreal(rowindex,Ez(i-1,j),1.0,matrix);
                putreal(rowindex,Ez(i,j+1),R*R,matrix);
                putreal(rowindex,Ez(i,j-1),R*R,matrix);
                putreal(rowindex,Ez(i,j),ksq*Dx*Dx-2*(1+R*R),matrix);
                putimag(rowindex,Ez(i,j),2*alpha*beta*Dx*Dx,matrix);

                rowindex++;

                putreal(rowindex,Hz(i+1,j),1.0,matrix);
                putreal(rowindex,Hz(i-1,j),1.0,matrix);
                putreal(rowindex,Hz(i,j+1),R*R,matrix);
                putreal(rowindex,Hz(i,j-1),R*R,matrix);
                putreal(rowindex,Hz(i,j),ksq*Dx*Dx-2*(1+R*R),matrix);
                putimag(rowindex,Hz(i,j),2*alpha*beta*Dx*Dx,matrix);

                rowindex++;
                }

/* BOTTOM WALL */

j=0;
for (i=1;i<=M-1;i++)
```

```
        {
        /* Ez=-Zs*Hx */

        putreal(rowindex,Ez(i,j),2.0*Dx*ksq,matrix);
        putimag(rowindex,Ez(i,j),4*Dx*alpha*beta,matrix);
        putreal(rowindex,Ez(i,j+1),-2*R*Xs*w*eps,matrix);
        putimag(rowindex,Ez(i,j+1),2*R*Rs*w*eps,matrix);
        putreal(rowindex,Ez(i,j),2*R*Xs*w*eps,matrix);
        putimag(rowindex,Ez(i,j),-2*R*Rs*w*eps,matrix);
        putreal(rowindex,Hz(i+1,j),-(alpha*Rs-beta*Xs),matrix);
        putimag(rowindex,Hz(i+1,j),-(beta*Rs+alpha*Xs),matrix);
        putreal(rowindex,Hz(i-1,j),alpha*Rs-beta*Xs,matrix);
        putimag(rowindex,Hz(i-1,j),beta*Rs+alpha*Xs,matrix);

        rowindex++;

        /* Ex=Zs*Hz  */

        putreal(rowindex,Hz(i,j),2*Dx*(Rs*ksq-2*alpha*beta*Xs),matrix);
        putimag(rowindex,Hz(i,j),2*Dx*(Xs*ksq+2*alpha*beta*Rs),matrix);
        putimag(rowindex,Hz(i,j+1),2*w*mu*R,matrix);
        putimag(rowindex,Hz(i,j),-2*w*mu*R,matrix);
        putreal(rowindex,Ez(i+1,j),alpha,matrix);
        putimag(rowindex,Ez(i+1,j),beta,matrix);
        putreal(rowindex,Ez(i-1,j),-alpha,matrix);
        putimag(rowindex,Ez(i-1,j),-beta,matrix);

        rowindex++;

        }

/* TOP WALL */

j=N;
for (i=1;i<=M-1;i++)
        {
        /* Perfect Electric Boundary */

        /* Ez=0 */

        putreal(rowindex,Ez(i,j),1.0,matrix);

        rowindex++;

        /* Ex=0  */

        putimag(rowindex,Hz(i,j),2*w*mu*R,matrix);
        putimag(rowindex,Hz(i,j-1),-2*w*mu*R,matrix);
        putreal(rowindex,Ez(i+1,j),alpha,matrix);
        putimag(rowindex,Ez(i+1,j),beta,matrix);
        putreal(rowindex,Ez(i-1,j),-alpha,matrix);
        putimag(rowindex,Ez(i-1,j),-beta,matrix);

        rowindex++;
```

```
        /* Perfect Magnetic Boundary

Hz=0

        putreal(rowindex,Hz(i,j),1.0,matrix);

        rowindex++;

Hx=0

        putimag(rowindex,Ez(i,j),2*w*eps*R,matrix);
        putimag(rowindex,Ez(i,j-1),-2*w*eps*R,matrix);
        putreal(rowindex,Hz(i+1,j),-alpha,matrix);
        putimag(rowindex,Hz(i+1,j),-beta,matrix);
        putreal(rowindex,Hz(i-1,j),alpha,matrix);
        putimag(rowindex,Hz(i-1,j),beta,matrix);

        rowindex++;
        */


        }

/* LEFT WALL  */

i=0;
for (j=1;j<=N-1;j++)
        {

        /* Ez=Zs*Hy  */

        putreal(rowindex,Ez(i,j),2*Dx*ksq,matrix);
        putimag(rowindex,Ez(i,j),4*Dx*alpha*beta,matrix);
        putreal(rowindex,Ez(i+1,j),-2*Xs*w*eps,matrix);
        putimag(rowindex,Ez(i+1,j),2*Rs*w*eps,matrix);
        putreal(rowindex,Ez(i,j),2*Xs*w*eps,matrix);
        putimag(rowindex,Ez(i,j),-2*Rs*w*eps,matrix);
        putreal(rowindex,Hz(i,j+1),alpha*R*Rs-beta*R*Xs,matrix);
        putimag(rowindex,Hz(i,j+1),beta*R*Rs+alpha*R*Xs,matrix);
        putreal(rowindex,Hz(i,j-1),-(alpha*R*Rs-beta*R*Xs),matrix);
        putimag(rowindex,Hz(i,j-1),-(beta*R*Rs+alpha*R*Xs),matrix);

        rowindex++;

        /* Ey=-Zs*Hz  */

        putreal(rowindex,Hz(i,j),2*Dx*(Rs*ksq-2*alpha*beta*Xs),matrix);
        putimag(rowindex,Hz(i,j),2*Dx*(Xs*ksq+2*alpha*beta*Rs),matrix);
        putimag(rowindex,Hz(i+1,j),2*w*mu,matrix);
        putimag(rowindex,Hz(i,j),-2*w*mu,matrix);
        putreal(rowindex,Ez(i,j+1),-R*alpha,matrix);
        putimag(rowindex,Ez(i,j+1),-R*beta,matrix);
        putreal(rowindex,Ez(i,j-1),R*alpha,matrix);
```

```
        putimag(rowindex,Ez(i,j-1),R*beta,matrix);

        rowindex++;

        }

/*  RIGHT WALL */

i=M;
for (j=1;j<=N-1;j++)
        {
        /* Perfect Magnetic Boundary */

        /*Hz=0 */

    putreal(rowindex,Hz(i,j),1.0,matrix);

    rowindex++;

        /*Hy=0*/

    putimag(rowindex,Ez(i,j),2*w*eps,matrix);
    putimag(rowindex,Ez(i-1,j),-2*w*eps,matrix);
    putreal(rowindex,Hz(i,j+1),R*alpha,matrix);
    putimag(rowindex,Hz(i,j+1),R*beta,matrix);
    putreal(rowindex,Hz(i,j-1),-R*alpha,matrix);
    putimag(rowindex,Hz(i,j-1),-R*beta,matrix);

    rowindex++;


        /* Perfect Electric Boundary

Ez=0

        putreal(rowindex,Ez(i,j),1.0,matrix);

        rowindex++;

Ey=0

        putimag(rowindex,Hz(i,j),2*w*mu,matrix);
        putimag(rowindex,Hz(i-1,j),-2*w*mu,matrix);
        putreal(rowindex,Ez(i,j+1),-R*alpha,matrix);
        putimag(rowindex,Ez(i,j+1),-R*beta,matrix);
        putreal(rowindex,Ez(i,j-1),R*alpha,matrix);
        putimag(rowindex,Ez(i,j-1),R*beta,matrix);

        rowindex++;
        */
        }

/* CORNERS */
```

```
i=0;
j=0;

        /* Ez=-Zs*Hx */

        putreal(rowindex,Ez(i,j),Dx*ksq,matrix);
        putimag(rowindex,Ez(i,j),2*Dx*alpha*beta,matrix);
        putreal(rowindex,Ez(i,j+1),-R*Xs*w*eps,matrix);
        putimag(rowindex,Ez(i,j+1),R*Rs*w*eps,matrix);
        putreal(rowindex,Ez(i,j),R*Xs*w*eps,matrix);
        putimag(rowindex,Ez(i,j),-R*Rs*w*eps,matrix);
        putreal(rowindex,Hz(i+1,j),-(alpha*Rs-beta*Xs),matrix);
        putimag(rowindex,Hz(i+1,j),-(beta*Rs+alpha*Xs),matrix);
        putreal(rowindex,Hz(i,j),alpha*Rs-beta*Xs,matrix);
        putimag(rowindex,Hz(i,j),beta*Rs+alpha*Xs,matrix);

        rowindex++;

        /* Ex=Zs*Hz  */

        putreal(rowindex,Hz(i,j),Dx*(Rs*ksq-2*alpha*beta*Xs),matrix);
        putimag(rowindex,Hz(i,j),Dx*(Xs*ksq+2*alpha*beta*Rs),matrix);
        putimag(rowindex,Hz(i,j+1),w*mu*R,matrix);
        putimag(rowindex,Hz(i,j),-w*mu*R,matrix);
        putreal(rowindex,Ez(i+1,j),alpha,matrix);
        putimag(rowindex,Ez(i+1,j),beta,matrix);
        putreal(rowindex,Ez(i,j),-alpha,matrix);
        putimag(rowindex,Ez(i,j),-beta,matrix);

        rowindex++;

i=M;
j=0;

        /* Ez=-Zs*Hx

        putreal(rowindex,Ez(i,j),Dx*ksq,matrix);
        putimag(rowindex,Ez(i,j),2*Dx*alpha*beta,matrix);
        putreal(rowindex,Ez(i,j+1),-R*Xs*w*eps,matrix);
        putimag(rowindex,Ez(i,j+1),R*Rs*w*eps,matrix);
        putreal(rowindex,Ez(i,j),R*Xs*w*eps,matrix);
        putimag(rowindex,Ez(i,j),-R*Rs*w*eps,matrix);
        putreal(rowindex,Hz(i,j),-(alpha*Rs-beta*Xs),matrix);
        putimag(rowindex,Hz(i,j),-(beta*Rs+alpha*Xs),matrix);
        putreal(rowindex,Hz(i-1,j),alpha*Rs-beta*Xs,matrix);
        putimag(rowindex,Hz(i-1,j),beta*Rs+alpha*Xs,matrix);

        rowindex++;

        Ex=Zs*Hz

        putreal(rowindex,Hz(i,j),Dx*(Rs*ksq-2*alpha*beta*Xs),matrix);
        putimag(rowindex,Hz(i,j),Dx*(Xs*ksq+2*alpha*beta*Rs),matrix);
        putimag(rowindex,Hz(i,j+1),w*mu*R,matrix);
```

```
        putimag(rowindex,Hz(i,j),-w*mu*R,matrix);
        putreal(rowindex,Ez(i,j),alpha,matrix);
        putimag(rowindex,Ez(i,j),beta,matrix);
        putreal(rowindex,Ez(i-1,j),-alpha,matrix);
        putimag(rowindex,Ez(i-1,j),-beta,matrix);

        rowindex++;
        */

        /* Perfect Magnetic Boundary */

        /*Hz=0 */

    putreal(rowindex,Hz(i,j),1.0,matrix);

    rowindex++;

        /*Hy=0*/

    putimag(rowindex,Ez(i,j),w*eps,matrix);
    putimag(rowindex,Ez(i-1,j),-w*eps,matrix);
    putreal(rowindex,Hz(i,j+1),R*alpha,matrix);
    putimag(rowindex,Hz(i,j+1),R*beta,matrix);
    putreal(rowindex,Hz(i,j),-R*alpha,matrix);
    putimag(rowindex,Hz(i,j),-R*beta,matrix);

    rowindex++;


        /* Perfect Electric Boundary

Ez=0

        putreal(rowindex,Ez(i,j),1.0,matrix);

        rowindex++;

Ey=0

        putimag(rowindex,Hz(i,j),w*mu,matrix);
        putimag(rowindex,Hz(i-1,j),-w*mu,matrix);
        putreal(rowindex,Ez(i,j+1),-R*alpha,matrix);
        putimag(rowindex,Ez(i,j+1),-R*beta,matrix);
        putreal(rowindex,Ez(i,j),R*alpha,matrix);
        putimag(rowindex,Ez(i,j),R*beta,matrix);

        rowindex++;
        */


i=0;
j=N;

/* Ez=+Zs*Hx
```

```
        putreal(rowindex,Ez(i,j),Dx*ksq,matrix);
        putimag(rowindex,Ez(i,j),2*Dx*alpha*beta,matrix);
        putreal(rowindex,Ez(i,j),R*Xs*w*eps,matrix);
        putimag(rowindex,Ez(i,j),-R*Rs*w*eps,matrix);
        putreal(rowindex,Ez(i,j-1),-R*Xs*w*eps,matrix);
        putimag(rowindex,Ez(i,j-1),R*Rs*w*eps,matrix);
        putreal(rowindex,Hz(i+1,j),alpha*Rs-beta*Xs,matrix);
        putimag(rowindex,Hz(i+1,j),beta*Rs+alpha*Xs,matrix);
        putreal(rowindex,Hz(i,j),-(alpha*Rs-beta*Xs),matrix);
        putimag(rowindex,Hz(i,j),-(beta*Rs+alpha*Xs),matrix);

        rowindex++;

Ex=-Zs*Hz

        putreal(rowindex,Hz(i,j),Dx*(-Rs*ksq+2*alpha*beta*Xs),matrix);
        putimag(rowindex,Hz(i,j),-Dx*(Xs*ksq+2*alpha*beta*Rs),matrix);
        putimag(rowindex,Hz(i,j),w*mu*R,matrix);
        putimag(rowindex,Hz(i,j-1),-w*mu*R,matrix);
        putreal(rowindex,Ez(i+1,j),alpha,matrix);
        putimag(rowindex,Ez(i+1,j),beta,matrix);
        putreal(rowindex,Ez(i,j),-alpha,matrix);
        putimag(rowindex,Ez(i,j),-beta,matrix);

        rowindex++;

*/

        /* Perfect Electric Boundary */

        /* Ez=0 */

        putreal(rowindex,Ez(i,j),1.0,matrix);

        rowindex++;

        /* Ex=0  */

        putimag(rowindex,Hz(i,j),w*mu*R,matrix);
        putimag(rowindex,Hz(i,j-1),-w*mu*R,matrix);
        putreal(rowindex,Ez(i+1,j),alpha,matrix);
        putimag(rowindex,Ez(i+1,j),beta,matrix);
        putreal(rowindex,Ez(i,j),-alpha,matrix);
        putimag(rowindex,Ez(i,j),-beta,matrix);

        rowindex++;

        /* Perfect Magnetic Boundary

Hz=0

    putreal(rowindex,Hz(i,j),1.0,matrix);
```

```
      rowindex++;
Hx=0

            putimag(rowindex,Ez(i,j),w*eps*R,matrix);
            putimag(rowindex,Ez(i,j-1),-w*eps*R,matrix);
            putreal(rowindex,Hz(i+1,j),-alpha,matrix);
            putimag(rowindex,Hz(i+1,j),-beta,matrix);
            putreal(rowindex,Hz(i,j),alpha,matrix);
            putimag(rowindex,Hz(i,j),beta,matrix);

            rowindex++;
            */



i=M;
j=N;

            /* Ez=+Zs*Hx

            putreal(rowindex,Ez(i,j),Dx*ksq,matrix);
            putimag(rowindex,Ez(i,j),2*Dx*alpha*beta,matrix);
            putreal(rowindex,Ez(i,j),R*Xs*w*eps,matrix);
            putimag(rowindex,Ez(i,j),-R*Rs*w*eps,matrix);
            putreal(rowindex,Ez(i,j-1),-R*Xs*w*eps,matrix);
            putimag(rowindex,Ez(i,j-1),R*Rs*w*eps,matrix);
            putreal(rowindex,Hz(i,j),alpha*Rs-beta*Xs,matrix);
            putimag(rowindex,Hz(i,j),beta*Rs+alpha*Xs,matrix);
            putreal(rowindex,Hz(i-1,j),-(alpha*Rs-beta*Xs),matrix);
            putimag(rowindex,Hz(i-1,j),-(beta*Rs+alpha*Xs),matrix);

            rowindex++;

            Ex=-Zs*Hz

            putreal(rowindex,Hz(i,j),Dx*(-Rs*ksq+2*alpha*beta*Xs),matrix);
            putimag(rowindex,Hz(i,j),-Dx*(Xs*ksq+2*alpha*beta*Rs),matrix);
            putimag(rowindex,Hz(i,j),w*mu*R,matrix);
            putimag(rowindex,Hz(i,j-1),-w*mu*R,matrix);
            putreal(rowindex,Ez(i,j),alpha,matrix);
            putimag(rowindex,Ez(i,j),beta,matrix);
            putreal(rowindex,Ez(i-1,j),-alpha,matrix);
            putimag(rowindex,Ez(i-1,j),-beta,matrix);

            rowindex++;
*/

            /* Hz=0 */

      putreal(rowindex,Hz(i,j),1.0,matrix);

      rowindex++;

            /* Ez=0 */
```

```
        putreal(rowindex,Ez(i,j),1.0,matrix);

        rowindex++;

        /* Ex=0

        putimag(rowindex,Hz(i,j),w*mu*R,matrix);
        putimag(rowindex,Hz(i,j-1),-w*mu*R,matrix);
        putreal(rowindex,Ez(i,j),alpha,matrix);
        putimag(rowindex,Ez(i,j),beta,matrix);
        putreal(rowindex,Ez(i-1,j),-alpha,matrix);
        putimag(rowindex,Ez(i-1,j),-beta,matrix);

        rowindex++;
*/

return;
}


void initmatrix(A)
float A[ROWLENGTH][ROWLENGTH][2];
{
int i,j,k;

for (i=0;i<=ROWLENGTH-1;i++)
        for (j=0;j<=ROWLENGTH-1;j++)
                for (k=0;k<=1;k++)
                        A[i][j][k]=0.0;
return;
}


void putreal(rowindex,colindex, value, matrix)
int rowindex,colindex;
float value, matrix[ROWLENGTH][ROWLENGTH][2];
{
/* For FORTRAN calculations reverse colindex and rowindex
   i.e., Transpose the matrix    */
matrix[colindex][rowindex][0]+=value;
return;
}


void putimag(rowindex,colindex, value, matrix)
int rowindex,colindex;
float value, matrix[ROWLENGTH][ROWLENGTH][2];
{
/* For FORTRAN calculations reverse colindex and rowindex
   i.e., Transpose the matrix    */
matrix[colindex][rowindex][1]+=value;
return;
}
```

```
int Ez(i,j)
int i,j;
{
return(2*i+2*j*(M+1));
}


int Hz(i,j)
int i,j;
{
return(2*i+2*j*(M+1)+1);
}


float determinant(gamma,matrix,params)
float *gamma, *matrix, *params;
{       void matr();
        float mag;
        fortran void  CGEFA();
        fortran void  CGED();
        static float det[3];
        int info, ipvt[ROWLENGTH];
matr(gamma,matrix,params);
CGEFA(matrix,ROWLENGTH,ROWLENGTH,ipvt,&info);
CGED(matrix,ROWLENGTH,ROWLENGTH,ipvt,det);
mag=0.5*log10(SQR(det[0])+SQR(det[1]))+det[2]-(float)(M+N+1)*log10(-
SQR(gamma[2])+SQR(2*M_PI*params[3])*4*M_PI*1e-7*8.854e-12*params[2]);
return(mag);
}


float *svd(gamma,matrix,params)
float *gamma, *matrix, *params;
{    void matr();
     fortran void  CGEBRD();
     fortran void  CBDSQR();
     fortran void  CUNGBR();
     int info;
     char upper, vect;
     float E[ROWLENGTH-1], TAUP[ROWLENGTH][2], TAUQ[ROWLENGTH][2],
work[64*ROWLENGTH][2];
     static float D[ROWLENGTH];
upper='U';
vect='P';
matr(gamma,matrix,params);
CGEBRD(ROWLENGTH,ROWLENGTH,matrix,ROWLENGTH,D,E,TAUQ,TAUP,work,64*ROWLEN
GTH,info);
printf("\nFirst Info: %d\n",info);
CUNGBR(&vect,ROWLENGTH,ROWLENGTH,ROWLENGTH,matrix,ROWLENGTH,TAUP,work,64*
ROWLENGTH,info);
printf("Second Info: %d\n",info);
```

```
CBDSQR(&upper,ROWLENGTH,ROWLENGTH,0,0,D,E,matrix,ROWLENGTH,&info,1,&info,1,work,
&info);
printf("Third Info: %d\n",info);
return(&D[0]);
}


void amoeba(p,y,ndim,ftol,argtol,funk,nfunk,matrix,params)
float (*funk)(),p[4][3],ftol,argtol,y[],*matrix,*params;
int *nfunk,ndim;
{
        float amotry();
        int i,ihi,ilo,inhi,pihi[3],pilo[3],pinhi[3],j,mpts=ndim+1;
        float rtol,sum,swap,ysave,ytry,*psum,ptol[3];

        psum=vector(1,ndim);
        *nfunk=0;
        GET_PSUM
        for (;;) {
                ilo=1;
                ihi = y[1]>y[2] ? (inhi=2,1) : (inhi=1,2);
                for (i=1;i<=mpts;i++) {
                        if (y[i] <= y[ilo]) ilo=i;
                        if (y[i] > y[ihi]) {
                                inhi=ihi;
                                ihi=i;
                        } else if (y[i] > y[inhi] && i != ihi) inhi=i;
                }
                for (j=1;j<=ndim;j++)
                        {
                pilo[j]=1;
                        pihi[j] = p[1][j]>p[2][j] ? (pinhi[j]=2,1) : (pinhi[j]=1,2);
                        for (i=1;i<=mpts;i++) {
                if (p[i][j] <= p[pilo[j]][j]) pilo[j]=i;
                      if (p[i][j] > p[pihi[j]][j]) {
                   pinhi[j]=pihi[j];
                   pihi[j]=i;
                       } else if (p[i][j] > p[pinhi[j]][j] && i != pihi[j]) pinhi[j]=i;
                }
                ptol[j]=2.0*fabs(p[pihi[j]][j]-p[pilo[j]][j])/(fabs(p[pihi[j]][j])+fabs(p[pilo[j]][j]));
                }
                rtol=2.0*fabs(y[ihi]-y[ilo])/(fabs(y[ihi])+fabs(y[ilo]));
                if (rtol < ftol) {
                        SWAP(y[1],y[ilo])
                        for (i=1;i<=ndim;i++) SWAP(p[1][i],p[ilo][i])
                        break;
                }
                if (ptol[1]<= argtol && ptol[2] <= argtol) break;
                if (*nfunk >= NMAX) nrerror("NMAX exceeded");
                *nfunk += 2;
                ytry=amotry(p,y,psum,ndim,funk,ihi,-1.0,matrix,params);
                if (ytry <= y[ilo])
                        ytry=amotry(p,y,psum,ndim,funk,ihi,2.0,matrix,params);
                else if (ytry >= y[inhi]) {
```

```
                        ysave=y[ihi];
                        ytry=amotry(p,y,psum,ndim,funk,ihi,0.5,matrix,params);
                        if (ytry >= ysave) {
                                for (i=1;i<=mpts;i++) {
                                        if (i != ilo) {
                                                for (j=1;j<=ndim;j++)
                                                        p[i][j]=psum[j]=0.5*(p[i][j]+p[ilo][j]);
                                                y[i]=(*funk)(psum,matrix,params);
                                        }
                                }
                                *nfunk += ndim;
                                GET_PSUM
                        }
                } else --(*nfunk);
        }
        free_vector(psum,1,ndim);
}
#undef SWAP
#undef GET_PSUM
#undef NMAX


float amotry(p,y,psum,ndim,funk,ihi,fac,matrix,params)
float (*funk)(),p[4][3],fac,psum[],y[],*matrix,*params;
int ihi,ndim;
{
        int j;
        float fac1,fac2,ytry,*ptry;

        ptry=vector(1,ndim);
        fac1=(1.0-fac)/ndim;
        fac2=fac1-fac;
        for (j=1;j<=ndim;j++) ptry[j]=psum[j]*fac1-p[ihi][j]*fac2;
        ytry=(*funk)(ptry,matrix,params);
        if (ytry < y[ihi]) {
                y[ihi]=ytry;
                for (j=1;j<=ndim;j++) {
                        psum[j] += ptry[j]-p[ihi][j];
                        p[ihi][j]=ptry[j];
                }
        }
        free_vector(ptry,1,ndim);
        return ytry;
}


float *EH_Power_calc(gamma,result,params,z,t,ex,ey,ez,hx,hy,hz)
float complex gamma, result[ROWLENGTH];
float
*params,z,t,ex[2*N+1][2*M+1],ey[2*N+1][2*M+1],hx[2*N+1][2*M+1],hy[2*N+1][2*M+1],ez[2*N+1][
2*M+1],hz[2*N+1][2*M+1];
{
int Ez(), Hz();
int i,j;
```

```
float Dx,Dy;
float a,b,eps,mu,w;
float complex prefac;
float complex Ex,Ey,Hx,Hy;
float complex Power=CMPLXF(0.0,0.0);
float complex Ptemp=CMPLXF(0.0,0.0);
static float Power_Hmax[3]={0.0,0.0,0.0};
float H_bot_temp, H_lef_temp;
a=params[0];
b=params[1];
eps=params[2]*8.854e-12;
w=2*M_PI*params[3];
mu=4*M_PI*1e-7;
Dx=a/(2*M);
Dy=b/(2*N);

prefac=-1/(w*w*mu*eps+gamma*gamma);

H_bot_temp=0.0;
H_lef_temp=0.0;

/*INSIDE*/

for (j=1;j<=N-1;j++)
        for (i=1;i<=M-1;i++)
                {
                Ex=prefac*(gamma*(result[Ez(i+1,j)]-result[Ez(i-
1,j)])/(2*Dx)+J*w*mu*(result[Hz(i,j+1)]-result[Hz(i,j-1)])/(2*Dy));
                Hy=prefac*(J*w*eps*(result[Ez(i+1,j)]-result[Ez(i-
1,j)])/(2*Dx)+gamma*(result[Hz(i,j+1)]-result[Hz(i,j-1)])/(2*Dy));
                Ey=prefac*(gamma*(result[Ez(i,j+1)]-result[Ez(i,j-1)])/(2*Dy)-
J*w*mu*(result[Hz(i+1,j)]-result[Hz(i-1,j)])/(2*Dx));
                Hx=prefac*(-J*w*eps*(result[Ez(i,j+1)]-result[Ez(i,j-
1)])/(2*Dy)+gamma*(result[Hz(i+1,j)]-result[Hz(i-1,j)])/(2*Dx));

                Ptemp+=Ex*conj(Hy)-Ey*conj(Hx);

                ex[j][i]=creal(Ex*cexp(J*w*t-gamma*z));
                hy[j][i]=creal(Hy*cexp(J*w*t-gamma*z));
                ey[j][i]=creal(Ey*cexp(J*w*t-gamma*z));
                hx[j][i]=creal(Hx*cexp(J*w*t-gamma*z));
                ez[j][i]=creal(result[Ez(i,j)]*cexp(J*w*t-gamma*z));
                hz[j][i]=creal(result[Hz(i,j)]*cexp(J*w*t-gamma*z));

/*Depending on type of Right and Top walls pick the right symmetry equation */

                /*ex[j][2*M-i]= ex[j][i];*/
                ex[j][2*M-i]=-ex[j][i];

                /*ex[2*N-j][i]= ex[j][i];*/
                ex[2*N-j][i]=-ex[j][i];

                ex[2*N-j][2*M-i]= ex[j][i];
```

```
                    /*ex[2*N-j][2*M-i]=-ex[j][i];*/

                    hx[j][2*M-i]= hx[j][i];
                    /*hx[j][2*M-i]=-hx[j][i];*/

                    hx[2*N-j][i]= hx[j][i];
                    /*hx[2*N-j][i]=-hx[j][i];*/

                    hx[2*N-j][2*M-i]= hx[j][i];
                    /*hx[2*N-j][2*M-i]=-hx[j][i];*/

                    ey[j][2*M-i]= ey[j][i];
                    /*ey[j][2*M-i]=-ey[j][i];*/

                    ey[2*N-j][i]= ey[j][i];
                    /*ey[2*N-j][i]=-ey[j][i];*/

                    ey[2*N-j][2*M-i]= ey[j][i];
                    /*ey[2*N-j][2*M-i]=-ey[j][i];*/

                    /*hy[j][2*M-i]= hy[j][i];*/
                    hy[j][2*M-i]=-hy[j][i];

                    /*hy[2*N-j][i]= hy[j][i];*/
                    hy[2*N-j][i]=-hy[j][i];

                    hy[2*N-j][2*M-i]= hy[j][i];
                    /*hy[2*N-j][2*M-i]=-hy[j][i];*/

                    ez[j][2*M-i]= ez[j][i];
                    /*ez[j][2*M-i]=-ez[j][i];*/

                    /*ez[2*N-j][i]= ez[j][i];*/
                    ez[2*N-j][i]=-ez[j][i];

                    /*ez[2*N-j][2*M-i]= ez[j][i];*/
                    ez[2*N-j][2*M-i]=-ez[j][i];

                    /*hz[j][2*M-i]= hz[j][i];*/
                    hz[j][2*M-i]=-hz[j][i];

                    hz[2*N-j][i]= hz[j][i];
                    /*hz[2*N-j][i]=-hz[j][i];*/

                    /*hz[2*N-j][2*M-i]= hz[j][i];*/
                    hz[2*N-j][2*M-i]=-hz[j][i];
                    }
Power=4*Ptemp;
Ptemp=CMPLXF(0.0,0.0);

/*SIDES*/

/*Bottom Side*/
j=0;
```

```
for (i=1;i<=M-1;i++)
        {
        Ex=prefac*(gamma*(result[Ez(i+1,j)]-result[Ez(i-1,j)])/(2*Dx)+J*w*mu*(result[Hz(i,j+1)]-
result[Hz(i,j)])/Dy);
        Hy=prefac*(J*w*eps*(result[Ez(i+1,j)]-result[Ez(i-1,j)])/(2*Dx)+gamma*(result[Hz(i,j+1)]-
result[Hz(i,j)])/Dy);
        Ey=prefac*(gamma*(result[Ez(i,j+1)]-result[Ez(i,j)])/Dy-J*w*mu*(result[Hz(i+1,j)]-result[Hz(i-
1,j)])/(2*Dx));
        Hx=prefac*(-J*w*eps*(result[Ez(i,j+1)]-result[Ez(i,j)])/Dy+gamma*(result[Hz(i+1,j)]-
result[Hz(i-1,j)])/(2*Dx));


        H_bot_temp=sqrt(0.5*(SQR(cabs(Hx))+SQR(cabs(result[Hz(i,j)]))+sqrt(SQR(SQR(creal(Hx))-
SQR(cimag(Hx))+SQR(creal(result[Hz(i,j)]))-
SQR(cimag(result[Hz(i,j)])))+4*SQR(creal(Hx)*cimag(Hx)+creal(result[Hz(i,j)])*cimag(result[Hz(i,j)])))
);
        if (H_bot_temp>Power_Hmax[0]) H_bot_temp=Power_Hmax[0];

        Ptemp+=Ex*conj(Hy)-Ey*conj(Hx);

        ex[j][i]=creal(Ex*cexp(J*w*t-gamma*z));
        hy[j][i]=creal(Hy*cexp(J*w*t-gamma*z));
        ey[j][i]=creal(Ey*cexp(J*w*t-gamma*z));
        hx[j][i]=creal(Hx*cexp(J*w*t-gamma*z));
        ez[j][i]=creal(result[Ez(i,j)]*cexp(J*w*t-gamma*z));
        hz[j][i]=creal(result[Hz(i,j)]*cexp(J*w*t-gamma*z));

/*Depending on type of Right and Top walls pick the right symmetry equation */

        /*ex[j][2*M-i]= ex[j][i];*/
        ex[j][2*M-i]=-ex[j][i];

        /*ex[2*N-j][i]= ex[j][i];*/
        ex[2*N-j][i]=-ex[j][i];

        ex[2*N-j][2*M-i]= ex[j][i];
        /*ex[2*N-j][2*M-i]=-ex[j][i];*/

        hx[j][2*M-i]= hx[j][i];
        /*hx[j][2*M-i]=-hx[j][i];*/

        hx[2*N-j][i]= hx[j][i];
        /*hx[2*N-j][i]=-hx[j][i];*/

        hx[2*N-j][2*M-i]= hx[j][i];
        /*hx[2*N-j][2*M-i]=-hx[j][i];*/

        ey[j][2*M-i]= ey[j][i];
        /*ey[j][2*M-i]=-ey[j][i];*/

        ey[2*N-j][i]= ey[j][i];
        /*ey[2*N-j][i]=-ey[j][i];*/

        ey[2*N-j][2*M-i]= ey[j][i];
```

```
        /*ey[2*N-j][2*M-i]=-ey[j][i];*/

        /*hy[j][2*M-i]= hy[j][i];*/
        hy[j][2*M-i]=-hy[j][i];

        /*hy[2*N-j][i]= hy[j][i];*/
        hy[2*N-j][i]=-hy[j][i];

        hy[2*N-j][2*M-i]= hy[j][i];
        /*hy[2*N-j][2*M-i]=-hy[j][i];*/

        ez[j][2*M-i]= ez[j][i];
        /*ez[j][2*M-i]=-ez[j][i];*/

        /*ez[2*N-j][i]= ez[j][i];*/
        ez[2*N-j][i]=-ez[j][i];

        /*ez[2*N-j][2*M-i]= ez[j][i];*/
        ez[2*N-j][2*M-i]=-ez[j][i];

        /*hz[j][2*M-i]= hz[j][i];*/
        hz[j][2*M-i]=-hz[j][i];

        hz[2*N-j][i]= hz[j][i];
        /*hz[2*N-j][i]=-hz[j][i];*/

        /*hz[2*N-j][2*M-i]= hz[j][i];*/
        hz[2*N-j][2*M-i]=-hz[j][i];
        }
Power+=4*Ptemp;
Ptemp=CMPLXF(0.0,0.0);

/*Left Side*/

i=0;
for (j=1;j<=N-1;j++)
        {
        Ex=prefac*(gamma*(result[Ez(i+1,j)]-result[Ez(i,j)])/Dx+J*w*mu*(result[Hz(i,j+1)]-
result[Hz(i,j-1)])/(2*Dy));
        Hy=prefac*(J*w*eps*(result[Ez(i+1,j)]-result[Ez(i,j)])/Dx+gamma*(result[Hz(i,j+1)]-
result[Hz(i,j-1)])/(2*Dy));
        Ey=prefac*(gamma*(result[Ez(i,j+1)]-result[Ez(i,j-1)])/(2*Dy)-J*w*mu*(result[Hz(i+1,j)]-
result[Hz(i,j)])/Dx);
        Hx=prefac*(-J*w*eps*(result[Ez(i,j+1)]-result[Ez(i,j-1)])/(2*Dy)+gamma*(result[Hz(i+1,j)]-
result[Hz(i,j)])/Dx);

        Ptemp+=Ex*conj(Hy)-Ey*conj(Hx);

        ex[j][i]=creal(Ex*cexp(J*w*t-gamma*z));
        hy[j][i]=creal(Hy*cexp(J*w*t-gamma*z));
        ey[j][i]=creal(Ey*cexp(J*w*t-gamma*z));
        hx[j][i]=creal(Hx*cexp(J*w*t-gamma*z));
        ez[j][i]=creal(result[Ez(i,j)]*cexp(J*w*t-gamma*z));
        hz[j][i]=creal(result[Hz(i,j)]*cexp(J*w*t-gamma*z));
```

```
/*Depending on type of Right and Top walls pick the right symmetry equation */

        /*ex[j][2*M-i]= ex[j][i];*/
        ex[j][2*M-i]=-ex[j][i];

        /*ex[2*N-j][i]= ex[j][i];*/
        ex[2*N-j][i]=-ex[j][i];

        ex[2*N-j][2*M-i]= ex[j][i];
        /*ex[2*N-j][2*M-i]=-ex[j][i];*/

        hx[j][2*M-i]= hx[j][i];
        /*hx[j][2*M-i]=-hx[j][i];*/

        hx[2*N-j][i]= hx[j][i];
        /*hx[2*N-j][i]=-hx[j][i];*/

        hx[2*N-j][2*M-i]= hx[j][i];
        /*hx[2*N-j][2*M-i]=-hx[j][i];*/

        ey[j][2*M-i]= ey[j][i];
        /*ey[j][2*M-i]=-ey[j][i];*/

        ey[2*N-j][i]= ey[j][i];
        /*ey[2*N-j][i]=-ey[j][i];*/

        ey[2*N-j][2*M-i]= ey[j][i];
        /*ey[2*N-j][2*M-i]=-ey[j][i];*/

        /*hy[j][2*M-i]= hy[j][i];*/
        hy[j][2*M-i]=-hy[j][i];

        /*hy[2*N-j][i]= hy[j][i];*/
        hy[2*N-j][i]=-hy[j][i];

        hy[2*N-j][2*M-i]= hy[j][i];
        /*hy[2*N-j][2*M-i]=-hy[j][i];*/

        ez[j][2*M-i]= ez[j][i];
        /*ez[j][2*M-i]=-ez[j][i];*/

        /*ez[2*N-j][i]= ez[j][i];*/
        ez[2*N-j][i]=-ez[j][i];

        /*ez[2*N-j][2*M-i]= ez[j][i];*/
        ez[2*N-j][2*M-i]=-ez[j][i];

        /*hz[j][2*M-i]= hz[j][i];*/
        hz[j][2*M-i]=-hz[j][i];

        hz[2*N-j][i]= hz[j][i];
        /*hz[2*N-j][i]=-hz[j][i];*/
```

```
        /*hz[2*N-j][2*M-i]= hz[j][i];*/
        hz[2*N-j][2*M-i]=-hz[j][i];
        }
Power+=4*Ptemp;
Ptemp=CMPLXF(0.0,0.0);

/*Top Side*/
j=N;
for (i=1;i<=M-1;i++)
        {
        Ex=prefac*(gamma*(result[Ez(i+1,j)]-result[Ez(i-1,j)])/(2*Dx)+J*w*mu*(result[Hz(i,j)]-
result[Hz(i,j-1)])/Dy);
        Hy=prefac*(J*w*eps*(result[Ez(i+1,j)]-result[Ez(i-1,j)])/(2*Dx)+gamma*(result[Hz(i,j)]-
result[Hz(i,j-1)])/Dy);
        Ey=prefac*(gamma*(result[Ez(i,j)]-result[Ez(i,j-1)])/Dy-J*w*mu*(result[Hz(i+1,j)]-result[Hz(i-
1,j)])/(2*Dx));
        Hx=prefac*(-J*w*eps*(result[Ez(i,j)]-result[Ez(i,j-1)])/Dy+gamma*(result[Hz(i+1,j)]-
result[Hz(i-1,j)])/(2*Dx));

        Ptemp+=Ex*conj(Hy)-Ey*conj(Hx);

        ex[j][i]=creal(Ex*cexp(J*w*t-gamma*z));
        hy[j][i]=creal(Hy*cexp(J*w*t-gamma*z));
        ey[j][i]=creal(Ey*cexp(J*w*t-gamma*z));
        hx[j][i]=creal(Hx*cexp(J*w*t-gamma*z));
        ez[j][i]=creal(result[Ez(i,j)]*cexp(J*w*t-gamma*z));
        hz[j][i]=creal(result[Hz(i,j)]*cexp(J*w*t-gamma*z));

/*Depending on type of Right and Top walls pick the right symmetry equation */

        /*ex[j][2*M-i]= ex[j][i];*/
        ex[j][2*M-i]=-ex[j][i];


        hx[j][2*M-i]= hx[j][i];
        /*hx[j][2*M-i]=-hx[j][i];*/

        ey[j][2*M-i]= ey[j][i];
        /*ey[j][2*M-i]=-ey[j][i];*/

        /*hy[j][2*M-i]= hy[j][i];*/
        hy[j][2*M-i]=-hy[j][i];

        ez[j][2*M-i]= ez[j][i];
        /*ez[j][2*M-i]=-ez[j][i];*/

        /*hz[j][2*M-i]= hz[j][i];*/
        hz[j][2*M-i]=-hz[j][i];
        }

Power+=2*Ptemp;
Ptemp=CMPLXF(0.0,0.0);

/*Right Side*/
```

```
i=M;
for (j=1;j<=N-1;j++)
        {
        Ex=prefac*(gamma*(result[Ez(i,j)]-result[Ez(i-1,j)])/Dx+J*w*mu*(result[Hz(i,j+1)]-
result[Hz(i,j-1)])/(2*Dy));
        Hy=prefac*(J*w*eps*(result[Ez(i,j)]-result[Ez(i-1,j)])/Dx+gamma*(result[Hz(i,j+1)]-
result[Hz(i,j-1)])/(2*Dy));
        Ey=prefac*(gamma*(result[Ez(i,j+1)]-result[Ez(i,j-1)])/(2*Dy)-J*w*mu*(result[Hz(i,j)]-
result[Hz(i-1,j)])/Dx);
        Hx=prefac*(-J*w*eps*(result[Ez(i,j+1)]-result[Ez(i,j-1)])/(2*Dy)+gamma*(result[Hz(i,j)]-
result[Hz(i-1,j)])/Dx);

        Ptemp+=Ex*conj(Hy)-Ey*conj(Hx);

        ex[j][i]=creal(Ex*cexp(J*w*t-gamma*z));
        hy[j][i]=creal(Hy*cexp(J*w*t-gamma*z));
        ey[j][i]=creal(Ey*cexp(J*w*t-gamma*z));
        hx[j][i]=creal(Hx*cexp(J*w*t-gamma*z));
        ez[j][i]=creal(result[Ez(i,j)]*cexp(J*w*t-gamma*z));
        hz[j][i]=creal(result[Hz(i,j)]*cexp(J*w*t-gamma*z));

/*Depending on type of Right and Top walls pick the right symmetry equation */

        /*ex[2*N-j][i]= ex[j][i];*/
        ex[2*N-j][i]=-ex[j][i];

        hx[2*N-j][i]= hx[j][i];
        /*hx[2*N-j][i]=-hx[j][i];*/

        ey[2*N-j][i]= ey[j][i];
        /*ey[2*N-j][i]=-ey[j][i];*/

        /*hy[2*N-j][i]= hy[j][i];*/
        hy[2*N-j][i]=-hy[j][i];

        /*ez[2*N-j][i]= ez[j][i];*/
        ez[2*N-j][i]=-ez[j][i];

        hz[2*N-j][i]= hz[j][i];
        /*hz[2*N-j][i]=-hz[j][i];*/
        }
Power+=2*Ptemp;
Ptemp=CMPLXF(0.0,0.0);

/*CORNERS*/
i=0;
j=0;

Ex=prefac*(gamma*(result[Ez(i+1,j)]-result[Ez(i,j)])/Dx+J*w*mu*(result[Hz(i,j+1)]-result[Hz(i,j)])/Dy);
Hy=prefac*(J*w*eps*(result[Ez(i+1,j)]-result[Ez(i,j)])/Dx+gamma*(result[Hz(i,j+1)]-result[Hz(i,j)])/Dy);
Ey=prefac*(gamma*(result[Ez(i,j+1)]-result[Ez(i,j)])/Dy-J*w*mu*(result[Hz(i+1,j)]-result[Hz(i,j)])/Dx);
Hx=prefac*(-J*w*eps*(result[Ez(i,j+1)]-result[Ez(i,j)])/Dy+gamma*(result[Hz(i+1,j)]-
result[Hz(i,j)])/Dx);
```

```
        H_bot_temp=sqrt(0.5*(SQR(cabs(Hx))+SQR(cabs(result[Hz(i,j)]))+sqrt(SQR(SQR(creal(Hx))-
SQR(cimag(Hx))+SQR(creal(result[Hz(i,j)]))-
SQR(cimag(result[Hz(i,j)])))+4*SQR(creal(Hx)*cimag(Hx)+creal(result[Hz(i,j)])*cimag(result[Hz(i,j)])))))
);
        if (H_bot_temp>Power_Hmax[0]) Power_Hmax[0]=H_bot_temp;


        H_lef_temp=sqrt(0.5*(SQR(cabs(Hy))+SQR(cabs(result[Hz(i,j)]))+sqrt(SQR(SQR(creal(Hy))-
SQR(cimag(Hy))+SQR(creal(result[Hz(i,j)]))-
SQR(cimag(result[Hz(i,j)])))+4*SQR(creal(Hy)*cimag(Hy)+creal(result[Hz(i,j)])*cimag(result[Hz(i,j)])))))
);
        if (H_lef_temp>Power_Hmax[1]) Power_Hmax[1]=H_lef_temp;

Ptemp+=Ex*conj(Hy)-Ey*conj(Hx);

ex[j][i]=creal(Ex*cexp(J*w*t-gamma*z));
hy[j][i]=creal(Hy*cexp(J*w*t-gamma*z));
ey[j][i]=creal(Ey*cexp(J*w*t-gamma*z));
hx[j][i]=creal(Hx*cexp(J*w*t-gamma*z));
ez[j][i]=creal(result[Ez(i,j)]*cexp(J*w*t-gamma*z));
hz[j][i]=creal(result[Hz(i,j)]*cexp(J*w*t-gamma*z));

/*Depending on type of Right and Top walls pick the right symmetry equation */

/*ex[j][2*M-i]= ex[j][i];*/
ex[j][2*M-i]=-ex[j][i];

/*ex[2*N-j][i]= ex[j][i];*/
ex[2*N-j][i]=-ex[j][i];

ex[2*N-j][2*M-i]= ex[j][i];
/*ex[2*N-j][2*M-i]=-ex[j][i];*/

hx[j][2*M-i]= hx[j][i];
/*hx[j][2*M-i]=-hx[j][i];*/

hx[2*N-j][i]= hx[j][i];
/*hx[2*N-j][i]=-hx[j][i];*/

hx[2*N-j][2*M-i]= hx[j][i];
/*hx[2*N-j][2*M-i]=-hx[j][i];*/

ey[j][2*M-i]= ey[j][i];
/*ey[j][2*M-i]=-ey[j][i];*/

ey[2*N-j][i]= ey[j][i];
/*ey[2*N-j][i]=-ey[j][i];*/

ey[2*N-j][2*M-i]= ey[j][i];
/*ey[2*N-j][2*M-i]=-ey[j][i];*/

/*hy[j][2*M-i]= hy[j][i];*/
hy[j][2*M-i]=-hy[j][i];
```

```
/*hy[2*N-j][i]= hy[j][i];*/
hy[2*N-j][i]=-hy[j][i];

hy[2*N-j][2*M-i]= hy[j][i];
/*hy[2*N-j][2*M-i]=-hy[j][i];*/

ez[j][2*M-i]= ez[j][i];
/*ez[j][2*M-i]=-ez[j][i];*/

/*ez[2*N-j][i]= ez[j][i];*/
ez[2*N-j][i]=-ez[j][i];

/*ez[2*N-j][2*M-i]= ez[j][i];*/
ez[2*N-j][2*M-i]=-ez[j][i];

/*hz[j][2*M-i]= hz[j][i];*/
hz[j][2*M-i]=-hz[j][i];

hz[2*N-j][i]= hz[j][i];
/*hz[2*N-j][i]=-hz[j][i];*/

/*hz[2*N-j][2*M-i]= hz[j][i];*/
hz[2*N-j][2*M-i]=-hz[j][i];

Power+=4*Ptemp;
Ptemp=CMPLXF(0.0,0.0);

i=M;
j=0;

Ex=prefac*(gamma*(result[Ez(i,j)]-result[Ez(i-1,j)])/Dx+J*w*mu*(result[Hz(i,j+1)]-result[Hz(i,j)])/Dy);
Hy=prefac*(J*w*eps*(result[Ez(i,j)]-result[Ez(i-1,j)])/Dx+gamma*(result[Hz(i,j+1)]-result[Hz(i,j)])/Dy);
Ey=prefac*(gamma*(result[Ez(i,j+1)]-result[Ez(i,j)])/Dy-J*w*mu*(result[Hz(i,j)]-result[Hz(i-1,j)])/Dx);
Hx=prefac*(-J*w*eps*(result[Ez(i,j+1)]-result[Ez(i,j)])/Dy+gamma*(result[Hz(i,j)]-result[Hz(i-1,j)])/Dx);

        H_bot_temp=sqrt(0.5*(SQR(cabs(Hx))+SQR(cabs(result[Hz(i,j)]))+sqrt(SQR(SQR(creal(Hx))-
SQR(cimag(Hx))+SQR(creal(result[Hz(i,j)]))-
SQR(cimag(result[Hz(i,j)])))+4*SQR(creal(Hx)*cimag(Hx)+creal(result[Hz(i,j)])*cimag(result[Hz(i,j)]))))
);
        if (H_bot_temp>Power_Hmax[0]) Power_Hmax[0]=H_bot_temp;

Ptemp+=Ex*conj(Hy)-Ey*conj(Hx);

ex[j][i]=creal(Ex*cexp(J*w*t-gamma*z));
hy[j][i]=creal(Hy*cexp(J*w*t-gamma*z));
ey[j][i]=creal(Ey*cexp(J*w*t-gamma*z));
hx[j][i]=creal(Hx*cexp(J*w*t-gamma*z));
ez[j][i]=creal(result[Ez(i,j)]*cexp(J*w*t-gamma*z));
hz[j][i]=creal(result[Hz(i,j)]*cexp(J*w*t-gamma*z));

/*Depending on type of Right and Top walls pick the right symmetry equation */

/*ex[2*N-j][i]= ex[j][i];*/
ex[2*N-j][i]=-ex[j][i];
```

```
hx[2*N-j][i]= hx[j][i];
/*hx[2*N-j][i]=-hx[j][i];*/

ey[2*N-j][i]= ey[j][i];
/*ey[2*N-j][i]=-ey[j][i];*/

/*hy[2*N-j][i]= hy[j][i];*/
hy[2*N-j][i]=-hy[j][i];

/*ez[2*N-j][i]= ez[j][i];*/
ez[2*N-j][i]=-ez[j][i];

hz[2*N-j][i]= hz[j][i];
/*hz[2*N-j][i]=-hz[j][i];*/

Power+=2*Ptemp;
Ptemp=CMPLXF(0.0,0.0);

i=0;
j=N;

Ex=prefac*(gamma*(result[Ez(i+1,j)]-result[Ez(i,j)])/Dx+J*w*mu*(result[Hz(i,j)]-result[Hz(i,j-1)])/Dy);
Hy=prefac*(J*w*eps*(result[Ez(i+1,j)]-result[Ez(i,j)])/Dx+gamma*(result[Hz(i,j)]-result[Hz(i,j-1)])/Dy);
Ey=prefac*(gamma*(result[Ez(i,j)]-result[Ez(i,j-1)])/Dy-J*w*mu*(result[Hz(i+1,j)]-result[Hz(i,j)])/Dx);
Hx=prefac*(-J*w*eps*(result[Ez(i,j)]-result[Ez(i,j-1)])/Dy+gamma*(result[Hz(i+1,j)]-result[Hz(i,j)])/Dx);

        H_lef_temp=sqrt(0.5*(SQR(cabs(Hy))+SQR(cabs(result[Hz(i,j)]))+sqrt(SQR(SQR(creal(Hy))-
SQR(cimag(Hy))+SQR(creal(result[Hz(i,j)]))-
SQR(cimag(result[Hz(i,j)])))+4*SQR(creal(Hy)*cimag(Hy)+creal(result[Hz(i,j)])*cimag(result[Hz(i,j)])))
);
        if (H_lef_temp>Power_Hmax[1]) Power_Hmax[1]=H_lef_temp;

Ptemp+=Ex*conj(Hy)-Ey*conj(Hx);

ex[j][i]=creal(Ex*cexp(J*w*t-gamma*z));
hy[j][i]=creal(Hy*cexp(J*w*t-gamma*z));
ey[j][i]=creal(Ey*cexp(J*w*t-gamma*z));
hx[j][i]=creal(Hx*cexp(J*w*t-gamma*z));
ez[j][i]=creal(result[Ez(i,j)]*cexp(J*w*t-gamma*z));
hz[j][i]=creal(result[Hz(i,j)]*cexp(J*w*t-gamma*z));

/*Depending on type of Right and Top walls pick the right symmetry equation */

/*ex[j][2*M-i]= ex[j][i];*/
ex[j][2*M-i]=-ex[j][i];


hx[j][2*M-i]= hx[j][i];
/*hx[j][2*M-i]=-hx[j][i];*/

ey[j][2*M-i]= ey[j][i];
/*ey[j][2*M-i]=-ey[j][i];*/
```

```
/*hy[j][2*M-i]= hy[j][i];*/
hy[j][2*M-i]=-hy[j][i];

ez[j][2*M-i]= ez[j][i];
/*ez[j][2*M-i]=-ez[j][i];*/

/*hz[j][2*M-i]= hz[j][i];*/
hz[j][2*M-i]=-hz[j][i];

Power+=2*Ptemp;
Ptemp=CMPLXF(0.0,0.0);

i=M;
j=N;

Ex=prefac*(gamma*(result[Ez(i,j)]-result[Ez(i-1,j)])/Dx+J*w*mu*(result[Hz(i,j)]-result[Hz(i,j-1)])/Dy);
Hy=prefac*(J*w*eps*(result[Ez(i,j)]-result[Ez(i-1,j)])/Dx+gamma*(result[Hz(i,j)]-result[Hz(i,j-1)])/Dy);
Ey=prefac*(gamma*(result[Ez(i,j)]-result[Ez(i,j-1)])/Dy-J*w*mu*(result[Hz(i,j)]-result[Hz(i-1,j)])/Dx);
Hx=prefac*(-J*w*eps*(result[Ez(i,j)]-result[Ez(i,j-1)])/Dy+gamma*(result[Hz(i,j)]-result[Hz(i-1,j)])/Dx);

Ptemp+=Ex*conj(Hy)-Ey*conj(Hx);

ex[j][i]=creal(Ex*cexp(J*w*t-gamma*z));
hy[j][i]=creal(Hy*cexp(J*w*t-gamma*z));
ey[j][i]=creal(Ey*cexp(J*w*t-gamma*z));
hx[j][i]=creal(Hx*cexp(J*w*t-gamma*z));
ez[j][i]=creal(result[Ez(i,j)]*cexp(J*w*t-gamma*z));
hz[j][i]=creal(result[Hz(i,j)]*cexp(J*w*t-gamma*z));

Power+=Ptemp;
Power_Hmax[2]=0.5*creal(Power)*Dx*Dy;
return(Power_Hmax);
}


void calc_long(hx_long, hz_long, ex_long, ez_long, hy_long, hz_long2, ey_long, ez_long2, ex, ey, ez, hx,
hy, hz, params, gamma, result)
float hx_long[2*M+1][NOOFDZ+1], hz_long[2*M+1][NOOFDZ+1], ez_long[2*M+1][NOOFDZ+1],
ex_long[2*M+1][NOOFDZ+1], hz_long2[2*N+1][NOOFDZ+1], hy_long[2*N+1][NOOFDZ+1],
ez_long2[2*N+1][NOOFDZ+1], ey_long[2*N+1][NOOFDZ+1], *params;
float ex[2*N+1][2*M+1], ey[2*N+1][2*M+1], hx[2*N+1][2*M+1], hy[2*N+1][2*M+1],
ez[2*N+1][2*M+1], hz[2*N+1][2*M+1];
float complex gamma,result[ROWLENGTH];
{
float *EH_Power_calc();
float Dz;
int i,j;
Dz=params[0]/(2*M);
for (i=0;i<=NOOFDZ;i++)
        {
        EH_Power_calc(gamma,result,params,i*Dz,0.0,ex,ey,ez,hx,hy,hz);
        for (j=0;j<=2*M;j++)
                {
                hx_long[j][i]=hx[N][j];
```

```
                hz_long[j][i]=hz[N][j];
                ex_long[j][i]=ex[N][j];
                ez_long[j][i]=ez[N][j];
                }
        for (j=0;j<=2*N;j++)
                {
                hy_long[j][i]=hy[j][2*M];
                hz_long2[j][i]=hz[j][2*M];
                ey_long[j][i]=ey[j][M];
                ez_long2[j][i]=ez[j][M];
                }
        }
return;
}


void plotmatr(xmatr,ymatr,m,n)
float *xmatr, *ymatr;
int m,n;
{
fortran void EZVEC();

EZVEC(xmatr,ymatr,&m,&n);
return;
}


void openplot()
{
fortran void OPNGKS();
fortran void GQCNTN();
fortran void GSELNT();
fortran void WTSTR();
int ierr,icn;
static char string[]="Title";
OPNGKS();
GQCNTN(&ierr,&icn);
GSELNT(0);
WTSTR(.1,.96,string,2,0,-1);
GSELNT(&icn);
return;
}


void closeplot()
{
fortran void CLSGKS();
CLSGKS();
return;
}


float *vector(nl,nh)
long nh,nl;
```

```
/* allocate a float vector with subscript range v[nl..nh] */
{
      float *v;

      v=(float *)malloc((unsigned int) ((nh-nl+2)*sizeof(float)));
      if (!v) nrerror("allocation failure in vector()");
      return(v-nl+1);
}


void free_vector(v,nl,nh)
float *v;
long nh,nl;
/* free a float vector allocated with vector() */
{
      free((char*) (v+nl-1));
}


void nrerror(error_text)
char error_text[];
/* Error print routine */
{

          fprintf(stderr,"Run-time error ... \n");
          fprintf(stderr,"%s\n",error_text);
          fprintf(stderr," ... now exiting to system ... \n");
          exit(1);
}
```

Appendix E

Sample Output (for a WR90 HTS Waveguide) of *wg_sweep*

```
Warning: no access to tty; thus no job control in this shell...
>>>>>>>> NCCS   Cray Y-MP C98/6256   UNICOS 7.C.3  Node: charney <<<<<<<<
 Technical Assistance Group   Bldg 28 Rm S201   tag@nccs.gsfc.nasa.gov
 MVS support 0900-1100, (301)286-9120; other hours, leave message
 Cray/Convex support 0830-1700, Tue & Thu 0830-1600, (301)286-CRAY/2729
 Current system status: enter 'statinfo' or call (301)286-1392.
======== URGENT INFORMATION! as of 17:37 Fri, Sep 3, 1993
09/02 Account renewal forms were due to the NCCS on September 1, 1993.
    See "consult news 1295" for more information.
======== SCHEDULED SYSTEM UNAVAILABILITY as of 17:37 Fri, Sep 3, 1993
       From--To    System(s) -- Reason
09/06 Mon 0800--1600  UniTree -- UltraNet and silo testing
09/07 Tue 0600--0900  UniTree/Convex -- Backups and silo testing
09/07 Tue 0600--0900  Cray C98 -- scheduled preventive maintenance
09/08 Wed 0600--0900  UniTree -- Convex 3820 UltraNet and silo testing
09/09 Thu 0600--0900  UniTree -- Convex 3820 UltraNet and silo testing
09/10 Fri 1200 to
09/14 Tue 0900        UniTree/Convex -- Upgrade to Convex 3820
======== Recent CONSULT ARTICLES as of 17:35 Thu, Sep 2, 1993
09/02 NEWS     1297  Planned Schedule for UniTree Move From Convex
               C3240 to C3820 (same as UNITREE 1010)
08/30 CRAY     1216  Cray C98 NQS Job Queue Scheduling (updated)
08/30 CRAY     1210  Transition to the Cray C98 (updated)
08/27 CRAY     1214  How to be Certified for Multitasking on the C98
------------------------------------------------------------------------
news: statinfo cray.consult cray.1210 cray.1120 cray.1216 cray.1021 cray.1206
 SCC30.news CF7750.news cray.1214 cray.1211 CF7760.news Pascal4.2 cray.1213
 cray.2160 cray.1212 cray.1118 cray.1009 cray.2070 cray.1050 cray.1028
 cray.1130 cray.1048 cray.1010 cray.1174 cray.1072 cray.1015 cray.1089
 cray.1088 cray.1069 cray.1109 cray.1139 cray.1155 cray.1044 cray.1022
 cray.1004 cray.1023 cray.1208 cray.1063 cray.1144 cray.1064 cray.1158
 cray.1105 cray.1027 cray.1053 cray.1157 cray.1046 cray.1202 cray.1127
 cray.1207 cray.1209 cray.1205 unicos70.ro cray.1203 cray.1037 cray.1201
 cray.1200 cray.1187 cray.2132 cray.2142 cray.1196 cray.1195 cray.1194
 cray.1193 cray.1078 cray.1101 cray.1094 cray.1036 cray.1192 cray.1188
 cray.1024 cray.1019 cray.1045 cray.1186 cray.1128 cray.1185 cray.1183
 cray.1182 cray.1181 cray.1180 cray.1171 cray.1005 cray.1179 cray.1178
 cray.1177 cray.1125 cray.1176 cray.1175 cray.1173 cray.1172 cray.1111
 cray.1170 cray.1169 cray.1166 cray.1168 cray.1167 cray.1165 cray.1164
 cray.1163 cray.1161 cray.1160 cray.2150 cray.2140 cray.2130 cray.2050
 cray.2040 cray.2030 cray.2020 cray.2010 cray.2000 cray.1159 cray.1153
 cray.1151 cray.1150 cray.1149 cray.1147 cray.1146 cray.1145 cray.1141
 cray.1140 cray.1138 cray.1137 cray.1136 cray.1135 cray.1134 cray.1132
 cray.1131 cray.1126 cray.1124 cray.1123 cray.1119 cray.1115 cray.1108
 cray.1107 cray.1098 cray.1097 cray.1096 cray.1095 cray.1090 cray.1085
 cray.1084 cray.1076 cray.1075 cray.1074 cray.1062 cray.1055 cray.1052
 cray.1051 cray.1043 cray.1039 cray.1033 cray.1030 cray.1026 cray.1012
 cray.1000 cray.1154 CF77_5.0 cray.1148 mvs_disk_fail news.consult cray.1034
 cray.1018
Sat Sep  4 13:26:25 PDT 1993
```

Enter width of waveguide cross-section : Enter height of waveguide cross-section : Enter relative dielectric constant of waveguide interior : Enter effective zero-temperature penetration depth of HTS walls : Enter normal conductivity of HTS walls : Enter temperature of HTS walls : Enter critical temperature of HTS

walls : Enter 'm' of the mode you are interested in : Enter 'n' of the mode you are interested in : Enter starting frequency : Enter stopping frequency : Enter number of points in frequency range :

Starting on frequency 8.000000e+09 Hz

Fc: 6.557210e+09 Hz
Theoretical TE10 alpha : 1.056854e-03 Nepers/m
Lossless beta: 9.604952e+01 rad/m

(1.0569e-03,9.6050e+01)
(1.0780e-03,9.5089e+01)
(1.0357e-03,9.5089e+01)
(1.0569e-03,9.4129e+01)
(1.0569e-03,9.3168e+01)
(1.0991e-03,9.4129e+01)
(1.0780e-03,9.3168e+01)
(1.0780e-03,9.4609e+01)
(1.0780e-03,9.3648e+01)
(1.0780e-03,9.4369e+01)
(1.0357e-03,9.4369e+01)
(1.0569e-03,9.4609e+01)
(1.0569e-03,9.4249e+01)
(1.0569e-03,9.4489e+01)
(1.0569e-03,9.4309e+01)
(1.0569e-03,9.4429e+01)
(1.0569e-03,9.4339e+01)
(1.0991e-03,9.4339e+01)
(1.1308e-03,9.4324e+01)
(1.0780e-03,9.4309e+01)
(1.0780e-03,9.4354e+01)
(1.1203e-03,9.4354e+01)
(1.1520e-03,9.4361e+01)
(1.0991e-03,9.4369e+01)
(1.0991e-03,9.4346e+01)
(1.0991e-03,9.4361e+01)
(1.0991e-03,9.4350e+01)
(1.0991e-03,9.4357e+01)
(1.0991e-03,9.4352e+01)
(1.1414e-03,9.4352e+01)
(1.1203e-03,9.4350e+01)
(1.1203e-03,9.4353e+01)
(1.1203e-03,9.4351e+01)
(1.1203e-03,9.4352e+01)
(1.1203e-03,9.4351e+01)
(1.1203e-03,9.4352e+01)
(1.0780e-03,9.4352e+01)
(1.0991e-03,9.4352e+01)
(1.0991e-03,9.4352e+01)
(1.1414e-03,9.4352e+01)
(1.1203e-03,9.4352e+01)
(1.1203e-03,9.4352e+01)
(1.0780e-03,9.4352e+01)
(1.1255e-03,9.4352e+01)

(1.1044e-03,9.4352e+01)
(1.1163e-03,9.4352e+01)
(1.1427e-03,9.4352e+01)
(1.1100e-03,9.4352e+01)
(1.1008e-03,9.4352e+01)
(1.0945e-03,9.4352e+01)
(1.1109e-03,9.4352e+01)
(1.1201e-03,9.4352e+01)
(1.1056e-03,9.4352e+01)
(1.1064e-03,9.4352e+01)
(1.1091e-03,9.4352e+01)
(1.1039e-03,9.4352e+01)
(1.1091e-03,9.4352e+01)
(1.1056e-03,9.4352e+01)
(1.1082e-03,9.4352e+01)
(1.1117e-03,9.4352e+01)
(1.1071e-03,9.4352e+01)
(1.1063e-03,9.4352e+01)
(1.1084e-03,9.4352e+01)
(1.1095e-03,9.4352e+01)
(1.1089e-03,9.4352e+01)
(1.1088e-03,9.4352e+01)
(1.1085e-03,9.4352e+01)
(1.1092e-03,9.4352e+01)
(1.1085e-03,9.4352e+01)
(1.1081e-03,9.4352e+01)
(1.1081e-03,9.4352e+01)
(1.1084e-03,9.4352e+01)
(1.1088e-03,9.4352e+01)
(1.1082e-03,9.4352e+01)
(1.1081e-03,9.4352e+01)
(1.1082e-03,9.4352e+01)
(1.1083e-03,9.4352e+01)
(1.1083e-03,9.4352e+01)
(1.1081e-03,9.4352e+01)
(1.1082e-03,9.4352e+01)
(1.1082e-03,9.4352e+01)
(1.1084e-03,9.4352e+01)
(1.1082e-03,9.4352e+01)

At frequency 8.000000e+09 Hz, (alpha,beta)=(1.10820e-03,9.43519e+01)

80 Iterations.

Starting on frequency 8.800000e+09 Hz

Fc: 6.557210e+09 Hz
Theoretical TE10 alpha : 1.027177e-03 Nepers/m
Lossless beta: 1.230000e+02 rad/m

(1.0272e-03,1.2300e+02)
(1.0477e-03,1.2177e+02)

(1.0066e-03,1.2177e+02)
(1.0272e-03,1.2054e+02)
(1.0272e-03,1.2115e+02)
(1.0272e-03,1.2238e+02)
(1.0272e-03,1.2146e+02)
(1.0272e-03,1.2208e+02)
(1.0272e-03,1.2162e+02)
(1.0683e-03,1.2162e+02)
(1.0991e-03,1.2154e+02)
(1.0477e-03,1.2146e+02)
(1.0477e-03,1.2169e+02)
(1.0888e-03,1.2169e+02)
(1.0683e-03,1.2177e+02)
(1.0683e-03,1.2165e+02)
(1.0683e-03,1.2173e+02)
(1.0683e-03,1.2167e+02)
(1.0272e-03,1.2167e+02)
(1.0477e-03,1.2165e+02)
(1.0477e-03,1.2168e+02)
(1.0888e-03,1.2168e+02)
(1.1196e-03,1.2169e+02)
(1.0683e-03,1.2169e+02)
(1.0683e-03,1.2168e+02)
(1.0683e-03,1.2169e+02)
(1.0683e-03,1.2168e+02)
(1.1094e-03,1.2168e+02)
(1.0888e-03,1.2168e+02)
(1.0888e-03,1.2168e+02)
(1.0477e-03,1.2168e+02)
(1.0683e-03,1.2168e+02)
(1.0683e-03,1.2168e+02)
(1.1094e-03,1.2168e+02)
(1.0888e-03,1.2168e+02)
(1.0888e-03,1.2168e+02)
(1.0477e-03,1.2168e+02)
(1.0683e-03,1.2168e+02)
(1.0683e-03,1.2168e+02)
(1.1094e-03,1.2168e+02)
(1.0888e-03,1.2168e+02)
(1.0888e-03,1.2168e+02)
(1.0477e-03,1.2168e+02)
(1.0683e-03,1.2168e+02)
(1.0683e-03,1.2168e+02)
(1.1094e-03,1.2168e+02)
(1.0631e-03,1.2168e+02)
(1.0426e-03,1.2168e+02)
(1.0773e-03,1.2168e+02)
(1.0824e-03,1.2168e+02)
(1.0679e-03,1.2168e+02)
(1.0590e-03,1.2168e+02)
(1.0727e-03,1.2168e+02)
(1.0724e-03,1.2168e+02)
(1.0693e-03,1.2168e+02)
(1.0740e-03,1.2168e+02)

(1.0725e-03,1.2168e+02)
(1.0691e-03,1.2168e+02)
(1.0718e-03,1.2168e+02)
(1.0686e-03,1.2168e+02)
(1.0666e-03,1.2168e+02)
(1.0661e-03,1.2168e+02)
(1.0704e-03,1.2168e+02)
(1.0696e-03,1.2168e+02)
(1.0694e-03,1.2168e+02)
(1.0676e-03,1.2168e+02)
(1.0697e-03,1.2168e+02)
(1.0705e-03,1.2168e+02)
(1.0690e-03,1.2168e+02)
(1.0693e-03,1.2168e+02)
(1.0694e-03,1.2168e+02)
(1.0687e-03,1.2168e+02)
(1.0690e-03,1.2168e+02)
(1.0687e-03,1.2168e+02)
(1.0692e-03,1.2168e+02)
(1.0691e-03,1.2168e+02)
(1.0691e-03,1.2168e+02)
(1.0693e-03,1.2168e+02)
(1.0692e-03,1.2168e+02)
(1.0692e-03,1.2168e+02)
(1.0690e-03,1.2168e+02)
(1.0692e-03,1.2168e+02)
(1.0693e-03,1.2168e+02)
(1.0691e-03,1.2168e+02)

At frequency 8.800000e+09 Hz, (alpha,beta)=(1.06920e-03,1.21682e+02)

81 Iterations.

Starting on frequency 9.600000e+09 Hz

Fc: 6.557210e+09 Hz
Theoretical TE10 alpha : 1.057287e-03 Nepers/m
Lossless beta: 1.469514e+02 rad/m

(1.0573e-03,1.4695e+02)
(1.0784e-03,1.4548e+02)
(1.0361e-03,1.4548e+02)
(1.0573e-03,1.4401e+02)
(1.0573e-03,1.4622e+02)
(1.0573e-03,1.4475e+02)
(1.0573e-03,1.4585e+02)
(1.0996e-03,1.4585e+02)
(1.1313e-03,1.4603e+02)
(1.0784e-03,1.4622e+02)
(1.0784e-03,1.4567e+02)
(1.0784e-03,1.4603e+02)
(1.0784e-03,1.4594e+02)

(1.0784e-03,1.4576e+02)
(1.0784e-03,1.4590e+02)
(1.0784e-03,1.4580e+02)
(1.0784e-03,1.4587e+02)
(1.0784e-03,1.4583e+02)
(1.0784e-03,1.4586e+02)
(1.0784e-03,1.4584e+02)
(1.0784e-03,1.4586e+02)
(1.1207e-03,1.4586e+02)
(1.0996e-03,1.4586e+02)
(1.0996e-03,1.4585e+02)
(1.0573e-03,1.4585e+02)
(1.0784e-03,1.4585e+02)
(1.0784e-03,1.4585e+02)
(1.0784e-03,1.4585e+02)
(1.0784e-03,1.4585e+02)
(1.1207e-03,1.4585e+02)
(1.0996e-03,1.4585e+02)
(1.0996e-03,1.4585e+02)
(1.0573e-03,1.4585e+02)
(1.0784e-03,1.4585e+02)
(1.0784e-03,1.4585e+02)
(1.1207e-03,1.4585e+02)
(1.0996e-03,1.4585e+02)
(1.0996e-03,1.4585e+02)
(1.0573e-03,1.4585e+02)
(1.0784e-03,1.4585e+02)
(1.0784e-03,1.4585e+02)
(1.1207e-03,1.4585e+02)
(1.0996e-03,1.4585e+02)
(1.0996e-03,1.4585e+02)
(1.0573e-03,1.4585e+02)
(1.1049e-03,1.4585e+02)
(1.1260e-03,1.4585e+02)
(1.0903e-03,1.4585e+02)
(1.0956e-03,1.4585e+02)
(1.0986e-03,1.4585e+02)
(1.0841e-03,1.4585e+02)
(1.0997e-03,1.4585e+02)
(1.1079e-03,1.4585e+02)
(1.0947e-03,1.4585e+02)
(1.0958e-03,1.4585e+02)
(1.0979e-03,1.4585e+02)
(1.0930e-03,1.4585e+02)
(1.0980e-03,1.4585e+02)
(1.1011e-03,1.4585e+02)
(1.0963e-03,1.4585e+02)
(1.0964e-03,1.4585e+02)
(1.0975e-03,1.4585e+02)
(1.0959e-03,1.4585e+02)
(1.0964e-03,1.4585e+02)
(1.0952e-03,1.4585e+02)
(1.0969e-03,1.4585e+02)
(1.0969e-03,1.4585e+02)

(1.0965e-03,1.4585e+02)
(1.0959e-03,1.4585e+02)
(1.0967e-03,1.4585e+02)
(1.0965e-03,1.4585e+02)
(1.0965e-03,1.4585e+02)
(1.0969e-03,1.4585e+02)
(1.0965e-03,1.4585e+02)
(1.0963e-03,1.4585e+02)
(1.0964e-03,1.4585e+02)
(1.0966e-03,1.4585e+02)
(1.0965e-03,1.4585e+02)

At frequency 9.600000e+09 Hz, (alpha,beta)=(1.09651e-03,1.45853e+02)

75 Iterations.

Starting on frequency 1.040000e+10 Hz

Fc: 6.557210e+09 Hz
Theoretical TE10 alpha : 1.116978e-03 Nepers/m
Lossless beta: 1.691824e+02 rad/m

(1.1170e-03,1.6918e+02)
(1.1393e-03,1.6749e+02)
(1.0946e-03,1.6749e+02)
(1.1170e-03,1.6580e+02)
(1.1170e-03,1.6834e+02)
(1.1617e-03,1.6834e+02)
(1.1952e-03,1.6876e+02)
(1.1393e-03,1.6918e+02)
(1.1393e-03,1.6791e+02)
(1.1393e-03,1.6876e+02)
(1.1393e-03,1.6812e+02)

At frequency 1.040000e+10 Hz, (alpha,beta)=(1.13932e-03,1.68125e+02)

8 Iterations.

Starting on frequency 1.120000e+10 Hz

Fc: 6.557210e+09 Hz
Theoretical TE10 alpha : 1.195677e-03 Nepers/m
Lossless beta: 1.902968e+02 rad/m

(1.1957e-03,1.9030e+02)
(1.2196e-03,1.8839e+02)
(1.1718e-03,1.8839e+02)
(1.1479e-03,1.9030e+02)
(1.1120e-03,1.9125e+02)
(1.1718e-03,1.9220e+02)

(1.1718e-03,1.8935e+02)
(1.1239e-03,1.8935e+02)
(1.1479e-03,1.8839e+02)
(1.1479e-03,1.8982e+02)
(1.1479e-03,1.8887e+02)
(1.1479e-03,1.8958e+02)
(1.1479e-03,1.8911e+02)
(1.1479e-03,1.8946e+02)
(1.1957e-03,1.8946e+02)
(1.2315e-03,1.8952e+02)
(1.1718e-03,1.8958e+02)
(1.1718e-03,1.8940e+02)
(1.1718e-03,1.8952e+02)
(1.1718e-03,1.8943e+02)
(1.1718e-03,1.8949e+02)
(1.1718e-03,1.8945e+02)
(1.2196e-03,1.8945e+02)
(1.2555e-03,1.8944e+02)
(1.1957e-03,1.8943e+02)
(1.1957e-03,1.8946e+02)
(1.2435e-03,1.8946e+02)
(1.2794e-03,1.8946e+02)
(1.2196e-03,1.8946e+02)
(1.2196e-03,1.8945e+02)
(1.2674e-03,1.8945e+02)
(1.2435e-03,1.8945e+02)
(1.2435e-03,1.8945e+02)
(1.1957e-03,1.8945e+02)
(1.2196e-03,1.8946e+02)
(1.2196e-03,1.8945e+02)
(1.2674e-03,1.8945e+02)
(1.2435e-03,1.8945e+02)
(1.2435e-03,1.8945e+02)
(1.2435e-03,1.8945e+02)
(1.2435e-03,1.8945e+02)
(1.1957e-03,1.8945e+02)
(1.2196e-03,1.8945e+02)
(1.2196e-03,1.8945e+02)
(1.2196e-03,1.8945e+02)
(1.2196e-03,1.8945e+02)
(1.2196e-03,1.8945e+02)
(1.2196e-03,1.8945e+02)
(1.2674e-03,1.8945e+02)
(1.2136e-03,1.8945e+02)
(1.2375e-03,1.8945e+02)
(1.2330e-03,1.8945e+02)
(1.2629e-03,1.8945e+02)
(1.2259e-03,1.8945e+02)
(1.2364e-03,1.8945e+02)
(1.2381e-03,1.8945e+02)
(1.2540e-03,1.8945e+02)
(1.2329e-03,1.8945e+02)
(1.2258e-03,1.8945e+02)
(1.2391e-03,1.8945e+02)

(1.2356e-03,1.8945e+02)
(1.2358e-03,1.8945e+02)
(1.2297e-03,1.8945e+02)
(1.2367e-03,1.8945e+02)
(1.2339e-03,1.8945e+02)
(1.2353e-03,1.8945e+02)
(1.2391e-03,1.8945e+02)
(1.2345e-03,1.8945e+02)
(1.2359e-03,1.8945e+02)
(1.2362e-03,1.8945e+02)
(1.2337e-03,1.8945e+02)
(1.2360e-03,1.8945e+02)
(1.2374e-03,1.8945e+02)
(1.2352e-03,1.8945e+02)
(1.2353e-03,1.8945e+02)
(1.2354e-03,1.8945e+02)
(1.2347e-03,1.8945e+02)
(1.2356e-03,1.8945e+02)
(1.2359e-03,1.8945e+02)
(1.2354e-03,1.8945e+02)
(1.2356e-03,1.8945e+02)
(1.2355e-03,1.8945e+02)
(1.2358e-03,1.8945e+02)
(1.2355e-03,1.8945e+02)
(1.2356e-03,1.8945e+02)
(1.2356e-03,1.8945e+02)
(1.2357e-03,1.8945e+02)
(1.2355e-03,1.8945e+02)

At frequency 1.120000e+10 Hz, (alpha,beta)=(1.23554e-03,1.89454e+02)

85 Iterations.

Starting on frequency 1.200000e+10 Hz

Fc: 6.557210e+09 Hz
Theoretical TE10 alpha : 1.288667e-03 Nepers/m
Lossless beta: 2.106307e+02 rad/m

(1.2887e-03,2.1063e+02)
(1.3144e-03,2.0852e+02)
(1.2629e-03,2.0852e+02)
(1.3402e-03,2.1063e+02)
(1.3789e-03,2.1168e+02)
(1.3144e-03,2.1274e+02)
(1.3144e-03,2.0958e+02)
(1.3660e-03,2.0958e+02)
(1.4046e-03,2.0905e+02)
(1.3402e-03,2.0852e+02)
(1.3402e-03,2.1010e+02)
(1.3918e-03,2.1010e+02)
(1.3660e-03,2.1063e+02)

(1.3660e-03,2.0984e+02)
(1.3144e-03,2.0984e+02)
(1.2758e-03,2.0971e+02)
(1.3402e-03,2.0958e+02)
(1.3402e-03,2.0997e+02)
(1.3402e-03,2.0971e+02)
(1.3402e-03,2.0991e+02)
(1.3402e-03,2.0978e+02)
(1.3402e-03,2.0987e+02)
(1.2887e-03,2.0987e+02)
(1.3144e-03,2.0991e+02)
(1.3144e-03,2.0986e+02)
(1.3144e-03,2.0989e+02)
(1.3144e-03,2.0987e+02)
(1.3144e-03,2.0988e+02)
(1.3144e-03,2.0987e+02)
(1.3144e-03,2.0988e+02)
(1.3144e-03,2.0987e+02)
(1.3660e-03,2.0987e+02)
(1.3402e-03,2.0987e+02)
(1.3402e-03,2.0987e+02)
(1.3402e-03,2.0987e+02)
(1.3402e-03,2.0987e+02)
(1.2887e-03,2.0987e+02)
(1.3144e-03,2.0987e+02)
(1.3144e-03,2.0987e+02)
(1.3144e-03,2.0987e+02)
(1.3144e-03,2.0987e+02)
(1.3144e-03,2.0987e+02)
(1.3144e-03,2.0987e+02)
(1.3660e-03,2.0987e+02)
(1.3467e-03,2.0987e+02)
(1.3209e-03,2.0987e+02)
(1.3354e-03,2.0987e+02)
(1.3676e-03,2.0987e+02)
(1.3277e-03,2.0987e+02)
(1.3165e-03,2.0987e+02)
(1.3240e-03,2.0987e+02)
(1.3164e-03,2.0987e+02)
(1.3306e-03,2.0987e+02)
(1.3269e-03,2.0987e+02)
(1.3275e-03,2.0987e+02)
(1.3341e-03,2.0987e+02)
(1.3316e-03,2.0987e+02)
(1.3285e-03,2.0987e+02)
(1.3301e-03,2.0987e+02)
(1.3342e-03,2.0987e+02)
(1.3292e-03,2.0987e+02)
(1.3325e-03,2.0987e+02)
(1.3300e-03,2.0987e+02)
(1.3285e-03,2.0987e+02)
(1.3308e-03,2.0987e+02)
(1.3309e-03,2.0987e+02)
(1.3302e-03,2.0987e+02)

(1.3295e-03,2.0987e+02)
(1.3305e-03,2.0987e+02)
(1.3306e-03,2.0987e+02)
(1.3302e-03,2.0987e+02)
(1.3305e-03,2.0987e+02)
(1.3303e-03,2.0987e+02)
(1.3300e-03,2.0987e+02)
(1.3304e-03,2.0987e+02)
(1.3303e-03,2.0987e+02)
(1.3303e-03,2.0987e+02)
(1.3305e-03,2.0987e+02)
(1.3303e-03,2.0987e+02)

At frequency 1.200000e+10 Hz, (alpha,beta)=(1.33038e-03,2.09872e+02)

76 Iterations.

Starting on frequency 1.280000e+10 Hz

Fc: 6.557210e+09 Hz
Theoretical TE10 alpha : 1.393510e-03 Nepers/m
Lossless beta: 2.303909e+02 rad/m

(1.3935e-03,2.3039e+02)
(1.4214e-03,2.2809e+02)
(1.3656e-03,2.2809e+02)
(1.3378e-03,2.3039e+02)
(1.2960e-03,2.3154e+02)
(1.3656e-03,2.3269e+02)
(1.3656e-03,2.2924e+02)
(1.3099e-03,2.2924e+02)
(1.3378e-03,2.2809e+02)
(1.3378e-03,2.2981e+02)
(1.3935e-03,2.2981e+02)
(1.4353e-03,2.3010e+02)
(1.3656e-03,2.3039e+02)
(1.3656e-03,2.2953e+02)
(1.3656e-03,2.3010e+02)
(1.3656e-03,2.2967e+02)
(1.4214e-03,2.2967e+02)
(1.4632e-03,2.2960e+02)
(1.3935e-03,2.2953e+02)
(1.3935e-03,2.2974e+02)
(1.3935e-03,2.2960e+02)
(1.3935e-03,2.2971e+02)
(1.4493e-03,2.2971e+02)
(1.4911e-03,2.2972e+02)
(1.4214e-03,2.2974e+02)
(1.4214e-03,2.2969e+02)
(1.4214e-03,2.2972e+02)
(1.4214e-03,2.2970e+02)
(1.4771e-03,2.2970e+02)

(1.4493e-03,2.2969e+02)
(1.4493e-03,2.2970e+02)
(1.4493e-03,2.2969e+02)
(1.4493e-03,2.2970e+02)
(1.3935e-03,2.2970e+02)
(1.4214e-03,2.2970e+02)
(1.4214e-03,2.2970e+02)
(1.4214e-03,2.2970e+02)
(1.4214e-03,2.2970e+02)
(1.4214e-03,2.2970e+02)
(1.4214e-03,2.2970e+02)
(1.4214e-03,2.2970e+02)
(1.4771e-03,2.2970e+02)
(1.4493e-03,2.2970e+02)
(1.4493e-03,2.2970e+02)
(1.4493e-03,2.2970e+02)
(1.4493e-03,2.2970e+02)
(1.3935e-03,2.2970e+02)
(1.4562e-03,2.2970e+02)
(1.4283e-03,2.2970e+02)
(1.4440e-03,2.2970e+02)
(1.4789e-03,2.2970e+02)
(1.4358e-03,2.2970e+02)
(1.4236e-03,2.2970e+02)
(1.4318e-03,2.2970e+02)
(1.4348e-03,2.2970e+02)
(1.4552e-03,2.2970e+02)
(1.4315e-03,2.2970e+02)
(1.4222e-03,2.2970e+02)
(1.4386e-03,2.2970e+02)
(1.4419e-03,2.2970e+02)
(1.4393e-03,2.2970e+02)
(1.4431e-03,2.2970e+02)
(1.4368e-03,2.2970e+02)
(1.4375e-03,2.2970e+02)
(1.4383e-03,2.2970e+02)
(1.4359e-03,2.2970e+02)
(1.4374e-03,2.2970e+02)
(1.4370e-03,2.2970e+02)
(1.4394e-03,2.2970e+02)
(1.4368e-03,2.2970e+02)
(1.4354e-03,2.2970e+02)
(1.4376e-03,2.2970e+02)
(1.4378e-03,2.2970e+02)
(1.4370e-03,2.2970e+02)
(1.4376e-03,2.2970e+02)
(1.4371e-03,2.2970e+02)
(1.4366e-03,2.2970e+02)
(1.4373e-03,2.2970e+02)
(1.4375e-03,2.2970e+02)
(1.4377e-03,2.2970e+02)
(1.4377e-03,2.2970e+02)
(1.4373e-03,2.2970e+02)
(1.4374e-03,2.2970e+02)
(1.4374e-03,2.2970e+02)

(1.4372e-03,2.2970e+02)
(1.4374e-03,2.2970e+02)

At frequency 1.280000e+10 Hz, (alpha,beta)=(1.43738e-03,2.29700e+02)

82 Iterations.

Starting on frequency 1.360000e+10 Hz

Fc: 6.557210e+09 Hz
Theoretical TE10 alpha : 1.508819e-03 Nepers/m
Lossless beta: 2.497136e+02 rad/m

(1.5088e-03,2.4971e+02)
(1.5390e-03,2.4722e+02)
(1.4786e-03,2.4722e+02)
(1.4485e-03,2.4971e+02)
(1.4032e-03,2.5096e+02)
(1.4786e-03,2.5221e+02)
(1.4786e-03,2.4847e+02)
(1.4183e-03,2.4847e+02)
(1.4485e-03,2.4722e+02)
(1.4485e-03,2.4909e+02)
(1.5088e-03,2.4909e+02)
(1.5541e-03,2.4940e+02)
(1.4786e-03,2.4971e+02)
(1.4786e-03,2.4878e+02)
(1.4786e-03,2.4940e+02)
(1.4786e-03,2.4893e+02)
(1.4786e-03,2.4925e+02)
(1.4786e-03,2.4901e+02)
(1.4786e-03,2.4917e+02)
(1.4786e-03,2.4905e+02)
(1.4786e-03,2.4913e+02)
(1.4786e-03,2.4907e+02)
(1.5390e-03,2.4907e+02)
(1.5843e-03,2.4906e+02)
(1.5088e-03,2.4905e+02)
(1.5088e-03,2.4908e+02)
(1.5692e-03,2.4908e+02)
(1.6144e-03,2.4908e+02)
(1.5390e-03,2.4909e+02)
(1.5390e-03,2.4907e+02)
(1.5390e-03,2.4908e+02)
(1.5390e-03,2.4908e+02)
(1.5390e-03,2.4908e+02)
(1.5390e-03,2.4908e+02)
(1.5993e-03,2.4908e+02)
(1.5692e-03,2.4908e+02)
(1.5692e-03,2.4908e+02)
(1.5692e-03,2.4908e+02)
(1.5692e-03,2.4908e+02)

(1.5088e-03,2.4908e+02)
(1.5767e-03,2.4908e+02)
(1.6069e-03,2.4908e+02)
(1.5560e-03,2.4908e+02)
(1.5635e-03,2.4908e+02)
(1.5678e-03,2.4908e+02)
(1.5470e-03,2.4908e+02)
(1.5544e-03,2.4908e+02)
(1.5662e-03,2.4908e+02)
(1.5585e-03,2.4908e+02)
(1.5452e-03,2.4908e+02)
(1.5508e-03,2.4908e+02)
(1.5549e-03,2.4908e+02)
(1.5546e-03,2.4908e+02)
(1.5469e-03,2.4908e+02)
(1.5556e-03,2.4908e+02)
(1.5593e-03,2.4908e+02)
(1.5530e-03,2.4908e+02)
(1.5540e-03,2.4908e+02)
(1.5544e-03,2.4908e+02)
(1.5518e-03,2.4908e+02)
(1.5527e-03,2.4908e+02)
(1.5542e-03,2.4908e+02)
(1.5533e-03,2.4908e+02)
(1.5550e-03,2.4908e+02)
(1.5561e-03,2.4908e+02)
(1.5561e-03,2.4908e+02)
(1.5540e-03,2.4908e+02)
(1.5545e-03,2.4908e+02)
(1.5545e-03,2.4908e+02)
(1.5554e-03,2.4908e+02)
(1.5562e-03,2.4908e+02)
(1.5559e-03,2.4908e+02)
(1.5556e-03,2.4908e+02)
(1.5560e-03,2.4908e+02)
(1.5552e-03,2.4908e+02)
(1.5551e-03,2.4908e+02)
(1.5555e-03,2.4908e+02)
(1.5557e-03,2.4908e+02)
(1.5553e-03,2.4908e+02)

At frequency 1.360000e+10 Hz, (alpha,beta)=(1.55545e-03,2.49078e+02)

76 Iterations.

Starting on frequency 1.440000e+10 Hz

Fc: 6.557210e+09 Hz
Theoretical TE10 alpha : 1.633745e-03 Nepers/m
Lossless beta: 2.686931e+02 rad/m

(1.6337e-03,2.6869e+02)

(1.6664e-03,2.6601e+02)
(1.6011e-03,2.6601e+02)
(1.5684e-03,2.6869e+02)
(1.5194e-03,2.7004e+02)
(1.6011e-03,2.7138e+02)
(1.6011e-03,2.6735e+02)
(1.6011e-03,2.7004e+02)
(1.6011e-03,2.6802e+02)
(1.5357e-03,2.6802e+02)
(1.5684e-03,2.6735e+02)
(1.5684e-03,2.6836e+02)
(1.5684e-03,2.6769e+02)
(1.5684e-03,2.6819e+02)
(1.5684e-03,2.6785e+02)
(1.5684e-03,2.6811e+02)
(1.6337e-03,2.6811e+02)
(1.6828e-03,2.6815e+02)
(1.6011e-03,2.6819e+02)
(1.6011e-03,2.6806e+02)
(1.6011e-03,2.6815e+02)
(1.6011e-03,2.6808e+02)
(1.6011e-03,2.6813e+02)
(1.6011e-03,2.6809e+02)
(1.6011e-03,2.6812e+02)
(1.6011e-03,2.6810e+02)
(1.6011e-03,2.6811e+02)
(1.6011e-03,2.6810e+02)
(1.6011e-03,2.6811e+02)
(1.6011e-03,2.6810e+02)
(1.6011e-03,2.6811e+02)
(1.6011e-03,2.6810e+02)
(1.6011e-03,2.6811e+02)
(1.6011e-03,2.6811e+02)
(1.6011e-03,2.6811e+02)
(1.6011e-03,2.6811e+02)
(1.6664e-03,2.6811e+02)
(1.7154e-03,2.6811e+02)
(1.6337e-03,2.6811e+02)
(1.6337e-03,2.6811e+02)
(1.6337e-03,2.6811e+02)
(1.6337e-03,2.6811e+02)
(1.6991e-03,2.6811e+02)
(1.7318e-03,2.6811e+02)
(1.7073e-03,2.6811e+02)
(1.6746e-03,2.6811e+02)
(1.6930e-03,2.6811e+02)
(1.6521e-03,2.6811e+02)
(1.6935e-03,2.6811e+02)
(1.7200e-03,2.6811e+02)
(1.6798e-03,2.6811e+02)
(1.6803e-03,2.6811e+02)
(1.6898e-03,2.6811e+02)
(1.6762e-03,2.6811e+02)
(1.6805e-03,2.6811e+02)

(1.6905e-03,2.6811e+02)
(1.6825e-03,2.6811e+02)
(1.6732e-03,2.6811e+02)
(1.6856e-03,2.6811e+02)
(1.6876e-03,2.6811e+02)
(1.6823e-03,2.6811e+02)
(1.6854e-03,2.6811e+02)
(1.6847e-03,2.6811e+02)
(1.6813e-03,2.6811e+02)
(1.6824e-03,2.6811e+02)
(1.6848e-03,2.6811e+02)
(1.6829e-03,2.6811e+02)
(1.6806e-03,2.6811e+02)
(1.6837e-03,2.6811e+02)
(1.6842e-03,2.6811e+02)
(1.6837e-03,2.6811e+02)
(1.6845e-03,2.6811e+02)
(1.6833e-03,2.6811e+02)
(1.6832e-03,2.6811e+02)
(1.6830e-03,2.6811e+02)
(1.6836e-03,2.6811e+02)
(1.6832e-03,2.6811e+02)
(1.6829e-03,2.6811e+02)
(1.6828e-03,2.6811e+02)
(1.6834e-03,2.6811e+02)
(1.6834e-03,2.6811e+02)
(1.6836e-03,2.6811e+02)
(1.6833e-03,2.6811e+02)

At frequency 1.440000e+10 Hz, (alpha,beta)=(1.68342e-03,2.68105e+02)

80 Iterations.

Starting on frequency 1.520000e+10 Hz

Fc: 6.557210e+09 Hz
Theoretical TE10 alpha : 1.767737e-03 Nepers/m
Lossless beta: 2.873976e+02 rad/m

(1.7677e-03,2.8740e+02)
(1.8031e-03,2.8452e+02)
(1.7324e-03,2.8452e+02)
(1.6970e-03,2.8740e+02)
(1.6440e-03,2.8883e+02)
(1.7324e-03,2.9027e+02)
(1.7324e-03,2.8596e+02)
(1.7324e-03,2.8883e+02)
(1.7324e-03,2.8668e+02)
(1.6617e-03,2.8668e+02)
(1.6970e-03,2.8596e+02)
(1.6970e-03,2.8704e+02)
(1.6970e-03,2.8632e+02)

(1.6970e-03,2.8686e+02)
(1.7677e-03,2.8686e+02)
(1.8208e-03,2.8695e+02)
(1.7324e-03,2.8704e+02)
(1.7324e-03,2.8677e+02)
(1.7324e-03,2.8695e+02)
(1.7324e-03,2.8681e+02)
(1.7324e-03,2.8690e+02)
(1.7324e-03,2.8684e+02)
(1.7324e-03,2.8688e+02)
(1.7324e-03,2.8685e+02)
logout